ISSN: 0019-4824

The Indian Geographical Journal

Volume 96 2021 No.1 & 2

The Indian Geographical Society
Department of Geography
University of Madras
Guindy Campus
Chennai-600 025,India

Editor: K.Kumaraswamy
Assistant Editor: K.Balasubramani

Governing Council of The Indian Geographical Society

President:	Prof. N. Sivagnanam
Vice Presidents:	Prof. B. Hema Malini
	Prof. Sulochana Shekhar
	Prof. Smita Bhutani
	Prof. Subhash Anand Prof. Aravind Mulimanian
General Secretary:	Dr. R. Jaganathan
Joint Secretaries:	Prof. R. Jegankumar
	Dr. S. Sanjeevi Prasad Dr. G. Geetha
Treasurer:	Prof. M. Sakthivel
Council Members:	Prof. P.S. Tiwari
	Prof. V. Emayavaramban
	Prof. B. Srinagesh
	Prof. Dhanaraj Gownamani
	Dr. B. Mahalingam Dr. S. Eswari
Member Nominated to the EC:	Prof. P.S. Tiwari
Editor:	Prof. K. Kumaraswamy
Assistant Editor:	Dr. K. Balasubramani

For details about the IGS, visit: www.igschennai.org

Information to Authors

The Indian Geographical Journal is published half-yearly in June and December by The Indian Geographical Society, Chennai. The UGC-Care listed / peer-reviewed journal invites manuscripts of original research on any geographical field, providing information of importance to geography and related disciplines with an analytical approach. The manuscript should be submitted only through the **online submission form https://forms.gle/SLfL1wodtvLEVPcV8**

The manuscript should be uploaded in Microsoft Word Document (.doc, .docx) as follows: 1) **Title Page**: Title of the Manuscript, Author Name and Address (complete postal address with contact details including phone and email ID) and acknowledgements (if any). 2) **Full-Length Manuscript**: The main text part should not contain the author(s) name or identities. The main text can be divided into the sections viz. Title, Abstract, Keywords, Introduction (Background/Literature review), Study area, Methodology, Results, Discussion, Conclusion and References. 3) **Tables**: All tables should be consolidated in a single MS Word document with proper captions and footnotes (if applicable). 4) **Figures**: All figures/graphs/charts/maps should be submitted in JPEG/PNG format within a single MS Word document. Each figure should have a concise caption describing accurately what the figure depicts. The tables and figures should be numbered in a sequence (Table 1, Table 2 etc. and Figure 1, Figure 2 etc.) and cited in the manuscript at appropriate places.

The title should be brief, specific and amenable to indexing. No more than five keywords should be indicated separately; these should be chosen carefully and not phrases of several words. The abstract should be limited to 100-250 words and convey the main points of the study, outline the methods and results and explain the significance of the results. Acknowledgements of people, grants, funds, etc., should be placed in a separate section in the title page. The names of funding organisations should be written in full. The title page should also be accompanied by a letter stating that it has not been published or sent to any other journal and will not be submitted elsewhere for publication.

Maps and charts should be submitted in the final or near-final form. The authors should, however, agree to revise the maps and charts for reproduction after the article is accepted for publication. If you include figures that have already been published elsewhere, you must obtain permission from the copyright owner(s) for both the print and online format. Please be aware that some publishers do not grant electronic rights for free, and it is informed that IGS will not be able to refund any costs that may have occurred to receive these permissions.

References should be listed in alphabetical order as per MLA format. The list of references (limited to 20-25) should include only the published works or sites that are cited in the main text. You may refer to the IGS website (http://igschennai.org/IGJ.php) for detailed guidelines.

Corresponding Email: editorigs1926@gmail.com

The Indian Geographical Journal

Contents

The Indian Geographical Journal
Volume 96 (1) June - 2021, pp 1-14
ISSN 0019-4824

INTRA-DISTRICT VARIATIONS AND EMERGING CONCERNS IN AGRICULTURAL DEVELOPMENT OF SIDDHARTHNAGAR DISTRICT, UTTAR PRADESH

Rajesh Kumar Abhay[1] and Shweta Rani[1]

[1]Department of Geography, Dyal Singh College, University of Delhi, New Delhi
E-mail : rkabhay@dsc.du.ac.in

Abstract

A higher level of development in the agriculture sector contributes positively to the economic condition and livelihood security of the farmers. In India, more than 60% of the population lives in villages and is highly dependent on agriculture for their socio-economic well-being. Agricultural development is one of the major challenges in the less developed districts in the country as these are poor in terms of natural resources and also in socio-economic aspects. The study area, Siddharthnagar district, has more than 93% of rural population which is mainly dependent on agriculture. The present study is concerned with the analysis of intra-district variations in agricultural development measured with the help of 10 selected indicators which are processed through the composite index method. The study uses secondary data sources on various indicators which are combined into 4 groups representing agricultural extent, fertilizers use and cropping intensity, irrigation status, and availability of modern tools and technology. The results show wide variations in the agricultural development at the block level which ranges from 0.89 in Mithwal and Khesraha blocks to 1.16 in Uska Bazar blocks and represent the least and very highly developed block in agriculture, respectively. The study also identifies emerging concerns like limited scope to extend agriculture, high dependence on food grain crops, comparatively low cropping intensity, efficient use of water in irrigation, etc. which requires policy intervention. The findings recommend that proper decision-making in these areas can help in achieving the rural development of the area through agricultural development.

***Keywords*:** Agriculture, Irrigation, Disparities, Rural Development, Siddharthnagar

Introduction

Agriculture is the largest economic activity performed in the world and the biggest use of land by men (Foley, 2011). Agriculture is an important sector of economy which has a considerable impact on the gross domestic product of any region. The development of agriculture plays a crucial role for the rural poor depending upon agriculture as it helps in improving the economic condition and purchasing power for the livelihood (Hajer et al., 2016). The whole rural local economy revolves around the primary activities in general and agriculture in particular. In the present time, agriculture is facing several challenges (Foley

et al., 2011) and agricultural development is one of them in developing countries like India where regional disparities are widening inspite of various governmental efforts (Kurian, 2000).

Agriculture and allied activities contribute to one-fourth of the GDP of the Indian economy and engage three-fifth of the total workforce (Singh, 2007). Agriculture has experienced various peaks and valleys in its development since India's independence. The marginalized and peripheral states and districts of India have always suffered from the negligence of government and also received least researcher's attention. Their contribution to economic development has never been emphasized. Over the period, regional disparities in development have widened and a need is felt to redesign policies for socio-territorial justice (Singh, 2005). Regional disparities in India have been examined through the social, economic, demographic and agricultural points of view at the state and district level. Most of them have been focusing on socio-economic development using demographic, social and economic activities related indicators (Kurian, 2000; Sohal and Kaur, 2006). A range of work has been done in the field of identifying regional disparities in the levels of development by taking different types of indicators (Das, 2018). But, again it is limited to mainland areas of the country. Further, various studies have also been found on analyzing the different dimensions of agricultural development like agricultural modernization tubewell irrigation (Sohal and Kaur, 2006; Ali and Abustan 2013). But, very few studies have been conducted to explain the block-level agricultural disparities in the districts of Uttar Pradesh.

Equipped with the most basic resources, Siddharthnagar district is lagging far behind the rest of other major developed districts in the state of Uttar Pradesh. The agricultural land provides a base and huge potential for the development of various economic activities. Yet it is rural, poor socio-economic condition, low agricultural production, poor agricultural benefits, least infrastructural development, and rate of rural and economic development is very slow. Therefore, the Siddharthnagar district presents a good example to analyze the above-mentioned issues. The present study has addressed two research objectives: Firstly, it measures the intra-district variations in the levels of agricultural development, and secondly, identifies concern areas required to achieve future agricultural prosperity and sustainability in Siddharthnagar.

Study Area

The Siddharthnagar district is located in the north-eastern part of Uttar Pradesh and shares an international border with Nepal towards its northern side (Figure 1A). The district lies between 27^{o} 0' to 27^{o} 28' North latitude and 82^{o} 45' to 83^{o} 10' East longitude covering a geographical area of 2895 sq km. It is one of the 75 districts of Uttar Pradesh. The state capital, Lucknow, is located approx. 43 km in the southwest of the Siddharthnagar district (Figure 1B). It is surrounded by six districts of Uttar Pradesh, namely Maharajganj and Gorakhpur district on the east; Gonda, Basti and Sant Kabir Nagar districts in the south; and Balrampur district in the west (Census of India, 2011). The district has 5 tehsils, namely Naugarh, Shoharatgarh, Bansi, Itwa and Domariyaganj. Further, the district is also divided

into 14 CD Blocks (Vikas Khand). These blocks are Bansi, Barhni Bazar, Bhanwapur, Birdpur, Domariyaganj, Itwa, Jogia Khas, Khesraha, Khuniyaon, Lotan, Mithwal, Naugarh, Shoharatgarh and Uska Bazar (Figure 1C; District Census Handbook, 2011).

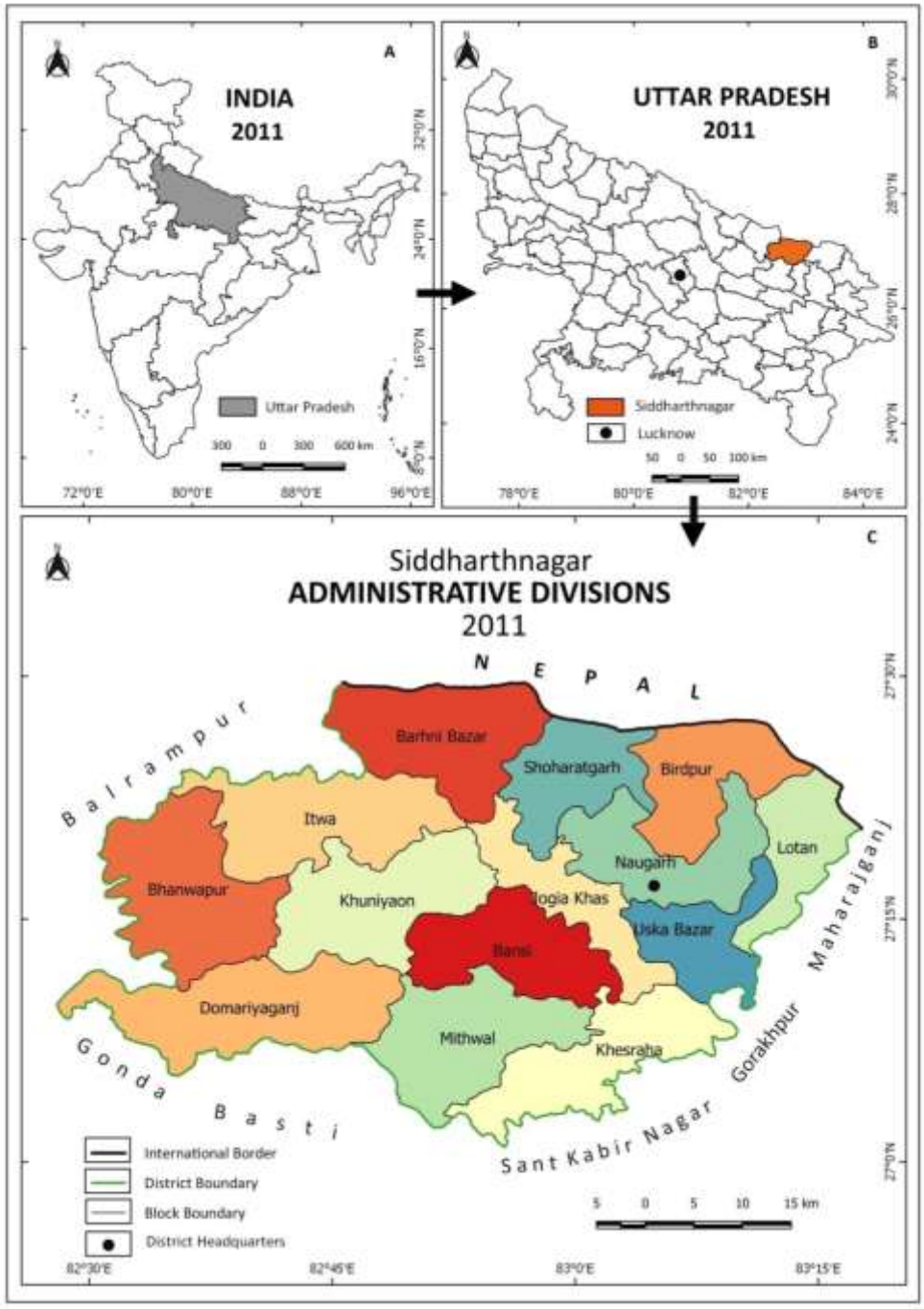

Fig. 1. Location of the Study Area

The study area, Siddharthnagar district, is adjoining to Nepal in the north and lies in the *Tarai* region. It is a part of Indo- Gangetic Plains (Middle-Ganga Plain Region) of India. Most of the land represents plain topography and the soil is very much fertile that provides suitable conditions for the cultivation. Many rivers flow in the Siddharthnagar district, such as Rapti, Budhi Rapti, Baanganga, Parasi, etc which provides sufficient water to irrigate fields and also contributes to groundwater recharge.

The total population of the district is 25,59,297, of which 93.72% is rural and the remaining is urban. The density of population in the district is 884 persons per sq km (Census of India, 2011). Agriculture is the backbone of the district economy. Rabi, Kharif and Zaid are the three agricultural seasons. Crops sown in the Rabi season are Wheat, Barley, potato, sugarcane, pulses (Masoor, Gram, Pea and Arhar), oilseeds, etc. and in the Kharif season Paddy, Maize, Urad, Moong, etc. and the Zaid season is mainly dominated by different vegetables (District Census Handbook, 2011).

Database and Methodology

The study is based on secondary data sources collected from District Census Handbook, Directorate of Statistics and Economics, Uttar Pradesh (2011), and Statistical Patrika Internet-based Data Entry and Retrieval System (SPIDER) (2016-17). This study is conducted at the block level. As mentioned above, the district comprises of 5 tahsils, and 14 blocks, therefore, a block is a viable unit of analysis. Regional variations will emerge convincingly at the block level as they are more in number in comparison to tehsils level which are just 5 in number. On the other hand, at the village level (2505 in number), it was not feasible due to the non-availability of data on several indicators. Data at the block level is easily available from reliable sources, therefore, chosen as a viable scale of study. In the present study, from a wide range of indicators, 10 indicators have been selected to reflect the agricultural development and have been combined into four groups. All the indicators have been chosen very carefully to reflect the overall status of agricultural development considering the study area and availability of data. The 4 groups of indicators are: (i) extent of agriculture and major crops, (ii) fertilizers use and cropping intensity, (iii) irrigation status, and (iv) modern tools and technology (Table 1).

The first indicator *Net Sown Area* (NSA) represents how much area is cropped, and the second indicator explains the agriculture under the major crops grown in the Siddharthnagar district under the first group of indicators, i.e. extent of agriculture and major crops. *NSA* is the actual land area cropped in a year as a proportion to the total geographical area of the block. The second indicator is the *area under food grain crops* which represents the main cereal crops cropped by a majority of the population in the block. It particularly includes rice and wheat in the study area. Fertilizers use and cropping intensity directly help in improving the farm income of the farmer. Agricultural development has been guided by package technology in which fertilizers played an important role (Qureshi, 2019). *Fertilizer consumption* helps in increasing production if used judiciously and *cropping intensity* is directly linked with agricultural productivity. The fourth indicator is

the *copping intensity* which is a measure of land efficiency and defined as the extent to which the NSA is cropped or sown (Singh and Ashraf, 2012). Assured irrigation provides physical support to the development of agriculture. Over time, the increase in certainty of irrigation facilities contributes to assured production. It is analyzed through four indicators: net irrigated area (NIA), net irrigated area to NSA, irrigation by state canals, and irrigation by tube wells in the district. *NIA* includes the area on which irrigation is applied for growing crops in an agricultural year. *NIA to NSA* indicator shows that the actual percentage of the area irrigated at least once a year. Canals are one of the most important sources of irrigation. *Irrigation by Tube Wells* is also a very important indicator of agricultural development which reflects the use of groundwater extraction. These modern tools and technology in the Siddharthnagar district are studied by analyzing the availability of harrow, harvesters and advanced threshing machines within 10 sq km of area. The *availability of advanced threshing machines* has become crucial for separating wheat, gram and other grains and seeds from their chaff and straw as it saves labour, cost and time. The agricultural development is positively related to all the indicators like net sown area, irrigation, the intensity of cropping, use of modern technology like advanced harrows and threshing machines. Hence it is chosen for the study.

Table 1. Selected indicators to Measure Agricultural Development in Siddharthnagar

Group		Indicators	
A	Extent of Agriculture and Major Crops	X_1	Net Sown Area (%)
		X_2	Area under Foodgrain Crops (%)
B	Fertilizers Use and Cropping Intensity	X_3	Consumption of Fertilisers (Kg/ ha)
		X_4	Cropping Intensity (%)
C	Availability of Irrigation Facilities	X_5	Net Irrigated Area (%)
		X_6	Net Irrigated Area to Net Sown Area (%)
		X_7	Irrigation by State Canals (%)
		X_8	Irrigation by Tubewells (%)
D	Availability of Modern Tools and Technology	X_9	Availability of Advanced Harrow and Cultivators (Per 10 sq km)
		X_{10}	Availability of Advanced Threshing Machines (Per 10 sq km)

***Source**: Compiled by Authors*

For the present study, we have applied *"Kundu's method of normalization of data through calculation of composite index"* (Kundu, 1980). At the block level, the information on 10 indicators is computed. This is followed by the computation of the scale-free index obtained by dividing each observation (block-level value) of a particular indicator by its column mean. Scale-free values are then combined for each of the blocks, followed by dividing the summed value by *N (Eq. 1)*. Such an index avoids the dominance of the composite index by one or two of these variables.

$$\text{Composite Index} = \sum_{i=1}^{n} \left(\frac{X_i}{\bar{X}_i}\right)/N \qquad \text{------ Eq. 1}$$

Where, X_i is indicator i.

$\bar{X}_i$, mean of indicator i.

and, N is the number of indicators. There are 10 indicators.

Finally, obtained scores are arranged in descending order with their respective blocks for easy interpretation and analysis. Here, higher the index value represents a higher level of development. The agricultural development is measured at the block level which is classified into very high, high, moderate and low levels of agricultural development. The data below this scale is not available. Further, various underlying factors have been explained which causes these disparities based on which policy interventions have been recommended.

Results and Discussion

Indicators of Agricultural Development

All the chosen indicators, to measure the overall status of agricultural development, are combined into 4 groups. These are discussed below:

Extent of Agriculture and Major Crops

These indicators represent the extent of agriculture in the district based on two indicators, i.e. net sown area and area under major food grain crops (Figure 2). The total NSA of the district is 76.10%. It ranges from 70.26 (Birdpur) to 81.46 % in Khesraha. Four districts that have a very high percentage of the NSA: Khesraha, Domariyaganj, Mithwal and Khuniyaon located in the south-central part of the district (more than 79, Figure 2A). The second indicator is the *area under food grain crops* which covers two-third area (66.8%) of the district. It is the highest in the Domariyaganj (79 %) while lowest in Lotan (61.1 %). Blocks growing very high percentage of food grain crops are Domariyaganj, Bansi, Uska Bazar and Mithwal (More than 69 %), while the northeastern blocks (Lotan, Naugarh and Jogia Khas) have a low percentage of area under food grain crops (less than 63 %, Figure 2B). Both indicators point towards that agriculture is an extensively pursued activity in the district where wheat and rice crops are dominantly grown by the local farmers.

Fertilizers Use and Cropping Intensity

Fertilizers are used for enhancing productivity and production. It was found that per hectare average consumption of chemical fertilizers in Siddharthnagar district is 156 kg per hectare (ha). The use of chemical fertilizers in the block ranges from 98.6 kg (Khesraha block) to 208 kg per ha in Jogia Khas block. Overall, high consumption of chemical fertilizers is found in northern parts of the district than in the south (Figure 2C). Overall cropping intensity in Siddharthnagar district is 169 %. The Domariyaganj (137.77 %) has the lowest and Lotan block (192.39) has the highest cropping intensity. The regional patterns reflect that the northeastern parts show very high (more than 180%) cropping intensity (Birdpur, Naugarh, Lotan and Uska Bazar block) while blocks in southeastern parts (Bansi, Mithwal and Domariyaganj block) show low (less than 160%) cropping intensity (Figure 2D).Higher consumption of fertilizer is attributed to the fact of high cropping

intensity. High cropping intensity reduces soil fertility which further requires fertilizer application to keep it productive. Therefore, it creates a great challenge to the farmers and planners to keep the soil sustainable for the future.

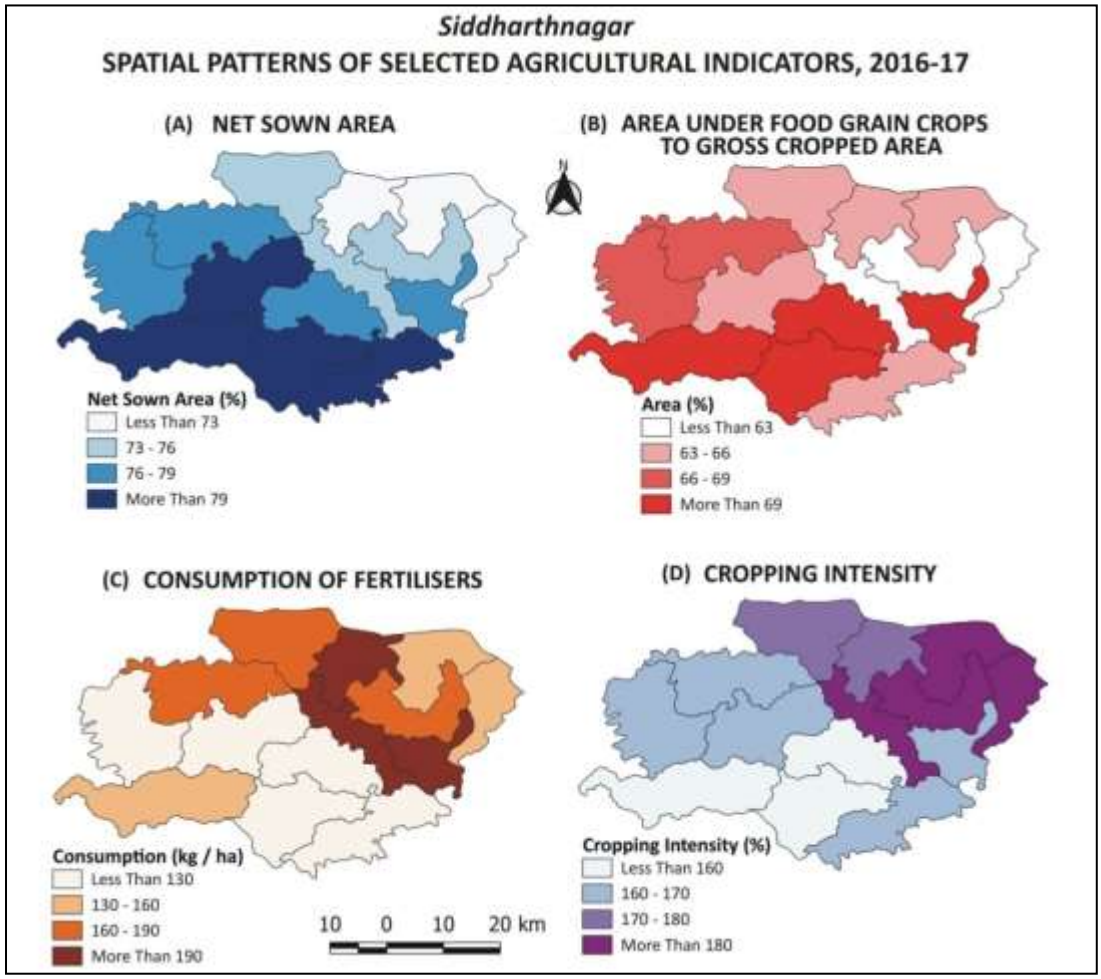

Fig. 2. Spatial Patterns of Selected Agricultural Indicators, 2016-17

Irrigation Status

The total net irrigated area in the district is 59.36% and ranges from 42.01 in Birdpur (lowest) to 84.73 % in the Bansi block (highest) (Figure 3A). It is high in the blocks of Bansi, Uska Bazar and Domariyaganj (more than 70%) located towards the southern half of the district. While blocks in northern parts show less percentage of irrigated area. In the district, net irrigated area to the net sown area is 77.61 % ranges from 67.17 % (Shoharatgarh) to 91.69 % (Domariyaganj) (Figure 3B). There are two blocks-Domariyaganj and Itwa- which have a very high percent of NIA to NSA. Two blocks-Shoharatgarh and Birdpur-have low percent of the area and they are located at the border areas (Figure 3).

Wide regional variations are visible in the NIA, and NIA to NSA at the block level which can be attributed to the drainage factor. Mostly rivers cross the district from the west to east direction in the district. They are less in the northern parts which affect the local irrigation patterns.

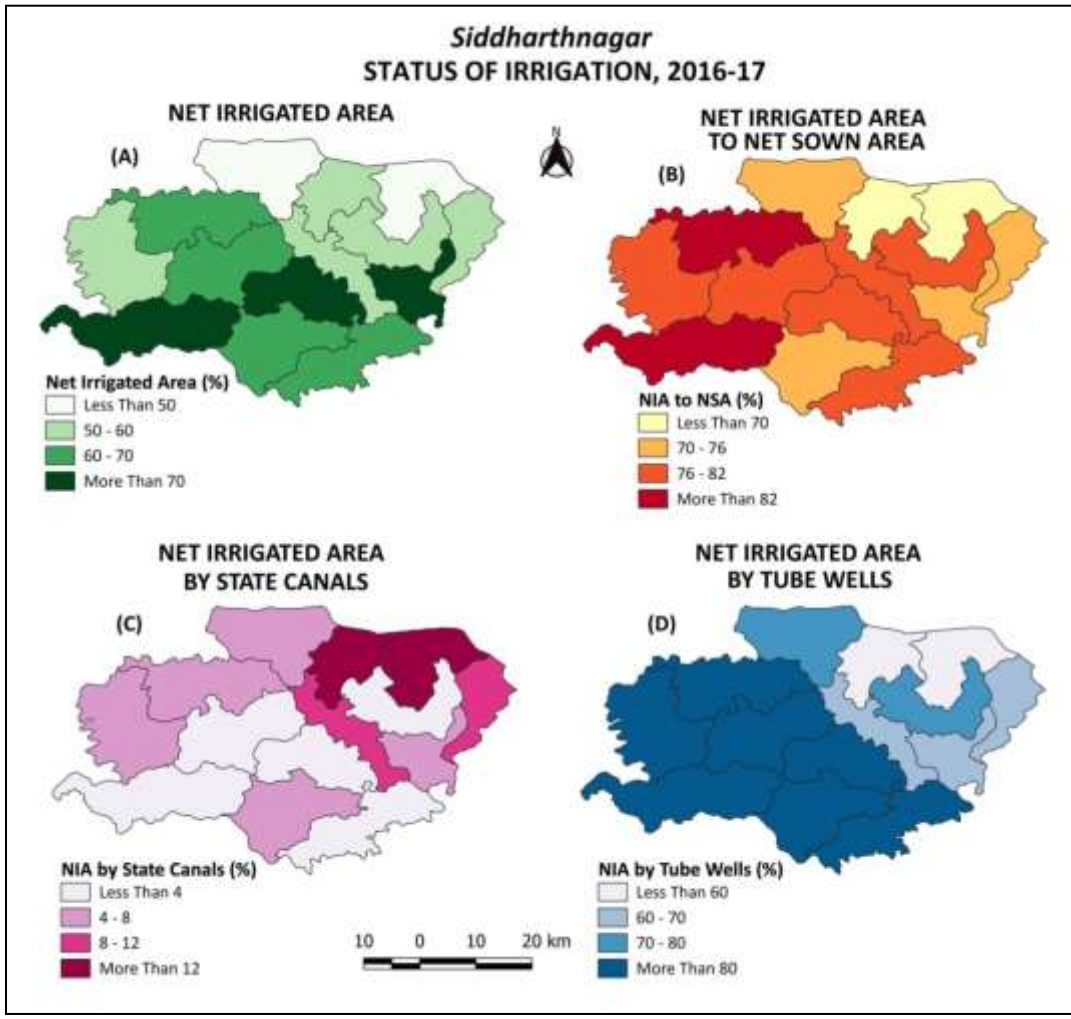

Fig. 3. Status of Irrigation in the Siddharthnagar District

The percentage of NIA by state canals is 6.9 % in the district. It is maximum in Shoharatgarh block (19.05) followed by Birdpur located along the Nepal border. It is the lowest in the Naugarh block (1.67) alongwith four blocks having less area irrigated by state canals in the district (Figure 3C).Most of the study area depends upon tube well irrigation covering approximately 74.83 % of the district. It ranges from 56.09 % in Shoharatgarh block to 85.65 % in the Domariyaganj (Figure 3D). Overall south-western blocks of the district are highly dependent on tube wells for irrigation (Figure 3). It is inferred that despite having many rivers in the district, the percentage of area irrigated by the canals is very less.

It is inferred that there is a huge scope for the development of canals for the agricultural development in the study area.

Availability of Modern Tools and Technology

The average availability of advanced harrow and cultivators in the district is 34 per 10 sq km or 3 to cover a square kilometer of area. It ranges from 28.89 (Domariyaganj) to 50.16 (Uska Bazar) in different blocks of the district (Figure 4A). Overall blocks on the periphery towards the north-west, west and south-west parts have low availability of harrow and cultivators.The average availability of threshing machines in the district is 55 per 10 sq km. The availability ranges from 22.83 in Khesraha to 107.31 in Bhanwapur per 10 sq km of area (Figure 4B). In all the blocks, the numbers of advanced threshing machines are not uniformly distributed. It explains that blocks are facing variations related to the availability of modern machinery within a very short distance.

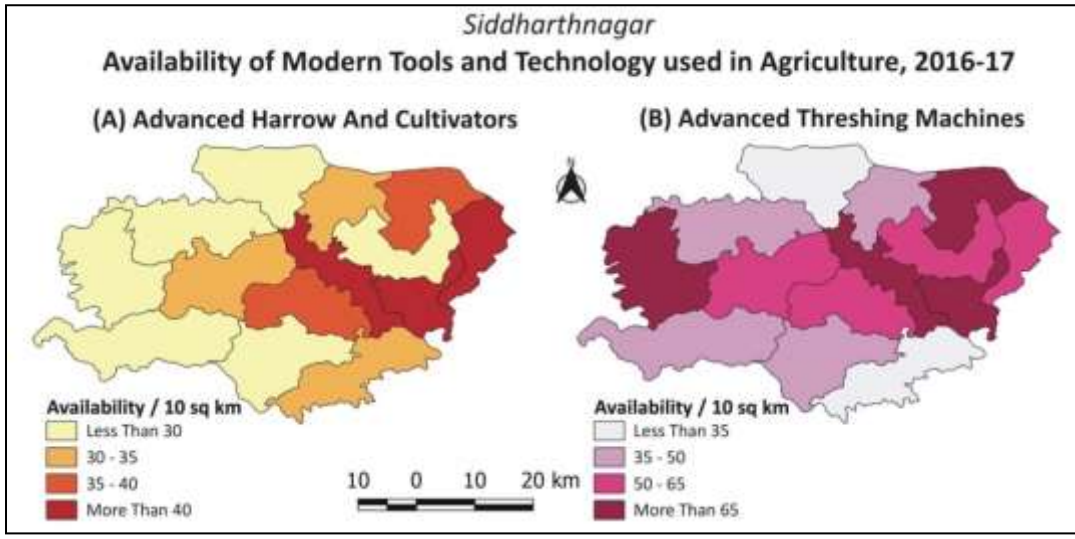

Fig. 4. Availability of Modern Farm Implements in Siddharthnagar District

Intra-District Variations in Agricultural Development

Based on the composite index score, agricultural development in Siddharthnagar district is assessed. The score ranges from 0.89 in Mithwal and Khesraha blocks to 1.16 in Uska Bazar block which represents the least developed block and very highly developed block in agriculture respectively (Figure 5). Very high agricultural development is found in 3 blocks, namely Uska Bazar, Jogia Khas and Shoharatgarh (score is more than 1.08; Figure 5). These blocks are located in the north-central parts and towards the east. The development is reasoned due to the proximity to district headquarters which acts as a nearby market and helps in getting more profit. The low transport cost alongwith easy availability of various inputs at low price contributes to getting more profit from agriculture. These benefits also help farmers in the purchase of modern farm implements, fertilizers,

and various other inputs which helps in the process of agricultural development. Four blocks are in the high agricultural development category with a composite score between 1.00 and 1.08 (Birdpur, Bhanwapur, Bansi and Lotan blocks). These are mainly located in the surrounding areas of very highly developed blocks except Bhanwapur located in the west.

Low-developed blocks scored a lower value in terms of agricultural development. These are Barhni Bazar, Mithwal and Khesraha block with a composite score of less than 0.92. These blocks show low fertilizers consumption and low availability of modern machinery. The low irrigation facility through the canal is also contributing to the low agricultural development of these blocks. Four blocks have moderately developed (Domariyaganj, Itwa, Khuniyaon and Naugarh) scoring between 0.92 to 1.0 . Interestingly, Itwa and Domriyaganj are the only blocks where some percentage of the urban population exists, but nevertheless they have attained moderate agricultural development. These blocks are located inside the above-discussed categories and towards the western parts of the district. These disparities are the result of the performance of the selected indicators in the district contributing positively as well as negatively in different blocks.

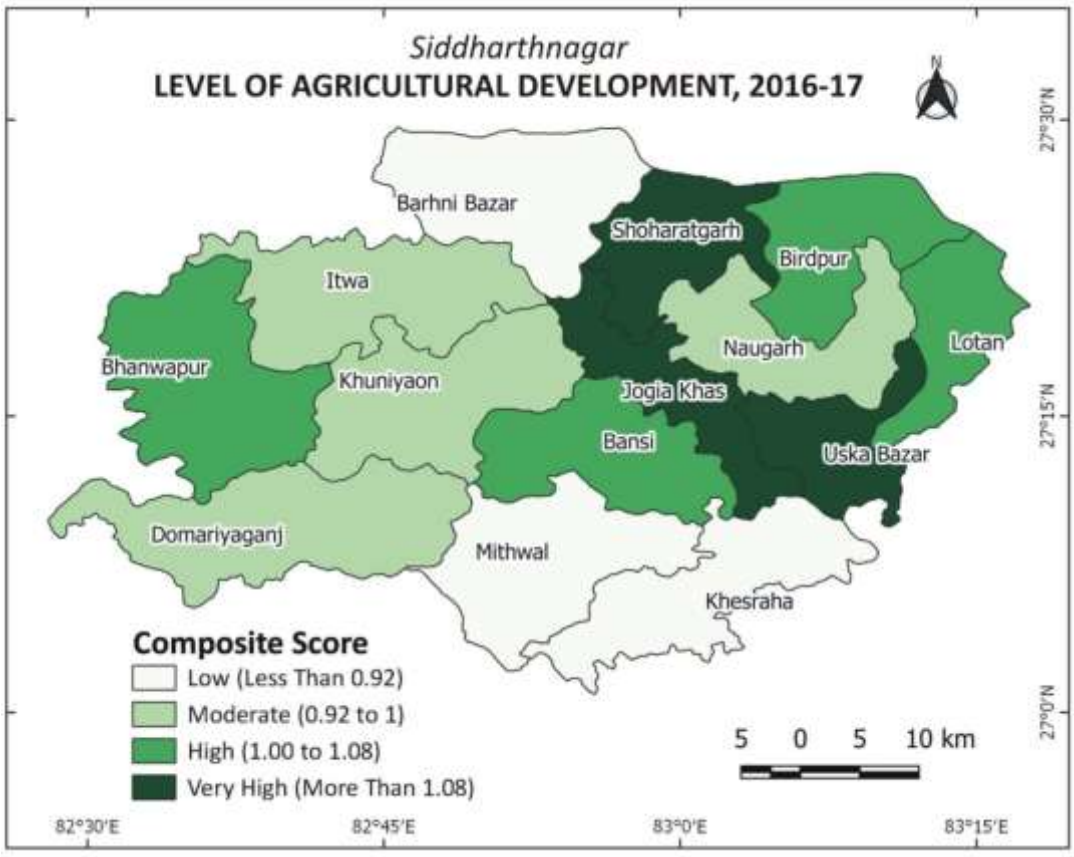

Fig. 5. Level of Agricultural Development in Siddharthnagar District

Besides, physical and economic factors affecting agricultural development discussed above, social factors also play a significant role in producing the disparities in agricultural development in the district. In the study carried out by Garia (2008), it is found that 79% of farmers have the lowest size of landholding (less than 1 ha), and 14% have 1-2 ha size in Siddharthnagar district. Both these categories cover 55% geographical area of the district. The small agricultural landholdings are not profitable for cultivation and income. It puts a great challenge to the economic development of the Siddharthnagar district. Smaller sizes of holdings alongwith a higher rate of fragmentation reduce productivity and make agriculture unsustainable in long run. The literacy rate in the district is very low (59%). The high literacy rates have a positive association with the level of awareness. Newspaper reading provides information about government subsidies, market prices about various inputs (seed quality), crop production, farm management, etc. This information help farmers to make appropriate decisions about the farming practices, ultimately leading to agricultural development.

Emerging Concerns for Policy Interventions

While mapping the intra-district variations in agricultural development, many issues and concerns have emerged which require policy interventions. The development of the agriculture sector and rural sustainability should not be seen in isolation. More than 93 % of population of the district depends upon agriculture for their livelihood, therefore, the economic prosperity of the region is very much dependent upon agricultural development. It is found that there is no more scope for extending agriculture as more than three-fourth area of Siddharthnagar is already the net sown area. The land is also required for other types of infrastructure development. Thus, an important concern is that more focus should be on improving production with higher productivity. Another concern is that area under food grain crops is high, so it is important to promote crop diversification and crop rotation.

Cropping intensity in the study area (169 %) as well as in the state (Uttar Pradesh, 159 %) is low in comparison to the agriculturally developed state of the country (Roy and Ahmad, 2015). The state of Punjab has a cropping intensity of more than 180 % since 2000-2001 (Grover et al., 2016) and also the Haryana state (186.9 % in 2015-16; Panwar and Dimri, 2018). Looking at the production potential, Siddharthnagar has a very high potential to produce more with more intensity as it forms the part of the Middle-Ganga Plain. The annual floods revitalize the soil fertility along the river course, so flood-resistant variety of seeds to be given to the farmers for further agricultural development. Fertilizer consumption is highly varied in blocks. It ranges from 98.6 kg/ha in the Khesraha block to 208 kg/ha in the Jogia Khas block. Its availability, distribution, accessibility, and reasonability are important concerns of the farmers. Further, there is also a need to rationalize fertilizer use without yielding any loss, for which farmers need to be educated. It will not only help in keeping the land productive, but also ensure an ultimate rural sustainability of land resources of the area.

Another concern is to use the resources efficiently, particularly water in irrigation. Foley (2011) estimated that to grow one calorie of food, on average, it takes about one litre of irrigation water. In the study area, due to the easy availability of water through rivers, canals, and tubewells, farmers are not using the water resource efficiently. More than three-fourth area of the net sown area is irrigated (Table 2). Canal irrigation is the least developed, inspite of many perennial rivers like Rapti, Burhi, etc. crossing the district. Mostly, the groundwater is used through tubewells and pump sets. If the existing groundwater extraction scenario remains to continue, the district will face rapid depletion of groundwater resources due to increasing aridity and associated problems. Therefore, irrigation management is a big concern in the near future.

Table 2. Comparison of Highly and Least Developed Block based on Indicators (2016-17)

Indicator	Unit	Siddharthnagar District	Highest Agricultural Development Uska Bazar Block)	Least Agricultural Development (Khesraha Block)
1. Net Sown Area	%	76.10	78.19	81.46
2. Area under Foodgrain Crops	%	66.8	69.30	66.00
3. Consumption of Fertilizers	Kg/ ha	156	192.70	98.60
4. Cropping Intensity	%	169	166.49	165.66
5. Net Irrigated Area	%	59.36	70.92	68.33
6. Net Irrigated Area to Net Sown Area	%	76.61	70.29	79.82
7. Irrigation by State Canals	%	6.9	7.95	3.96
8. Irrigation by Tubewells	%	74.83	67.65	82.47
9. Availability of Advanced Harrow and Cultivators	Per 10 sq km	34	50	31
10. Availability of Advanced Threshing Machines	Per 10 sq km	55	91	23

***Source**: Statistical Patrika Internet-based Data Entry and Retrieval System (SPIDER) (2016-17), Uttar Pradesh*

Agriculture is under continuous modification (Talukder et al., 2020) and there is a need to modernize it by efficient means of modern machinery. These tools manage land effectively and efficiently. In the study area, the status of modern tools and technology is very poor. Distribution andaccessibility are major challenges for the farmers.All these

issues need immediate attention from agricultural planners and policy-makers for proper decision-making in these areas, so that, rural development can be achieved through agricultural development.

Conclusions

The above analyses clearly explain the variations in agricultural development with the help of selected indicators. Based on the selected indicators like net sown area, cropping intensity, fertilizer consumption, irrigation and modern technology, and wide variations,the agricultural development is identified at the block level in the Siddharthnagar. Identified concerns require policy interventions from the policy-makers for the agricultural development at micro-level. The population of the Siddharthnagar district is highly dependent on agriculture for the livelihood. The emerging concerns have the potential to become critical, if not tackled in a time-bound manner. The present research provides critical insights into the agricultural development aspects of the Siddharthnagar district. We hope this work can initiate goal-oriented dialogues among the policy-makers and administrators for achieving agricultural sustainability in the study area.

Acknowledgements

The authors are thankful to the authorities of the Indian Council of Social Science Research (ICSSR), New Delhi and MHRD (IMPRESS Scheme) for the financial support (F.No. IMPRESS/P2171/644/SC/2018-19/ICSSR), and Head of the institution, Dyal Singh College for providing necessary facilities. Acknowledgements are also due to Mr. Satish Kumar Saini, Research Assistant for providing required help in data collection and map preparations, and to reviewers for their constructive comments on the paper.

References

1. Ali, M.H. and Abustan, I. (2013). Irrigation Management Strategies for Winter Wheat using Aqua Crop model. *Journal of Natural Resources and Development*, 3, 106-113.
2. Census of India, (2011). *Final Population Totals. Siddharthnagar*, Uttar Pradesh, Directorate of Census Operations, Uttar Pradesh.
3. Das, J. (2018). Regional Disparity in the Level of Development in West Bengal: A Geographical Analysis. *Indian Journal of Regional Science*, 50(1), 53-63.
4. District Census Handbook (2011). *Siddharthnagar, Uttar Pradesh*, Series-10, Part XII-A and B, Directorate of Census Operations, Uttar Pradesh.
5. Foley, J.A. (2011). Can We Feed The World Sustain The Planet?.*Scientific American*, 305(5), 60-65.
6. Foley, J.A., Ramankutty, N., Brauman, K.A., et al. (2011). Solutions for a Cultivated Planet. *Nature*, 478, 337-342.
7. Garia, P.S. (2008) Baseline Survey in the Minority Concentrated Districts of Uttar Pradesh: Report of Siddharthnagar District, Giri Institute of Development Studies, Lucknow.
8. Grover, D.K., Singh, J.M, Singh, J. and Kumar, S. (2016). State Agricultural Profile – Punjab, AERC Study No. 43, Agro-Economic Research Centre Department of

Economics and Sociology Punjab Agricultural University Ludhiana December. http://www.aercpau.com/assets/docs/AERC%2043.pdf. (Accessed on April 05, 2021)

9. Hajer, M.A., Westhoek, H., Ingram, J., van Berkum, S., and Ozay, L. (2016). Food Systems and Natural Resources. United Nations Environmental Programme. https://wedocs.unep.org/handle/20.500.11822/7592. (Accessed on April 05, 2021)
10. Kundu, A. (1980). *Measurement of Urban Processes: A Study in Regionalization*. Popular Prakashan Private Limited, Bombay.
11. Kurian, N.J. (2000). Widening Regional Disparities in India: Some Indicators. *Economic and Political Weekly*, 35(7), 538-550.
12. Panwar, S. and Dimri, A.K. (2018). Trend Analysis of Production and Productivity of Major Crops and its Sustainability: A Case Study of Haryana, *Indian Journal Agricultural Research,* 52(5), 571-575.
13. Qureshi, M.H. (2019). Agricultural Development and Environmental Issues in India. *Annals of the National Association of Geographers, India*, 39(2), 163-173.
14. Roy, R. and Ahmad, H. (2015). State Agricultural Profile of Uttar Pradesh, 2014-2015, Agro-Economic Research Centre, University of Allahabad, Allahabad, Uttar Pradesh.
15. Singh, G. (2007). Judicious Management of Land, Water and Climate Resources for Sustainable Agriculture. *Punjab Geographer*, 3, 1-11.
16. Singh, G. and Ashraf, S.W.A. (2012). Spatial Variation in Level of Agricultural Development in Bulandshahar District of Western Uttar Pradesh (India). *International Journal of Development and Sustainability*, 1(1), 47-56.
17. Singh, J. (2005). Can the Indian States' Achieve a Future of the Sustainable Agricultural development and Face Challenges to Agriculture during the 21st Century?.*Punjab Geographer*, 1, 1-3.
18. Sohal, K.S. and Kaur, S. (2006). Regional Disparities in Agricultural Modernization in Punjab. *Punjab Geographer*, 2, 63-72.
19. SPIDER [Statistical Patrika Internet-based Data Entry and Retrieval System], (2016-17). Various Tables for Siddharthnagar Districthttp://updes.up.nic.in/spideradmin/Hpage1.jsp(Accessed during May–September 2020).
20. Talukder, B., Blay-Palmer, A., vanLoon, G.W. and Hipel, K.W. (2020). Towards Complexity of Agricultural Sustainability Assessment: Main Issues and Concerns. *Environment and Sustainability Indicators*, 6, 38-53.

The Indian Geographical Journal
Volume 96 (1) June - 2021, pp 15-30
ISSN 0019-4824

ACCELERATING AGEING IN INDIA: TRENDS AND EXPLANATIONS

Smita Bhutani*, Harmanjot Antal

Department of Geography, Panjab University, Chandigarh, 160014, India.
E-mail: prof.smitabhutani@gmail.com; harmanantal@gmail.com

Abstract

In the 21st century population ageing is an exigent factor in the world, and dwindling demographics have become a major concern for many countries. But India with a huge population base still boasts of the demographic dividend. However, the drivers of ageing population in India are interplaying conspicuously for an ageing future. The paper attempts to elucidate the link between demographic transition and population ageing in India, to gain an insight into how the trends in the drivers of population ageing – the fertility and mortality – are carving out ageing India. Further, the size, growth, and sex ratio of the older population in India are discussed to understand their demographic situation. It emerges that the trends in fertility and mortality are declining, and life expectancy is increasing along with the resultant onset of decline in absolute numbers of persons and change in age structure. All the demographic variables in India are in line with the concept of population ageing. Also, the size, share, growth of the older population is witnessing an upward trend.

Keywords: Population Ageing; Demographic Transition; Older Population; India

Introduction

The initiation of global concern for population ageing can be traced back to the various actions undertaken by the United Nations. In 1982, the General Assembly called the first World Assembly on Ageing that brought the issues of aged people at the forefront. It constructed the first-ever global instrument named Vienna International Plan of Action on Ageing that gave 62-point recommendations to function as a foundation for the formulation of policy and programmes for the older people (United Nations, 1982). Later in 1991, the general assembly laid out 18 rights essential to older people by bringing into effect the United Nations Principles for Older Persons (United Nations: General Assembly, 1991). Thereafter, the International Conference on Ageing, 1992, adopted Proclamation on Ageing. Further, the year 1999 was declared as the International Year of Older Persons. The international attention and commitment towards addressing the issues of the elderly continued in 2002 when the Second World Assembly adopted the Political Declaration and the Madrid International Plan of Action on Ageing (United Nations, 2002). The action plan called for a change at levels to recognise and harness the enormous potential of the ageing world. It prioritised three target areas: "older persons and development; advancing health

and well-being into old age; and ensuring enabling and supportive environments (United Nations, Department of Economic and Social Affairs, 2002)."

Ageing is a natural and a universal phenomenon which is inevitable especially for humans during existence. When there is a growth in the number and proportion of older adults in a population, the population is considered to be ageing. Ageing of the population is also known as demographic ageing or population ageing. It is a term which refers to shift in the age distribution of a population towards older ages. The United Nations defines a country as ageing, where the share of people aged '60 and above' in the total population hits the 7 per cent mark (Prakash, 1999). Further, the United Nations refers to it as one of the four "mega-trends" that defines the global population in the 21st century (United Nations Department of Economic and Social Affairs, 2020). The continual strides in social, economic, medical, and public health domains have reduced fertility and mortality and added years to life. Consequently, the relative sizes of different age groups in a population have decreased in favour of older age-cohorts. Hence there are changes in population age-structure. In an instrumental study on the ageing process, Antonio Golini provided a conceptual framework that clearly describes the determinants and consequences of the ageing process (Golini, 2002). In this model, the population ageing is described as a macro-level concept of ageing, which is driven by reductions in fertility and mortality rates, and migration flows. Further, it shows that ageing of the population has consequences on myriad aspects, such as health, economy, policy and international relations.

The scope of the present paper pertains to the macro-level concept of ageing, i.e., population ageing for the country of India. Also, it discusses the course of demographic transition in India by analysing the trends in fertility and mortality during the documented demographic history of the country. Its effect on the life expectancy, the growth of population, and change in the age structure is examined further. The paper culminates with a discussion of select demographic dimensions of the older population in India (their size, growth, and sex composition) to better understand their demographic situation in India.

Data and Method

Scale of Work

The present study is a macro-scale study in terms of the chosen concept and spatial unit. The concept of population ageing is a macro-level concept which deals with the ageing of the entire population. The spatial unit of the study - the country of India - is a macro-scale unit. The study attempts to see the trends in drivers of population ageing and the demographic situation of older adults at the national scale.

Sources of Data

The data for the present study is extracted from Census of India, Sample Registration System, National Sample Survey and various reports and documents from the Office of the Registrar General and Census Commissioner of India, the Central Statistics

Office: Ministry of Statistics and Programme Implementation, Central Bureau of Health Intelligence and international organisations like the United Nations and World Health Organization. Also, the research papers available on the internet are referred for the study. Among various datasets, the World Population Prospects, 2019 by the United Nations is the most relevant data which is found particularly useful. A detailed list of the data tables and reports used for is provided in Table 1.

Moreover, the data relating to the crude birth and death rates, and life expectancy for the years 1901 to 2011 are compiled from multiple sources because the national level survey system responsible for providing data on fertility and mortality indicators, i.e., the Sample Registration System, started providing regular estimates only from the year 1971. So, for the current year (i.e. 2020) the data from the United Nations' projections is utilised. However, future trends for some demographic variables are discussed depending on the purpose and availability of the data.

Results and Discussion

Linking Demographic Transition and Population Ageing

Population ageing is linked to the demographic transition. The demographic transition is a mechanism that drives a society from a demographic system, marked by an initial phase of high fertility rates and mortality rates, to a phase denoted by lower fertility and mortality rates. During this transformation the age structure is put through various influences, and it changes accordingly. The change in age structure, as a society experiences demographic transition, denotes that the population is ageing. Therefore, to have an insight into population ageing in India, it is imperative to first understand the demographic history of the country and then the trends in fertility, mortality and life expectancy, and their effect on its population growth and age structure. These findings would illustrate how India is moving towards an ageing future.

Demographic History of India

The demographic background of India as summarised in Table 2 helps in visualising how the fertility rates and mortality rates interplayed through time which aids in understanding the population growth patterns, change in age structure, and how India is transforming demographically. In India we see that both fertility and mortality were initially very high, which nullified each other resulting in a period of low population growth. Later, between 1921 and 1951, the growth was steady as fertility remained high, whereas the mortality rate witnessed a sharp decline. Further, between 1951 and 1981, there was a spurt in the growth as the mortality fell substantially, and fertility experienced just the initial decline. It was between 1981 and 2011, the growth of the population in India witnessed a noticeable decline as mortality was at the lowest and the trend of decline in fertility was established.

Table 1: Sources of population data, India

Agency	Data source	Type of data extracted
Office of the Registrar General and Census Commissioner of India	Demographic Transition in India	Demographic history of India
	Compendium of India's Fertility and Mortality Indicators, 1971 – 2013, Sample Registration System	Crude birth rate and crude death rate (1971-2011)
	SRS based Abridged Life Tables 2013-17	Life expectancy at birth (1970-2015)
	Primary Census Abstract, 2011: A-2 data table - Decadal Variation in Population Since 1901	Decadal population growth in absolute numbers (1901-2011)
	SRS Statistical Report, 2018	Crude birth rate, crude death rate, infant mortality rate, total fertility rate (1971 and 2018)
	C-6 table from Census of India, 1991 and C-14 Tables from Census of India, 2001 and 2011	Age composition of the population (1991, 2000 and 2011)
	Population Projections for India and States 2011-2036	Projection of age composition of the population (year 2036)
	Census of India (1951-2011)	Size, share, decadal growth rate and sex ratio of the older population (1951/61-2011)
Indian Statistical Institute	National Sample Survey, 14th round, July 1958-July 1959, number 48	Crude birth rate and crude death rate (1901-1961)
Central Bureau of Health Intelligence	Health Information of India, 2000-2001	Life expectancy at birth (1901-1961)
Central Statistics Office: Ministry of Statistics and Programme Implementation, India	Elderly in India, 2016	Size, share, decadal growth rate and sex ratio of the older population (1951/61-2011)
United Nations, Department of Economic and Social Affairs, Population Division	World Population Prospects 2019, Volume II: Demographic Profiles	Crude birth rate, crude death rate, life expectancy at birth, total population (2020)

Source: *Prepared by the authors.*

Table 2: Demographic history of India

Till 1921	• High fertility and equally high mortality • Period of low and uncertain population growth
Between 1921 and 1951	• Fertility remained high, and mortality experienced a sharp decline • The steady growth of population
Between 1951 and 1981	• The initial decline in fertility and a substantial fall in mortality • The unprecedented growth of population
Between 1981 and 2011	• Fertility decline got established and mortality at the lowest level • A sharp decline in India's growth rate of population

Source: *Demographic Transition in India: a report by the Census of India (Office of the Registrar General of India, 2014).*

Fertility, Mortality and Life Expectancy: Trends and Effect

A perusal of the trends in birth and death rates reveals that India has witnessed a substantial decrease in crude birth rate and the total fertility rate. Crude birth rate suffered a decline from 49.2 per thousand in 1911 to 21.8 per thousand in 2011 (Figure 1). Also, this trend is likely to be maintained as the projections for 2020 reveal that the birth rates have dropped to a further low of 18 per thousand(United Nations, Department of Economic and Social Affairs, 2019).Similarly, the total fertility rate declined from 5.2 children per woman in 1971 to 2.7 children in 2011. The reduced fertility is attributed to the use of contraceptives, family planning measures, and socio-economic awakening among the people. Initially, the effect of fertility changes on the ageing of the population may not be apparent. But a slow and steady fall in fertility (as reflected in decline in crude birth rate and total fertility rate) is noticeable in the newer birth cohorts, which shrinks as compared to the preceding birth cohorts. Therefore, reduction in fertility narrows the size of the youngest age groups compared to that of the older age groups.

Moreover, a continuous fall in death rate ever since 1921 (Figure 1) because of improving conditions of food supply and medical services led to a substantial increase in the total population of the country. Due to advancement in the medical and socio-economic levels and a substantial decline in mortality, life expectancy has increased. A remarkably low death rate of 7.1 per thousand was recorded in India in 2011, which was less than the death rates of many developed countries like Japan, the United Kingdom, Sweden, Germany, the United States of America (though due to a large proportion of aged population). However, an increasing trend in crude death rate is expected of India as well due to expected rise in ageing of population, as a slight increase in death rate to 7.2 per thousand was projected for the year 2020. In India, the life expectancy took a significant leap from 23.8 years in 1901 to 68.3 years in 2011-2015 (Figure 2) with 23.63 years for males and 23.96 for females in 1901 to 66.9 years for males and 70 years for females in 2011-2015. The latest value of 69.3 years for the year 2020 indicates that the upward trend of life expectancy is likely to continue.

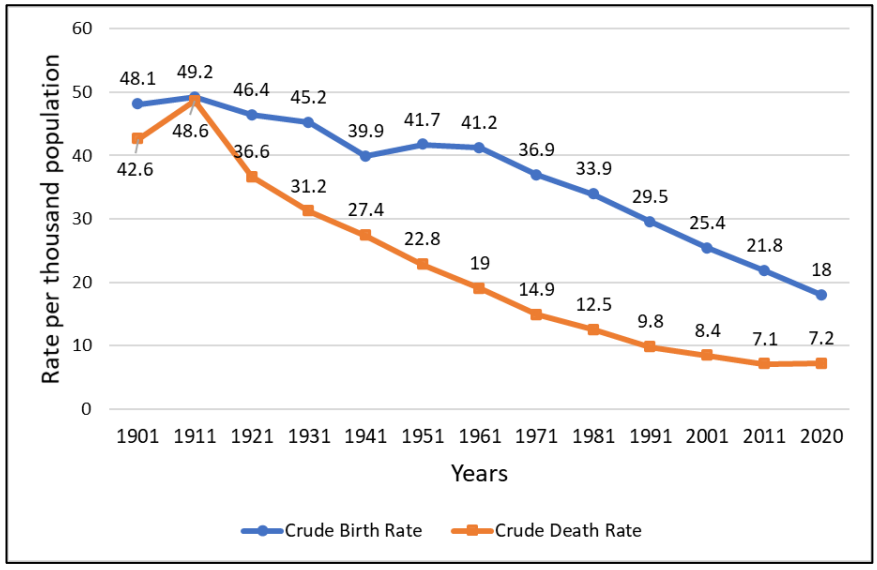

Figure 1: Trends in crude birth rate and crude death rate, India, 1911-2020

Sources*: National Sample Survey, 14th round, July 1958-July 1959, number 48 (Indian Statistical Institute, 1961); Compendium of India's Fertility and Mortality Indicators, 1971 – 2013, Sample Registration System (Office of the Registrar General & Census Commissioner of India, 2013); World Population Prospects 2019, Volume II: Demographic Profiles (United Nations, Department of Economic and Social Affairs, 2019).*

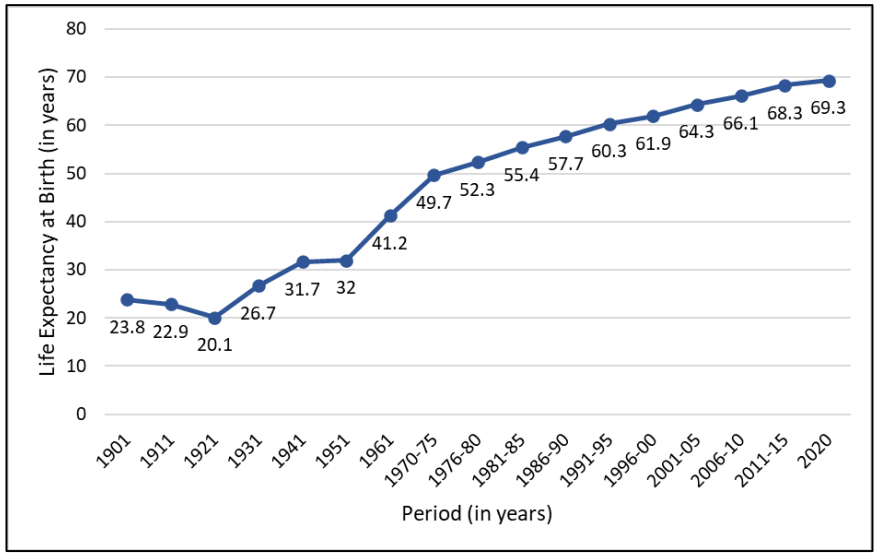

Figure 2: Trends in life expectancy at birth (in years), India, 1901-2020

Sources*: Health Information of India, 2000-2001; SRS based Abridged Life Tables 2013-17 (Central Bureau of Health Intelligence, n.d.; Office of the Registrar General & Census Commissioner of India, 2019); World Population Prospects 2019, Volume II: Demographic Profiles (United Nations, Department of Economic and Social Affairs, 2019).*

A slow decline in fertility, a rapid decline in mortality and an increase in life expectancy led to an enormous growth of population (Figure 3). Given the further expected lower values of mortality rate and an increase in life expectancy in the offing, what India needs today for the full realisation of demographic transformation is further fall in fertility which may lead to accelerated ageing.

It is important to mention here that with a chequered demographic history, trends in fertility, mortality and life expectancy have left a considerable effect on population growth in the country. A huge total of 1.21 billion in 2011 was accumulated in about 110 years as the country started with a population of 238 million in 1901 (Figure 3). In its documented demographic history, each successive census of the country, before the 2011 census (except the decade 1911-1921), registered an increase in absolute numbers – always higher than the increase in the immediately preceding census. In the 2011 census, for the first time in the demographic history of the country, the increase in absolute numbers was smaller than the increase in the immediately preceding census. During 1991-2001 a total of 182.3 million had been added but the decade that followed 2001-2011 –only 181.5 million people were added. The slight decline in absolute numbers in the year 2011 is a welcome change, though the population of India has increased more than 5-folds since the beginning of the 20th century. Additionally, the population of India was expected to reach an ever so big number of 1.38 billion in 2020 as per the United Nations projections.

Table 3. Demographic achievements of India (1971 to 2020)

Demographic drivers of population ageing	1971	2020	Trend
Crude birth rate	36.9 per thousand	18 per thousand	Downward
Crude death rate	14.9 per thousand	7.2 per thousand	Downward
Infant mortality rate	129 per 1000 live births	32 per 1000 live births	Downward
Total fertility rate	5.2 children per woman	2.24 children per woman	Downward
Life expectancy	32 years	69.3 years	Upward

Sources: *SRS based Abridged Life Tables 2013-17; SRS Statistical Report, 2018 (Office of the Registrar General and Census Commissioner of India 2019, 2020); World Population Prospects 2019, Volume II: Demographic Profiles (United Nations, Department of Economic and Social Affairs 2019).*

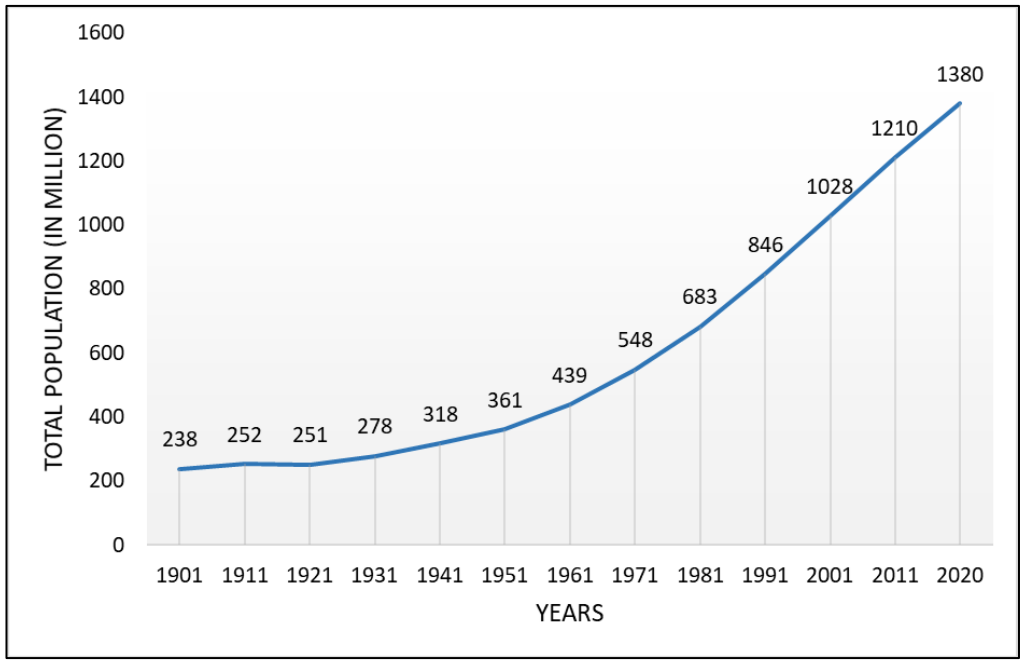

Figure 3: Trends in growth of total population in absolute numbers, India, 1901-2020

Source: *Census of India, 2011 (Office of the Registrar General & Census Commissioner of India, 2011); World Population Prospects 2019, Volume II: Demographic Profiles (United Nations, Department of Economic and Social Affairs, 2019).*

Changing Age Structure: Narrating Population Ageing

India's demographic transition not only resulted in explosive population growth; but also led to a dramatic change in the structure of its population. Such a demographic change reflects a complicated interplay of alterations in mortality and fertility. Firstly, due to considerable improvement in child survival as evident from the substantial decline in infant mortality rate and below five child mortality rate, the size of young cohorts increased. Secondly, large-sized young cohorts moved into adulthood overtime. Thirdly, owing to substantial fertility decline during the second stage of the demographic transition, relative size of young cohorts declined.

It means that the initial large size of age group 0-14, because of high fertility, dominated in India's age structure in 1971-1991. By 2011, the size of the 'less than 15' age group declined because of decline in the crude birth rate and total fertility rate, and thus the share of the reproductive and working-age group (15-59) swelled and constituted a much larger share of the population (Figure 4). The proportion of reproductive and working age-group population attained the largest ever proportion of about 62.7 per cent in 2011 in the demographic history of the country. The percentage is likely to increase to 65.1 per cent in the year 2036. This is rightly termed as "demographic dividend" or "window of demographic

opportunity." The increasing share of older population with time and its implication are, however, not to be overlooked (Figure 4).

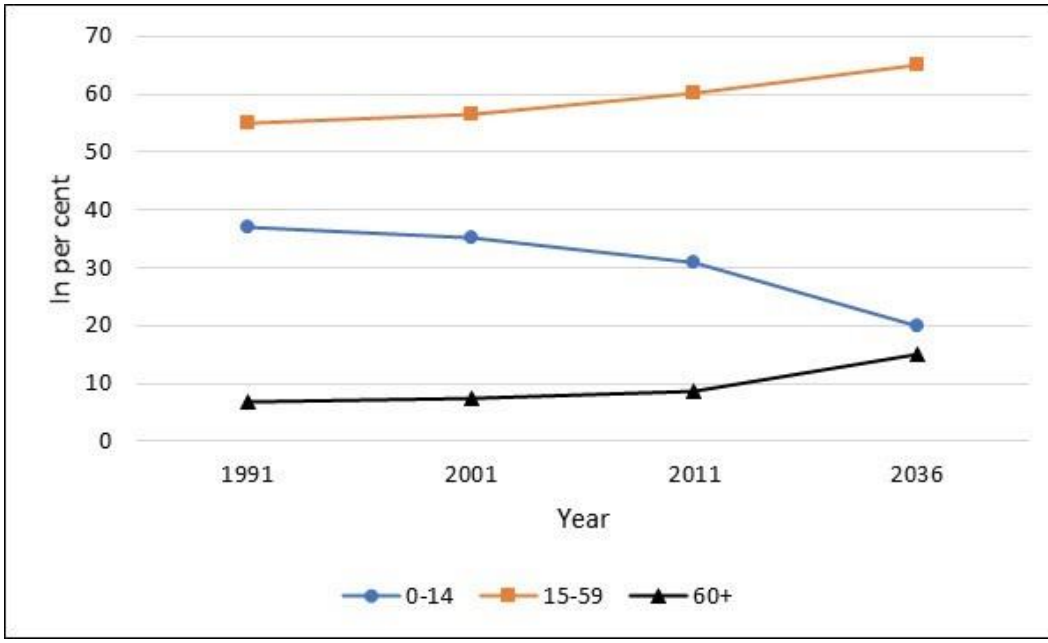

Figure 4: Trends in age-specific population, India, 1991-2036

Sources**:** *Census of India, 1991, 2001, 2011 (C6 and C14 Tables); Population Projections for India and States 2011 – 2036 (Technical Group on Population Projections: Census of India 2011, 2019).*

To further elucidate the age-sex structure of population, a graphical method of population pyramids can be effective, wherein younger populations are represented by a pyramid with a broad base and narrow peak. On the other hand, older populations are shown by a 'pillar/column-like' shape representing a more or less even distribution of population in all the age groups. When the shift from pyramids to pillars/columns occurs, the ratio of older age groups to the preceding younger cohorts rises, so the population shifts from a youthful to an older one. As the trends in fertility and mortality unfolded through the demographic history of India, the population pyramids transitioned from pyramid-like in the 1960s (with a broad base of children and a peak of older people) to the one with bulge at the middle in 2011 (with a shrunk base and a bulging middle). Due to fall in fertility and a subsequent decline in relative size of young cohorts make the cohorts shift into adulthood which results in bulging at the middle. Moreover, the transformation from pyramids to pole-like is predicted by the mid of the 21st century, when the population pyramid would get flattened at the top (Figure 5). By the turn of the next century, it is likely to acquire the form of inverted pyramids. So there would be very little population growth at the bottom of the pyramid and rapid growth of the aged population at the top. Graphically, it is evident that the age structure has started shifting towards older age cohorts (Figure 5).

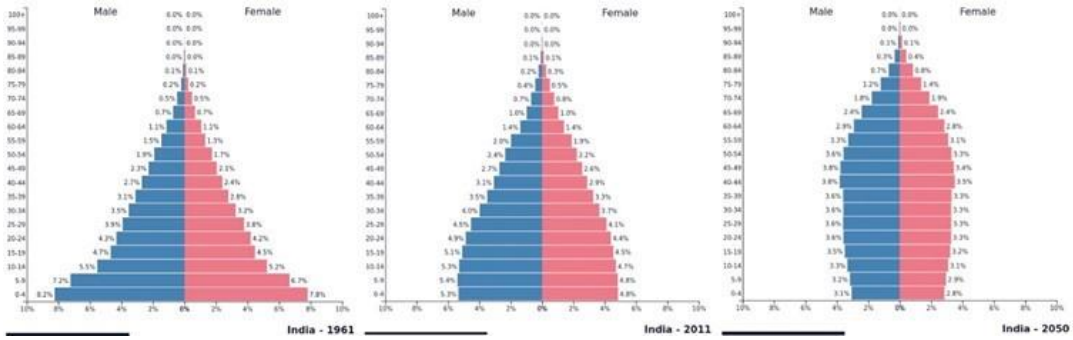

Figure 5: Population pyramids, India (years - 1961, 2011, 2050)

Source*: Population Pyramid.net (Population Pyramids of the World from 1950 to 2100, 2019).*

Therefore, India's population is ageing in two ways. F Firstly, as a result of reduced fertility (5.2 children per woman in 1971 which declined to 2.7 children in 2011) the proportion of 0-4 age group population declined which led to slower growth at the base of population pyramid. Secondly, reduced mortality and enhanced life expectancy increased the size of population pyramid at the top**.** The overall result of the demographic transition and related demographic achievements is that India supported more than 100 million people aged '60 and above' as of 2011, which formed more than 8 per cent of the total population. Indeed, the demographic transition in India indicates an ageing demographic future as we see how the trends in fertility, mortality have been declining, and life expectancy has been increasing – all demographic variables in place to drive population ageing. The resultant onset of decline in absolute numbers of persons and change in age structure from pyramids to columns are also in line with the concept of population ageing. This is exactly how the demographic statistics become drivers of ageing population.

At this conjuncture, it becomes crucial to look closely at the ageing population in India. For this, the paper proposes to study select demographic dimensions of the elderly to better understand their demographic situation..

Large Size of Aged Population

India has the second largest aged population in the world next to China. In 2011, there were 103.8 million people whose age was 60 years or above. Moreover, India's aged population is increasing both in absolute numbers as well as in terms of proportion to the total population. Looking at the older population in India in terms of absolute numbers: at the beginning of the twentieth century, there were 12 million older people; this figure rose to 24.7 million by the year 1961; it further climbed to 77 million in 2001. The population statistics released by the 2011 census revealed that the country had nearly 104 million older population. There has been a gradual rise in number of the older population through the decades, and it is expected to reach 319 million by 2050(International Institute for Population Sciences (IIPS) et al., 2020). There is also a stark difference in the rural-urban distribution of the older population in India – about 73 million aged people were living in

rural areas as compared to 30.6 million in urban areas in 2011. Moreover, there were more elderly females than elderly males in 2011; however, it has not always been like this. The entire previous census recorded a greater number of males than females except for the year 2001 when this trend reversed.

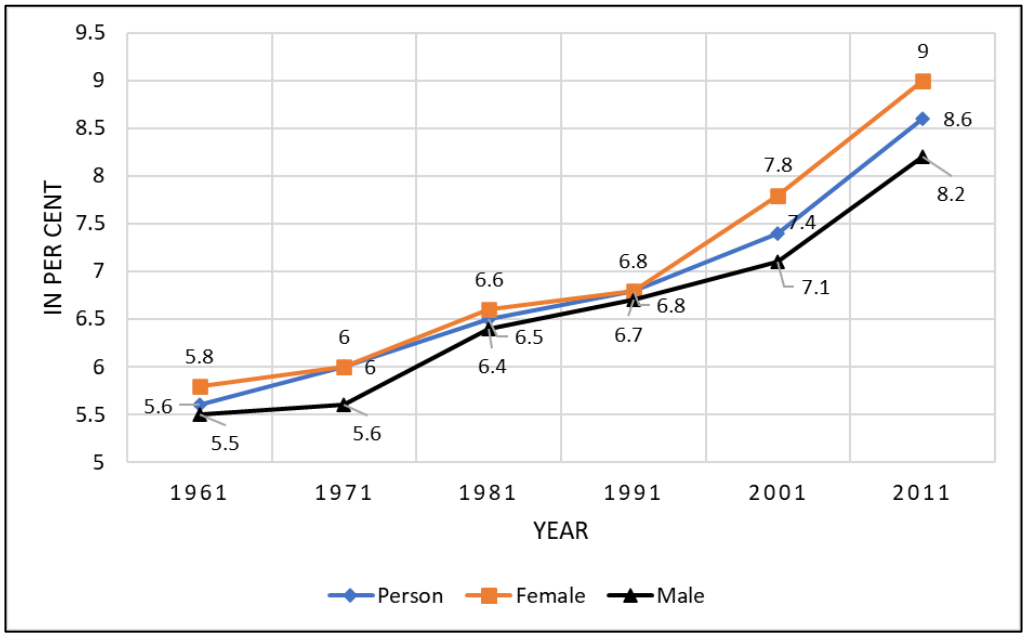

Figure 6: Share of older population by sex in total population (in per cent), India, 1961-2011

Sources: *Census of India (1951-1961); Central Statistics Office: Ministry of Statistics and Programme Implementation, India, 2016.*

Besides the increase in absolute number, the per cent share of older people in the total population has also witnessed an upward trend since 1961 (Figure 6). Their proportion to the total population has increased from 5.6 per cent in 1961 to 8.6 per cent in 2011, and it is projected to rise 11.4 per cent in 2025 and 19.5 per cent in 2050 (International Institute for Population Sciences (IIPS) et al., 2020).The proportion of aged females was higher (9 per cent) as compared to their male (8.2 per cent) counterparts in 2011. Also, in 2011, the proportion of the aged population in rural areas was higher (8.8 per cent) than urban areas (8.1 per cent), attributable to a general trend of out-migration of young population from rural areas which introduces age-structure imbalances (Kundu & Saraswati, 2012). Further, the gap in the proportion of older females to the total population and proportion of older males to the total population is widening (Figure 6). Whereas, the difference between per cent share of the older population of the urban in total population and per cent share of the older population of the rural in the total population is narrowing (Figure 7). Certainly, population ageing has emerged as a phenomenal issue in India.

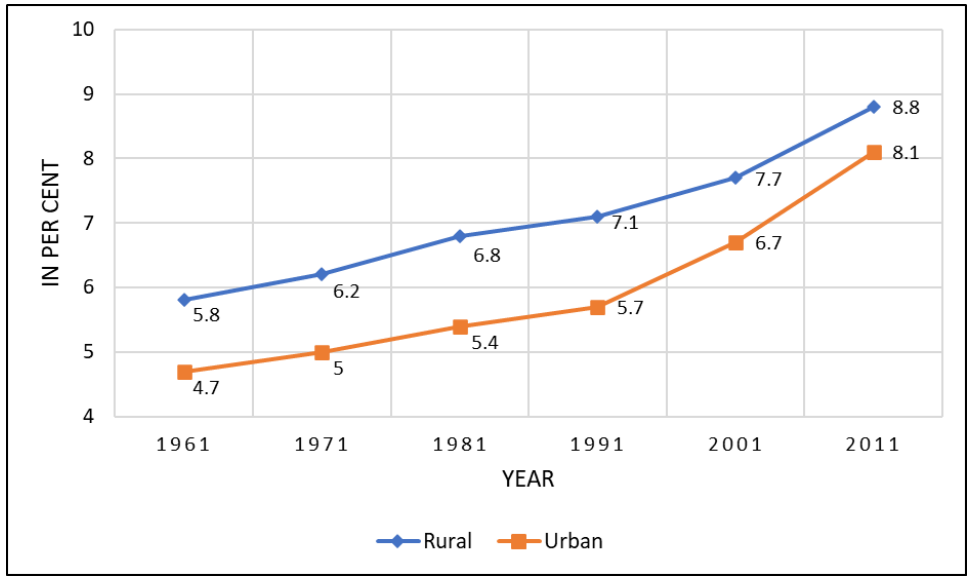

Figure 7: Share of older population by residence in total population (in per cent), India, 1961-2011

Sources: *Census of India (1951-1961); Central Statistics Office: Ministry of Statistics and Programme Implementation, India, 2016.*

A distinctive feature of India's aged population is a higher degree of unevenness in its distribution in different states. Amongst various Indian states, Uttar Pradesh had the largest chunk of the aged population (14.9 per cent to total aged population) in the country. Maharashtra, Andhra Pradesh, West Bengal, Bihar, Tamil Nadu, Karnataka, Madhya Pradesh, Rajasthan, Gujarat, Kerala, Odisha, and Punjab altogether contributed about three-fourths (72 per cent) of the aged population in the country. A large number of small states, such as Goa, Meghalaya, Nagaland, Mizoram, Arunachal Pradesh, Sikkim, and all the union territories contributed less than 2 per cent of the aged population.By comparison, all the union territories, except Puducherry, had a lower proportion of the aged population than the national average. As per the 2011 Census, all these centrally governed territories were generally highly urbanized territories, and urban areas attracted migrants of working age-group at a large scale.

Growth of Aged Population

The rapid growth of the aged population was observed for the decade 2001-2011 when their growth rate escalated to 35.5 per cent from 25.2 per cent in the previous decade of 1991-2001. While for the total population, the decadal growth rate declined from 21.5 per cent to 17.7 per cent for the same period. Also, the decade 2001-11 saw a huge leap when compared to the growth rate of older people in the previous three decades (1971-1981,

1981-1991, 1991-2001) as the growth rate experienced a downward trend during these years (Figure 8).

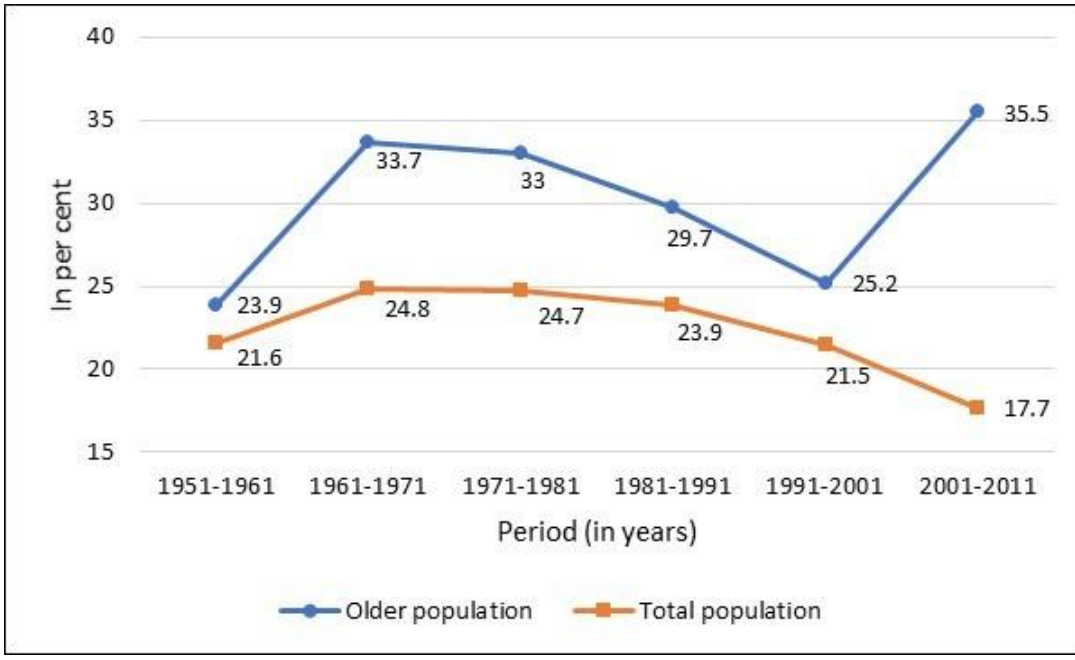

Figure 8: Decadal growth rate of older population and total population (in per cent), India, 1951-2011

Sources: *Census of India (1951-1961); Central Statistics Office: Ministry of Statistics and Programme Implementation, India, 2016*.

The reason for such a huge trend-reversal jump in the growth of the older population as opposed to the declining growth of the total population during the decade 2001-11 seems to correspond with the trends in fertility and mortality of the total population. As discussed in the demographic history of India (Table 2), between 1981 and 2011, declining trend in fertility was established and the mortality reached the lowest level,; so India's growth rate of population witnessed a sharp decline. Consequently, the fall in fertility shrunk the size of the youngest age group and increased the proportion of the older age group. The reduced mortality increased the life expectancy. Hence the growth of the older population experienced a spurt during 2001-11, whereas the growth of general population declined.

The annual growth rate of the aged population was also higher (3 per cent) as compared to the growth rate of the total population (1.9 per cent) in 2011. And the fastest-growing group is the "oldest old" (above 80 years of age) as their number is increasing at an unprecedented higher rate of 4.2 per cent per annum. The population projections show that by 2050, the elderly population in India will surpass the population of children below 14 years.

One significant feature of India's growth of the aged population was that there continued to be a contrast between the growth of the older population in urban and rural areas. While there was an increase in the growth rate of the aged population in urban areas from 54.6 per cent in 1991-2001 to 59.3 per cent during 2001-2011, the corresponding figure for rural areas declined to 27.6 per cent from 29.7 per cent. It was because of the age-selective out-migration from rural areas and significant improvement in health facilities which led to increased life expectancy, particularly in urban areas.

The rapidly increasing size of the aged population will not only affect the age structure of India's population by the next few decades but also cause strain on the resources and environment. Hence, adequate savings and infrastructure is needed to have a decent lifestyle for the aged people.

Sex Composition of Aged Population

Although the Indian population, like that of other developing countries, continued to suffer from a considerable paucity of females in general, yet the number of aged females remained higher as against their male counterparts throughout the first half of the 20th century. However, in the second half of the 20th century until the 1991 census, the number of aged females was lower than their male counterparts. It was during the inter-censual period of 1991-2001 that the number of aged females, as compared to their male counterparts, started to increase again.

According to the recent census of 2011, the sex ratio of the aged population of the country, as a whole, was recorded as 1033 females per 1000 males. It was the result of a higher life expectancy of females (63.9 years) than males (62.7 years). Moreover, the sex ratio of the aged population was relatively higher than the general population (Figure 9). The figure was 933 for the general population.

The sex ratio of elderly population in favour of females can be attributed to the higher life expectancy of females at birth as well as at the age of 60 years. However, viewed in its regional perspective, the sex ratio of India's aged population varied from one part of the country to the other. Among the states, Kerala was on the top with a sex ratio of 1226 females for every 1000 males in the country, At the other end of the scale, Sikkim recorded the lowest sex ratio of only 813 aged females per 1000 males. As far as the union territories were concerned, Daman and Diu was characterised with a sex ratio of 1331 females per 1000 males, which was the highest among the centrally administered territories and the states. However, Andaman and Nicobar Islands, recorded the lowest.

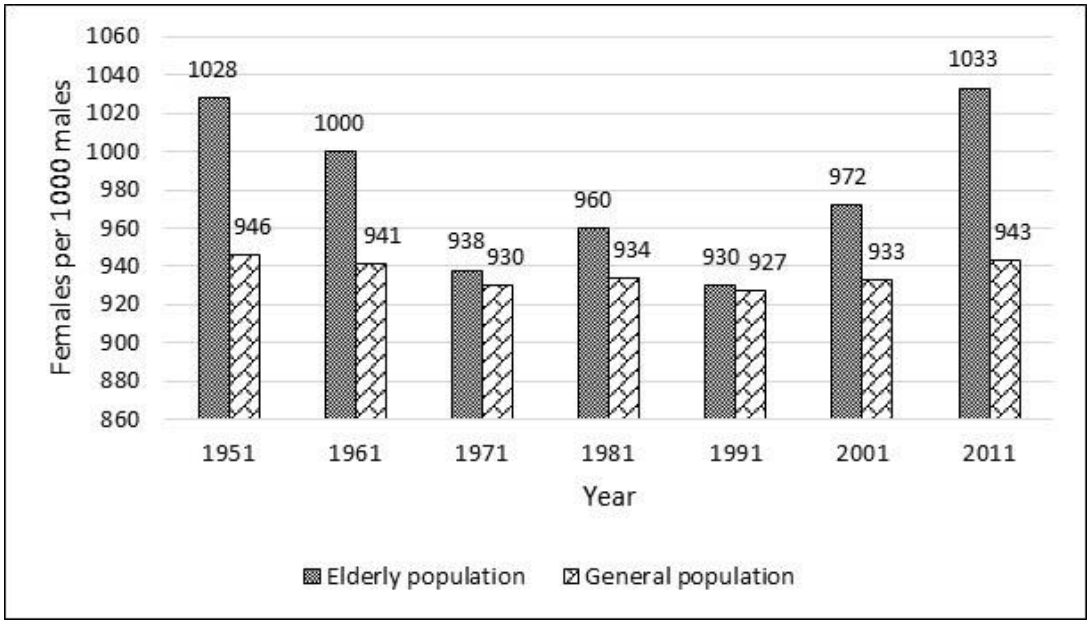

Figure 9: Trends in sex ratio for the elderly and general population, India, 1951-2011

Sources: *Census of India (1951-1961); Central Statistics Office: Ministry of Statistics and Programme Implementation, India, 2016.*

Conclusion

By tracing the declining trends in fertility and mortality in India along with their effects on population growth and change in age-structure, it is evident that the demographic future of India is ageing. The window of demographic opportunity in terms of demographic dividend is now wide open to be harnessed, but over the time, the current bulge in the working and reproductive age group is likely to shift upwards towards older age cohorts which then would pose serious challenges. Moreover, the size, share, and growth of older population in India is already following an upward trend. Considering all these in unison, it is apparent that the population ageing is an emerging as well as a pressing issue in India which needs an immediate attention. Also, preparing socially, economically, and medically for an ageing future must become a priority of the political, social and scientific institutions in the country.

References

1. Golini, A. (2002). Teaching demography of aging. *Genus*, *58*(3–4), 135–163. https://www.jstor.org/stable/pdf/29788740.pdf?refreqid=excelsior%3A97715328e0164a934e3cd1c168bf3b05
2. International Institute for Population Sciences (IIPS), National Programme for Health

Care of Elderly, (NPHCE), MoHFW, Harvard T. H. Chan School of Public Health (HSPH), & the University of Southern California (USC). (2020). *Longitudinal Ageing Study in India (LASI) Wave 1, 2017-18, India Report*. https://www.iipsindia.ac.in/sites/default/files/LASI_India_Report_2020_compressed.pdf

3. Kundu, A., & Saraswati, L. R. (2012). Migration and Exclusionary Urbanisation in India. *Economic and Political Weekly*, *47*(26–27), 219–227. https://www.epw.in/journal/2012/26-27/special-articles/migration-and-exclusionary-urbanisation-india.html
4. Prakash, I. J. (1999). *Ageing in India*. https://apps.who.int/iris/bitstream/handle/10665/65965/WHO_HSC_AHE_99.2.pdf;jsessionid=7788C3ABD3EF1778DB0898E9E55766BF?sequence=1
5. United Nations, Department of Economic and Social Affairs, D. F. I. S. D. (2002). *Political Declaration and Madrid International Plan of Action on Ageing*. http://www.un.org/esa/socdev/documents/ageing/MIPAA/political-declaration-en.pdf
6. United Nations, Department of Economic and Social Affairs, Population Division (2019). *World Population Prospects 2019, Volume II: Demographic Profiles (ST/ESA/SER.A/427)*. https://population.un.org/wpp/Publications/Files/WPP2019_Volume-II-Demographic-Profiles.pdf
7. United Nations: General Assembly. (1991). *United Nations Principles for Older Persons*. https://www.ohchr.org/Documents/ProfessionalInterest/olderpersons.pdf
8. United Nations. (1982). *Report of the World Assembly on Aging, Vienna, 26 July to 6 August 1982*. https://www.un.org/esa/socdev/ageing/documents/Resources/VIPEE-English.pdf
9. United Nations. (2002). *Report of the Second World Assembly on Ageing*. https://undocs.org/A/CONF.197/9
10. United Nations Department of Economic and Social Affairs. (2020). *World Population Ageing 2019 (ST/ESA/SER.A/444)*.
11. United Nations Population Fund, & HelpAge International. (2012). *Ageing in the Twenty-First Century: A Celebration and A Challenge*. https://www.unfpa.org/sites/default/files/pub-pdf/Ageing report.pdf

The Indian Geographical Journal
Volume 96 (1) June - 2021, pp 31-44
ISSN 0019-4824

VULNERABILITY OF STREET VENDORS IN AIZAWL CITY, INDIA

Lalnghakmawia Thangluah and Benjamin L. Saitluanga

Dept. of Geography and Resource Management, Mizoram University
E-mail: nghaka1230@gmail.com, bena.sailo@gmail.com

Abstract

Street vending is one of the most visible informal occupations and a notable source of income for the urban poor. Contrary to what is projected in urban planning models, informal sector proliferates in cities of the Global South due to the combined processes of increasing urbanisation and globalisation. The present paper is an attempt to measure spatial vulnerability of street vendors in Aizawl City where street vendors work under diversified legal and socio-environmental conditions. By using simple random sampling method, 400 street vendors from five prominent street markets were interviewed through scheduled questionnaire. Vendors' Vulnerability Index (VVI) was developed with the help of 14 indicators which are categorized under three broad dimensions - socio-economic, occupational and environmental dimensions. The analysis of data shows that the socio-economic condition of street vendors and the environmental quality of street markets varies spatially and, low level of vulnerability is highly interlinked with presence of proper regulation and provision of basic infrastructures. The second part of the study examines how street vendors in the city negotiated and adapted to remain in the informal sector and, lastly, it appraises the role of the local government and communities in the process of regulation of street vending for livelihood protection of street vendors.

Keywords: Street vending, Vulnerability Index, Spatial Analysis, Aizawl, Mizoram

1. Introduction

The urban economy in the Global South is characterised by predominance of an informal sector (Martinez et al., 2017; Martinez et al, 2018; Ojeda &Pino, 2019). Although there is no reliable information for most of the countries, it is estimated that the informal sector accounts for more than half of total employment in the Global South (Vanek et al., 2014). Contrary to what is projected in urban planning models, informal sector proliferates in less developed cities due to the combined processes of increasing urbanisation and globalisation mainly due to privatisation, lowering production cost and increasing competition which often resulted in unemployment for low and un-skilled workers (Gauvain, 2007; Bhowmick, 2005; Kiaka et al., 2020).

Street vending is one of the most visible informal occupations and a notable source of income for the urban poor (Roever & Skinner, 2016; Martinez et al., 2018). It is either

"mobile or space-bound, predominantly urban economic activity" (Graaff and Ha, 2015:2) that takes place on sidewalks, parks, intersections, leftover spaces and privately owned spaces such as outdoor shopping malls (Cupers, 2015). Also known as street trading or hawking, it is considered as one of the most vulnerable occupations due to absence of regulation, social acceptance, provision of infrastructure, low profit and difficulty in access to resources (Chen, 2012;). In spite of negative perceptions from shopkeepers, local communities and municipal authorities, it remains a structural feature of cities due to lack of opportunities in the formal sector. As a free entry segment which does not require financial capital in the two-fold classification of informal sector (see Fields, 1990), less educated and poorer migrants see street as an economic space that provides opportunities to carry out business (Williams, 2010). A strong representation of low skilled rural-urban migrants as well as skilled unemployed who were terminated from the formal sector due to economic restructuring is observed among street vendors in cities of the Global South (Bhowmik, 2005; Turner & Schoenberger, 2012).

Street markets are diversified and spatial difference in environmental conditions of vending places as well as income and quality of life of vendors are observed (Martinez et al. 2018). The profitability of street vending is determined by location of vending and length of occupancy (Cohen et al., 2000; Sales, 2018). Generally, street vendor prefers to occupy vacant spaces nearby prime locations including city centres, traffic intersections and entrances of shopping centers and stations (Kamalipour and Peimani, 2019). There is a competition for good location in every market among street vendors. Having a good space for vending is one of the significant factors that affect the income of street vendors (Cohen et al., 2000). In Hanoi, stationary or fixed stalls are dominated by long-term city residents of the city while mobile or itinerant vendors most belong to recent migrants (Turner & Schoenberger, 2012). Maintaining a consistent presence in almost exactly the same market spot is a critical component of business practice within the industry. Even though different spots in a market may be only a few meters apart, many vendors insist on staying in one place (Lauermann, 2013). In Mumbai, good spots are controlled by long time vendors who even 'sublet' to other vendors while less favourable isolated spots are occupied by more vulnerable groups like migrants, lower caste, women and elderly (Sales, 2018).

Assessment of level of vulnerability of street vendors has been conducted by a few scholars (see Esayas and Mulugeta, 2020). However, previous studies have neglected the spatial dimension of vulnerability. In this paper, an attempt has been made to analyse the spatial vulnerability of street vendors in Aizawl City by using vulnerability index. Measurement of spatial variation in vulnerability of informal street vendors is crucial for planning and implementation of the government policies pertaining to street vendors. The study also discusses how street vendors in the city negotiated, appropriated and adapted to remain in the informal sector and, the role of the local government and communities in the process of regulation of street vending for livelihood protection of street vendors. The entire study will expand the project of better understanding of the geographies of urban informal economy in the Global South.

2. Study Area

Aizawl is the capital city of Mizoram which is located at the southern corner of the north-eastern region of India. Founded in 1894, it is one of the fastest growing hill cities in India. As per 2011 Census of India, the city has a population of 293,416 that constitute 26.89 per cent of the entire Mizoram population. Aizawl City is governed by the Aizawl Municipal Corporation (AMC). The city is divided into 19 Municipal Wards and 83 Local Councils.

In 1941, the population of Aizawl was 4780 only and massive rural-urban migration to Aizawl took place after the Independence of India in 1947. The end of strict migration control policy of the British India after the Independence, the *Rambuai* or the 20 years of armed struggle to attain Independence during 1966 – 1986 that resulted in large-scale migration into the relatively safer Aizawl town and, the unprecedented increase in job opportunities in the government sector with the attainment of Union Territory in 1972 were considered as the main reasons behind the large-scale migration into Aizawl city (Saitluanga, 2017). With recent stagnation in the growth of government jobs and limited avenues in other employment sectors, urban poverty has risen considerably. It is estimated that 6.5% of the city's urban households belong to Below Poverty Line (BPL) (Zothanmawia, 2017). Many of the poor households were absorbed in the informal sector. According to GoI (2011), street vendors alone constitute 1.29 per cent the city's population which is much higher than the average figures for Mizoram (0.92%) and India (0.65%). Besides the permanent vendors, there are non-resident weekly street vendors most of which belongs to cultivators from neighbouring villages who came to the city to sell their agricultural products on Saturday market. With the passage of the Street Vendors (Protection of Livelihood and Regulation of Street Vending) Act, 2014 by the Parliament of India, the state of Mizoram has also notified the Mizoram Street Vendors (Protection of Livelihood and Regulation of Street Vending) Rules, 2017. The implementation of the Street Vendors Rules, 2017 including the formation of Town Vending Committee was put under the AMC by the state government.

Five major market areas of Aizawl city viz. Bawngkawn, Bara Bazar, Treasury Square, Thakthing and Vaivakawn were selected for the present study (see Fig. 1 & Fig.2). These markets are located at various traffic intersections of the city. Bara Bazar is the central business district while Treasury square is not essentially a traditional *bazaar* type market but a specially designated street vending market due to the presence of government offices including Assembly secretariat, old secretariat and Aizawl District Commissioner's office.

3. Data and Method

Random sampling technique was employed to collect primary data from 400 street vendors in the five selected markets with the help of scheduled questionnaires. From the obtained data, a total of 14 indicators were selected and categorized them into three

dimensions - Socio-economic, Occupational and Environmental dimensions to measure Vendor's Vulnerability Index (VVI) (see Table 2). The selected indicators were standardized using the following equation

$$\text{Index}_{s_d} = \frac{S_h - S_{min}}{S_{max} - S_{min}}$$

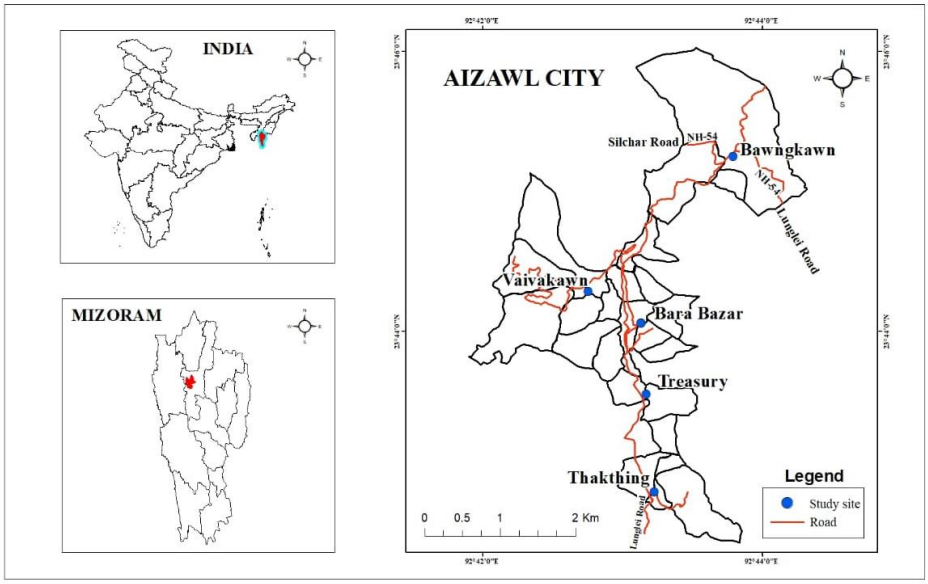

Fig. 1. The Study Area – Aizawl, Mizoram

3. Data and Method

Random sampling technique was employed to collect primary data from 400 street vendors in the five selected markets with the help of scheduled questionnaires. From the obtained data, a total of 14 indicators were selected and categorized them into three dimensions - Socio-economic, Occupational and Environmental dimensions to measure Vendor's Vulnerability Index (VVI) (see Table 2). The selected indicators were standardized using the following equation

$$\text{Index}_{s_d} = \frac{S_h - S_{min}}{S_{max} - S_{min}}$$

Where, S_{min} and S_{max} are the minimum and maximum values of each vending market. These values were used to transform the indicator into a standardized index. After each indicator was standardized, the indicators were averaged using the following formula to calculate the value of each dimension:

$$\mathbf{M_d} = \frac{\sum_{i=1}^{n} \mathbf{Index_{s_d i}}}{\mathbf{n}}$$

Where, M_d is one of the dimensions for each market and $\mathrm{Index}_{s_{di}}$ represents the standardized index for the i^{th} dimension and n is the number of each indicator in each dimension. Lastly, Vendors' Vulnerability Index of each market is obtained by the formula given below.

$$\mathrm{VVI_d} = \frac{\sum_{i=1}^{3} w_{mi} M_{di}}{\sum_{i=1}^{3} w_{m_i}}$$

Where, VVI_d is the Vendor's Vulnerability Index for a particular market, $\sum_{i=1}^{3} w_{mi} M_{di}$ is the weighted average of three dimensions while W_{mi} represents the number of total indicators. Since the concept of vulnerability bears negative connotation, the highest ranked market represents the most vulnerable market and vice versa.

Secondly, intra-market vendors' vulnerability is measured with binary-composite vulnerability index which was computed using the following formula

$$V = \frac{VI_1 + VI_2 + VI_3 + \ldots + VI_{14}}{N}$$

Where, V refers to the composite vulnerability index, $VI_{1,2,3...}$ refers to vulnerability indicators and N is the total number of indicators. Here, each vendor is assigned a binary value (0=No, Yes=1) for each indicator. Depending on the assigned values, the index score for a particular vendor lies between 0 and 1. Standard deviation method is employed to categorize vendors into five classes – not vulnerable, mildly vulnerable, vulnerable, strongly vulnerable and extremely vulnerable.

4. Results

4.1 Socio-Demographic profile of street vendors

Street vending in Aizawl is dominated by females with low level of education. Only 15 per cent of the respondents were male and 80 per cent of the total vendors have not completed High School. In Mizoram, it is a common tradition among rural students to drop out of school when they failed to pass High School board examination. The age distribution of the street vendors showed that the highest number of street vendors was found in the age group of 41-50 years (38.3%), and a few of them were found to be older than 60 years (8.2%) (see Table 1).

4.2 Levels of Vulnerability of Street Vendors

As shown in Table 2, more than half of the respondents were migrant workers from different parts of Mizoram and a few non-local population from neighbouring states and countries, particularly Assam and Myanmar. It is also observed street vending is taken up by old aged vendors who constitute 23.25 per cent of the total respondents. Majority of the street vendors were illegal vendors who did not have license or permission. Robbery and harassment are the two most common forms of social insecurity faced by the street vendors in Aizawl City. A small number of vendors had reported health related problems due to pollution and rain.

Table 1. Profile of Street Vendors in Aizawl City

Indicators		Total	Percentage
Sex	Male	61	15.25
	Female	339	84.75
Age	Less than 30 years	50	12.50
	31-40 years	104	26.00
	41-50 years	153	38.25
	51-60 years	60	15.00
	More than 60 years	33	8.25
Education	Below High School	321	81.00
	Below Higher Secondary	64	16.00
	Graduate	6	1.50
	Above Graduate	6	1.50

Source: Authors' Survey, 2019

Table 2. Selected Indicators of Vulnerability

Dimension	Indicators	Code of Indicators	Percentage (N=400)
Socio-demographic	Percentage of unmarried vendors	X1	17.3
	Percentage of vendors who have studied below High School	X2	80.3
	Percentage of vendors who have migrated from outside	X3	66.0
	Percentage of vendors who have rented a house	X4	55.3
	Percentage of vendors with income less than average income	X5	53.3
	Percentage of vendors more than 51 years	X6	23.3
	Percentage of non-local vendors	X7	5.3
Occupational	Percentage of vendors without vendor's license	X8	61.5
	Percentage of vendors with no affiliation in any association	X9	45.5
	Percentage of vendors who have faced robbery	X10	30.0
	Percentage of vendors who have faced harassment	X11	15.5
Environmental	Percentage vendors who reported problems due to street flood in vending spots	X12	38.7
	Percentage of vendors who reported health problems due to rain or pollution	X13	9.0
	Percentage of vendors who reported injury due to road traffic while vending	X14	10.7

Source: Authors' Survey, 2019

Spatial analysis of our data shows that street vendors in Bawngkawn market are the most vulnerable vendors in socio-demographic dimension (See Table 3). The reported income of vendors in Bawngkawn market is also the lowest among all the street markets. Majority of vendors were less educated, migrant and tenants. The market has also relatively higher percentage of old age vendors in comparison to other vending places. On the other hand, vendors in Treasury Square market are the least vulnerable ones. The average income of the vendors in Treasury Square is the highest among all vending markets. Again, vendors in Bawngkawn market are the most vulnerable vendors in occupational dimension. The market has the highest number of vendors who did not possess license or permission from any authority. More than two-third of the vendors were not affiliated to any kind of vending association. On the other hand, vendors in Thakthing market are the least vulnerable vendors in occupational dimension. Incidence of robbery and harassment was very low in Thakthing market. In environmental dimension, Vaivakawn market is the least ranked market. In this market, majority of the vendors were severely affected by street flood due to absence of proper drainage and, health problems like cold and fever were reportedly prevalent among the street vendors. On the other hand, vendors in Treasury Square market reported fewer problems with respect to pollution, flood and road accidents.

Table 3. Vendors' Vulnerability Index (VVI), Aizawl City

Dimension	Indicators	Bawngkawn	Bara Bazar	Treasury Square	Thakthing	Vaivakawn
Socio-demographic	X1	0.117	0.223	0.117	0.200	0.115
	X2	0.800	0.750	0.783	0.875	0.865
	X3	0.583	0.628	0.767	0.688	0.673
	X4	0.700	0.608	0.450	0.338	0.673
	X5	0.683	0.595	0.367	0.438	0.519
	X6	0.385	0.209	0.200	0.238	0.212
	X7	0.033	0.088	0.033	0.075	0.038
	M_d	**0.413**	**0.388**	**0.340**	**0.356**	**0.387**
Occupational	X8	0.450	0.412	0.000	0.300	0.308
	X9	0.700	0.345	0.583	0.313	0.558
	X10	0.233	0.412	0.250	0.175	0.308
	X11	0.050	0.230	0.117	0.075	0.231
	M_d	**0.358**	**0.350**	**0.238**	**0.216**	**0.351**
Environmental	X12	0.233	0.135	0.100	0.875	0.865
	X13	0.150	0.068	0.033	0.010	1.000
	X14	0.083	0.135	0.050	0.138	0.077
	M_d	**0.156**	**0.113**	**0.061**	**0.341**	**0.460**
VVI		**0.372**	**0.346**	**0.275**	**0.338**	**0.460**

Source: Authors' Survey, 2019

As shown in Table 4 and Figure 2, the lowest VVI is observed in Treasury Square while Vaivakawn market has the highest VVI. Treasury Square is located nearby the old central secretariat where the state government has properly reserved vending space. Most of the vendors were given license and are locally called 'hawkers' (see Fig. 3a & b). Roads are relatively wider and proper sidewalk is constructed for the pedestrians. Most of the vendors were provided roofed vending stalls or kiosks by the state government. The average income of vendors in Treasury market was also relatively higher than those in other markets. On the other hand, our analysis shows that vendors in Vaivakawn market were the most vulnerable vendors in the city. This market stretches along one of the busiest intersections in Aizawl city. The market has no proper sidewalk and the busy roads leave inadequate space for vendors. Besides, the catchment area of the market mainly includes the less developed and peripheral parts of the city.

Table 4. Classification of Vending Market based on Vendors' Vulnerability Index (VVI), Aizawl City

Class	Range of Vulnerability	Market
Weakly Vulnerable	0 - 0.29	Treasury Square
Mildly Vulnerable	0.30 - 0.32	
Vulnerable	0.33 - 0.39	Thakthing, Bara Bazar, Bawngkawn
Strongly Vulnerable	0.40 - 0.43	
Extremely Vulnerable	0.44 - 0.46	Vaivakawn

Source: Authors' Survey, 2019

4.3 Intra-market Vulnerability

Variation in vulnerability is not confined only at inter-market level. Intra-market analysis of vulnerability shows that significant variation is observed among street vendors in different markets of the city. Table 5 shows that Treasury Square which has the lowest VVI has the least percentage of vendors under 'extremely vulnerable' and the highest percentage of vendors under 'weakly vulnerable' category. On the other hand, Vaivakawn market has the highest percentage of 'extremely vulnerable' and 'strongly vulnerable' vendors. Bawngkawn market is another vending area where relatively large percentage of more vulnerable street vendors is found.

5. Discussion

Spatial disparity in vulnerability of street vendors in Aizawl City is related to variations in availability of vending spot and institutional management of vendors. The state government has earmarked vending spots and freely distributed vending stalls to licensed hawkers in and around Treasury Square market Apart from this, the state government has hardly taken up welfare measures for the street vendors. Street vendors in other markets were not given permission by the state government but were recognised by the local community councils. These vending markets are usually crowded without leftover spaces for vending activities.

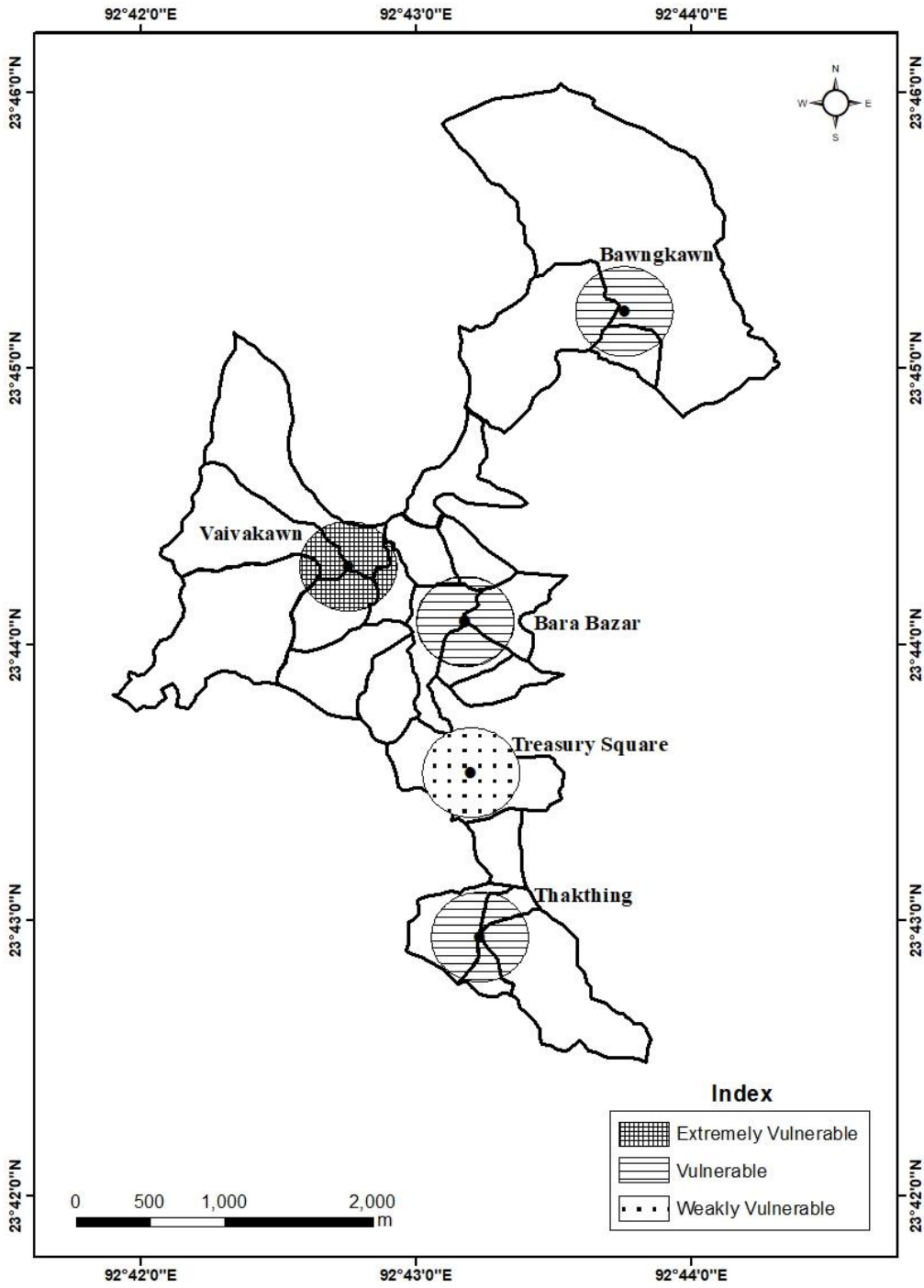

Fig. 2. Vendor's Vulnerability Index (VVI), Aizawl, Mizoram

Table 5. Vulnerability Class of Street Vendors in Aizawl City

Class	Range	Bawng-kawn	Bara Bazar	Treasury Square	Thakthing	Vaiva-kawn
Weakly Vulnerable	0 - 0.19	1.67	4.73	6.67	2.50	1.92
Mildly Vulnerable	0.20 - 0.30	5.00	14.86	8.33	3.75	1.92
Vulnerable	0.31 - 0.52	66.67	62.84	68.33	77.50	59.62
Strongly Vulnerable	0.53 - 0.63	21.67	16.89	16.67	13.75	30.77
Extremely Vulnerable	0.64 - 0.74	5.00	0.68	0.00	2.50	5.77

Source: Authors' Survey, 2019

In the absence of proper regulation from the state government, local communities have actively involved in regulating street vendors within their neighbourhoods. The Local Councils (LCs) – the lowest tier of the urban local body - have been entrusted to by the municipal corporation to manage and issue license to vendors in the nearby markets. They also supervise vending arrangement of the weekly Saturday market by allocating seats and vending time for the vegetable street vendors. In some places, they alter the street traffic by turning the two-way road into one-way during the vending period to make the vending spaces more spacious. There is only one market in the city that is Bara Bazar where the street is open for vegetable vendors during weekdays. In this market, vegetable vendors are allowed to occupy the whole street in the evening. Vendors would come close to the street and when the whistle goes exactly at 5 PM, they would rush to occupy a good spot. Among them are the vendors or co-vendors having permanent seats inside the market. Knowing that the street is more profitable than inside, they changed their location by trying to maximise their incomes.

In many cities, the appropriation and modification of public space by street vendors have been negatively perceived by other stakeholders including shopkeepers, local communities and municipal authorities that often resulted in harassment of vendors (Donovan, 2008). In Aizawl city, harassment in the work place is reported by a few vendors only as street vendors negotiated to avoid conflict with shop owners by paying 'rent' to sell their items in front of the shops. By doing this, they avoid complaint and harassment from the local authorities. Unfixed or mobile vendors in Bara Bazar area carry their few products in a wooden structure so that they can move freely without paying fees to anyone. Some other vendors hang a few items, usually clothes and belts, around their necks and stand along the main roads. When they finished selling, they collect new items from the nearby shop and sell again. These kinds of arrangement enable the street vendors to avoid spatial conflict and trading competitions with other stakeholders on the market.

Fig. 3(a). Treasury Square – Street Vendors in Treasury Square have the least vulnerability in Aizawl

Fig. 3(b). Vaivakawn – Street Vendors in Vaivakawn have the highest vulnerability in Aizawl

In spite of the positive relationship between street vendors and the public, street vendors in Aizawl city are also facing a range of socio-economic and environmental problems which affected their social well-being. Vending areas are not equipped with either any form of infrastructure like garbage discharge space, clean drinking water or sanitation facilities. They are frequently disturbed by rain and flood during rainy season. Provision of street vendors with basic services in their work spaces is one of the most pressing issues to enhance the quality of life of street vendors. Jha (2018) has rightly argued that street vending has been neglected in India for a long time until the passage of the Street Vendors Act, 2014. Unlike other workers, vendors are often harassed and relocated as the public perceives street trading is associated with social disorder. The vulnerability and negative perception of street vendors may be reduced through the intervention of the state in the form of legalisation and proper regulation. However, we observed that the introduction of the Mizoram Street Vendors Rules, 2017 has little significance towards the enhancement of quality of life of street vendors in Mizoram due to poor implementation. At the same time, one of the biggest hurdles in the process of regulation of street vending is that vendors have preferred location like crowded activity centres, streets with high pedestrian flow and more visible places while rejecting locations which are better suited for provision of amenities (Kamalipour and Peimani, 2019). In a hill city like Aizawl with narrow and crowded roads, all streets along markets are not suitable and permissible for street vending. But street vendors are willing to occupy the most profitable spots and even developed collective tactics to 'own' their preferred locations.

Conclusion

Street vending is an important informal economic activity in Aizawl City. It generates not only income and employment to the urban poor but also provides goods and services to the communities. Majority of street vendors in Aizawl City are less educated, middle-aged female who have either migrated recently or a few decades ago from rural areas. They concentrate along the roads, footpaths or bus stops which are not designed for vending. Due to congestion of public spaces, the utilization of sidewalks and leftover spaces along the streets in market areas has been perceived negatively by the public. Vendors in crowded markets are more vulnerable to various dimensions of well-being. On the other hand, vendors in a designated vending site like those in Treasury Square are less vulnerable to social, occupational and environmental problems. With the introduction of the Mizoram Street Vendors Rules, 2017, the state government and the municipal corporation have been given increasing role to protect, accommodate and enhance the livelihood of the street vendors, particularly the extremely vulnerable street vendors which are found in different markets. Until now, street vendors have informally negotiated for space with other formally recognised stakeholders to avoid spatial conflicts and trading competitions. Provision of special vending sites with proper regulation would help in reduction of harassment, confiscation of vending items and livelihood enhancement of the most vulnerable sections of street vendors.

References

1. Bhowmik, S. K. (2005). Street Vendors in Asia: A Review. *Economic and Political Weekly*,40 (22/23), 2256-2264.
2. Chen, M.A. (2012). *The Informal Economy: Definitions, Theories and Policies*. Working Paper, WIEGO, 1(26), 90141-90144.
3. Cohen, M., Bhatt, M., & Horn, P. (2000). *Women Street Vendors: The Road to Recognition*, New York, NY: The Population Council.
4. Cupers, K. (2015). The urbanism of Los Angeles Vending. In K. Graaff & N. Ha (Eds.), *Street Vending in the Neoliberal City: A Global Perspective on the Practices and Politics of a Marginalized Economy* (Pp. 139-163). New York: Berghahn.
5. Donovan, M. G. (2008). Informal Cities and the Contestation of Public Space: The Case of Bogotá's Street Vendors, 1988—2003. *Urban Studies*, 45(1), 29–51.
6. Esayas, E., & Mulugeta, S. (2020). Analysis of socioeconomic vulnerability of street vendors, *Theoretical and Empirical Researches in Urban Management*, 15 (2), 49-65
7. Fields, G.S. (1990). Labor Market Modeling and the Urban Informal Sector: Theory and Evidence. In D. Turnham, B. Salomé and A. Schwarz (Eds.), *The Informal Sector Revisited* (Pp. 49–69). Paris: OECD.
8. Government of India (GoI) (2011). *Socio Economic and Caste Census 2011*. Ministry of Housing and Urban Poverty Alleviation, Government of India, New Delhi.
9. Graaff, K., & Ha, N. (2015). Introduction. In K. Graaff & N. Ha (Eds.), *Street Vending in the Neoliberal City: A Global Perspective on the Practices and Politics of a Marginalized Economy* (Pp. 1 -15). New York: Berghahn.
10. Jha, R. (2018). *Strengthening Urban India's Informal Economy: The Case of Street Vending*. Observer Research Foundation Issue Brief, 249.
11. Kamalipour, H., & Peimani, N. (2019). Negotiating Space and Visibility: Forms of Informality in Public Space. *Sustainability*, 11(17), 1-19.
12. Kiaka, R., Chikulo, S,. Sloother, S., & Hebinck, P., (2021). "The street is ours". A comparative analysis of street trading, Covid-19 and new street geographies in Harare, Zimbabwe and Kisumu, Kenya. *Food Security*, https://doi.org/10.1007/s12571-021-01162-y.
13. Lauermann, J. (2013). Practicing space: Vending practices and street markets in Sana'a Yemen. *Geoforum*, 47, 65–72.
14. Martinez, L., Short, J,. & Estrada, D. (2017). The urban informal economy: Street vendors in Cali, Colombia. *Cities*, 66, 34–43.
15. Martinez, L., Short, J,. & Estrada, D. (2018). The diversity of the street trading: A case study of street vending in Cali. *Cities*, 79, 18-25.
16. Ojeda, L., & Pino, A. (2019). Spatiality of street vendors and sociospatial disputes over public space: The case of Valparaíso, Chile. *Cities*, 95, https://doi.org/10.1016/j.cities.2019.02.005
17. Roever, S. (2014). *Informal Economy Monitoring Study Sector Report: Street Vendors*, WIEGO, Cambridge.

18. Roever, S., & Skinner, C. (2016). Street vendors and cities. *Environment and Urbanization*, 28(2), 359–374.
19. Saitluanga, B.L. (2017). *Himalayan quality of life: A study of Aizawl City*, Springer.
20. Sales, L. (2017). The Street Vendors Act and the right to public space in Mumbai. *Articulo: Journal of Urban Research*, 17-18, https://journals.openedition.org/articulo/3631 (Retrieved 12 July, 2021).
21. Turner, S., & Schoenberger, L. (2011). Street Vendor Livelihoods and Everyday Politics in Hanoi, Vietnam. *Urban Studies*, 49(5), 1027–1044.
22. Vanek, J., Chen, M.A., Carre, F., Heintz, J., & Hussmanns, R. (2014). *Statistics on the Informal Economy: Definitions, Regional Estimates and Challenges*. WIEGO Working paper 48, https://www.wiego.org/sites/default/files/publications/files/Vanek-Statistics-WIEGO-WP2.pdf (Accessed on 02 June 2021).
23. Williams, C.C. (2010). Entrepreneurship and the informal economy: an overview. *Journal of Developmental Entrepreneurship*, 15 (4), 361–378.
24. Zothanmawia, R. (2017). A study of urban poverty in Mizoram with special reference to Aizawl Municipal Corporation (AMC) area. *Senhri Journal of Multidisciplinary Studies,* 2(2), 117-141.

The Indian Geographical Journal
Volume 96 (1) June - 2021, pp 45-59
ISSN 0019-4824

AIR QUALITY ANALYSIS DURING THE FIRST LOCKDOWN OF COVID-19: A CASE STUDY OF CHENNAI METROPOLITAN AREA

Swetha S and Sulochana Shekar

Department of Geography, Central University of Tamil Nadu, Thiruvarur, India
E-mail: swethasuresh238@gmail.com, suloshekhar@gmail.com

ABSTRACT

Despite the economic crisis and the loss of human life caused by COVID-19, the first complete lockdown period had shown a positive side from an environmental perspective. This lockdown has restricted the country's vehicular and industrial activities, power plants, construction activities, biomass burning, road dust resuspension, restaurants, etc., which led to a decrease in pollution levels due to reduction in pollutant sources and emissions. The study has identified significant changes in the air quality of the Chennai Metropolitan area during the first lockdown (March-May 2020). The Sentinel-5P, MODIS, and OMI/Aura satellite datasets have been used for the analysis with the help of Google Earth Engine API and NASA's GIOVANNI tool, which indicated the decreased levels of NO2, SO2, CO, and Aerosol Optical depth in various parts of the study area. The results have been acquired by carrying out change detection analysis between the satellite data of pre- lockdown and the first- lockdown phase of the year 2020, calculating per-pixel change between them. Ground-based air quality monitoring data has been used to support the trend shown by satellite data analysis. A significant decrease in the concentration level of pollutants can be seen in the industrial regions of the city. Some pockets of the city, especially the residential areas, resulted in increasing levels of pollutants with peak concentrations during April-May 2020. To validate the results, the study also analyzed the pattern of pollutant concentrations during March to May months of three consecutive years 2019,2020 and 2021, of which 2019 was taken to be a normal year, whereas 2020 and 2021 were the years with Covid-19 restrictions showing a decreasing trend of pollution. Also, the study has identified that the northern Chennai industrial regions, including Manali, Ponneri, Ennore, and the central commercial part of the city, are the significant hotspots of pollution, which need suitable air pollution control measures considering not only the COVID-19 situation but also to help in mitigation of Climate change and Global warming substantially.

Keywords: COVID-19, Air quality, Pollutant concentration, Sentinel-5P, MODIS, Google Earth Engine, GIOVANNI, Chennai

1. INTRODUCTION

The COVID-19, infection due to novel coronavirus from the Wuhan province of China, was declared a public health emergency of international concern on 30th January

2020. As of 23rd December 2021, 275,233,892 confirmed cases had been reported globally, including 5,364,996 deaths due to this infection (The Times of India, 2021; WHO, 2021). After the first case of COVID-19 reported on 30th January in India, the cases gradually increased and peaked in the following months. This has led to a nationwide public curfew on 22nd March 2020, followed by a complete lockdown (first) of the nation from 24th March 2020 (*My Gov*, 2020). This lockdown was extended until May 30th as the pandemic continued in Tamil Nadu. The first lockdown was imposed on four stages to flatten the infection curve, each with different plans, strategies, and rules (The Hindu, 2020). Chennai, at most times placed in the red category region, indicates the method devised by the Government of India to identify the pockets of severity into red, orange, and green based on the confirmed number of cases where red meant the highest severity. The rules and relaxations were based on this category (DM II, 2020). The state capital Chennai was the most affected region within Tamil Nadu by COVID-19 with 8228 confirmed cases during the first phase of lockdown (Mar-May,2020) as per the reports of 21st May 2020 (*Greater Chennai Corporation*, 2020; The Times of India, 2021)

Chennai is one of the cities highly prone to air pollution, which has recorded severe air quality crises even in the recent past. The presence of heavy industries and ports in northern Chennai served as a hotspot of pollution and has resulted in an unhealthy air quality many times in the previous years, the most recent observed during May-July, 2019 (The New Indian Express, 2020). Also, the Center for Science and Environment reported that Chennai has one of India's worst vehicular pollutions after Delhi produces 3200 tonnes of CO2 per day. PM 2.5 (Particulate Matter 2.5) concentration increase was the primary concern in the city as it has ailed the health of people living in the hotspots. The year 2018-2019 has seen a maximum PM 2.5 in the city where the peak level of PM 2.5 ever (173microgram/cubic meter) was recorded in Nungambakkam (Citizen Matters Chennai, 2019).

The study aims to identify any changes in the air quality of the study area during the first lockdown period of Covid-19 compared to the pre-lockdown and post- lockdown situations. Also, it aims to make use of the advancements in remote sensing and GIS analysis like the availability of Sentinel-5P data specially developed for monitoring real-time atmospheric trace gases and Google Earth Engine API, which makes complex geospatial workflows fast and more accessible with more readily available data.

2. STUDY AREA

Chennai is one of the four metropolitan cities of India, geographically located between 12°50'49" and 13°17'24" N latitude and 79°59'53" and 80°20'12" E longitude *(Figure 1)*. It is a port city with proximity to the Bay of Bengal that gives easy access to the markets in East Asia. The economic base of Chennai has its foundation in trade and shipping. It has many ventures of automobile industries, chemical and petrochemical enterprises, IT companies, medical care facilities, and manufacturing hubs (Urban Emissions. Info, 2017). Chennai is the administrative capital of Tamil Nadu, with people

residing in the region from all over Tamil Nadu and also has a large floating population(CMDA, 2020). The Greater Chennai region has a population of 8,696,010. At the same time, Chennai alone holds a population of 67,48,026 with a population density of 37,223 persons per sq. km. It is considered one of the most densely populated cities in the world (USA Today, 2019). Nearly 820,000 people of Chennai live in slum conditions which is a matter of concern. The people in slums already live in poor environmental conditions where waste management and disposal are uncontrolled and unregulated. The proximity to the pollution hotspots increases their risk to be affected by air pollution. 13% of households own a car, and 47% own a motorcycle. (JICA, 2017)

The city can be divided into four regions: North, Central, South, and West. While the northern Chennai region serves as a manufacturing hub, the southern and western parts of the city are concentrated with Information Technology firms, financial companies, and call centres. At the same time, the central region remains a commercial hub (Statistical Handbook, 2017).

Chennai is a tropical region with a mean annual temperature of 24.3 to 32.9 °C. Late May to early June is the hottest part of the year, with maximum temperatures peaking between 35–40 °C, and January with minimum temperatures around 15–22 °C is considered the coolest part of the year. The humidity usually ranges between 65 and 84%. Prevailing winds in Chennai are generally southwesterly between April and October, and it is northeasterly during the rest of the year. The northeast monsoon brings the rains during October, November, and December, with an average annual rainfall is 1200 mm (CMDA, 2008; TNPCB, 2020)

3. MATERIALS AND METHODS

3.1 DATA

The study is based on the satellite data of the pre and post lockdown period of Chennai (Table 1 & 2) from the Sentinel 5-precursor mission, which provides near real-time global coverage data on the atmospheric concentration of NO2, SO2, O3, CO, Methane, Formaldehyde, and UV aerosol properties from TROPOMI (Tropospheric Monitoring Instrument) (van Geffen et al., 2019; Veefkind et al., 2012) and OMI/Aura NO2 Cloud-Screened Total and Tropospheric Column Level 3 data used for a total column and tropospheric column of NO2 (OMI, 2012; Earthdata, n.d.) MODIS Multi-Angle Implementation of Atmospheric Correction (MAIAC) product MCD19A2 V6 has been used for mapping Aerosol optical depth in the study area. The ground-based air quality measurements have been collected from the Continuous Ambient Air Quality Monitoring station data of TNPCB (Tamil Nadu Pollution Control Board) and CPCB (Central Pollution Control Board). The TNPCB have 4 CAAQMS in the study area that includes Kodungayyur, Koyambedu, Perungudi, and Royapuram. At the same time, the CPCB has four monitoring stations around Chennai in the places like Manali, Manali Village, Velachery Residential area, and Alandur Bus Depot. This Air quality monitoring stations measure

many atmospheric parameters like PM2.5, PM10, NOx, NO2, SO2, CO, O3, etc. Combining CPCB and TNPCB stations, eight stations data around the study area limit were obtained(CPCB, 2020.; *TNPCB*, 2020).

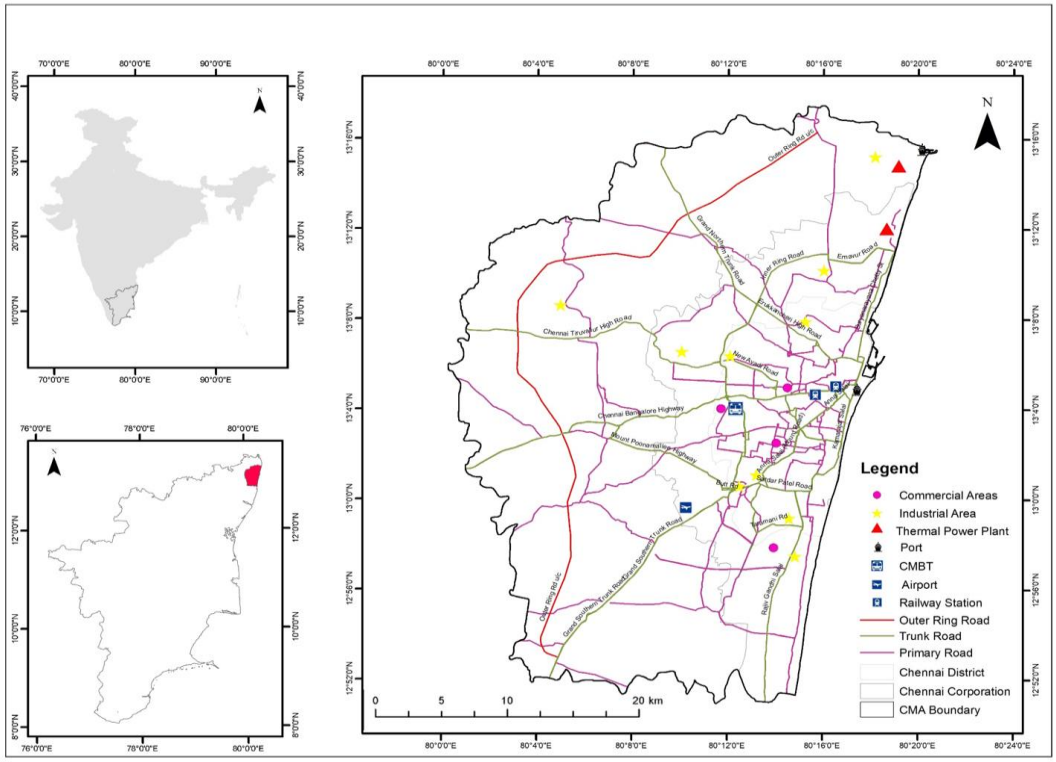

Figure 1 Location of Study

Table1: Data used and its sources

Pollutant	Data	Band Name	Source
Nitrogen Dioxide	OMNO2d	Total column NO2	Giovanni
	Sentinel 5-P NRTI/L3_NO2	NO2_column_number_density	Google Earth Engine
Sulphur Dioxide	Sentinel 5-P NRTI/L3_SO2	SO2_column_number_density	
Carbon Monoxide	Sentinel 5-P NRTI/L3_CO	CO_column_number_density	
Ozone	Sentinel 5-P NRTI/L3_O3	O3_column_number_density	
UV Aerosol Index	Sentinel 5-P NRTI/L3_AER_A	absorbing_aerosol_index	
Land Aerosol Optical Depth	MCD19A2 V6	Optical_Depth_047	

Table 2: Dates for which satellite data is acquired for all the pollutants

	Year	Date
Pre- Lockdown	2019	March 1 to May 31
	2020	January 1to March 23
Lockdown	2020	March 24to May 10
Post- Lockdown	2021	March 1 to May 31

Table3) National Air Quality Standards

Pollutant	Concentration in µg/m³		
	Time Weighted Average	Industrial, Residential and Other Rural areas	Ecologically Sensitive Areas
NO2	24 Hours	80	80
SO2	24 Hours	80	80
CO	24 Hours	1	1

3.2 METHODS

In this study, the Google Earth Engine, a cloud-based platform that has an analysis-ready data catalogue, was utilized to make maps on mean concentrations of NO2, SO2, CO, UV Aerosol Index, Ozone, and AOD from Sentinel 5p and MODIS imageries (Tobías et al., 2020; Veefkind et al., 2012) The platform was accessed through internet-based API and code editor by giving python or java based codes (Gorelick et al., 2017). A comparison study has been made using time-series graphs retrieved using the google earth engine for 2019, 2020, and 2021 during the intended study period (Mar-May). The GIOVANNI, a tool from NASA for accessing, visualizing, and analyzing the remote sensing data, was used to make time-series graph and time-averaged maps on NO2 concentrations using OMI/Aura Cloud-Screened Total and Tropospheric Column L3 Global Gridded data with 0.25°x 0.25° spatial resolution (OMI, 2012; Saikawa et al., 2019; Prados et al., 2010).

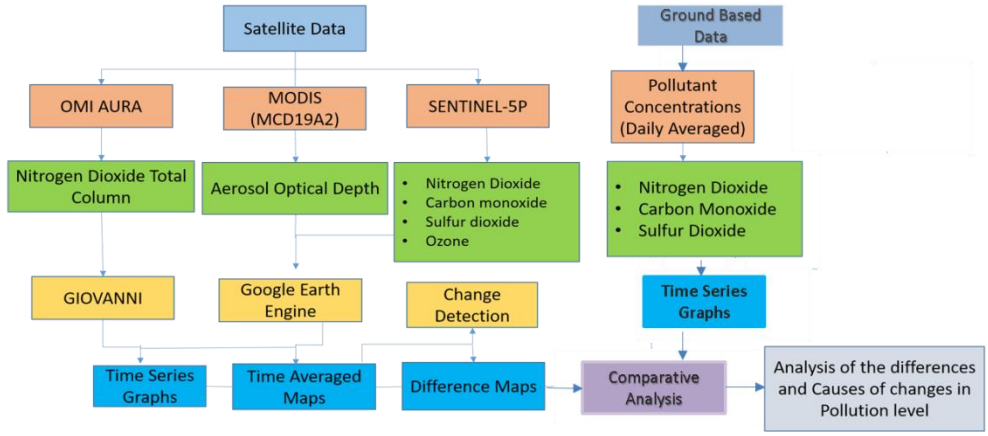

Figure 2 Methodology of the study

Further, change detection analysis was performed with ERDAS Imagine 2014 using the image difference tool. This tool calculates the change in pixel values of two raster images. The acquired time-averaged maps of NO2, SO2, and CO during the period before lockdown, which was from Feb 1st, 2020 to Mar 23rd, 2020, and the period after lockdown, which is from Mar 24th, 2020 to May 10th, 2020, had been used for difference calculation.

4. RESULTS

4.1. Nitrogen Dioxide:

The overall concentration of NO2 varies from -0.00005 to 0.0009 mol/m² during the lockdown period. From the Sentinel 5-P data, more than a 30% decrease in the concentration of NO2 *(Figure 3b & 4e)* can be noticed in the Northern and Central parts of the study area from March to May, which is the prime location for many industrial estates and commercial hubs. The MODIS data shows a similar result but with less accuracy than Sentinel 5-P *(Figure 4c & d).* The Ennore port, known for the high movement of vehicles during regular days, had the lowest concentration of NO2 during this period compared to the pre-lockdown time. April 1st to 10th of 2020 recorded low concentrations of NO2, and later on, it started increasing gradually *(Figure 3a & b)*. The Tambaram area shows a slight increase in the concentrations of NO2 during this period. From *Figure 3b,* a prominent decrease in the trend of NO2 concentration due to lockdown compared to 2019 and 2021 can be observed. It should be noted that from day 130 (May 10th) of 2021, when the 2nd phase of complete lockdown was imposed, it shows a similar decrease inNO2 concentration. The CAAQM's data also shows a similar trend of NO2 concentration for the year 2020 in line with the satellite data *(Figure 3c)*.

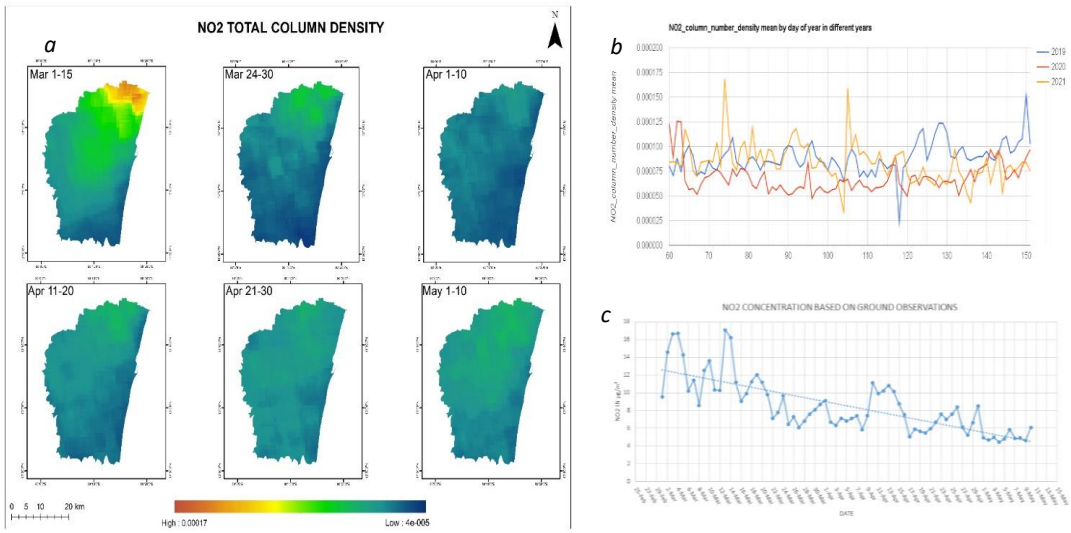

Figure 3 a) NO2 concentration weekly range from Sentinel 5P, b) Graph showing NO2 levels during 2019,2020 & 2021, c) NO2 levels of lockdown period retrieved through CAAQM's

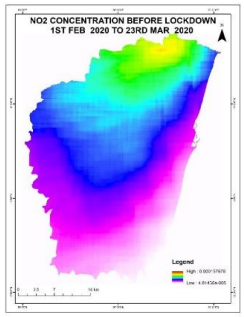

4a)

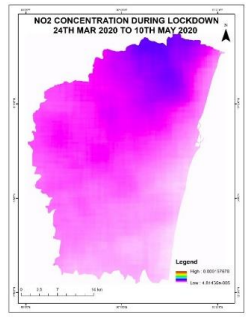

4b)

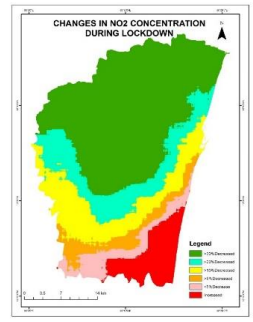

4e)

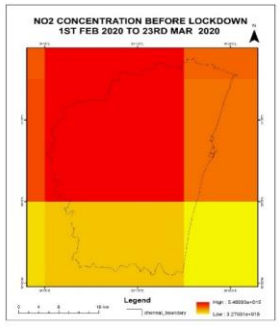

4c)

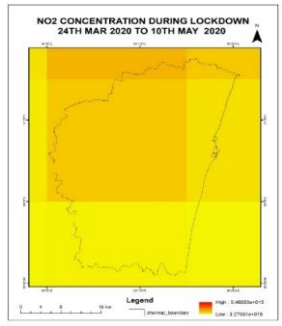

4d)

Figure 4 a) NO2 concentration before lockdown retrieved from Sentinel 5P, b) NO2 concentration during lockdown retrieved from Sentinel 5P, c) NO2 concentration before lockdown retrieved from MODIS, d) NO2 concentration during lockdown retrieved from MODIS, e) Changes in NO2 concentration in percentage

4.2. Sulphur Dioxide

In the case of SO2, there isn't an overall decrease, but a dynamic trend in the concentration can be noted during the lockdown. In some parts of the city like Ambattur, Tambaram, Chengalpattu, and Sriperumbudhur, the SO2 concentration was higher than normal days from March to May in 2020 *(Figure 5 a & 6b)*. Ambattur is an industrial area with many small-scale industries. There is a satellite earth station by Tata Consultancy situated at Redhills. Whereas Tambaram and Chengalpattu were residential areas, the anthropogenic activities didn't cease in that areas amidst lockdown. More than 30% reduction of SO2 than normal days was recorded during the 1st ten days in April 2020, which is evident in the Manali and Ennore industrial regions where the significant emitters of SO2 like the power plants, metals processing, and smelting facilities are situated *(Figure 5a & 6c).* The overall concentration of SO2 ranges from -0.0004 to 0.0005 mol/m² *(Figure 5b).* As observed from CAAQM's data Koyambedu region recorded 8 out of 10 highest SO2 recordings during the lockdown period. Before lockdown, in the year 2020, the SO2 concentration had reached the highest values of 60.08 µg/m³ in the Manali area, but during the lockdown, it recorded less than ten µg/m³ throughout. In the Velachery residential area,

both the highest and lowest concentrations were recorded during the lockdown period, and the highest recordings were the consecutive days from April 11 to 14,2020. Analyzing the successive years, 2020 shows overall minimal concentrations of SO2 compared with the years 2019 and 2021 *(Figure 5b).*

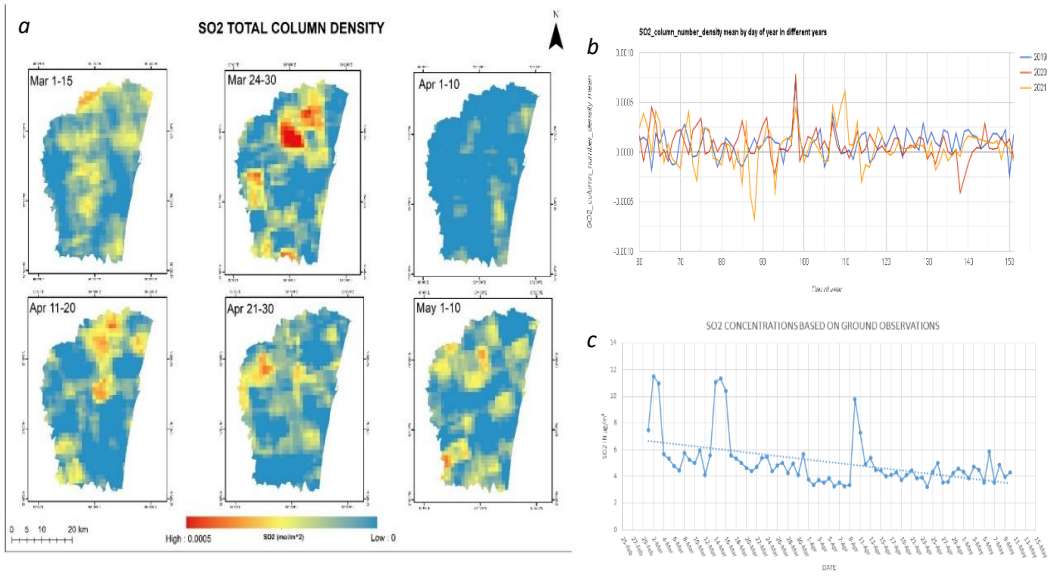

Figure 5 a) SO2 concentration weekly range from Sentinel 5P, b) Graph showing SO2 levels during 2019,2020 & 2021, c) SO2 levels of lockdown period retrieved through CAAQM's

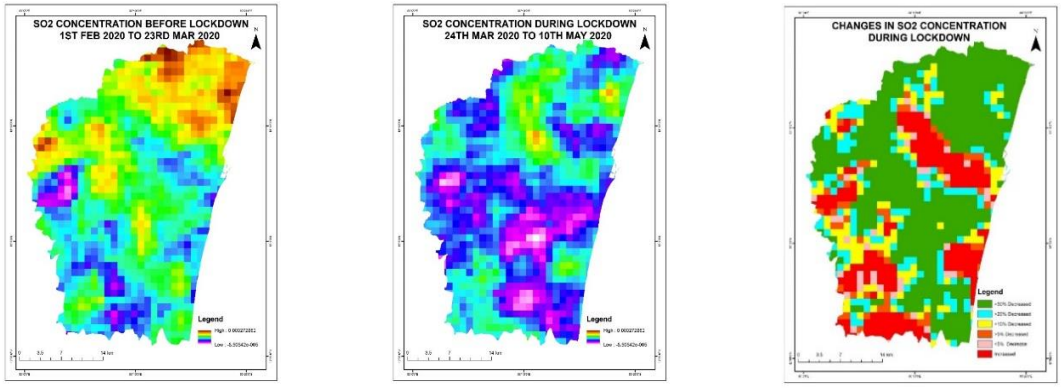

a) *b)* *c)*

Figure 6 a) & b) Mean SO2 concentrations before and during lockdown,c) Changes in SO2 concentration mapped in percentage

4.3 Carbon Monoxide:

Comparing the pre- lockdown phase, the concentration level of CO showed a decrease in most of the places. Especially in the central parts of the study area, more than 30% decreased level of CO was recorded *(Figure 8c).* A more significant reduction in concentration was seen from March 23rd to March 31st in the year 2020*(Figure 7a).* Although recorded a traceable decrease during the lockdown period, the mean concentration of CO didn't reduce in the northern and southern regions. The concentrations increased in the Ennore industrial area and Sholinganallur but were traceable. The comparison of the concentration of CO shows a clear difference in May month *(Figure 8c & d).* From *Figure 7c*, it is seen that CO maintained a similar trend to the normal years in 2020.

According to CAAQM's data, the highest concentrations of CO were recorded in Royapuram between March and mid-April, but a significant decrease was noticed in the same area from the 2nd half of April and till May 10th in the year 2020. In Manali, an industrial area, it could be noticed that most of the days exceeded the limit set by the pollution control board before lockdown. But, it never exceeded the national standards *(Table 3)* during the first part of lockdown. In contrast, Velachery residential area recorded an increasing concentration of CO during the lockdown.

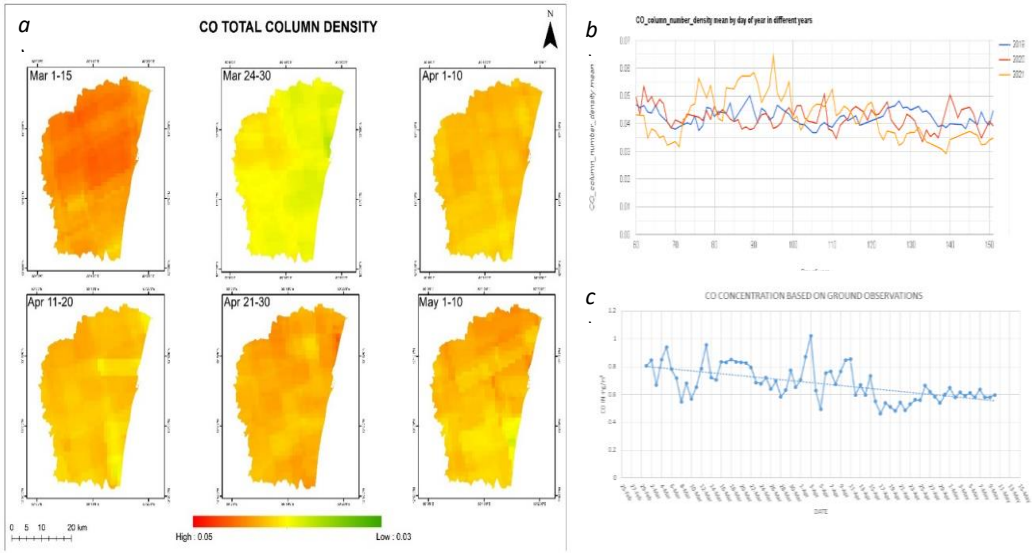

Figure 7 a) CO concentration weekly range from Sentinel 5P, b) Graph showing CO levels during 2019,2020 & 2021, c) CO levels of lockdown period retrieved through CAAQM's

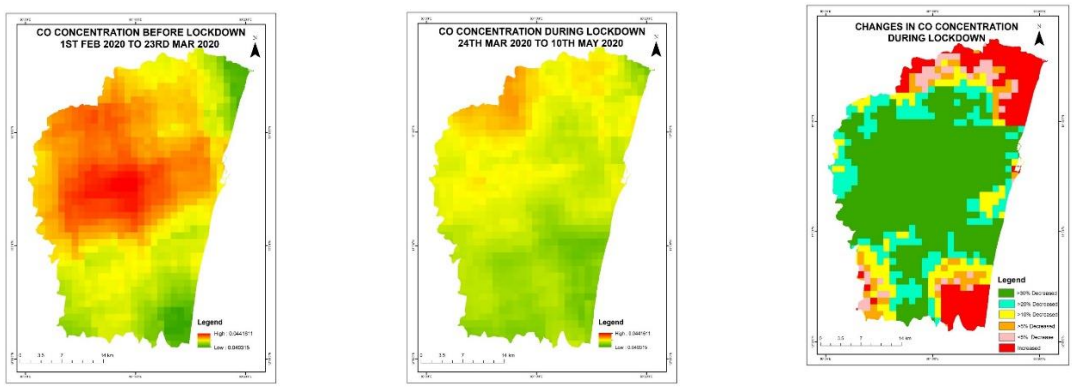

a *b* *c*

Figure 8 a) & b) Mean CO concentrations before and during lockdown,c) Changes in CO concentration mapped in percentage

4.4 Ozone:

The ozone layer shields the earth from ultraviolet radiation in the stratosphere, whereas the tropospheric ozone acts as an efficient cleansing agent. The total ozone column density, as well as the tropospheric ozone concentration, had increased. It relates to the decrease in Nitrogen Oxide in the atmosphere, resulting in the lowering of ground-level ozone consumption. (Mahato et al., 2020) The comparison analysis of the normal years showed a similar trend of increasing ozone density, but the overall concentration is significantly higher in 2020 than in 2019*(Figure 9 a&b).*

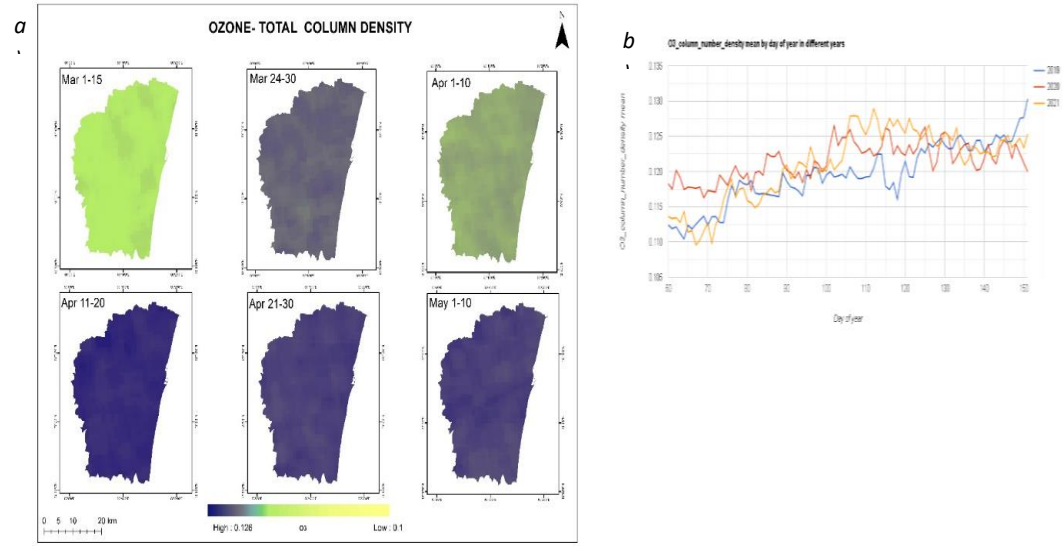

Figure 9 a) Ozone concentration weekly range from Sentinel 5P, b) Graph showing O3 levels during 2019,2020 & 2021

4.5 Aerosol Optical Depth:

The Absorbing Aerosol Index (AAI) and Aerosol Optical Depth (AOD) indicate the presence of UV absorbing aerosols in the atmosphere like dust and smoke if their values are positive. The Northwestern part of the study area, which had a very high concentration of Aerosols before lockdown, shows a significant decrease in the concentration during the lockdown. The AOD ranges from 20 to 1650 altogether, and during the lockdown, it was up to 955. Overall the year 2020 shows a decreased concentration of AAI compared to the year 2019 *(Figure 10).*

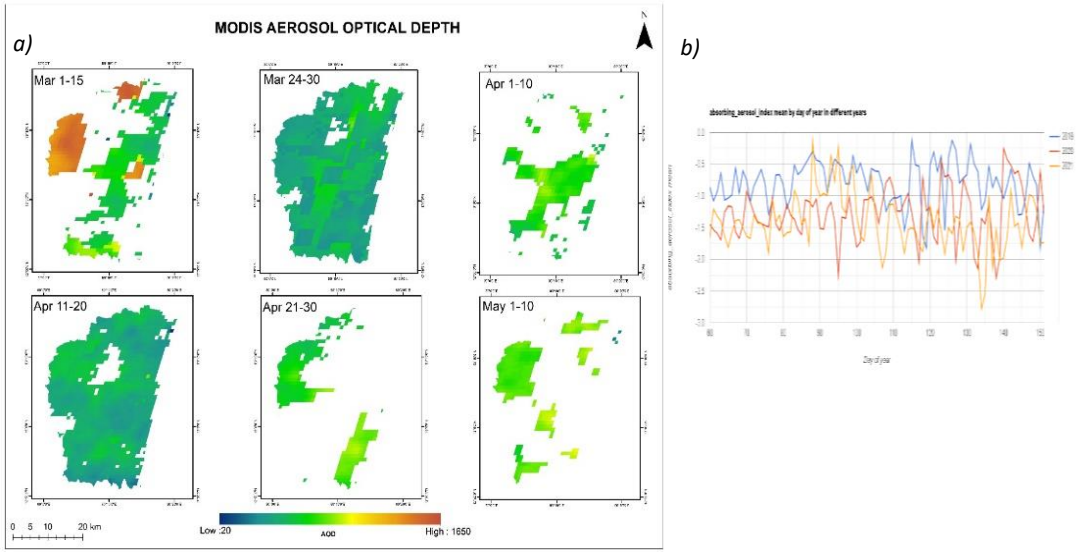

Figure 10 a) Aerosol Optical Depth retrived from MODIS, b) Graph showing Absorbing Aerosol Index during 2019,2020 & 2021 retrived from Sentinel 5P

5. DISCUSSION

The Covid-19 pandemic resulted in a series of lockdowns all over the globe. Studies have shown improved air quality in major cities of India like Delhi, Bangalore, and Mumbai. Also, the same scenario is seen in the study area where the air quality has improved during the lockdown, which started on March 24, 2020, and extended till May 3, 2020, without any relaxation to the public or business people. Whereas the essential works and services continued without any restrictions. On April 23, 2020, a relaxation was provided for heavy industries, and IT's to work with 33% of staff, but then it was taken back in the next two days due to the increase in the number of Covid-19 cases. Markets like Koyembedu continued to serve, but public entry was prohibited. Thus the movement of people has not entirely cut off in the lockdown period but has been reduced tremendously. Also, the complete closure of heavy industries was one of the main interests of the study (The Hindu, 2020b).

The primary sources of NO2 include burning fuel like coal, oil, biomass, and gas in power plants, manufacturing units, and emissions from vehicles Arora, 2019; van Geffen et al., 2019), and in the case of SO2, it is burning of coal, vehicles running with fuel containing high Sulphur content, metal extraction from an ore and some natural processes like decomposition and combustion of organic matter, spray from sea and volcanic eruptions (Dahiya & Myllyvirta, 2019; NSW.gov, 2019). For CO, the sources are residential and commercial combustion. Nearly 60% of CO emissions are due to anthropogenic activities (Kumar et al., 2013). The results also indicate that the city's industrial areas recorded a decrease in the concentration of all the pollutants during the lockdown.

In Chennai Metropolitan Area, it has been found that 48% of pollution is due to transport emission, and the industrial areas are the next source of pollution (Guttikunda et al., 2014) as the city is a base for around 30 percent of India's automobile industry and 40 percent of the auto components industry. The major automobile industries like BMW, Ford, Renault-Nissan, and related companies are in the industrial parks in the suburbs of Chennai (JICA, 2017). The Ambattur–Padi industrial zone houses many textile manufacturers, and the special economic zone (SEZ) in the city's southern suburbs contains many footwear manufacturing industries. Pharmaceuticals giant Pfizer and chemicals giant Dow Chemicals have research and development facilities in Chennai. (UrbanEmissions.Info, 2017) As of the traffic survey conducted in the city, more than 200,000 vehicles per day are passing on NH45 and Inner Ring Road, and the traffic volume in the suburbs is less than 70,000 per day. 70% of traffic on the Inner Ring Road and NH205 is due to Motorcycles. More than 3,000-4,000 container trucks go in and out of Chennai Port every day (JICA, 2017). Also, it should be noted that Chennai is one of the largest commercial and industrial hubs but has not been included under the National Clean Air Program of 2019, launched by the Ministry of Environment, Forest and Climate Change (MoEFCC).

The Northern Chennai region, especially the areas like Manali, Thiruvottriyur, Ennore, Gummidipoondi, has the highest source of pollution causing industries and has a significant movement of heavy vehicles. In southern Chennai, the movement of Individual cars and public transport is higher due to commercial, residential areas and some of the critical transport terminals (JICA, 2017). Thus, these regions can be considered the major pollution hotspots in the study area.

All the pollutant concentrations gradually increased during the last 20 days of the lockdown during the study period. The Government announced relaxations from the lockdown for various activities during this period. From April 20, relaxation from lockdown has been given to many sectors, including Industries at the outskirts, Special Economic Zones, IT companies, Vehicle repair, Brick industries, Agri Equipments, Coal and other mining, Construction based industries, Fishing, Fertilizer industries, and daily wage workers with some restrictions. This could be the reason for the gradual increase in air pollution lately.

Even though there was a reduction in pollution levels in different parts of the city during the first lockdown, it has not contributed much to the overall decrease in the pollutant concentration at a significant difference compared to the previous year. Traffic over major road junctions have been noticed like Padi flyover, Anna salai- Chinna malai road, Anna salai- Thiruvallikeni road, Aayiram Vilakku area, and Smith road, etc. which is due to the essential service and the unawareness of the general public *(Photo 1).*

During summer, the atmospheric temperature near the earth's surface is maximum, which enhances the vertical mixing height and increases the mixing layer height. As Chennai is a coastal region, the sea breeze starts to flow towards the landward side in the afternoon controlling the particulate matter's vertical mixing. An increase in temperature also elevates the ambient particulate level, usually. It also causes the pollutants to move inland, creating more pollution inland (Jayamurugan et al., 2013; Sudhakar et al., 2014). This indicates that even though a favorable situation prevails for pollution levels, the reduction in the pollution causing activities shows a noticeable change in the air quality.

Photo 1: Huge traffic on Padi Flyover amidst lockdown on1st April 2020
Source: The Times of India

6. CONCLUSION

It is evident from the study that restricted industrial and vehicular activities had a significant impact on improving the air quality. This should be taken into concern, and steps should be taken to maintain the air quality. Methods and plans to restrict the pollution caused by industries and vehicles are necessary even after the lockdown to ensure the good air quality of the human habitat, positively affecting society and the environment taking into account the lack of major air quality monitoring programs in the city. The results acquired using Google Earth Engine cloud-based API and Sentinel 5-P data which is readily available, prove it is a very efficient tool to study air pollution, especially in this lockdown period where it is challenging to collect ground-based primary data. Also, these

advancements make researchers and climatologists quickly analyze real-time data of every corner of the globe to provide up-to-date information and make further plans accordingly to mitigate air pollution and build a sustainable urban environment. This study suggests using these techniques to monitor and prevent air pollution on a regional scale. It is paramount to control air pollution to improve the livable conditions of the city and the health of the citizens, especially during this pandemic.

REFERENCES

1. Chaudhary, S., Kumar, S., Antil, R., & Yadav, S. (2021). Air Quality Before and After COVID-19 Lockdown Phases Around New Delhi, India. *Journal of Health & Pollution*, *11*(30), 210602. https://doi.org/10.5696/2156-9614-11.30.210602
2. Citizen Matters Chennai. (2019). *'Smart' T Nagar among top five polluted neighbourhoods in Chennai: Report*. https://chennai.citizenmatters.in/chennai-air-pollution-data-pm2-5-12831
3. CMDA. (2008). *2nd Master Plan for Chennai Metropolitan Area-2026*. http://www.cmdachennai.gov.in/Volume1_English_PDF/Vol1_Chapter00_Introduction.pdf
4. CMDA. (2020). *Chennai Metropolitan Development Authority*. http://www.cmdachennai.gov.in/
5. *CPCB*. (2021). https://cpcb.nic.in/
6. DM II. (2020). *Guidelines for Demarcation of Contaminent Zone to control Corona Virus*. Revenue and Disaster Management Department. https://cms.tn.gov.in/sites/default/files/go/revenue_e_221_2020.pdf
7. Gorelick, N., Hancher, M., Dixon, M., Ilyushchenko, S., Thau, D., & Moore, R. (2017). Google Earth Engine: Planetary-scale geospatial analysis for everyone. *Remote Sensing of Environment*, *202*, 18–27. https://doi.org/10.1016/j.rse.2017.06.031
8. *Greater Chennai Corporation*. (2020). http://covid19.chennaicorporation.gov.in/c19/
9. JICA. (2017). *Data Collection Survey for Chennai Metropolitan Region : Intelligent Transport Systems- Final Report*.
10. *my Gov*. (2020). https://www.mygov.in/covid-19/
11. OMI. (2012). *Ozone Monitoring Instrument (OMI) Data User ' s Guide*. https://acdisc.gesdisc.eosdis.nasa.gov/data/s4pa/Aura_OMI_Level2G/OMTO3G.003/doc/README.OMI_DUG.pdf
12. Prados, A. I., Leptoukh, G., Lynnes, C., Johnson, J., Rui, H., Chen, A., & Husar, R. B. (2010). Access, Visualization, and Interoperability of Air Quality Remote Sensing Data Sets via the Giovanni Online Tool. *IEEE Journal of Selected Topics in Applied Earth Observations and Remote Sensing*, *3*(3), 359–370. https://doi.org/10.1109/JSTARS.2010.2047940
13. Sathe, Y., Gupta, P., Bawase, M., Lamsal, L., Patadia, F., & Thipse, S. (2021). Surface and satellite observations of air pollution in India during COVID-19 lockdown: Implication to air quality. *Sustainable Cities and Society*, *66*, 102688. https://doi.org/https://doi.org/10.1016/j.scs.2020.102688
14. Statistical Handbook. (2017). *District statistical handbook Chennai district 2016-2017*.

15. The Hindu. (2020a). *Extended lockdown will help flatten the curve in Tamil Nadu : State Health Minister C . Vijayabaskar*. https://www.thehindu.com/news/national/tamil-nadu/extended-lockdown-will-help- flatten-the-curve-in-Tamil-Nadu/article31485127.ece
16. The Hindu. (2020b). *Tamil Nadu government extends COVID-19 lockdown till*.
17. The New Indian Express. (2020). *Chennai vehicles pollute nearly as much as Delhi's: CSE data*. https://www.newindianexpress.com/nation/2020/feb/11/chennai-vehicles-pollute-nearly-as-much-as-delhis-cse-data-2101650.html
18. The Times of India. (2021). *Chennai: How Covid-19 second wave rose like a tsunami and is crashing fast*. https://timesofindia.indiatimes.com/city/chennai/chennai-how-covid-19-second-wave-rose-like-tsunami-and-is-crashing-fast/articleshow/83328936.cms
19. *TNPCB*. (2020). https://www.tnpcb.gov.in/
20. UrbanEmissions.Info. (2017). *Air Pollution Knowledge Assessment (APnA) city pro*. http://www.urbanemissions.info/india-apna/chennai-india/
21. USA Today. (2019). *75,000 people per square mile? These are the most densely populated cities in the world*. https://www.usatoday.com/story/news/world/2019/07/11/the-50-most-densely-populated-cities-in-the-world/39664259/
22. Van Geffen, J. H. G. M., Eskes, H. J., Boersma, K. F., Maasakkers, J. D., & Veefkind, J. P. (2019). TROPOMI ATBD of the total and tropospheric NO2 data products. In *S5p/TROPOMI* (Issue 1.4.0). https://sentinel.esa.int/documents/247904/2476257/Sentinel-5P-TROPOMI-ATBD-NO2-data-products
23. Veefkind, J. P., Aben, I., McMullan, K., Förster, H., de Vries, J., Otter, G., Claas, J., Eskes, H. J., de Haan, J. F., Kleipool, Q., van Weele, M., Hasekamp, O., Hoogeveen, R., Landgraf, J., Snel, R., Tol, P., Ingmann, P., Voors, R., Kruizinga, B., … Levelt, P. F. (2012). TROPOMI on the ESA Sentinel-5 Precursor: A GMES mission for global observations of the atmospheric composition for climate, air quality and ozone layer applications. *Remote Sensing of Environment*, *120*(2012), 70–83. https://doi.org/10.1016/j.rse.2011.09.027
24. WHO. (2021). *Coronavirus (COVID-19) Dashboard*. https://covid19.who.int/

The Indian Geographical Journal
Volume 96 (1) June - 2021, pp 60-72
ISSN 0019-4824

ASSESSMENT OF FOREST COVER CHANGE IN PART OF THE NORTHERN WESTERN GHATS: A CASE STUDY OF THE KAS AND PANCHGANI PLATEAUS

Ravindra G. Jaybhaye, Yogesh P. Badhe* and Poorva K. Kale

Department of Geography, Savitribai Phule Pune University, Pune-411007, India
* E-mail: yogeshspb94@gmail.com

Abstract

The Kas and Panchgani plateaus in the Western Ghats are well-known for their peculiar features like laterite rich area, floral diversity, endemism and tourism. The area has serious concern because of threat to the natural environment by forest fragmentation of land use land cover change such as a built-up area expansion on agriculture land and numerous infrastructural development activities. In the process, forest fragmentation was examined using geospatial technology and Fragsat 4.2 programme for distinct classes using landscape metrics such as the Class Area (CA), Percentage of Land (PLAND), Edge Density (ED), and Largest Patch Index (LPI) at the class level. The analysis of spatial patterns on land use and land cover maps was created using Landsat 5, 7, and 8 digital data for the years 1989, 1999, 2006, and 2015. The findings of the foregoing investigation revealed that both the plateau have the problem of forest fragmentation and comparatively Panchgani plateau has more fragmentation. Landscape metrics revealed that the landscape has changed significantly and provides more precise information on the fragmented areas. The study has relevance in the context of measuring extend of degradation and necessary conservation actions.

Keywords: Forest Fragmentation, Fragstats, Landscape Metrics, Western Ghats.

Introduction

The deforestation problem is pertinent despite many conservation drives. Since 1990, the worldwide primary forest has decreased by more than 80 million hectares, and also habitat loss (Flowers et al., 2020) and forest degradation (Rahman et al., 2016) have been cited as serious risks to biological diversity. Deforestation and fragmentation are major concerns in tropical forest management and conservation activities, with worldwide implications. In India, the forests have dramatically changed over the last few decades in the Himalayas, Eastern Ghats and the Western Ghats (Reddy et al., 2010). Among them, Western Ghats have more fragmentation due to anthropogenic activity such as tourism activity, agricultural expansion, and maximum pressure on the forests for livelihood. Deforestation occurs mainly due to the fragmentation process which causes loss of forest covers in small patches and which results in huge loss over a longer period of time. Fragmentation of previously contiguous forests getting transformed into small patches

(Jaybhaye et al., 2016) and edge impacts within a forest-deforested boundary zone have also detrimental physical and biological effects on the forest (Gascon et al., 2000). Understanding the effects of forest cover change is critical for biodiversity conservation since large portions of tropical forests are spread along with agricultural landscapes (Hill et al., 2011). The term "forest fragmentation" refers to the separation of a big forest area into small parts (Liu et al., 2019). Fragmentation is a dynamic process in which a landscape's habitat pattern changes dramatically over time. Fragmentation is characterised as the conversion of major forest sections into smaller, non-contiguous pieces while simultaneously reducing forest area, increasing forest edge, and isolating big forest regions (Laurance, 2000).

Human development activities such as plantation, mining, road construction, agricultural activities, utility corridors, or human intrusion in forest areas usually separate these parts. Most landscape patterns presently consist of big human settlements, growing agricultural areas, and dispersed and isolated ecosystems as a result of human activities. Most conservation reserves are surrounded by rapidly changing forests and appear to be built to function as isolated natural systems over time (Bennett, 2003). Deforestation has several negative consequences, including loss of ecosystem, the defeat of a significant carbon sequestration source, effects on climate change and in tropical forests there are negative consequences for people's lives. Deforestation leads to the extinction of many species and has three consequences on biological diversity and habitat destruction (Badhe and Jaybhaye, 2021).

Remote sensing has been established as a sophisticated technique for forest monitoring systems that can improve data about fragmentation patterns and distribution of forests (Mayaux et al., 2005). Remote sensing data provide an opportunity to study change detection in forest cover and link additional environmental and human factors to the spatio-temporal pattern of such changes (Dewan et al., 2012). Riitters et al., (2004), use temporal land use land cover (LULC) to examine patterns of forest fragmentation on a global scale and also investigate species loss due to forest fragmentation on a local scale. Fynn, I. E., and Campbell, J. (2019) investigated the effects of various spatial resolutions on common fragmentation metrics using several images formats in their forest fragmentation research. Recent studies have used geospatial methods to investigate the impact of human activities on forest fragmentation (Riitters et al., 2016; Aditya et al., 2018; Shapiro et al., 2016; Sarkar, A. A. 2019) based on accessible geospatial data on forest cover (Rose et al., 2015). Batar et al., (2017) used geospatial tools to investigate forest fragmentation, the findings of the study demonstrate that human activities are the primary reasons for forest decline and fragmentation. The quantification of various levels of fragmentation is made easier due to multi-temporal satellite images and geospatial technology. FRAGSTATS is a programme that calculates landscape patterns (McGarigal et al., 2002) can be used to compute landscape pattern measurements and can assist forest loss and fragmentation are quantified and revealed in various ways (Riitters et al., 2004).

The study area is economically sensitive and has significant human interference with perspective tourism development and basic infrastructure development. This dynamic is necessary to maintain frequently and assess for development on sustainability. The impact of human interference is significant. Its impact has been assessed in terms of change in land use land cover and general identification of change in area under forest. The nature of deforestation needs to assess in detail in terms of different causes of subsequent different forms of loss of vegetation cover. Therefore the forest fragmentation is a process useful to explain the nature of deforestation which will be useful to design strategies for conservation measures.

Study Area

The Kas and Panchgani plateaus are selected for the study of forest cover change using landscape metrics such as class area (CA), percentage of land (PLAND), edge density (ED), and largest patch index (LPI). These are well-known tourist destinations of the Satara district of the Western Ghats region (Figure 1). Both have similar feature like the same elevation, ranging from 1100 to 1300 metres above sea level and also plateau in relief feature.

Panchgani plateau, an area of 170 sq. km is 1293 meters above sea level. There are many dams in the around the area: Wai, Bavdhan, and Nagewadi dams in the east; Gureghar in the west; Khingar in the south and Rajpuri and Dhom Dam is to the north.

The Kas Plateau, famously known as the Valley of Flowers, is located 25 kilometres from Satara, Maharashtra. In 2012, it was declared a UNESCO World Heritage Site. During the monsoon season, from August to early October, the entire grassland transforms into a valley of flowers. The Kas Plateau is recognized for its unique ecosystem, which includes a variety of herbs, shrubs, plants, butterflies, and insects, as well as its scenic beauty. The Kas Plateau is made up of four separate plateaus. The main tableland of Kas lies between Latitude 17°43'36.50" to 17°45'21.95" North and Longitude 73°47'29.13" to 73°50'56.51" East, covering an area of 150.2 sq. km. at an altitude of 1200 m. The Kas plateau is comes under the ecologically sensitive zone where variety of unique flora and fauna species are found.

Data and Methodology

LULC maps were derived from the data source of Landsat imagery for the years 1989, 1999, 2006 and 2015 (Table 1). These images formed the base for the classification of LULC as well as estimation of forest cover in the study areas. According to Chuvieco (1996), before the images could be used to study changes in forest cover and fragmentation, they had to be corrected geometrically, atmospherically, and topographically. The LULC maps are generated using hybrid classification technique based on Maximum Likelihood classifier in the supervised classification and ISO cluster unsupervised classification. At the time of taking training datasets for image processing, the representation of all classes of radiance according to spectral signature value was taken

into account (Chuvieco, 1996). The categories of LULC identified for the study were dense vegetation, open vegetation, scrubland, barren land, agriculture, water bodies, and wet land.

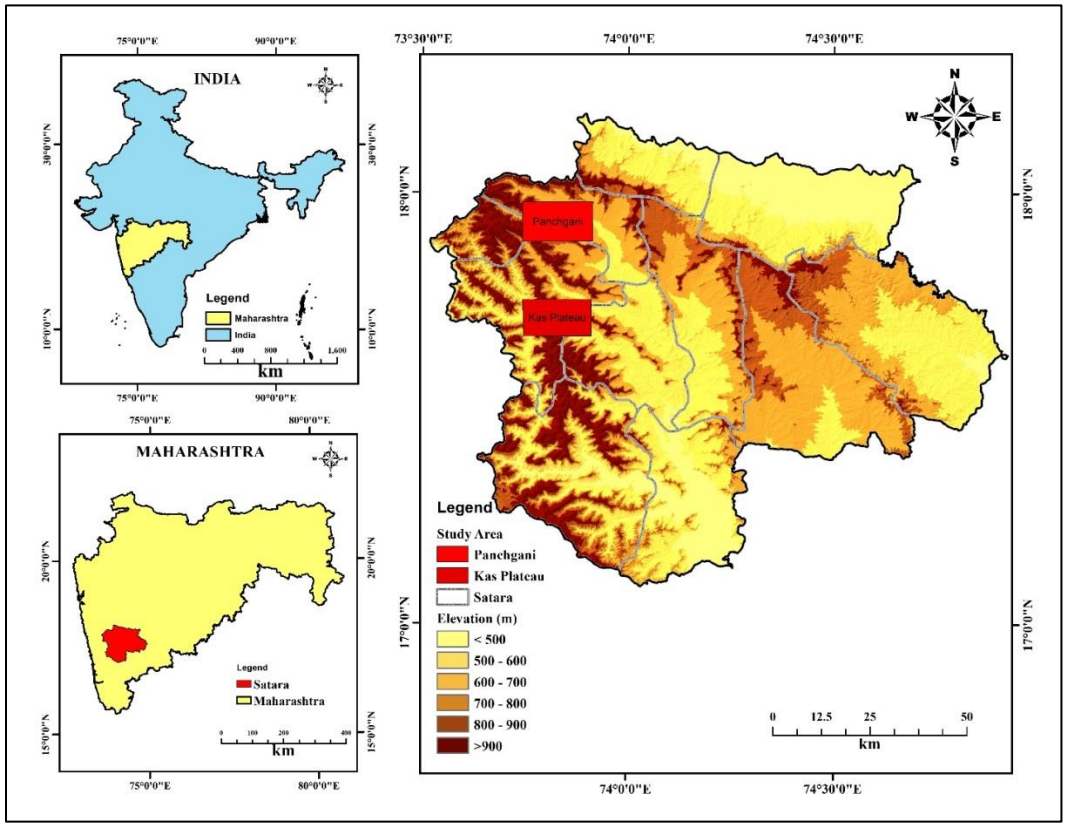

Figure 1. Location Map of the Study Area: Kas and Panchgani Plateaus

Table 1. The Satellite Data Source

Acquisition Date	Satellite	Sensor	Sources	Spatial Resolution
28th February 1989	Landsat 5	TM	USGS	30
14th November 1999	Landsat 7	ETM+	USGS	
18th February 2006	Landsat 7	ETM+	USGS	
19th February 2015	Landsat 8	OLI	USGS	

Image processing techniques are essential for this study which involves the preparation of base map and identifying the LULC of the study area. The fragmentation pattern was determined applying Fragstats statistical software for image analysis (Narmada et al., 2021). A set of four metrics comprising of class area (CA), percentage of land (PLAND), edge density (ED) and largest patch index (LPI) (present landscape consisting of

the largest patch) were chosen for the present study. The Fragstats software was utilized to compute these indices on the class metrics derived from LULC classified images.

Fragstats

FRAGSTATS is a programme for analysing spatial patterns and quantifying landscape elements, has been commonly used to predict landscapes features (McGarigal and Marks, 1994). FRAGSTATS generates indices that describe each mosaic patch, every patch class (class), and the entire landscape mosaic. The study areas are ecologically sensitive but become vulnerable due to irresponsible tourism activity and chaotic development. Hence, with the understanding of dynamism in forest degradation, there is a need to discover the extent of forest degradation with the spatio-temporal change in LULC and forest cover, and to assess the changes in various parameters of landscape metrics and compare the fragmentation of two different eco-sensitive areas of Western Ghats. To assess the transition in LULC categories and forest cover for the application of landscape spatial indices, ArcGIS 9.3 software was used. Fragstats software 4.2 was used to create these indices or spatial metrics (McGarigal et al., 2002). Fragstats software has the advantage of assisting in the comparison of the spatial pattern of landscape. The spatial configuration of native forest fragments was quantified and compared using the class area (CA), percentage of land (PLAND), edge density (ED), and largest patch index (LPI).

To assess landscape patterns, each metric must have the same spatial resolution (Cushman et al., 2008); changing the spatial resolution will result in a more inaccurate landscape assessment. To quantify and monitor a huge database of landscape features, landscape complexity must be defined (Papadimitriou, 2009). A variety of criteria define landscape characteristics, each with a different level of relevance depending on the classification category. As a result, the metrics used in this study were chosen to identify characteristics at various levels and to be studied to estimate forest cover change using landscape metrics.

Class Area (CA):

It is a landscape composition metric that identifies a specific patch type in the landscape. The class area is absolute area covered by each patch type. If a single patch type covers the entire landscape area then the class area (CA) equals the total landscape area (TA).

$$CA = \sum_{j=1}^{n} a_{ij}\left(\frac{1}{10{,}000}\right) \quad (1)$$

Where,

a_{ij} = area (m^2) of patch ij.

Percentage of land (PLAND):

It represents the proportion of the landscape that is composed of the corresponding

atch type. PLAND quantifies the relative ratio of each patch type in the landscape. It equals the sum of the area (m^2) of all patches of the corresponding patch type, divided by the total landscape area (m^2), and multiplied by 100 (to convert to percentage)

$$\text{PLAND} = P_i = \frac{\sum_{j=1}^{n} a_{ij}}{A}(100) \quad (2)$$

Where,

P_i = proportion of the landscape occupied by patch type (class) i.

a_{ij} = area (ha) of patch ij.

A = total landscape area (ha).

Edge Density (ED):

The sum of the lengths (m) of all edge segments, divided by the entire landscape area (sq. m), and multiplied by 10,000 for the conversion into the hectares.

$$ED = \frac{\sum_{k=1}^{m} e_{ik}}{A}\left(\frac{1}{10000}\right) \quad (3)$$

Where,

e_{ik} = total length (m) of edge in landscape involving patch type (class) i; includes landscape boundary and background segments involving patch type i.

A = total landscape area (m^2).

Largest patch index (LPI):

The largest patch index (LPI) shows percentage of the largest patch area in each class and helps to understand the fragmentation in the study area. When the corresponding patch type is small, LPI approaches 0 values, whereas when the entire landscape is formed up of a single patch type, it equals 100 values. The area of the largest patch divided by the total landscape are multiplied by 100.

$$\text{LPI} = \frac{\max_{j=1}^{n}(a_{ij})}{A}(100) \quad (4)$$

Where,

a_{ij} = area (ha) of patch ij.

A = total landscape area (ha).

Results and Discussion

Panchgani plateau

The PLAND describes the percentage of land covered by each LULC category (Table 2). Since 1999, the amount of land covered by dense vegetation has decreased. It has decreased from 6.7 % in 2006 to 3% in 2015. The area under forest has been decreased since last two decades of the study period. It has occupied by agriculture and

settlement, which have been increasing over the period. The dense vegetation categories have been increased from 1115.4 ha. (1989) to 1599.4 ha in 1999 at Panchgani plateau and again it reduced up to 1146.4 ha in 2006 and decreased converted in results of 503.3 ha in 2015. The Open vegetation category occupied the most land in 2006, but by 2015, it had decreased to 1800 ha. In the category of scrubland, the area covered in 2006 was higher than in 2015 (Figure 2). A significant increase in the area occupied by agricultural and settlement has occurred since 1989 (Table 2). The decrease in the land after 2006 is depicted by the open vegetation and scrub land category. Between 2006 and 2015, the area occupied by agriculture and settlement increased significantly.

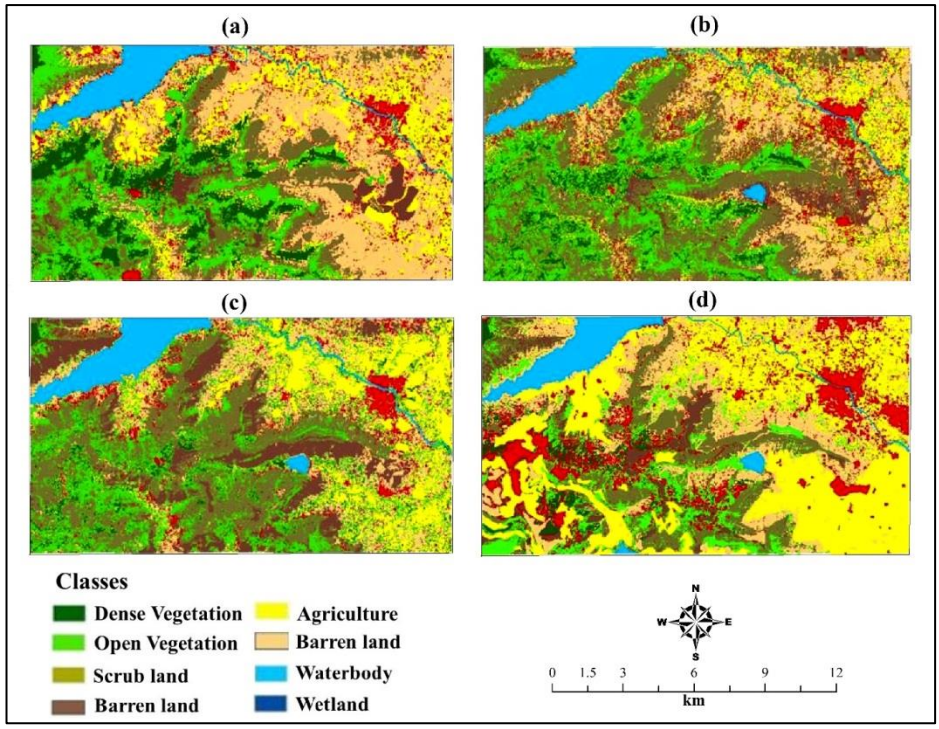

Figure 2. LULC of Panchgani Plateau: a. 1989 b. 1999 c. 2006 d. 2015

Between 1989 and 2006, the edge density of dense vegetation, open vegetation and scrubland categories increased, and then significantly decreased in 2015 (Table 3). The largest patch index indicates the proportion of the class area occupied by the largest patch. It describes the decline in vegetation type over time, resulting in forest fragmentation (Figure 3). The findings of this study imply that increasing agricultural, fallow land and settlement (built-up areas) are the primary drivers of forest fragmentation in Panchgani plateau. At the same time the study region is extremely susceptible due to irresponsible tourism activities, infrastructure construction, inappropriate land use, and forest fires. It is also vulnerable to changes in forest cover and increased forest fragmentation. The available habitat is declining due to fragmentation and forest loss caused by conversion to agriculture and other land uses.

Table 2. Class Area and Percentage of Land of Panchgani plateau

Class Name	Class Area (ha)				PLAND (%)			
	1989	1999	2006	2015	1989	1999	2006	2015
Dense Vegetation	1115.4	1599.4	1147.4	503.3	6.5	9.4	6.7	3
Open Vegetation	3084.2	2806.6	3295.1	1803.9	18.1	16.5	19.3	10.6
Scrub Land	4836.2	2608.8	4776.1	1987.5	28.4	15.3	28	11.7
Barren Land	1402	505.6	866.5	702.9	8.2	3	5.1	4.1
Agriculture	2666.3	2583.5	2042.1	5269.7	15.6	15.2	12	30.9
Fallow land	1569.1	4624.5	2575.6	3557.7	9.2	27.1	15.1	20.9
Settlement	1764.7	1226.4	1116.1	2320.8	10.4	7.2	6.5	13.6
Water body	609.6	1092.7	1228.6	901.7	3.6	6.4	7.2	5.3

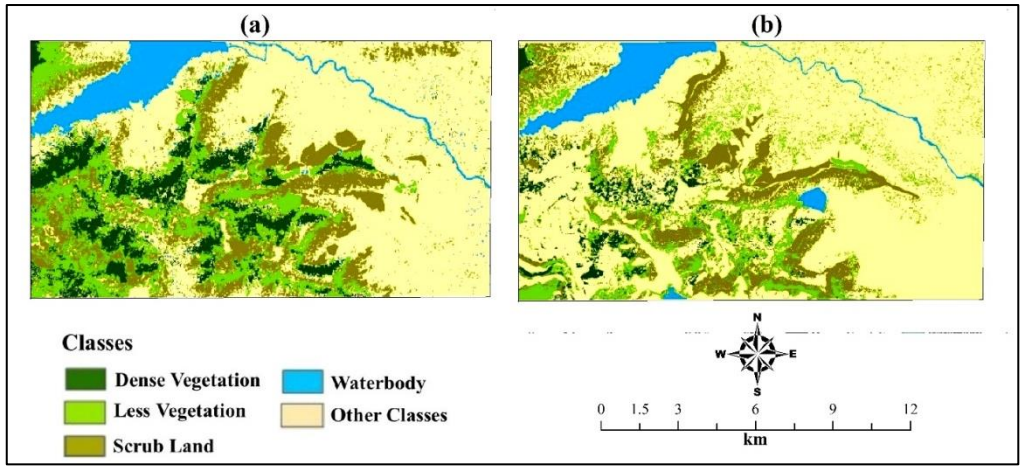

Figure 3. Forest Fragmentation of Panchgani Plateau: a. 1989 b. 2015

Table 3. Edge Density and Largest Patch Index for Panchgani plateau

Class Name	ED (ha)				LPI (%)			
	1989	1999	2006	2015	1989	1999	2006	2015
Dense Vegetation	16.3	29	42.3	18.6	1.3	1.3	0.7	0.2
Open Vegetation	31.2	58	113.8	73.5	7.8	4.8	5.3	0.5
Scrub Land	46.9	51.7	136.8	46.5	11.6	2	4.2	1.9
Barren Land	17.8	8.2	43.5	17.9	1.4	0.5	1	1.1
Agriculture	23.6	57.6	89.8	54.6	2.8	2.7	2.4	10.5
Fallow land	23.6	75.2	73.5	93.1	0.7	7.9	3.2	4.8
Settlement	39.6	53.7	61.9	73.2	0.3	0.5	0.5	1.1
Water body	13.4	8.6	19.5	4.2	1.3	5.7	5.8	4.4

Kas Plateau

The increasing tourism activity in the Kas plateau is creating threat to the surrounding area. The area of dense vegetation has decreased from 2006 (1957 ha) to 2015 (1523 ha), whereas the area of open vegetation has increased significantly (Table 4). The main reason for this is the increase in patchiness in the area. The percentage of land covered by vegetation is decreasing, from 13% in 2006 to 10.1% in 2015. In 2015, open vegetation increased by 23%, but scrub land dropped slightly (Figure 4) (Table 4).

Table 4. LULC Class Area and Percentage of land of Kas plateau

Class Name	**Class Area** (ha)				**PLAND** (%)			
	1989	**1999**	**2006**	**2015**	**1989**	**1999**	**2006**	**2015**
Dense Vegetation	962.2	1548.6	1957.6	1523.1	6.4	10.3	13	10.1
Open Vegetation	2894	3712.3	2942.2	3510.3	19.3	24.7	19.6	23.4
Scrub Land	4006.2	5741.2	4234.8	3896.3	26.7	38.2	28.2	25.9
Barren Land	2589.4	586.6	556.5	731.2	17.2	3.9	3.7	4.9
Agriculture	3736.8	1568.6	3151.1	3033.5	24.9	10.4	21	20.2
Water-body	418.5	1184.3	1540.3	1961.6	2.8	7.9	10.3	13.1
Wetland	414	679.5	638.6	365.1	2.8	4.5	4.3	2.4

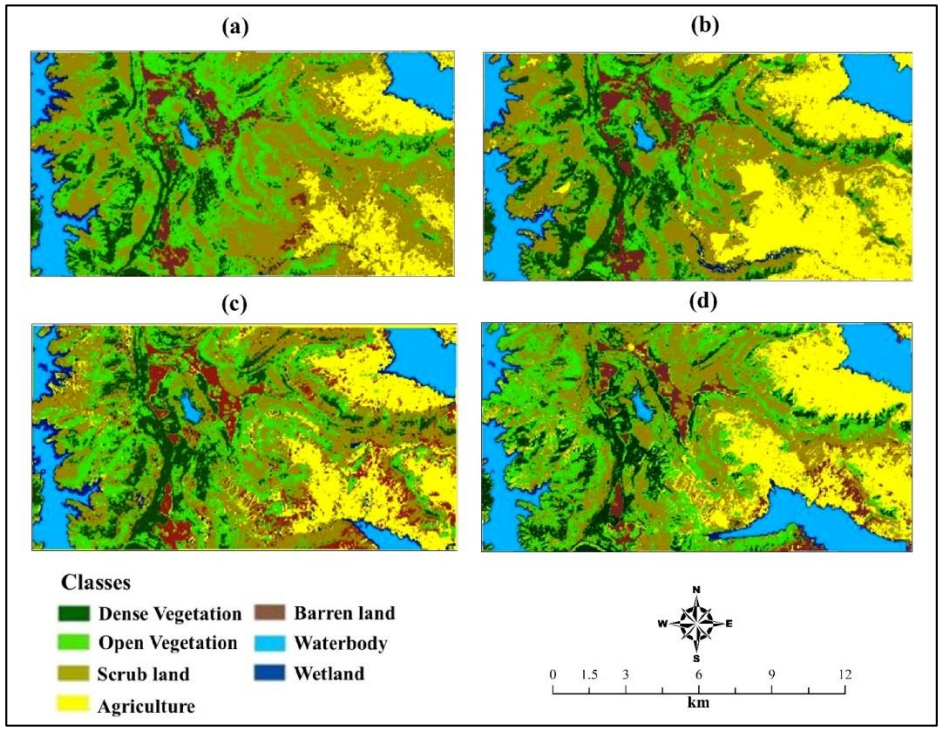

Figure 4. LULC of Kas Plateau: a. 1989 b. 1999 c. 2006 d. 2015

Between 1989 and 2006, the edge density of dense vegetation and scrubland categories increased, and then significantly decreased in 2015. From 1989 to 2015, there has been a steady increase in the category of open vegetation and also increase in agriculture category in the Kas Plateau (Table 5). The number of patches in the agriculture category has increased, followed by dense vegetation. If the number of patches for a specific category increases, the area is shown to be fragmented (Figure 5).

Table 5. Edge density and Largest patch index of Kas plateau

Class Name	**ED** (ha)				**LPI** (%)			
	1989	**1999**	**2006**	**2015**	**1989**	**1999**	**2006**	**2015**
Dense Vegetation	19.7	37.9	56.1	50.4	1.5	1.9	3.4	3.3
Open Vegetation	57.1	94.8	106.4	125.6	3.4	5.7	2.2	6.9
Scrub Land	58	112.6	142.2	111.1	11.1	21.5	7.8	10.3
Barren Land	56	16.3	16.5	20.7	1.1	0.8	0.7	1
Agriculture	57	25.4	62.1	72.8	7.8	4.3	12.4	7.3
Water-body	4.8	3.7	5	5.9	1.2	3.3	3.8	4.5
Wetland	9.7	26.8	40.9	19.3	0.7	0.7	0.6	0.5

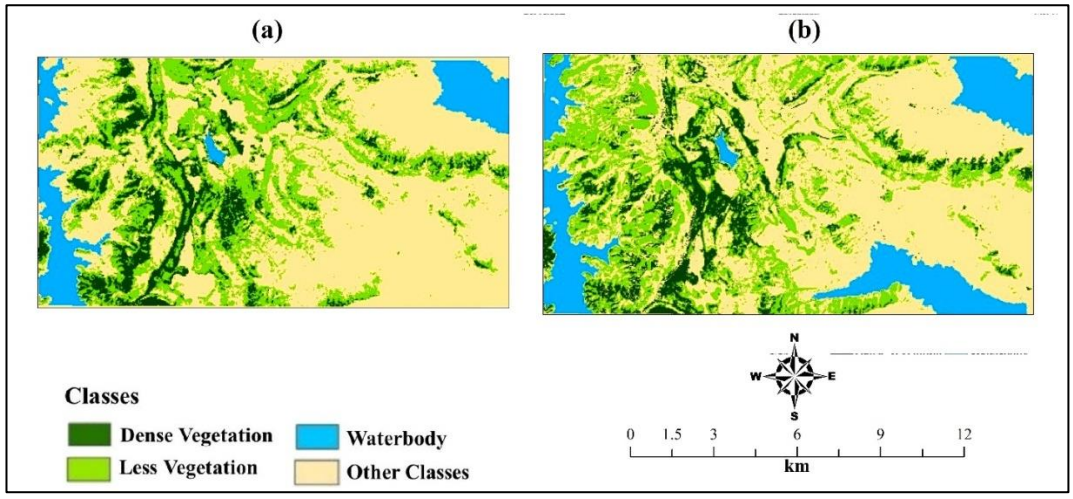

Figure 5. Forest Fragmentation of Kas plateau: a. 1989 b. 2015

Fragmentation in Kas and Panchgani Plateaus

Kas and Panchgani plateaus are two distinct places with few similarities in elevation, climate, and physiographic conditions with flora and fauna. Both of these locations are well-known tourist destinations. Though Kas and Panchgani plateaus are eco-sensitive zone but still there is a disturbance mainly due to increase in agriculture, water bodies and development activities, which degrade the ecosystem due to forest fragmentation. From the Landsat images, it was depicted that the settlements in the Kas

plateau are scattered and sparsely populated. In Panchgani plateau, the wetland area is absent. As compared to Kas Plateau, the Panchgani plateau is more fragmented because of decrease in vegetation cover. Fragmentation in Panchgani plateau is also the result of its popularity as a famous tourist destination. Another reason for fragmentation might be as a consequence of increase in area under agriculture. The area under dense vegetation is only 3% in Panchgani plateau and 10.1% in Kas plateau region whereas the open vegetation is high in Kas plateau (23.4 %) as compared to Panchgani plateau which is 10.6 % respectively. Agricultural land is expanding in the Panchgani plateau (30.9%) as compared to 20.2% in Kas region. The results reveal that the both plateau areas are degrading through fragmentation of natural forest but Panchgani Plateau and its surrounding areas are more fragmented as compared to Kas Plateau region. The conservation effects of the Kas Plateau region have improved.

Conclusions

Forest fragmentation is associated with a rapid increase in the number of small patches and a decrease in patch connectivity. The study areas are experiencing forest fragmentation due to unplanned tourism activity, farm houses, increasing settlements, expansion of agriculture area, infrastructure development and human encroachment in adjacent area of forest. Increased fragmentation is harmful to biodiversity because forest patches are more widely scattered throughout both plateaus. The comparison between geographical and geological distinct Kas and Panchgani plateau facing the negative impact of human interference and have changed forest cover over the period. It can be depicted that both these areas are under threat for ecological disturbance and especially Panchgani plateau has face more. The spatial configuration pattern of forest fragmentation, as well as how it fluctuates through time and space at the landscape level, should be addressed in conservation policy and land use planning for both the study area and the rest of the world.

Acknowledgements

We are grateful for the financial support provided by Savitribai Phule Pune University, Pune, under the Rashtriya Uchchatar Shiksha Abhiyan (RUSA/CBS/TH 1.3).

References

1. Aditya, S. K., Asok, V. S., Jerome, J., & Reghunath, R. (2018). Landscape Analysis Using GIS and Remote Sensing For Assessing Spatial Pattern in Forest Fragmentation in Shendurney Wildlife Sanctuary, Western Ghats, India. *Indian Journal of Ecology*, *45*(2), 299-304.
2. Badhe, Y. P., & Jaybhaye, R. G. (2021). Habitat Suitability Area Analysis for Leopard to Mitigate Human-Wildlife Conflict in Junnar Forest Division of Pune Forest Circle, 9(5), 524-542. doi: 10.12691/aees-9-5-2.
3. Batar, A. K., Watanabe, T., & Kumar, A. (2017). Assessment of land-use/land-cover change and forest fragmentation in the Garhwal Himalayan Region of India. *Environments*, *4*(2), 34.

4. Bennett, A. F. (2003). Linkages in the landscape: the role of corridors and connectivity in wildlife conservation *IUCN Forest Conservation Programme, Conserving Forest Ecosystem Series* (No. 1).
5. Chuvieco, E., & Salas, J. (1996). Mapping the spatial distribution of forest fire danger using GIS. *International Journal of Geographical Information Science*, *10*(3), 333-345.
6. Cushman, S. A., McGarigal, K., & Neel, M. C. (2008). Parsimony in landscape metrics: strength, universality, and consistency. *Ecological indicators*, *8*(5), 691-703.
7. Dewan, A. M., Yamaguchi, Y., & Rahman, M. Z. (2012). Dynamics of land use/cover changes and the analysis of landscape fragmentation in Dhaka Metropolitan, Bangladesh. *GeoJournal*, *77*(3), 315-330.
8. Flowers, B., Huang, K. T., & Aldana, G. O. (2020). Analysis of the habitat fragmentation of ecosystems in Belize using landscape metrics. *Sustainability*, *12*(7), 3024.
9. Fynn, I. E., & Campbell, J. (2019). Forest fragmentation analysis from multiple imaging formats. *Journal of Landscape Ecology*, *12*(1), 1-15.
10. Gascon, C., Williamson, G. B., & da Fonseca, G. A. (2000). Receding forest edges and vanishing reserves. *Science*, *288*(5470), 1356-1358.
11. Hill, J. K., Gray, M. A., Khen, C. V., Benedick, S., Tawatao, N., & Hamer, K. C. (2011). Ecological impacts of tropical forest fragmentation: how consistent are patterns in species richness and nestedness?. *Philosophical Transactions of the Royal Society B: Biological Sciences*, *366*(1582), 3265-3276.
12. Jaybhaye, G. R., Kale, K. P., & Joshi, P. (2016). The Relevance of Geospatial Techniques in the Assessment of Forest Fragmentation of Anjaneri Hill, Nasik District, Maharashtra, India. *J Environ Sci Toxicol Food Technol*, *10*(4).
13. Laurance, W. F. (2000). Do edge effects occur over large spatial scales?. *Trends in Ecology & Evolution*, *15*(4), 134-135.
14. Liu, J., Coomes, D. A., Gibson, L., Hu, G., Liu, J., Luo, Y., ... & Yu, M. (2019). Forest fragmentation in China and its effect on biodiversity. *Biological Reviews*, *94*(5), 1636-1657.
15. Mayaux, P., Holmgren, P., Achard, F., Eva, H., Stibig, H. J., & Branthomme, A. (2005). Tropical forest cover change in the 1990s and options for future monitoring. *Philosophical Transactions of the Royal Society B: Biological Sciences*, *360*(1454), 373-384.
16. McGarigal, K., & Marks, B. J. (1994). FRAGSTATS: spatial pattern analysis program for quantifying landscape structure. Version 2.0. *Forest Science Department, Oregon State University, Corvallis*, 67.
17. McGarigal, K., Cushman, S. A., Neel, M. C., & Ene, E. (2002). FRAGSTATS: spatial pattern analysis program for categorical maps. *Computer software program produced by the authors at the University of Massachusetts, Amherst. Available at the following web site: www. umass. edu/landeco/research/fragstats/fragstats. html*, *6*.
18. Narmada, K., Gogoi, D., & Bhaskaran, G. (2021). Landscape metrics to analyze the forest fragmentation of Chitteri Hills in Eastern Ghats, Tamil Nadu. *Journal of Civil Engineering and Environmental Sciences*, *7*(1), 001-007.

19. Papadimitriou, F. (2009). Modelling spatial landscape complexity using the Levenshtein algorithm. *Ecological Informatics*, *4*(1), 48-55.
20. Rahman, M., Jashimuddin, M., Islam, K., & Nath, T. (2016). Land use change and forest fragmentation analysis: A geoinformatics approach on Chunati Wildlife Sanctuary, Bangladesh. *J Civil Eng Environ Sci*, *2*(1), 020-029.
21. Reddy, C. S., Giriraj, A., Babar, S., Ugle, P., & Sudhakar, S. (2010). Assessment of fragmentation and disturbance patterns in Eastern Ghats: a case study in RV Nagar Range, Visakhapatnam district, Andhra Pradesh, India. *Journal of the Indian Society of Remote Sensing*, *38*(4), 633-639.
22. Riitters, K. H., Wickham, J. D., & Coulston, J. W. (2004). A preliminary assessment of Montreal process indicators of forest fragmentation for the United States. *Environmental Monitoring and Assessment*, *91*(1), 257-276.
23. Riitters, K., Wickham, J., Costanza, J. K., & Vogt, P. (2016). A global evaluation of forest interior area dynamics using tree cover data from 2000 to 2012. *Landscape Ecology*, *31*(1), 137-148.
24. Rose, R. A., Byler, D., Eastman, J. R., Fleishman, E., Geller, G., Goetz, S., ... & Wilson, C. (2015). Ten ways remote sensing can contribute to conservation. *Conservation Biology*, *29*(2), 350-359.
25. Sarkar, A. A. (2019). Geoinformatics Approach to Assess Land Use Dynamic and Landscape Fragmentation Due to Opencast Coal Mining in Raniganj Coalfield, India.
26. Shapiro, A. C., Aguilar-Amuchastegui, N., Hostert, P., & Bastin, J. F. (2016). Using fragmentation to assess degradation of forest edges in Democratic Republic of Congo. *Carbon Balance and Management*, *11*(1), 1-15.

The Indian Geographical Journal
Volume 96 (1) June - 2021, pp 73-78
ISSN 0019-4824

Archives - 1

TOPOGRAPHICAL SURVEYS

from The Indian Geographical Journal Formerly Known as The Journal of The Madras Geographical Association

(Volume XV, 1940, pp.255-259)

By

RAO BAHADUR K. N. NARASIMHACHARY,
Assistant Director of Survey, Madras.

There are different kinds of surveys, such as Marine Surveys, Land Surveys, Geological Surveys, Archaeological Surveys, etc. Land surveys only will be dealt with here. By land surveys is meant the surveys of the features on the earth's *surface.* Land surveys consist of two main branches: -" Topographical Surveys" and "Cadastral Surveys."

TOPOGRAPHICAL SURVEYS

Surveying is the process of accurately determining and recording the features on the earth's surface. Topography is the process of delineating these features in a map. Thus topographical surveying is the process of accurately determining and recording the natural and artificial features on the earth's surface and delineating them in a map. Natural features are rivers, hills, forests, lakes, etc., and artificial features are towns, roads, railways, and in short, whatever features are brought into existence on the earth's surface by human hands.

Only such features as can be legibly shown should be delineated in a map. Thus the amount of features that can be shown in a map depends upon the scale of the map and the nature of the country. In a small scale map - say 1 inch = 4 miles - only important details or features can be shown, whereas in a larger scale map -1 inch = 1 mile - more features can be shown. In a country where features are numerous, only such important ones as can be useful should be shown. The scale on which topographical surveys are carried out is generally 1 inch = 1 mile. Unless the surveys done and the maps prepared are accurate they are not only absolutely of no value but are misleading. Hence, for any work accuracy is most essential. For this purpose topographical surveys consist of two distinct process:-

(1) Triangulation or Trigonometrical Surveys to serve as framework, and

(2) Surveying and delineating the physical features on the framework or the skeleton prepared on the basis of triangulation.

TRIANGULATION

Triangulation is the process of covering the country with a net-work of triangles. Triangulation commences from a measured base and closes on another measured base. The process of triangulation as preliminary to topographical surveys was conceived only in 1735. The first country that was dealt with was South America and that by scientists from France and Belgium. It was only in 1745 the process began in England and it was not until 1792 it was completed. India was not far behind England in the commencement of such surveys. This work was started in India about 1800 and Madras was selected as a place to commence this operation as in the "Madras Observatory" observations for Longitudes and Latitudes were being taken since 1787 and calculated with reference to Greenwich; and thus it would be a proper fixed point to which the values-Longitude and Latitudes of the various triangulation points may be referred so that the map of India when prepared might occupy the place on the globe relative to the other countries. Thus the "Madras Observatory" is very important in the topographical sur- vey of India.

Triangulation consists of three distinct branches:-

(1) Selection of sites for base lines,
(2) Construction of range of triangles, and
(3) Check on triangulation by astronomical observations for Latitude and Longitude.

As already stated triangulation was first commenced in Madras; and a flat place near Madras was selected for a base. This base runs north to south; the north end of the base is in the Race Course and the south end is on the Perumbakkam Hill. The length of the base is 7½ miles. The base is measured with absolute care with chain or steel tapes several times, and after applying corrections for sag, expansion due to temperature, alignment, slope, etc., the measurement is reduced to mean sea level and then utilised in the computation. The accuracy of the measurement of the base is of utmost importance as the measurements of the sides of the range of the triangles depend on this measurement.

Then points are selected for the construction of range of triangles. These points are generally on tops of hills, temple, towers, church steeples and such eminent points so that large triangles may be obtained. Series of triangles are so formed and observations are taken at these points for angles, heights or depressions. The first series or range of triangles started from the Madras base and went westward to Bangalore and closed on a similarly measured base. This series was started by Col. Lambton. The series went up to west coast from Bangalore to Mangalore. Again another series started from Bangalore to Cape Comorin in the south and to Delhi in the north. These series are called Lambton's series. Several other series were also run along the coasts, parallel to and perpendicular to Delhi series, etc. Thus the whole of India was covered with a network of triangles. Between these series several ranges of triangles were also run to cover the country fully.

Accuracy of the triangulation was checked at intervals by observations taken for Latitude and Longitude. For this purpose proper points in the series at intervals were

selected and values of these points were computed direct from these observations and compared with those obtained by the solution of triangles - it must be remembered in passing that these triangles are spherical and not plane - starting from the measured base. Check is also exercised by comparing the measurement obtained by calculation of the base at the terminus of the series with that obtained by actual measurement of the base. For example, for the series from Madras to Bangalore, the length obtained by measurement of the base at Bangalore was compared with that obtained by the calculation of triangles.

As already said above, the Madras observatory was the starting fixed point for calculating the values of the various points fixed by triangulation. With reference to the values of this observatory the values of triangulation points were computed with a view to project or plot them on paper to serve as framework for topographical surveys.

For purposes of survey and issue of maps the whole of India is divided into quarter degree sheets and degree sheets, the former being on scale 1 inch = 1 mile and latter on 1 inch = 4 miles. Topographical survey - field observation - is carried on 1 inch=1 mile scale. Hence a skeleton or a framework showing the triangulation points fixed at the trigonometrically survey is prepared for cach quarter degree on scale 1 inch = 1 mile. It is mounted on a plane table head and taken to field for delineating the physical features in that part of the country.

The plane table is then set up on one of the fixed points and aligned in proper position by sighting other fixed points projected on the sheet. Then the magnetic meridian is marked by placing the magnetic compass on the table to indicate the magnetic north to facilitate the setting up of the table in other places.

Then the delineation of the features of the country round begins. To important physical features rays are drawn from the point after sighting them through the sight-vane. Temple towers in a village site or other prominent buildings, important bends along a road, or rivers etc., are generally sighted. Then the table is taken to another fixed point and another set of rays is struck to the same points. Thus the positions of these points are fixed by intersection and these are verified from a third fixed point. Thus the features are filled in by plane table survey minor details being sketched in by the eye.

Prismatic compass is also freely used in delineating the details. The whole sheet is thus filled in with details or features. The plane table surveyor should not only cover his sheet but also a portion of the sheets adjoining his so that there may be no difficulty in the combination of the sheets for a small scale map - say a degree sheet on 1" = 4 miles. In the case of big lakes and forests the outer boundary is fixed by inter-section, interpolation, compass survey etc. In drawing the contours of hills, clinometer is generally used in ascertaining the heights at different points along the slopes; and contours are marked by a process called stepping. i.e., by marking the intermediate points between two clinometer heights where the slope is roughly uniform. There are different methods of exhibiting the contours by joining the points of equal heights by continuous lines, by vertical hachures, by

layers etc. Thus the whole sheet is completed in field and sent to office for further work of publication.

There was at first no printing office in India. Hence the original plane table sheets had to be sent to England for publication. Even in England there was no Government department for printing maps. The work had to be entrusted to private agencies. Aaron Smith brought out in 1822 his atlas of South India based on Lambton' triangulation on scale 1" = 4 miles in 18 sheets from Krishna to Cape Comorin. The work of publishing the maps of the rest of India was entrusted to Mr. John walker who came of a family of engravers. For the purpose of publishing maps the whole of India Burmah and Ceylon was divided into 177 sheets each sheet t measure 40 inches by 27 inches. It was not until 1868 that arrangements were made to have the publication of maps done in India. By that time Mr. Walker had completed engraving of 84 sheets. Ever since, maps of India are being published systematically. Now degree sheets on scale 1" = 4 miles and quarter degree sheets on scale 1" = 1 mile are being issued and re-edited regularly by the Survey of India Department. In 1877 a very useful and valuable map of India on a scale of 64 miles to an inch was completed. Later on a general map of India on double the above scale was also published.

It may be of some interest to mention here that long before the publication of the map of India based on trigonometrical surveys, Major Rennell, the father of Indian Geography, brought out his famous map of India in 1788. This map was compiled mainly from route surveys carried out by the military staff at various times during the 18th century. When Bengal was acquired by Lord Clive, Major Rennell began his survey of the Province and after completing that survey he returned to England and spent his time in bringing out his atlas of Bengal and his famous map of India. This is the starting point in the history of Indian Government map- making.

In conclusion it may be said that topographical surveys have very materially helped towards the completion of our knowledge of the physical geography of the vast tracts of India. The Indian topographical surveying by theodolite and plane table based on major and minor triangulation cannot be excelled for general accuracy and rapidity. These surveys on scale 1"=1 mile are very useful for engineering, military, administrative and geographical purposes.

Archives - 2

NEWS AND NOTES

from The Indian Geographical Journal Formerly Known as The Journal of The Madras Geographical Association

(Volume XV, 1940, pp.297-298)

Four ordinary meetings of the Madras Geographical Association were held during the third quarter of the year (19). In the first two of them, held on 27th July and 3rd August,

192 respectively, Rao Bahadur K.N. Narasimhacharya (Asst. Director of Survey) delivered two lectures on *Topographical Surveys* and *Cadastral Surveys*.

* * * * *

In the third meeting held on 31st August 193 , Mr. M. Subrahmanya Aiyar spoke on *The Defence of India: A study in Historical Geography*. In the fourth meeting, held on 14th September 193 , Dr. S.M. Hussain Nainar (of the University Department of Oriental Research) delivered a lecture on *Arab Geographers of India*.

* * * * *

In this issue of the Journal (Volume Number), the papers on *Sugar and Red Hills Lake* are concluded: and some of the remaining papers of the Tinnevelly Conference such as Paddy Cultivation, Population, Trade-centres and Communications are included.

* * * * *

The 11th Geographical Conference of the Association will be held at the Rishi Valley in Chittoor District during next (193) summer; and along with it a Summer School of Geography will also be conducted there. It is not yet decided whether there would be a separate Summer School at Saidapet also.

* * * * *

Four important Resolution were passed at the business session of the Tinnevelly Conference, the first of which regarding the conversion of the Associate Members of the Association to Ordinary Members has been approved by the Executive Committee; and steps are being taken to have the rule altered before the next General Body Meeting.

* * * * *

As regards the other three resolutions – about the separate entry of the History and Geography marks in the S.S.L.C. book, the increase of the time for the question paper, and the inclusion of the World Regions for S.SL.C. Public Examination – a copy of the resolution has been submitted to the Board for consideration and necessary action.

* * * * *

We are glad to note that Mr. V. Kalyanasundaram, M.A., L.T., Dip. In Geog., has been appointed Junior Lecturer in the University Department of Geography, Madras.

* * * * *

While none of the Colleges in Madras (except Queen Mary's) has started Geography, it is gratifying to learn that two colleges in Mysore State (at Mysore and

Bangalore) have opened Geography at the Intermediate stage this academic year with the idea of continuing it in the degree course.

* * * * *

Of course, Aligarh stands pre-eminent with its well established M.A. and M.Sc., courses in Geography- thanks to the pioneering zeal and spade work of Dr. I.R Khan of the U.P. Educational Service and untiring zeal and steady work of Dr. S, M. Tahir Rizvi.

* * * * *

Dr. Rizvi is the President of the Geography and Geodesy Section of the Indian Science Congress Session to be held at Benares in January next (193). We are glad to learn that a good number of interesting papers have been contributed for this section- several from this province.

* * * * *

The All-India Federation of Teachers' Associations will meet at Udaipur from 27 to 30th December 1940. Teachers from South India who intend to attend the Benares Session of the Science Congress can make it easily convenient to attend the Udaipur Conference also on their way.

* * * * *

The Indian Geographical Journal
Volume 96 (1) June - 2021, pp 79-79
ISSN 0019-4824

THE INDIAN GEOGRAPHICAL SOCIETY

Department of Geography, University of Madras, Chennai - 600 025

11th IGS Online Talent Test – 2021

Date: 16.05.2021 Time: 11.00 a.m. - 12.00 Noon

WINNERS

Young Geographer (Under Graduate Programme)

The IGS Founder Prof. N. Subrahmanyam Award

Name of the Student	Name of the Institution	Total Score	Marks Scored	Rank
Mala K	Department of Geography Nirmala College for Women, Coimbatore	75	72	I
Nandhini R	Department of Geography Nirmala College for Women, (Autonomous), Coimbatore	75	69	II
Tamil Selvi M	Department of Geography Sri Vijay Vidhyalaya College of Arts and Science	75	66	III
Indu A V	Department of Geography Nirmala College for Women, (Autonomous), Coimbatore	75	66	II
Jenita I	Department of Geography Nirmala College for Women, (Autonomous), Coimbatore	75	66	III
Ashwini M	Department of Geography Sri Meenakshi Govt Arts College w(Autonomous), Madurai	75	66	III
Pooja Panicker	Department of Geography, Tourism and Travel Management, Madras Christian College (Autonomous), Chennai	75	66	III

Young Geographer (Post Graduate Programme)

Prof. A. Ramesh Award

Name of the Student	Name of the Institution	Total Score	Marks Scored	Rank
R.Abarna	Department of Geography, Central University of Tamil Nadu, Thiruvarur 610 005	75	66	I
Neeraja A R	Department of Geography, Central University of Tamil Nadu, Thiruvarur 610 005	75	60	II
Jishna T	Department of Geography, Central University of Tamil Nadu, Thiruvarur 610 005	75	60	II
Nimisha N Menon	Department of Geography, University of Madras, Guindy Campus, Chennai 600 025.	75	59	III

The Indian Geographical Journal
Volume 96 (2) December - 2021, pp 80-98
ISSN 0019-4824

UTILITY OF GRIDDED POPULATION DATASETS IN AGGREGATING CENSUS DATA FOR NON-ADMINISTRATIVE GEOGRAPHIES OF INDIA

Lazar. A[1], N. Chandrayudu[2]

[1]Office of the Registrar General India, New Delhi
[1& 2]Dept. of Geography, College of Sciences, Sri Venkateswara University, Tirupati, Andhra Pradesh, India.

lazar.rgi@gov.in

Abstract

Gridded datasets are very valuable for a wide variety of decision models in environmental, health, and climate change research. As the variables affecting the environment, health, and climate are contiguous, the census datasets published at administrative geographies often may not be usable and require recompilation. The open-access raster datasets of gridded population layers provide ample scope for aggregating census counts for non-administrative geographies. The existing gridded population datasets are prepared at global scale and suitable for national or regional scales, however, downscaling them for smaller non-administrative geographies is challenging and produce less accurate population counts. Thus, an attempt was made to analyse the utility of existing gridded population layers with census counts at different administrative levels (entire India, Karnataka State and Mysore city). Further, the fitness of use for different scales is also analysed. It is observed that the creation of gridded population layers using village/town level census counts along with the covariates improve the accuracy. The publication of census data as a gridded raster layer would greatly help researchers and planners to study the non-administrative geographies of India.

Keywords: Census data, Population grids, Areal weighting, Non-administrative geographies

Introduction

Humans are the most influential factor on earth's planet and will remain so (Palumbi, 2001). The carrying capacity of planet earth is likely to be challenged by the increasing population size, and these challenges pose a more significant threat to ecological balances (Hendry et al., 2017). It is estimated that the interaction of anthropogenic activities is so impactful that they trigger a series of changes and effects on their natural settings. The effects may be on localised, subregional, regional and global scales, depending upon the length and breadth of such collective activities (Gill and

Malamud, 2017). Increasing evidence points out that the effect of anthropogenic processes on the immediate environment can be both intentional and non-malicious, with differing magnitude and scale (RSUSNAS, 2020). It is essential to delineate the geographical spread of common disaster risks induced by these anthropogenic influences based on natural hazards' occurrence, frequency, and intensity and identify the population at risk. Through the evolution of humanity, natural features have often been used for demarcating the land borders, such as political, socio-cultural and legal boundaries. In general, the features like mountain ranges, valleys, watersheds, rivers, streams and major lakes were used as boundaries. During every Population and Housing Census cycle, the National Statistical Organizations (NSOs) produce immense data. The census results show how people and places change over time, how dense they are, where their distribution is likely to cause problems, and so on. The requirements for census count as per the administrative boundary systems for governance and service delivery are met through tabulation plans. However, NSOs do not publish aggregate population counts based on non-administrative boundaries. In addition to administrative boundary-based population counts, aggregated population counts based on natural boundaries is also vital for understanding the influence of human on natural resources. The natural boundaries are defined based on natural processes; in some cases, they stand for millions of years (e.g., physiography). However, they are subject to change due to temperature, rainfall, and soil, which were also used to define them (e.g., rainfall or drought regions). These changes are continuously monitored through scientific measures, and the extent of such boundaries is revised accordingly.

The geographies used for census counts often vary, and it is always a challenge to use them for temporal studies. To overcome this limitation, many methods were proposed in the past. Goodchild and Lam used areal interpolation for aggregating census track level counts to different zone level boundaries (Goodchild and Lam, 1980). Flowerdew et al. used ancillary variables to improve the accuracy of areal interpolation (Flowerdew et al., 1991) by applying Expectation-Maximization (EM) algorithm for the aggregating census counts for parliamentary constituencies. Reibel and Bufalino used street weighted interpolation for population estimation in incompatible zones (Reibel and Bufalino, 2005) by negating the homogeneity assumptions. Langford employed binary dasymetric mapping aided with ancillary covariates generated from multi-spectral satellite imageries (Landsat 7-Enhanced Thematic Mapper) to apply the perceived covariant influence on the presence or absence of population in each pixel (Langford, 2007). In recent studies by Stevens et al. and Lloyd et al., global scale remotely sensed data were used as population covariates, while aggregating pixel-level census counts (Stevens et al., 2015; Lloyd et al., 2017b). Leyk et al. (2019) analysed the global scale gridded population datasets and their fitness for use by comparing the accuracy matrices (Leyk et al., 2019). These recent studies at global scale were made possible due to the High-Performance Computing (HPC) capacities, which allowed researchers to use multivariate geostatistical analysis to model gridded layers by applying several ancillary variables to estimate the pixel level counts.

Gridded population datasets are prepared using various approaches to estimate population counts at grid cells (Lloyd et al., 2017a). Population details with regular grids are

the most appropriate model for assessing population distributions, as they offer several significant advantages over administrative geographies. It extends the utility of census data for various studies. The importance of accurate spatial datasets containing the population traits and distribution is critical in many research domains such as health, economic, and environmental fields across various temporal and spatial scales (Stevens et al., 2015). Despite its legacy of 15 uninterrupted censuses, the Census of India datasets are continued to get published as per administrative boundary systems. However, the research communities interested in non-administrative geographies like physiography, agroclimatic, soil region, watershed, river basin, and earthquake zone, often have to spend lots of time and energy for recompiling the census data as per their region of interest. There were many attempts such as WorldPop (2010, 2015 and 2020), Global Human Settlement Layer (1975, 1990, 2000 and 2015), Gridded population of the World (2000, 2005, 2010, 2015 and 2020) and Global Rural Urban Mapping (1990, 1995 and 2000) to create gridded population raster layers for meeting such demands. However, these attempts disaggregate coarser census geographies to arrive at finer resolutions, causing poor accuracy of census counts at smaller geographies. The present research reviews the utility of existing open-access gridded population datasets and suggests possible methods for publishing similar products using Census of India datasets.

Materials and Methods

Study Area

The present study was attempted at three levels viz., Country (India), State (Karnataka) and City (Mysuru) levels (Fig. 1). India lies entirely in the Northern Hemisphere and extends between 6°45' to 37°06' North latitudes and 68°07' to 97°25' East longitudes covering over an area of 3.28 million sq.km. (ORGI, 1988) and accounts for 2.42% of the world land area with a share of around 18% in the world population. As per the Census of India 2011, India consists of 28 States, 7 Union Territories (Fig.1a), 640 Districts, 5,924 Sub-Districts, 7,933 towns (4,041 Statutory Towns and 3,892 Census Towns) and 6,40,930 Villages. The total population as per Census 2011 is 1,21,05,69,573, out of which 68.8 per cent live in rural and the remaining 31.2 per cent in urban (ORGI, 2013).

The areal extent of Karnataka (Fig. 1b) in terms of latitudinal and longitudinal spread is approximately from 11°35' to 18°29' North latitudes and 74°03' to 78°35' East longitudes. As per Census 2011, The State is divided into 27 districts, 176 Sub-Districts, 347 Towns (including 127 Census Towns) and 29,340 Villages (including 1943 Uninhabited Villages). The total population of the State as per Census 2011 is 6,10,95,297, out of which 61.33 percent live in rural while the rest 38.67 percent in urban.

Mysuru Municipal Corporation (M. Corp.), covering over 90 sq.km of area (Fig. 1c), is the fourth largest city in Karnataka State with a total population of 8,93,062, (ORGI, 2013). The latitudinal and longitudinal spread is approximately from 12°12'09" to 12°21'18" North latitudes and 76°35'56" to 76°42'20" East longitudes. Situated in the southernmost

part of the State, the city has been divided into 65 wards. Though the number of wards has remained unchanged since the 2001 Census, the extent of wards consistently changed between censuses.

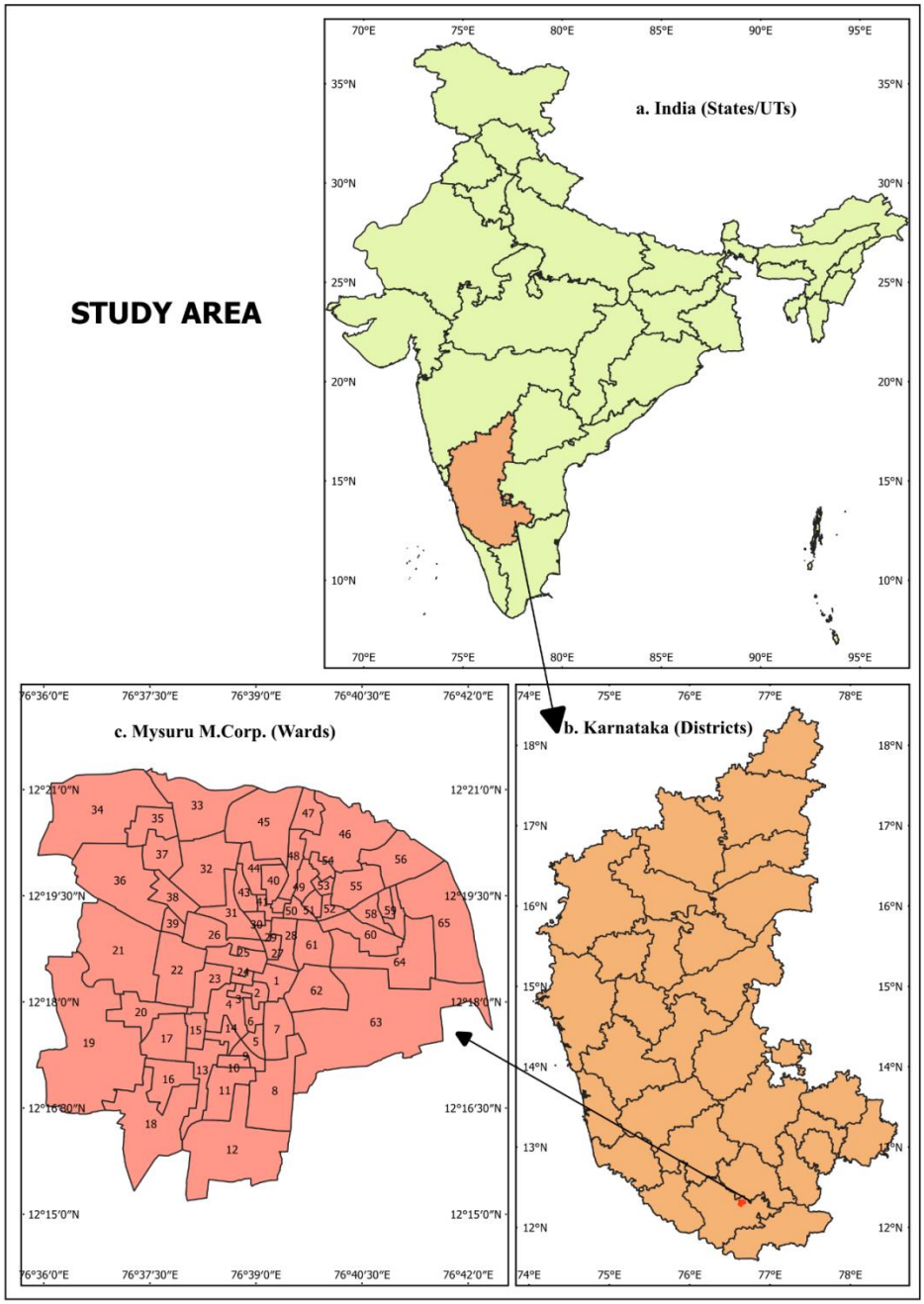

Fig.1: Administrative Units – a) India (States/UTs), b) Karnataka State (Districts), and c) Mysuru M. Corp (Wards)

Data Sources

Several initiatives have produced gridded population datasets (Table 1). In the present study, two open-source gridded population datasets, which were created using Census of India 2011 counts, namely WorldPop 2010 and Gridded Population of the World 2010 (GPW) have been downloaded from Center for International Earth Science Information Network (CIESIN, 2021) (https://sedac.ciesin.columbia.edu) and WorldPop (https://www.worldpop.org) portals. Both the datasets cover the entire country and are comparable to census counts from Census of India 2011. Each of these datasets provides different levels of accuracy and spatial resolution due to the modelling limitations. The WorldPop is a highly modelled gridded dataset created by employing random forest techniques based on multiple ancillary covariates for pixel level distribution of the census counts. It is also having the best spatial resolution of 100 m (3 arc sec) compared to other open-source gridded datasets (Stevens et al., 2015). On the other hand, the GPW datasets was produced at 1k resolution based on areal weighting without any ancillary variable. These raster datasets were clipped at three levels using ArcGIS Pro 2.8 with outline boundaries of India, Karnataka and Mysuru M. Corp. For spatial data analysis, district-level data for India, villages and town-level data for Karnataka State and ward level data for Mysuru have been considered, and the results were generated for each non-administrative geographies.

Table 1: Comparison of global level gridded population raster data sources

Open access Gridded data set	Produced by	Population Type	Method	Ancillary data	Modelling type and Resolution (Grid Cell Size) at Equator	File Types	Year of availability close to 2011 and Access Policy
Gridded Population of the World (GPW) ver. 4	CIESIN	Night-time population (population counted at place of domicile)	Areal weighted	Nil	Nil 1 km.	GeoTIFF, ASCII, and netCDF-4 format	2010 Open
Global Human Settlement Layer – Population (GHS-POP)	JRC and CIESIN	Night-time population (population counted at place of domicile)	Binary Dasymetric	Landsat-derived built up areas	Lightly Modelled 250 m and 1 km	GeoTIFF, Map service	2015 Open
World Population Estimate	ESRI	Mixed (45% of countries are night-time populations), based on available national population estimates, though progressing toward night-time with each new release	Dasymetric	Land cover for urban classes, road intersections, settlement locations, Landscape disturbance equating to human settlement	Highly modelled 250 m	Virtual Image Tile layer	2013 Commercial-ArcGIS Users
WorldPop	University of Southampton & CIESIN	Night-time population (population counted at place of domicile)	Random Forest	Settlement locations & extents, land cover, roads, built-up, health facility location, satellite nightlights, vegetation, topography, refugee camps	Highly modelled 100 m	GeoTiff	2011 Open
LandScan Global Population Datasets	Oak Ridge National Laboratory (ORNL)	Ambient Night-time population	Multi-layered, intelligent dasymetric, spatial modelling approach	Land cover, roads, slope, urban areas, village locations, and high-resolution imagery analysis	Highly modelled 1 km.	GeoTiff	2011 Commercial/Academic Research

Spatial Aggregation

The census counts were generated for selective non-administrative geographies through the zonal statistics algorithm of QGIS 3.16 by overlaying the vector layers on raster datasets. These non-administrative geographies are briefly elaborated in subsequent paras. A comparison of census counts at the district (India) and ward (Mysuru M.Corp) levels were also attempted for analysing the gridded layer fitness for use. Further, zonal statistics for agro-ecological regional level (as a test case) was calculated using vector layer (points) consisting of village/town level Karnataka State census counts and from that of gridded datasets to test the fitness of gridded population layers at a regional scale. Census counts at regional and administrative levels are tabulated and analysed using scatter plots to evaluate the linear relationship between raster datasets and the aggregates generated at regional, district and city scales using the JASP application (Jeffreys's Amazing Statistics Program).

Non-Administrative Geographies of India

The boundaries are defined and used by humans to meet specific purposes, and they are most often the conceptual toolkit used by the researchers for their enquiries (Lamont and Molnar, 2002). The boundary system can be natural, for example, boundaries created based on topographic features like elevation, soil and vegetation etc., or can be artificial based on political authority such as administrative land regions, cultural or socio-economic. The boundary systems created based on physiographical features are more visible than the artificial ones. In this study, except those created for political authority, all remaining boundary systems are treated as non-administrative geographies. Among the non-administrative boundaries, the four important geographies, namely, physiographic regions, agro-ecological regions, river basins and earthquake zones (Fig. 2) were chosen to assess the utility of gridded population datasets. The characteristics of these non-administrative geographies are briefly discussed in the following sections.

Physiographic Regions: The physiographical divisions of India were first attempted by Holdich in 1904, which is somewhat a broad geographical zone of India based on geological information only (Holdich, 1904). An attempt by Stamp (1922-24) produced a more substantive division named as 'natural regions' based on physiographic structure for three macro-regions and 22 subregions (Stamp and Dudley, 1928). Later, the regional divisions proposed by Spate were empirically derived and divided India into 35 regions of the first order (under the three macro-regions and excluding the islands), 74 second-order divisions with 225 subdivisions (Spate and Learmonth, 1954). During the Census 1981 phase, more profound work on regional divisions based on physiography, geological structure, climatic conditions, and soils was attempted and mapping all these regions using village/town level boundaries was also completed. In this frame, four Macro, 28 Meso (State boundaries used to split the 4 Macro regions) and 101 Micro regions (grouping Meso regions by using district boundaries) were outlined for the country (ORGI, 1988). Sub-micro regions were delineated within this frame of micro-regions by considering the village/town

boundaries. The analysis for the present research was done using the four Macro regions (Fig. 2a).

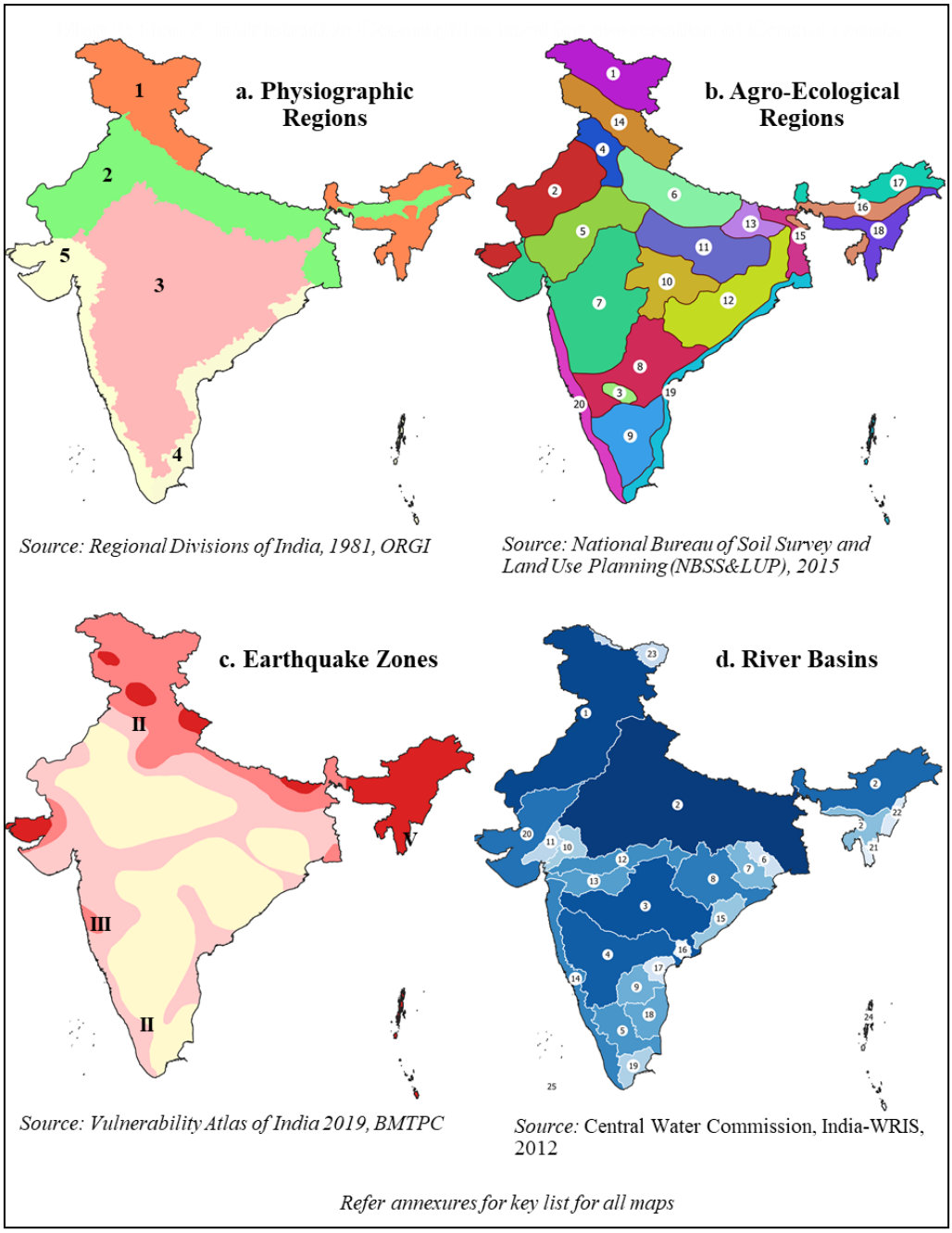

Fig. 2: Non-administrative geographies used for aggregation of census counts – a) Physiographic Regions, b) Agro-Ecological Regions, c) Earthquake Zones, and d) River Basins

Agro-Ecological Regions: The Agro-Ecological Regions (AER) are carved out based on agroclimatic conditions derived by superimposing climate parameters on landforms and soils. As the climate and soils are the modifiers of the length of the growing period, the agro-ecological regions are critical aspects for studies on agriculture-related issues. Krishnan and Singh (1968) delineated soil climatic zones by superimposing moisture index and mean air temperature isopleths on broad soil types of India (Virmani et al., 1980). The attempt by Murthy and Pandey (1978) used physiography, climate (rainfall and potential water surplus/deficit), major soils and agricultural regions. During 1988, under the Planning Commission, a similar attempt was made and 15 agroclimatic regions with 73 sub regions were delineated. The refined work of the National Bureau of Soil Survey and Land Use Planning (NBSS&LUP) has divided the country into 20 agro-ecological regions (AERs). The analysis for present research was done using the 20 AERs (Fig. 2b) defined by the NBSS&LUP (Mandal et al., 2014).

Earthquake Zones: As per the seismic zoning map of the country (BMTPC, 2019), the total area is classified into four seismic zones (Medvedev–Sponheuer–Karnik scale). Zone V is seismically the most active region, while zone II is the least. Approximately 11% area of the country falls in zone V, 18% in zone IV, 30% in zone III and remaining in zone II. For the present study, the analysis of the gridded population layer was done as per earthquake zone boundaries delineated in the Vulnerability Atlas of India, 2019 (Fig. 2c).

River Basins: The rivers are the soul of civilisation and a vital geophysical ecosystem engine that support and sustain life on earth. The term "river basin" encompasses many sub-systems such as surface (soil and land resources), subsurface water resources, wetlands and associated ecosystems, including those coastal and nearshore marine systems. The systematic delineation of river basins in India was attempted in 1949 by the erstwhile Central Waterways, Irrigation and Navigation Commission (now Central Water Commission). CWC has delineated 20 river basins, comprising 12 major river basins and 8 composite basins, using Survey of India (SOI) toposheets and contour maps. CWC revised the basin's boundaries and classified 32 basins, 94 sub-basins, and 3448 watersheds in the latest available data. The study used River Basin Atlas of India (Fig. 2d) sourced from the India-WRIS portal (India-WRIS, 2012) for river basin level analysis .

Comparisons of gridded datasets

The gridded population datasets were compared with the Administrative Atlas of India 2011 published by Office of the Registrar General, India, for ascertaining fitness of their use. The Gridded Population of World (GPW) (Fig. 4a) was created using simple areal weighting method to distribute the census counts proportionately and equally across the all grids (at given scale) (Fig. 3a). Whereas Global Human Settlement Layer (Fig. 4c) and World Population Estimates (Fig. 4d) are derived weights based on built-up and land use through dasymetric techniques (Fig. 3b & 3c). Similarly, the WorldPop dataset was created using dasymetric model based on statistically derived weights from multiple ancillary

variables for assigning census counts to each of the grids (Fig. 3d). As the gridded population layers (WorldPop and GPW) used Census of India 2011 counts, these two datasets were selected for the study for comparison. The village / town layers (Fig. 5b polygon centroids) sourced from Karnataka State Remote Sensing Application Centre were used to calculate zonal counts for agro-ecological regions (Fig. 5a) and used to compare with gridded datasets at state level. The ward level boundaries of Mysuru M. Corp. were used to compare ward level census counts from gridded datasets. It is important to note that variations may arise in population counts between GPW and WorldPop raster datasets due to limitation of zonal statistics algorithm. The over counts are possible due to the cells along the shared borders of zonal boundaries are also get counted more than once (called as edge effect), producing over representation of cell values across shared zonal boundaries. There is also possibility for over counts due to misalignment of boundaries used for creating gridded layers.

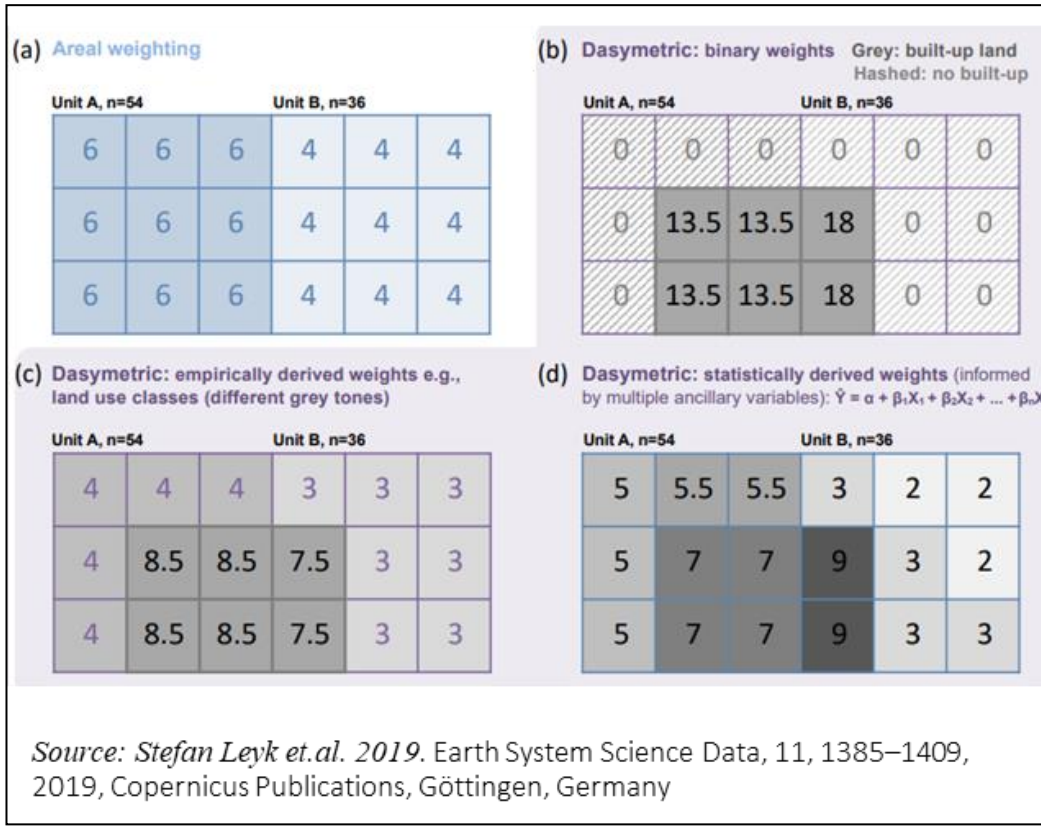

Fig. 3: Different statistical approach for assigning census population counts to grid cells – a) Areal Weights, b) Dasymetric: Binary Weights, c) Dasymetric: Empirically derived Weights, and d) Dasymetric: Statistically derived Weights

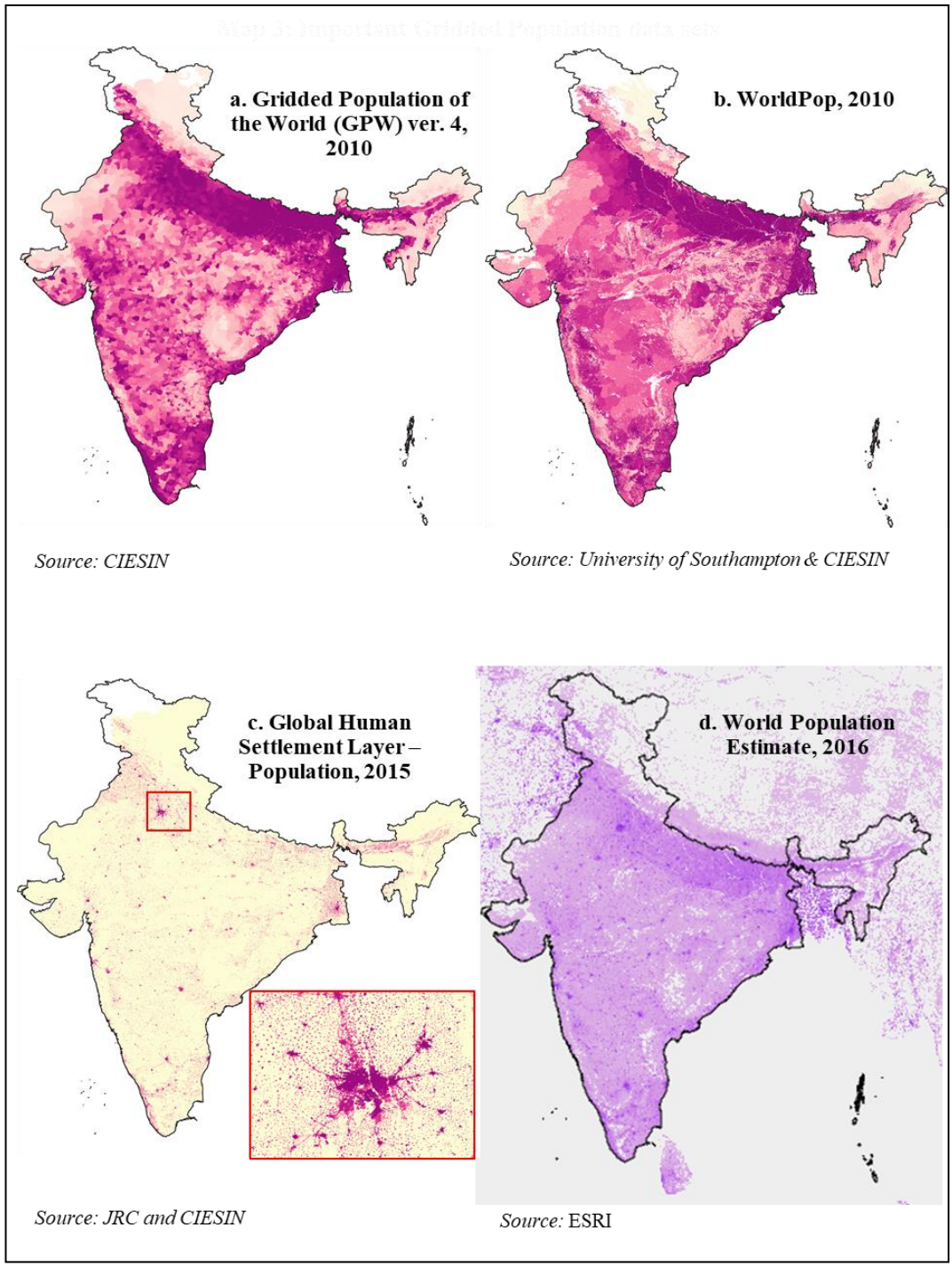

Fig. 4: Gridded population datasets of India – a) Gridded Population of the World, b) World Population, 2010, c) Global Human Settlement Layer – Population, 2015, and d) World Population Estimate, 2016

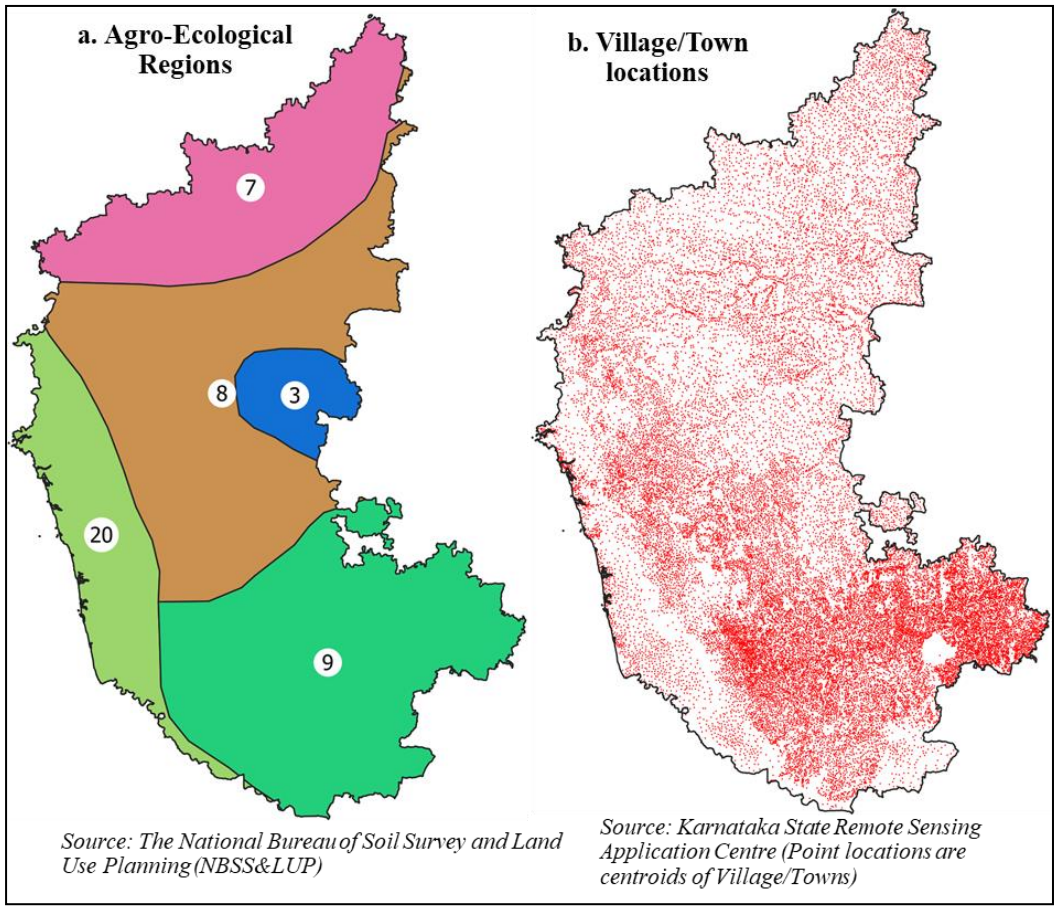

Fig. 5: (a) Agro-ecological regions of Karnataka State and (b) Location (centroids) points of villages and towns in Karnataka State

Results and Discussion

Aggregates of census counts for physiographic regions: The aggregates of Census count for four of the non-administrative geographies are presented in Tables 2 to 5. The highest proportion of the population lives in the Great Plains (GWP: 40.63%, WorldPop: 41.07%) and the Deccan Plateau (GWP: 36.20%, WorldPop: 36.18%). These two physiographic regions constitute 2.2 million sq.km of area (Table 2) and more than 3/4th of population of the country. The smallest proportion of population live in the Northern Mountain region (GWP: 4.72%, WorldPop: 4.29%). The difference in counts between GPW and WorldPop is less than half a percent and the highest is observed in the Northern Mountain region (0.43%)

Aggregates of census counts for earthquake zones: About 6.4% of people live in very high earthquake zone V (GWP: 6.46%, WorldPop: 6.42%), and near about 20% of people live in moderately high earthquake Zone IV (Table 3). The remaining 73% people

live in Zone III and II, which accounts for 72 percent (1.37 million sq.km.) of area in the country. The difference in census counts between GPW and WorldPop is less than half percent across all zones, and the highest could be observed in Zone II (0.30%).

Table 2: Aggregate census counts from gridded population data sets for physiographic regions of India

Physiographic Regions	Area	Aggregate population			
		GPW	Percentage share	WorldPop	Percentage share
Northern Mountains	5,42,819	5,82,82,328	4.72	5,42,48,996	4.29
The Great Plains	7,30,116	50,13,10,467	40.63	51,88,99,623	41.07
Deccan Plateau	15,20,788	44,65,88,010	36.20	45,70,85,023	36.18
Eastern Coastal Plains and Islands	1,89,519	9,34,13,365	7.57	9,50,55,985	7.52
Western Coastal Plains and Islands	2,90,926	13,41,68,782	10.87	13,81,49,696	10.93

Table 3: Aggregate census counts from gridded population data sets for earthquake zone of India

Earthquake Zone	Area	Aggregate population			
		GPW	Percentage share	WorldPop	Percentage share
II	13,73,944.32	40,07,60,240	32.48	41,41,89,957	32.78
III	9,83,973.32	50,24,97,084	40.73	51,26,70,815	40.58
IV	5,50,630.66	25,08,40,213	20.33	25,54,38,386	20.22
V	3,65,641.38	7,96,69,538	6.46	8,11,43,918	6.42

Aggregates of census counts for agro-ecological regions: Among the agro-ecological regions, the proportion of people living in the Northern Plain Middle Gangetic Plain is 16% and hot semiarid with moderately deep black soils region is 12%. Together, these two regions constitute more than 1/4th of population in the country (Table 4). Other significant proportion of population (between 5-10%) live in regions, which are hot semiarid spread over Deccan and hot subhumid spread over the coastal areas.

Aggregates of census counts for river basins: Among the river basins (Table 5), the Ganga basin alone constitutes around 44% of population in the country, and constitute 1/4th of the geographical area of the country (25.88%). Other river basins with significant share of population are Krishna (7%), Indus and West flowing rivers from Tapi to Kadri (around 6.5%) and Godavari Basins (6%). Remaining 20 basins have proportion of population less than 5 percent and all of them sum up to around 30 percent of population of the country and thus, top five river basins alone constitute 70 percent of country's population.

Table 4: Aggregate census counts from gridded population data sets for agro-ecological regions of India

AER Code	Agro-Ecological Region Name	Area in Sq.Km.	Aggregate population			
			GPW	Percentage share	WorldPop	Percentage share
1	Western Himalayas, cold arid eco-region with shallow skeletal soils	1,77,707	14,94,050	0.12	14,52,676	0.11
2	Western plains and Kutch Peninsula, hot arid ecoregion with desert saline soils	2,54,302	3,61,23,607	2.93	3,75,88,078	2.98
3	Deccan plateau, hot arid eco-region with mixed red and black soils	21,398	54,32,006	0.44	55,76,032	0.44
4	Hot semi-arid ecoregion with alluvium-derived soils	68,710	5,52,71,974	4.48	6,09,58,922	4.82
5	Deccan plateau, hot arid eco-region with mixed red and black soils	2,25,847	8,02,71,130	6.51	8,12,01,886	6.43
6	Northern Plain Middle Gangetic Plain with hot semiarid to sub humid climate and alluvial and Tarai soils	2,10,767	19,82,73,220	16.07	20,02,69,014	15.85
7	Hot Semiarid with moderately deep black soils	4,90,714	14,85,08,357	12.04	15,55,97,894	12.32
8	Deccan Plateau, hot semiarid eco-region with mixed red and black soils	2,48,400	7,17,70,347	5.82	7,52,77,639	5.96
9	Deccan Plateau, hot semiarid eco-region with red loamy soils	1,74,563	7,51,26,347	6.09	7,76,30,102	6.14
10	Hot sub humid eco-region with moderately deep black soils	1,55,184	4,03,13,460	3.27	4,10,88,435	3.25
11	Eastern Plateau (Bundelkhand Upland) hot sub humid eco-region with red and yellow soils	2,18,466	6,81,94,299	5.53	6,82,09,366	5.40
12	Eastern Plateau, hot sub humid eco-region with red and lateritic soils	2,66,098	6,85,11,715	5.55	7,15,24,174	5.66
13	Northern Plains (Lower Gangetic) hot, sub humid ecoregion with alluvial soils	57,540	7,17,58,182	5.82	7,29,69,089	5.78
14	Western Himalayas, warm to hot sub humid to humid sub montane shallow and skeletal hill soils	1,52,370	3,08,47,048	2.50	2,68,39,344	2.12
15	Bengal basin, hot, sub humid eco-region with loamy to clayey alluvial soils	51,929	7,47,24,799	6.06	7,59,77,269	6.01
16	Assam and North Bengal Plain, warm humid to per humid eco-region with alluvial soils	94,175	4,52,96,222	3.67	4,73,35,927	3.75
17	Eastern Himalayas, warm per humid eco-region with shallow and skeletal red soils	86,841	41,56,869	0.34	34,88,424	0.28
18	North Eastern hills (Purvanchal), warm per humid ecoregion with red and yellow soils	99,690	1,25,79,947	1.02	1,20,56,419	0.95
19	Eastern Coastal Plains and Island of Andaman and Nicobar, hot sub humid	1,17,721	7,34,46,547	5.95	7,48,18,023	5.92
20	Western Ghats Coastal Plains and Western Hills with red and lateritic and alluvium derived soils	1,01,768	7,16,66,950	5.81	7,35,84,363	5.82

Note: Due to edge effect, the population counts shall exceed the total population of the country.

Table 5: Aggregate census counts from gridded population data sets for the major river basins of India

WRIS Code	Name of the River Basins	Area in Sq.Km.	Aggregate population			
			GPW	Percentage share	WorldPop	Percentage share
1	Indus Basin	4,67,069	8,33,22,851	6.75	8,21,58,512	6.50
2a	Ganga Basin	8,39,786	53,84,94,209	43.65	55,49,63,879	43.92
2b	Brahmaputra Basin	1,92,743	4,11,82,969	3.34	4,11,26,851	3.26
2c	Barak & Others	49,083	1,00,87,177	0.82	99,19,183	0.79
3	Godavari Basin	3,10,257	7,35,57,884	5.96	7,45,85,567	5.90
4	Krishna Basin	2,60,212	8,54,56,361	6.93	8,91,32,362	7.05
5	Cauvery Basin	85,865	4,23,64,386	3.43	4,38,08,981	3.47
6	Subarnarekha Basin	26,721	1,20,21,764	0.97	1,22,52,814	0.97
7	Brahmani & Baildoni Basin	53,497	1,42,51,203	1.16	1,44,27,585	1.14
8	Mahanadi Basin	1,44,300	4,02,78,734	3.26	4,00,96,246	3.17
9	Pennar Basin	55,075	1,16,86,357	0.95	1,26,75,950	1.00
10	Mahi Basin	39,659	1,64,87,177	1.34	1,61,96,850	1.28
11	Sabarmati Basin	31,853	1,69,78,424	1.38	1,72,36,113	1.36
12	Narmada Basin	95,612	2,07,40,284	1.68	2,08,76,296	1.65
13	TapiBasin	65,524	2,26,64,944	1.84	2,19,19,670	1.73
14	West Flowing River from Tapi to Kadri	1,14,027	7,96,40,162	6.46	8,37,91,018	6.63
15	East Flowing Rivers between Mahanadi and Pennar	48,477	1,69,32,186	1.37	1,73,57,052	1.37
16	East flowing rivers between Godavari and Krishna	10,691	49,57,686	0.40	54,15,342	0.43
17	East flowing rivers between Krishna and Pennar	23,723	67,52,406	0.55	66,56,078	0.53
18	East Flowing Rivers between Pennar and Cauvery	64,096	4,03,78,277	3.27	4,17,69,403	3.31
19	East Flowing Rivers between Cauvery and Kannyakumari	38,312	1,69,83,703	1.38	1,72,17,482	1.36
20	West Flowing Rivers of Kutch and Saurashtra Including Lun	1,91,492	3,49,07,526	2.83	3,61,54,765	2.86
21	Minor Rivers draining into Myannmar and Bangladesh	12,645	5,05,198	0.04	5,25,889	0.04
22	Minor rivers draining into Myanmar	17,627	27,42,369	0.22	27,77,954	0.22
24	Drainage Area of ANI	6,842	3,37,271	0.03	3,45,273	0.03
25	Drainage Area of Lakshadweep	30	40,624	0.00	52,210	0.00

Comparisons of gridded population datasets with census counts: The comparisons of gridded layers done by matching of census counts published by ORGI (ORGI, 1988; ORGI, 2013) at the levels of districts (India) and wards (Mysuru M. Corp).

The dot plots created using ORGI District level counts and counts derived from gridded datasets exhibit relatively strong relationship (GPW: 0.9672, WorldPop: 0.9726). However, there are more outliers in GPW dataset than in the WorldPop (Fig. 6a & 6b). This is so because, the GPW was created using areal interpolation without covariates, whereas the WorldPop was created using multiple ancillary variables for estimating and distributing census counts.

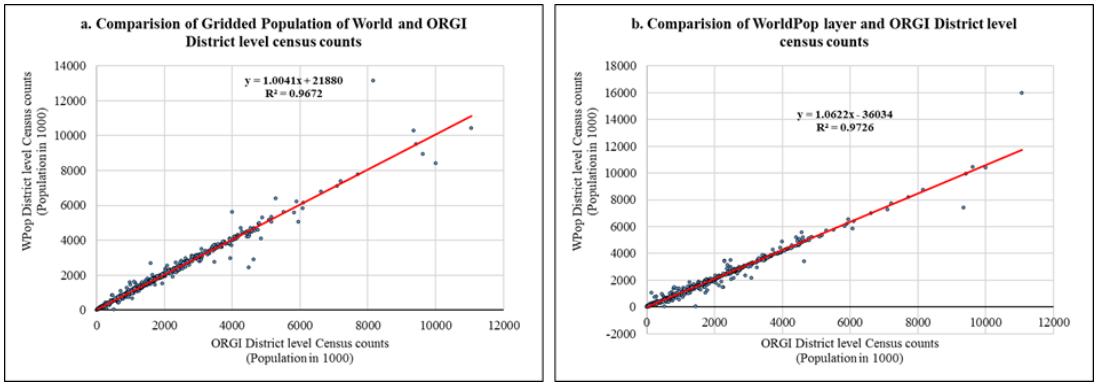

Fig. 6: a) Comparison between ORGI district level census counts and gridded population layers, and b) Comparison between ORGI district level census counts and World population layer

The ward level aggregates created from both GPW and WorldPop exhibit insignificant relationship (Fig. 7a & 7b) with ward level census counts from ORGI. Though insignificant, yet the WorldPop shows slightly better fit (R^2: 0.0202) than GPW (R^2: 0.0071) due to better pixel level resolution. As the distribution of census counts for the WorldPop dataset was created based on the built-up, land cover and other covariates, have profound control on the probability of assigning Census counts for known urban clusters. Yet, using these two datasets for ward level geographies that are smaller than sub-district level geographies may not yield accurate results, hence not fit for use.

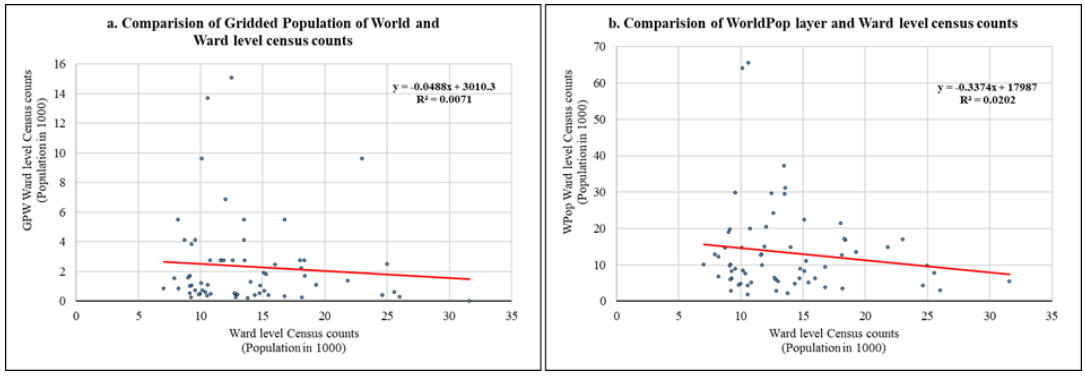

Fig. 7: a) Comparison of ORGI Mysuru M.Corp. ward level units census counts with the gridded population layers, and Comparison of ORGI Mysuru M.Corp. ward level units census counts with the World population layer

Improving accuracy of aggregates

CIESIN advices to keep the aggregate geographies either equal to that of geography used for modelling the grids or at least one step higher. As the sizes of the non-administrative geographies are higher than the sub-district level, both datasets are good enough to produce the census counts for non-administrative geographies of higher orders

i.e., above the size of districts. However, smaller geographies need better granularity of administrative geographies for creating gridded population raster datasets. In addition to increasing the granularity of lower-level administrative geographies, the accuracy can be further improved by using ancillary covariates, while distributing the census counts at village / town levels. As the granularity increases along with use of covariates such as built-up, land use, road density and night-time light data derived from remote sensing platforms, it is feasible to create more accurate gridded population datasets for India. By producing gridded population datasets with good accuracy, the population data gap can be filled in various domains of research such as climate change, public health, disease modelling, agriculture, disaster risk, impact assessment and so on.

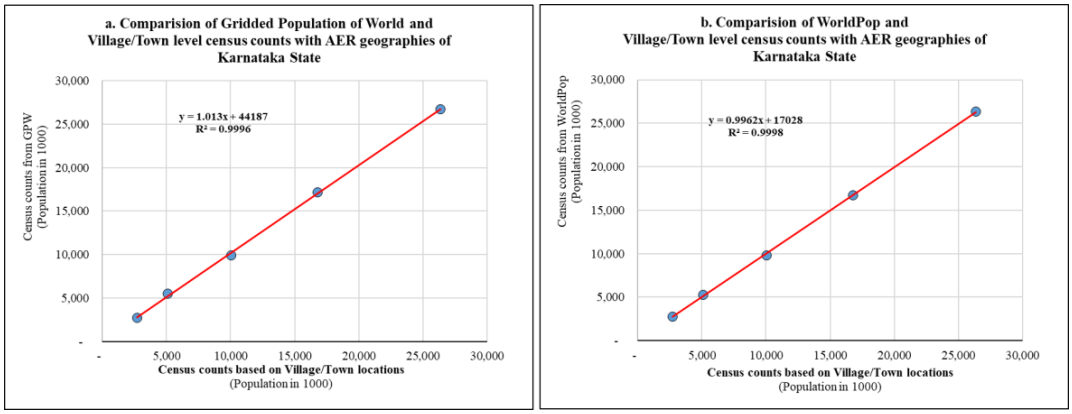

Fig. 8: a) Comparison between village/town level census counts with AER geographies of Karnataka State and gridded population of World, and b) Comparison between village/town level census counts with AER geographies of Karnataka State and World population layer

Conclusion

The evaluation of existing open access gridded population datasets for recompiling census counts for non-administrative geographies at different scales, attempted through zonal summary statistics algorithms in QGIS application. The comparisons of GPW (resolution 1K) and WorldPop (resolution 100 m) shows that there is a strong linear relationship (R^2 0.9334) between these datasets even though the latter was created using simple areal weighting method. However, the comparison of aggregates from gridded population datasets at district, city, village/town and ward level reveals that there are accuracy issues below the sub-district levels.

However, these accuracy issues can be addressed by creating gridded population layers using village/town level census counts along with the covariates. This approach is demonstrated at village/town level for the different agro-ecological geographies of Karnataka State. The results show perfect linear relationship (GPW: R^2 0.9996, WorldPop: R^2 0.9998) with the census counts (Table 6). It is feasible for the ORGI to generate such datasets for the larger interest of the research communities instead of merely providing

standards census tables. The gridded datasets can eliminate the amount of time and effort required for recasting census data for non-administrative boundaries. In addition, the preparation of micro-level gridded datasets can enhance the utility of census counts and will be very useful for all micro-level studies using non-administrative geographies.

Table 6: Comparison of GPW, WorldPop and actual census counts for agro-ecological regions of Karnataka State

Region Code	Agro-Ecological regions	Aggregated Population created from			Variation from aggregates of Village/Town level units (ORGI)	
		WorldPop	GPW	Village/Towns	WorldPop	GPW
3	Deccan plateau, hot arid eco-region with mixed red soil and black soils	27,54,962	27,06,542	27,39,572	-0.6	1.2
7	Hot Semiarid with moderately deep black soils	98,21,713	99,44,554	1,00,27,006	2.0	0.8
8	Deccan Plateau, hot semiarid eco-region with mixed red and black soils	1,67,40,429	1,71,72,664	1,67,92,564	0.3	-2.3
9	Deccan Plateau, hot semiarid eco-region with red loamy soils	2,63,31,258	2,67,35,340	2,63,66,025	0.1	-1.4
20	Western Ghats Coastal Plains and Western Hills with red and lateritic and alluvium derived soils	52,39,992	54,87,572	51,06,978	-2.6	-7.5
Total		6,08,88,354	6,20,46,672	6,10,32,145	0.2	-1.7

Note: Due to edge effect, the population counts shall exceed the total population of the State

References

1. BMTPC (2019). *Vulnerability Atlas of India (Third Edition).* Building Materials & Technology Promotion Council (BMTPC), New Delhi.
2. CIESIN (2021). *Documentation for the Gridded Population of the World, Version 4*. Center for International Earth Science Information Network (CIESIN), Columbia University. (Retrieved from https://sedac.ciesin.columbia.edu/binaries/web/sedac/collections/gpw-v4/gpw-v4-documentation-rev11.pdf)

3. Dudley, S.L. (1928). The natural regions of India. *Geography*, 14(*6*), 502-506.
4. Flowerdew, R., Green, M. and Kehris, E. (1991). Using areal interpolation methods in geographic information systems. *Papers in Regional Science,* 70(*3*), 303-315.
5. Gill, J.C. and Malamud, B.D. (2017). Anthropogenic processes, natural hazards, and interactions in a multi-hazard framework. *Earth-Science Reviews*, 166(*2017*), 246-269.
6. Goodchild, M.F. and Lam, N.S. (1980). Areal interpolation: A variant of the traditional spatial problem. *Geo-Processing,* 1, 297-312.
7. Hendry, A.P., Gotanda, K.M. and Svensson, E.I. (2017). Human influences on evolution, and the ecological and societal consequences. *Philosophical Transactions B*, 1-13. (https://doi.org/10.1098/rstb.2016.0028)
8. Holdich, T.H. (1904). *The Regions of the World-India.* Oxford University Press, London.
9. India-WRIS (2012). *River Basin Atlas of India.* WRIS and RRSC-West, NRSC-ISRO, Jodhpur.
10. Krishnan, A. and Singh, M. (1968). Soil climatic zones in relation to cropping patterns. *Proceedings Symposium on Cropping Patterns*, Indian Council of Agricultural Research, New Delhi, 172-185.
11. Lamont, M. and Molnar, V. (2002). The study of boundaries in the social sciences. *Annual Review of Sociology*, 28, 167-195.
12. Langford, M. (2007). Rapid facilitation of dasymetric-based population interpolation by means of raster pixel maps. *Computers, Environment and Urban Systems,* 31(*1*), 19-32.
13. Leyk, S., ….. and Pesaresi, M. (2019). The spatial allocation of population: a review of large-scale gridded population data products and their fitness for use. *Earth System Science Data,* 11(*3*), 1385–1409.
14. Lloyd, C.D., Catney, G., Williamson, P. and Bearman, N. (2017a). Exploring the utility of grids for analysing long term population change. *Computers Environment and Urban Systems*, 66, 1-12.
15. Lloyd, C.T., Sorichetta, A. and Tatem, A.J. (2017b). High resolution global gridded data for use in population studies. Scientific Data, 4-170001, DOI: 10.1038/sdata.2017.1.
16. Mandal, C., ….. and Thakre, S. (2014). Revisiting agro-ecological sub-regions of India – A case study of two major food production zones. *Current Science,* 107(*9*), 1519-1536.
17. Murthy, R.S. and Pandey, S. (1978). Delineations of agro-ecological regions of India. *In Paper presented in Commission V, 11th Congress of ISSS*, Edmonton, Canada, 19-27.
18. ORGI (1988). *Regional Divisions of India-A Cartographic Analysis.* Office of the Registrar General India, New Delhi.
19. ORGI (2013). *Primary Census Data Highlights - India.* Office of the Registrar General India, New Delhi.
20. Palumbi, S.R. (2001). Humans as the World's greatest evolutionary force. *Science*, 293(*5536*): 1786-1790. DOI: 10.1126/science.293.5536.1786.
21. Reibel, M. and Bufalino, M.E. (2005). Street-weighted interpolation techniques for demographic Street-weighted interpolation techniques for demographic. *Environment and Planning A Vol(37)*, 129-139.

22. RSUSNAS (2020). *Climate Change-Evidence and Causes- Update 2020 - An overview from the Royal Society and the U.S. National Academy of Sciences (RSUSNAS).* The National Academy of Sciences, Washington and The Royal Society, London.
23. Spate, O.H.K. and Learmonth, A.T.A. (1954). *India and Pakistan: A general and regional geography.* Methuen, London.
24. Stevens, F.R., Gaughan, A.E., Linard, C. and Tatem, A.J. (2015). Disaggregating census data for population mapping using random forests with remotely-sensed and ancillary data. *PLOS ONE*, 10(*2*): e0107042.
25. Virmani, S.M., Sivakumar, M.V.K. and Reddy, S.J. (1980). Climatic classification of semi-arid tropics in relation to farming systems research. *Consultants' Meeting on Climatic Classification,* ICRISAT (International Crops Research Institute for the Semi-Arid Tropics), Patancheru, 59-88.

The Indian Geographical Journal
Volume 96 (2) December - 2021, pp 99-112
ISSN 0019-4824

IDENTIFICATION OF GROUNDWATER VULNERABLE ZONES THROUGH GEOGRAPHICAL INFORMATION SYSTEM (GIS) IN NOYYAL RIVER BASIN, TAMIL NADU

R. Madhumitha, K. Kumaraswamy[1] and Deepthi N.[2]

[1] Department of Geography, Bharathidasan University, Tiruchirappalli, India
[2] Department of Geography, Central University of Tamil Nadu, Thiruvarur, India
Corresponding E-mail: kkumargeo@gmail.com

Abstract

The Noyyal basin is one of the active industrial regions in Tamil Nadu facing a critical groundwater contamination. The vulnerability zones of the basin are delineated by combining the physical factors (depth to the groundwater level, net recharge, aquifer media, soil texture, topography, impact of the vadose zone, hydraulic conductivity, lineament density, proximity from the river) and environmental factors (land use/land cover, population density, and source of contamination). All the selected factors and their sub-classes are weighted and ranked based on their tendency to contaminate the groundwater resources. Using these factors geospatial layers are generated which in turn integrated through Geographical Information System (GIS) to generate groundwater vulnerability zones (at village level). The result shows that 18 percent of the area is highly vulnerable, and 31 percent is moderately vulnerable to contamination. The spatial result is explicit that the villages present adjoining the main river are under moderate to high-vulnerability than other areas.

Keywords: Physical Factors, Environmental Factors, DRASTIC, Vulnerable Zone, Geographical Information System

Introduction

Groundwater is contaminated when the polluted water infiltrates through the soil and rocks, and eventually reaches the aquifer. Vulnerability assessment is one of the basic steps for monitoring and managing groundwater resources, and the factors of groundwater contamination can be identified from the source, pathway, receptor, and consequence (Zhang et al., 2013). The source of contamination is generally of both natural and anthropogenic origins. The transmission pathway of contaminants to the aquifer is on its aquifer medium, soil, fractures, etc. The people and environment are the receptors of contaminants. Consequences of the groundwater contamination are human health related issues, degradation of groundwater quality, agricultural productivity, soil infertility, etc.

Groundwater vulnerability is defined as the tendency of the aquifer for getting contaminated, and the zones of contamination can be delineated with vulnerability map

(Ducci,1999). The physically vulnerable regions can be delineated from the hydro-geological factors of the basin that controls the groundwater contamination. Index-based methods are commonly used for vulnerability zone delineation, such as SINTACS DRASTIC, DRIST, GOD, SEEPAGE, etc. to assess the intrinsic vulnerability of the groundwater (Al-Amoush et al., 2010; Muruganandam, 2015; Lathamani et al., 2015; Vaezihir and Tabarmayeh, 2015; Sakala et al., 2019). The DRASTIC model by Aller et al. (1987) is a relatively more reliable method to delineate the intrinsic groundwater vulnerability using the Geographical Information System (GIS). The model considers the factors such as Depth to the water level, net Recharge, Aquifer media, Soil, Topography, vadose zone Impact, and hydraulic Conductivity. Later, several modified DRASTIC models were adapted by the researchers to study the specific vulnerabilities by adding appropriate parameters. The pesticide DRASTIC model is used to study pollutant-based contamination (Meenakshi and Ganesh, 2019). Differences in vulnerability with distance from pollution sources such as industrial plants (Aylin et al., 2001) or landfill sites (Elliott et al., 2001) are important factors in environmental studies. The Geographical Information System (GIS) is an excellent tool for water resource management studies, and the integration of layers not only aids the visualisation but also makes the overall analysis more sound, objective, and simple (Simsek and Gunduz, 2007). Delineating the vulnerability zones using GIS is very much needed for the Noyyal River basin as it is an active industrial region. Noyyal basin is located in the western part of Tamil Nadu state, originates from Velliangiri hills in the Western Ghats, and flows through four districts- Coimbatore, Tiruppur, Erode, and Karur. Noyyal is the right bank tributary that drains a total area of 3,500 km^2 and runs 180 km long to drain into the River Cauvery at Noyyal village, Karur District. The Noyyal basin lies between 10º54’ N to 11º19’ N latitudes and 76º39’ E to 77º55’ E longitudes. The basin takes over a fern leaf-like structure with a broad central part and narrow edges (Figure 1). The climate of the region is dry and warm, the natural flow of the Noyyal is seasonal and occurs only during the north-east monsoon months, but the river exhibits perennial flows in a few stretches because of the sewage from the urban and industrial centres, and returns the flow from Lower Bhavani Project. The lithology of the area comprises hard rock and unconsolidated formations. Hard consolidated rocks cover a significant part of the basin, mainly as weathered and fractured granite gneisses, granites, and charnockites. Red sandy and red loamy are the dominant types of soil. The basin is highly urbanised with a population density of 120 people/km^2 in the rural settlements and 1000 people/km^2 in urban centres. The basin is the cotton belt of Tamil Nadu, with favourable geographic and climatic conditions that shelter the hosiery industries. Urban centres-Coimbatore and Tirupur are the industrial hubs with most textile industries. Land use shrinks from agriculture to industrial and urban, with rural to urban migration showing the changing nature of the occupation. Assessing groundwater vulnerability is important, because the region is a promising source of groundwater for agriculture and human consumption. Therefore, classifying the basin into different categories based on its degree of contamination is a powerful tool for conservation of groundwater.

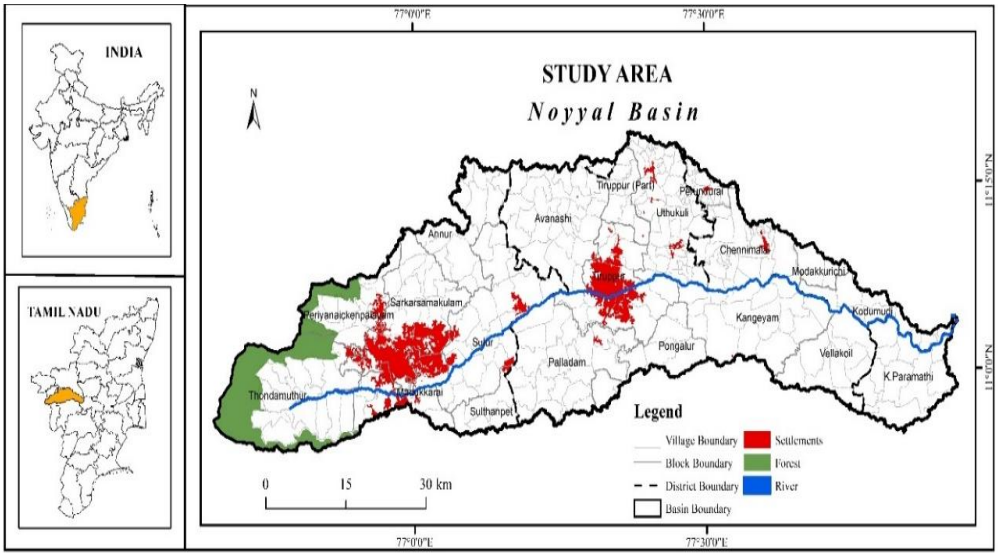

Figure 1: Location of the study area

Data and Methods

The study assesses the physical and environmental factors to prepare a groundwater vulnerability zone map for the Noyyal basin. Different data sources are used, and all the factors implemented are given in Table 1 below.

Table 1. Data sources and the type of data used for all the parameters

Factors	Data Used	Source
Depth to the Water and Net Recharge	Water Level and Rainfall (1987 - 2018)	State Ground and Surface Water Resources Data Centre (SG&SWRDC), Taramani, Chennai.
Aquifer Media	Geology	Geological Survey of India (GSI)
Soil Texture	Soil Data	Tamil Nadu Agricultural University (TNAU), Coimbatore
Topography	Aster 30m DEM	United States Geological Survey (USGS) - Earth Explorer
Impact of Vadose Zone and Hydraulic Conductivity	Vadose Zone and Conductivity	Central Ground Water Board (CGWB), Chennai
Lineament Density	Lineament	Web Map Service of Bhuvan, National Remote Sensing Centre (NRSC)
River Proximity and Land Use / Land Cover	Landsat 8 ETM+ 30m Resolution Imageries	USGS - Earth Explorer
Population Density	Demography	District Census Handbook, 2011

Physical Factors

DRASTIC

DRASTIC is a seven parameters model, i.e., Depth to water, net Recharge, Aquifer media, Soil media, Topography, Impact of the vadose zone, and hydraulic Conductivity. It is widely used because the input information is either readily available or from governmental agencies. The model is more suitable in the plain and coastal regions than in hard rock zones. Noyyal basin is the hard rock region that would not aid aquifer interactions. Therefore, a modified DRASTIC model was attempted. The weights given to all the seven parameters range from 1 to 5, based on the relative importance.

Depth to the Water Level

Water travels for a certain distance to reach the saturation zone; this distance gives the time taken by the pollutant to travel and the extent of the contamination. The shallow aquifers are more easily susceptible to contaminants than deep aquifers. The depth level data was collected from SG & SWRDC, and the basin is classified into three depth categories - <10m, 10-20m, and >20m. Regions with greater distance are less vulnerable to contamination, therefore, the greater the distance smaller the rating value.

Net Recharge

The net recharge is the total water infiltrates from the surface to the aquifer. The greater the recharge of the aquifer, the higher the transmission of contaminants. The recharge of the basin is mainly due to rainfall. The rainfall data from 1980 - 2018 was collected from SG & SWRDC. The rainfall values vary from <500 mm to >900 mm, and the ratings were assigned from 2 – 10.

Aquifer Media

The geological formation of the basin has both consolidated and unconsolidated materials that yield sufficient water for an aquifer. It controls the route and path length of a contaminant, which in turn determines the attenuation and purification capacity. The unconsolidated material enables to penetrate water into the aquifer than the hard rock. Aquifer media data was obtained from the Geological Survey of India, and a wide range of aquifer media are present in the basin, out of which fluvial and alluvium are given the highest rating of 10.

Soil Texture

Soil is the topmost layer of the vadose zone, and it has its potential influence on groundwater contamination (Saidi, 2011). Soil texture has a strong connection with permeability and porosity. Soil with a coarse texture can transmit contaminants more rapidly

than a fine texture. Soil texture data was collected from TNAU, and the rating was based on whether the soil texture was coarse or fine.

Topography

The topography represents the slope or land surface of the basin, and it was derived from the ASTER 30m DEM data. The topography indicates the possibilities of pollutant infiltration or run off, and here in the study area, the slope of the basin varies from <1% to >15%.

Impact of Vadose Zone

The vadose zone is the unsaturated or partially saturated zone that is present below the ground surface and above the aquifer. The vadose zone can control the water movement and the attenuation capacity (Meenakshi and Ganesh, 2019). Vadose zone data was collected from Central Ground Water Board. The thickness of the vadose zone influences the percolation of contaminants into the water table. The thicker the vadose zone, the time taken by the contaminants to reach the aquifer is also high. The basin is prominently covered by metamorphic and igneous hard rock having a low vadose zone impact, and a moderate impact zone has sand and gravel mixed with silt and clay.

Hydraulic Conductivity

Hydraulic conductivity is one of the important factors that control the groundwater flow within the aquifers. It is defined as the rate at which the groundwater will flow under a given hydraulic gradient. The rate of groundwater movement is directly proportional to the rate of contaminant transmission. Aquifer with high hydraulic conductivity leads to high transmission of contaminants. Hydraulic conductivity of the basin is calculated as follows,

$$K = T / h$$

Where, K is the Hydraulic conductivity in m/day;
T is the Transmissivity in m^2 per day and
h is thickness in metre.

Conductivity data was collected from Central Ground Water Board, and the hydraulic conductivity values of the basin range from <100 m/day to >700 m/day are categorised into four classes (<100m, 100-300m, 300-700m and >700m).

Other Physical Factors

Lineament Density

The interaction of aquifers within the study area is very low due to the hard rock formation. The lineaments provide the secondary porosity for water percolation. It acts as a conduit and enables groundwater interaction in the hard rock region. The higher intensity of

lineaments would increase the chance of contaminant movement towards groundwater (Abdullah, 2015). Lineament data was obtained from the Web Map Service of Bhuvan, National Remote Sensing Centre. Lineament density values range from <0.5 km/km^2 to >0.9 km/km^2.

River Proximity

Proximity from the river is one of the important factors considered for the delineation of the vulnerability zones in the Noyyal basin. The interaction of groundwater within the basin is very low because the majority of the region is of hard rock. However, the exchange happens through the sedimentary deposits found along the main river. Several industrial and bleaching units, CETPs (Common Effluent Treatment Plants), and STPs (Sewage Treatment Plants) are present on the bank of the river. Therefore, the proximity to the main river is an important factor that governs groundwater contamination. The groundwater wells that are present close to the main river are more prone to contamination than the farther wells, and the proximity values range from <1 km to >6 km, are ranked accordingly.

Environmental Factors

Source of Contamination

Point and non-point are the sources of pollutants. A point source is a discharge from a structure specially designed for the disposal of effluents, and on the other hand, a non-point source of contamination has widely distributed sources. Therefore, it is difficult to address the treatment of pollutants. In the basin, wastewater from the electroplating industries, bleaching and dyeing units, effluent treatment plants, sewage treatment plants, municipal dumping sites, and sewage are considered as point sources. The non-point source of contamination is mainly the agricultural land due to the use of fertilisers and pesticides, and these pollutants enter the riverine system through return flow. The intensity of contamination is high in the point source contamination. Hence, a high rating is given and a low rating to the non-point source of contamination.

Land Use / Land Cover

Land use/ land cover is a salient factor that could be utilised for the identification of the source of contaminants. Residential and agricultural land are the two-prime land-use types that supply pollutants to the groundwater (Sener, 2012). Sewage disposal, garbage dumping, and industrial wastewater are the sources of contaminants that are aggregated from the built-up land and contaminants like fertiliser and pesticides are from agricultural land use. The classes are rated depending on their pollutant intensity.

Population Density

In an urban environment, population density is one of the prominent factors used

for evaluating pollutant load (Nurroh et al., 2020). The region is vulnerable to contamination when the population density is high. Urban areas with high population density are the contributors of pollutants, such as municipal waste, sewage disposal, industrial wastewater, etc. (Vaezihir and Tabarmayeh, 2015).

Groundwater Vulnerability Index

Each of the above listed parameters are mapped in GIS by overlaying their appropriate factors. Weights and rating for all the parameters were assigned on the basis of level of vulnerability. The linear combination of the generated thematic layers and the assemblage of the weights leads to the creation of groundwater vulnerability zones (Kourgialas and Karatzas, 2015). Each factor is multiplied by its weight and ranked. Then all the factors were summed to produce the final resultant layer.

$$\mathbf{GVI} = \sum_{\mathbf{i=1}}^{\mathbf{n}} \mathbf{w_i x_i}$$

Where, GVI is the resultant layer, i is the appropriate factors for a particular index, n is the number of factors and x_i is the rank of factor i. The weightage and ratings of the factors are tabulated in Table 2.

Results

Groundwater Contamination

All the seven parameters of the DRASTIC model vary within the basin are as follows. Depth to water, the basin has a shallow aquifer in the eastern part, moderate in the central region, and deep aquifers in the western part. The Western Ghats is located in the western part of the basin, and the region receives more rainfall than the rest. Therefore, net recharge is substantial in this region. The geology of the study area is highly characterised by old crystalline, and metamorphic rocks belonging to the Archaean group, and the basin is entirely underlain by gneiss. The unconsolidated alluvial deposit is found under the foothill of the Western Ghats and could also be seen along the course of the river bed. Hydraulic conductivity is high along the river course. The coarser soil textures like sandy, loamy sand, and sandy loam are highly present in the eastern portion of the basin having a high tendency to transmit contaminants. The western part of the basin has a steep slope, and high vadose zone impact that is filled with pervious sand and gravel material. The spatial results reveal that the vulnerability of the region is high along the course of the main river than the peripheral parts. Figure 2 portrays modified DRASTIC layers with vulnerable zones.

Other Controlling Factors

The industrial cluster of the basin (3km buffer zone from the major source of pollutants) is considered as a point source of contamination, and the rest of the region is considered to be non-point source of contamination. Therefore, the region present within the one km buffer zone from the main river is highly vulnerable to groundwater

contamination. Coimbatore and Tiruppur corporations are regions with high population densities and are the sources of potential pollutants. Figure 3 show the source of contamination, land use/land cover, and population density vulnerable zones.

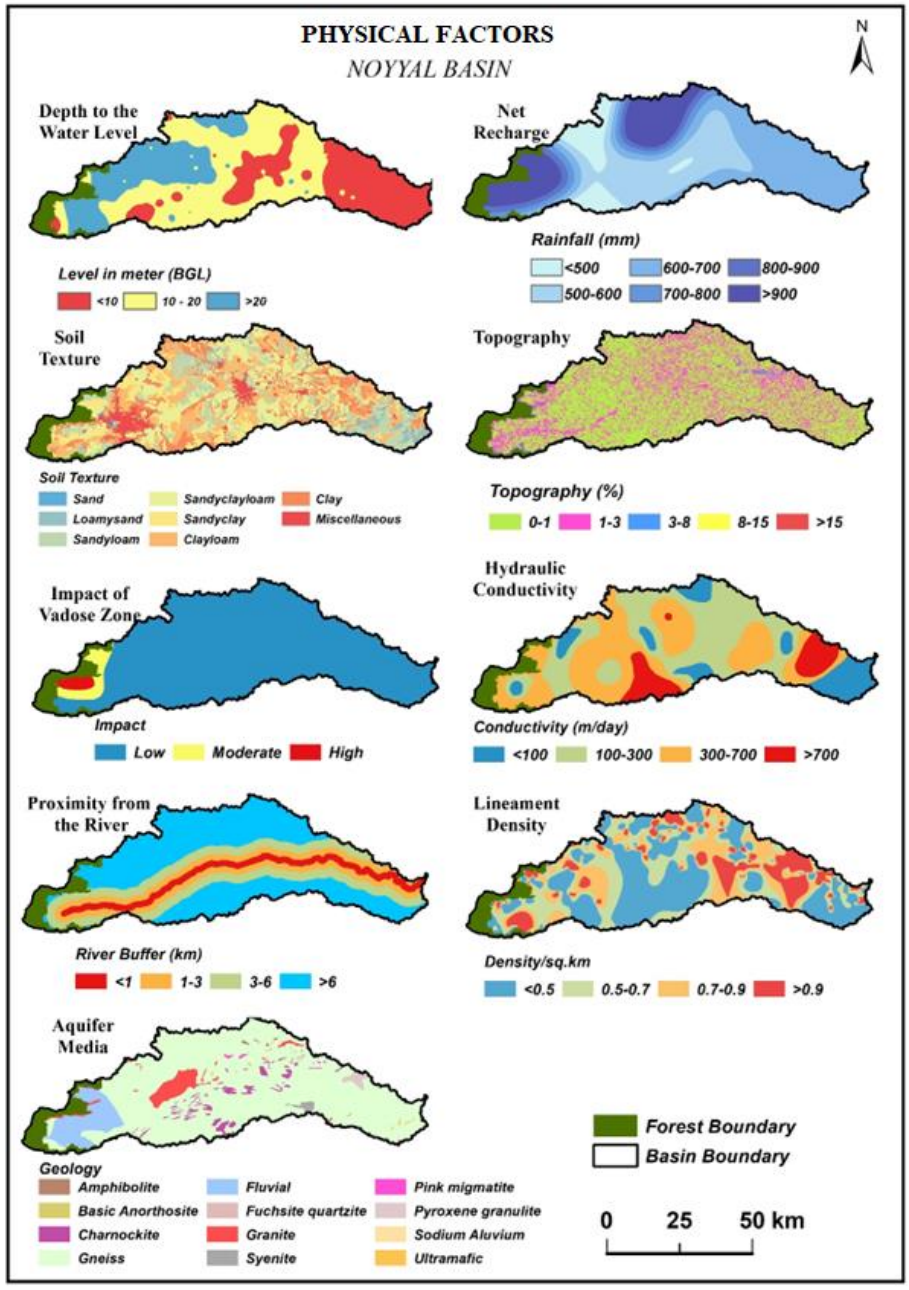

Figure 2: Physical factors - Depth to the water level, Net Recharge, Soil Texture, Topography, Impact of Vadose Zone, Hydraulic Conductivity, Proximity from the River, Lineament Density, Aquifer Media of the Noyyal Basin

Table 2. Weights and rating for all the parameters

Factors	Parameters	Sub-classes	Weightage (wi)	Ratings (xi)
DRASTIC	Depth to the Water Level (m)	<10	5	10
		10 - 20		6
		>20		2
	Net Recharge (mm)	<500	4	2
		500-600		2
		600-700		4
		700-800		6
		800-900		8
		>900		10
	Aquifer Media	Fluvial, Sodium Alluvium	3	10
		Gneiss		8
		Pyroxene granulite, Fuchsite Quartzite		6
		Amphibolite, Charnockite		4
		Anorthosite, Granite, Syenite, Pink migmatite and Ultramafic		2
	Soil Media	Miscellaneous	2	0
		Clay, Clay Loam		2
		Sandy clay		4
		Sandy clay loam		6
		Loamy sand, Sandy Loam		8
		Sand		10
	Topography (%)	<1	1	10
		1-3		8
		3 - 8		6
		8 - 15		4
		>15		2
	Impact of Vadose Zone	Metamorphic & Igneous	5	2
		Sand & Gravel with Significant Silt & Clay		6
		Sand & Gravel		10
	Hydraulic Conductivity (m/day)	<100	3	2
		100 - 300		6
		300 - 700		8
		> 700		10
Other Physical Factors	Lineament Density (km/km^2)	<0.5	5	2
		0.5 – 0.7		6
		0.7 – 0.9		8
		>0.9		10
	Proximity from the Main River (km)	<1	5	10
		1-3		8
		3 - 6		4
		>6		2
Environmental Factors	Source of Contamination	Point Source Contamination	5	10
		Non-Point Source Contamination		2
	Land Use / Land Cover	Built-up	4	10
		Agriculture Land		8
		Waterbody		6
		Wasteland, Scrubland		4
		Forest Land		2
	Population Density	<1500	3	2
		1500-3000		6
		3000-4500		8
		>4500		10

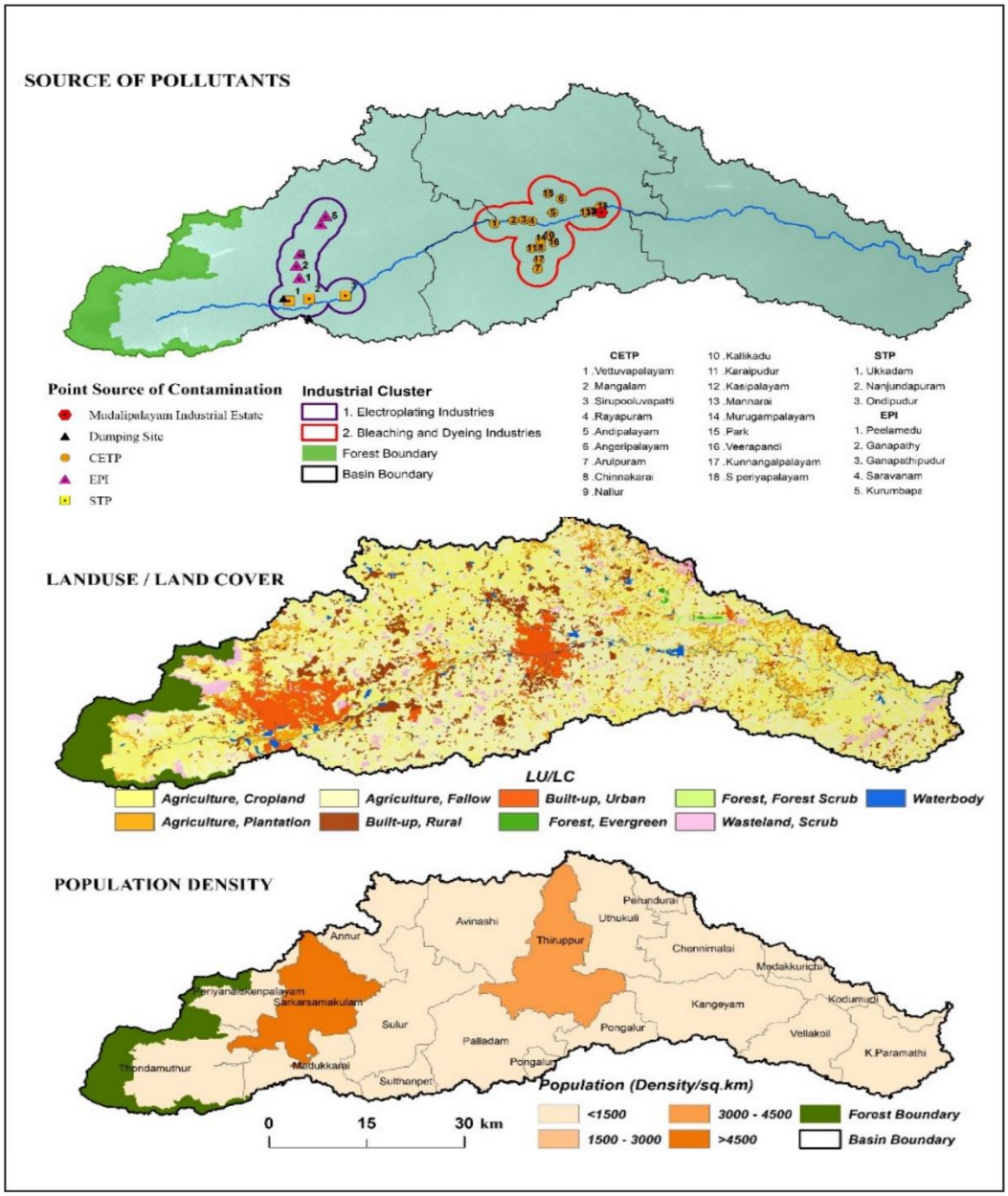

Figure 3: Environmental Factors - Point Source of Contamination, Land Use / Land Cover and Population Density of the Noyyal Basin

Groundwater Vulnerability Index

The groundwater vulnerability zones were delineated by overlaying all the physical and environmental layers (Figure 4). The result shows that 18 percent is highly vulnerable,

31 percent is moderately vulnerable and 51 percent is low vulnerable, of the total area. After generalising the result, it is pinpointed that among 285 villages, 18 villages are under the highly vulnerable zone, 105 villages are in the moderate zone, and the rest 162 villages are in the less-vulnerable zone. The Tiruppur corporation and the southern portion of the Coimbatore corporation are highly vulnerable. The spatial result shows that the villages adjacent to the main river are moderately to highly vulnerable to contamination due to the sedimentary deposits. The northern and southern portions of the basin are vulnerable to contamination because of the hard rock structure.

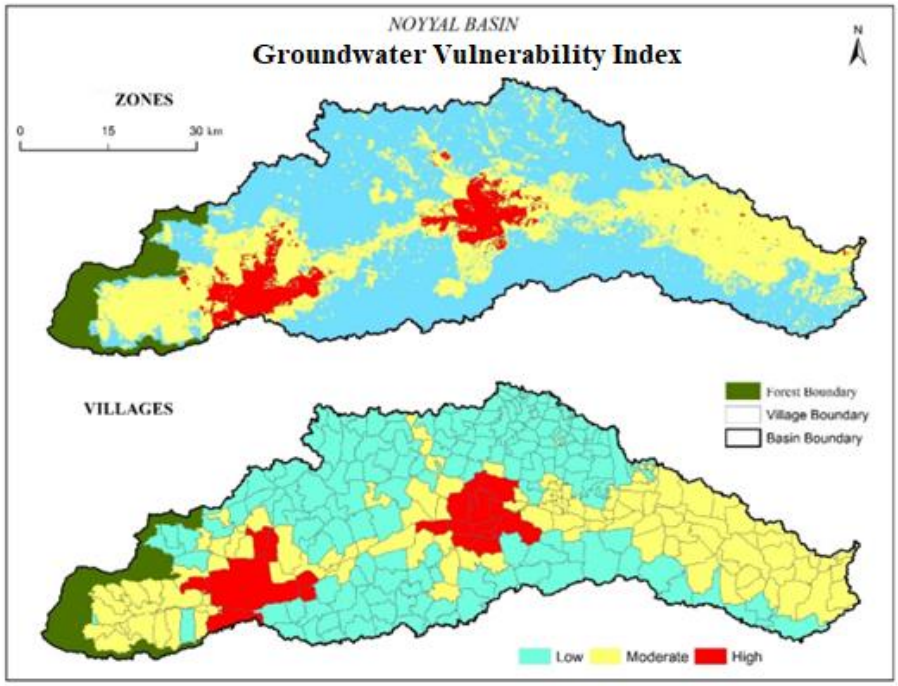

Figure 4: Groundwater Vulnerability Zones and Vulnerable Villages in the Noyyal Basin

Discussion

Groundwater quality analysis of the Noyyal basin has shown that the water from most parts of the area is unhealthy for human consumption and irrigation purposes. The reasons are anthropogenic and geological, i.e., less recharge, longer duration of contact, chemical weathering of rock-forming minerals (Selvarani and Shivakumar, 2020, Duraisamy et al., 2019). Here in the study, the western-most basin is under the foothills of the Western Ghats with uncontaminated freshwater, and the water quality index constitutes good in quality for drinking and irrigation purposes. However, the region tends to be highly vulnerable to groundwater contamination due to the presence of unconsolidated formation, high vadose zone impact, and recharge region. In parallel, the easternmost part is also

highly vulnerable because of a very porous soil texture (sand and sandy loam), shallow aquifer, and high lineament density.

The northern and southern peripheries of the basin remain less vulnerable. Due to the hard rock formation, these areas remain undisturbed by the contaminants. The central and the downstream area of the basin are at high vulnerability where agriculture is the main occupation of the people. The region within the buffer of one km is at high vulnerability, and the periphery is low to moderate vulnerability because of the hard rock formation with less lineament density, low hydraulic conductivity, and distant from the river. The villages adjoining the main river are at moderate to high vulnerability for trace element contamination. A high vulnerability to contamination is assessed in the southern portion of the Coimbatore corporation due to contamination from the hazardous dumping sites and sewage treatment plants. Shallow water table, gentle topography, sandy loamy soil, thinner vadose zone, and underlying geologic formations with well-developed fissures and fractures are the causes of high vulnerability in the Noyyal basin as suggested by (Saranya et al., 2021), and the outcome of the study is in congruence with it.

Conclusion

In the study, groundwater vulnerability assessment is implemented to find the potentially vulnerable zones of the basin. The modified DRASTIC model that includes the lineament density, proximity from the river, source of contamination, population density, and land use/land cover factors was employed to delineate the specific groundwater vulnerability zones. Contamination zones were depicted from the point source contamination of industrial clusters (hotspot for contamination) and water quality indices. All the layers were weighted and integrated into the GIS environment. The northern and southern portion of the basin remains at low vulnerability. Due to the bedrock formation, these areas remain undisturbed by the contaminants. The basin exhibits a higher vulnerability in 18 villages near the Coimbatore and Tiruppur corporations. The aquifers of these regions are more vulnerable to contaminants. The quality of the contaminated aquifers could be improved by the injection of harvested rainwater, along with suitable artificial recharge structures. Therefore, the vulnerable regions need proper management strategies.

Acknowledgment: The first author wishes to thank the University Grants Commission (UGC) for providing Basic Scientific Research Fellowship and the second author wishes to thank the Indian Council of Social Science Research (ICSSR) for providing Senior Fellowship to carry out the research in the Department of Geography, Bharathidasan University, Tiruchirappalli. The authors would also like to thank Defence Research & Development Organisation, Ministry of Defence, Government of India and Department of Environmental Sciences, Bharathiar University, Coimbatore for providing IC-PMS facility for groundwater element analysis.

Reference

1. Abdullah, T.O., Ali, S.S., Al-Ansari, N.A. and Knutsson, S. (2015) Groundwater Vulnerability Mapping Using Lineament Density on Standard DRASTIC Model: Case Study in Halabja Saidsadiq Basin, Kurdistan Region, Iraq. Engineering, 7, 644-667. https://doi.org/10.4236/eng.2015.710057
2. Al-Amoush, H., Hammouri, N. A., Zunic, F. and Salameh, E. (2010). Intrinsic Vulnerability Assessment for the Alluvial Aquifer in the Northern Part of Jordan Valley. *Water Resources Management, 24*(13), 3461-3485.
3. Aller, L., Bennett, T., Lehr, J. H., Petty, R. J. and Hackett, G. (1987). DRASTIC: A Standardized System for Evaluating Ground Water Pollution Potential Using Hydrogeologic Settings. *US EPA, Washington, DC*, 455.
4. Bera, A., Mukhopadhyay, B. P., Chowdhury, P., Ghosh, A. and Biswas, S. (2021). Groundwater vulnerability assessment using GIS-based DRASTIC model in Nangasai River Basin, India with special emphasis on agricultural contamination. *Ecotoxicology and Environmental Safety*, 214. https://doi.org/10.1016/j.ecoenv.2021.112085
5. Ducci D. (1999). GIS Techniques for Mapping Groundwater Contamination Risk, *Natural Hazards,* 20, 279–294.
6. Duraisamy, S., Govindhaswamy, V., Duraisamy, K. *et al.* Hydrogeochemical characterization and evaluation of groundwater quality in Kangayam taluk, Tirupur district, Tamil Nadu, India, using GIS techniques. *Environ Geochem Health* **41,** 851–873 (2019). https://doi.org/10.1007/s10653-018-0183-z
7. Elliott P., Briggs D., Morris S., ... and Jarup L. (2001). Risk of Adverse Birth Outcomes in Populations Living Near Landfill Sites. *BMJ,* 323(7309), 363-368.
8. Kourgialas, N. N. and Karatzas, G. P. (2015). Groundwater Contamination Risk Assessment in Crete, Greece, using Numerical Tools within a GIS framework. *Hydrological Sciences Journal, 60*(1), 111-132.
9. Lathamani, R., Janardhana, M. R., Mahalingam, B. and Suresha, S. (2015). Evaluation of Aquifer Vulnerability Using Drastic Model and GIS: A Case Study of Mysore City, Karnataka, India. *Aquatic Procedia*, 4, 1031-1038.
10. Meenakshi, P. and Ganesh, A. (2019). Evaluation of Groundwater Vulnerability to Contamination in Coimbatore District. Journal of Geography, *Environment and Earth Science International*, *20*(4), 1-17. https://doi.org/10.9734/jgeesi/2019/v20i430110
11. Muruganandam R. (2015). *Spatio-Temporal Analysis of Groundwater Vulnerability in Noyyal Basin, Tamil Nadu, India Using Geospatial Technologies*. Unpublished Ph.D. Thesis, Department of Geography, Bharathidasan University, Tiruchirappalli.
12. Nurroh S., Gunawan T. and Kurniawan A. (2020). Assessment of Groundwater Pollution Risk Potential Using DRASTIC Model in Yogyakarta City, Indonesia. In *E3S Web of Conferences,* 200, 02002. EDP Sciences.
13. Rahman, A. (2008). A GIS based DRASTIC model for assessing groundwater vulnerability in shallow aquifer in Aligarh, India. *Applied Geography*, 28, 32-53. https://doi.org/10.1016/j.apgeog.2007.07.008

14. Saidi S., Bouri S., Ben Dhia H. and Anselme B. (2011). Assessment of Groundwater Risk Using Intrinsic Vulnerability and Hazard Mapping: Application to Souassi Aquifer, Tunisian Sahel. *Agricultural Water Management*, 98(10), 1671–1682.
15. Sakala, E., Fourie F., Gomo, M. and Coetzee, H. (2019). Groundwater Vulnerability Mapping of Witbank Coalfield in South Africa Using Deep Learning Artificial Neural Networks. *South African Journal of Geomatics*, *8*(2), 282-293.
16. Saranya, T., Saravanan, S. Assessment of groundwater vulnerability using analytical hierarchy process and evidential belief function with DRASTIC parameters, Cuddalore, India. *Int. J. Environ. Sci. Technol.* (2022). https://doi.org/10.1007/s13762-022-03944-z
17. Selvarani. G A. and Sivakumar. (2020). Appraisment of phreatic water characteristic using water quality index modelling and GIS in industrialized region. *Materials Today: Proceedings.* (http://dx.doi.org/10.1016/j.matpr.2020.09.409)
18. Sener E. and Davraz A. (2012). Assessment of Groundwater Vulnerability Based on A Modified DRASTIC model, GIS and an Analytic Hierarchy Process (AHP) Method: The Case of Egirdir Lake Basin (Isparta, Turkey). *Hydrogeology Journal,* 21(3), 701–714.
19. Simsek C. and Gunduz O. (2007). IWQ Index: A GIS-Integrated Technique to Assess Irrigation Water Quality. *Environmental Monitoring and Assessment,* 128, 277-300.
20. Srinivasan, Veena & Kumar, Suresh & Chinnasamy, Pennan & Sulagna, Swati & Sakthivel, D. & Paramasivam, P & Lele, Sharachchandra. (2014). Water Management in the Noyyal River Basin: A Situation Analysis.
21. Vaezihir, A. and Tabarmayeh, M. (2015). Total Vulnerability Estimation for the Tabriz Aquifer (Iran) by Combining a New Model with DRASTIC. *Environmental Earth Sciences*, *74*(4), 2949-2965.
22. Zhang Q, Yang X, Zhang Y, Zhong M. Risk assessment of groundwater contamination: a multilevel fuzzy comprehensive evaluation approach based on DRASTIC model. ScientificWorldJournal. 2013 Dec 2;2013:610390. https://doi.org/10.1155/2013/610390

The Indian Geographical Journal
Volume 96 (2) December - 2021, pp 113 - 128
ISSN 0019-4824

SUB-SURFACE WATER QUALITY ASSESSMENT USING GIS TECHNIQUES IN SURAT-BHARUCH INDUSTRIAL REGION, GUJARAT, INDIA

Somnath Saha, Rolee Kanchan*

Faculty of Science, The Maharaja Sayajirao University of Baroda, Vadodara, Gujarat, India.
E-mail: roleekanchan@gmail.com

Abstract

Sub-surface water is essential for drinking, industries, irrigation and other domestic purposes. Demand for the sub-surface water is continuously increasing due to population growth which leads to over exploitation of water. The over-usage and industrial effluents may affect the quality of sub-surface water. The present study focuses on Surat-Bharuch industrial region that lies on the eastern flank of the Gulf of Khambhat, Gujarat. Based on 138 sub-surface water samples, collected from the region in May-June 2017, spatio-temporal analysis was undertaken. Physio-chemical parameters like pH, TDS, Calcium (Ca2+), Sodium (Na+) and Fluoride (F-) were analysed and a descriptive analysis was performed. Further, a mathematical model in terms of WQI was generated. WQI indicated that 7.97% of sub-surface samples were excellent for drinking, 15.94% were very good, 16.67% were good, whereas 14.49% were poor and 44.93% were unfit for drinking. The WQI classification shows that a significant part of the region had poor water quality making it, unfit for drinking.

Keywords: Sub-surface Water Quality, WQI, Spatial Distribution, Geographic Information System.

Introduction:

Sub-surface water is the most valuable resource on the earth and is currently of global concern (Villeneuve et al., 1990; Isa et al., 2012). It plays a significant role in water supply, ecosystem functioning and human well-being (Sheikhy Narany et al., 2014). Sub-surface water is one of the essential natural resources which have extensive usages. This resource is either inadequate or plenteous at times and is always very unevenly distributed, both over space and time. It is utilised for domestic, industrial and agricultural purposes. Its usage has recently increased and in the long run the trend would continue.

The physical and chemical composition of surface and sub-surface water changes throughout time and over space. It depends on factors such as atmospheric precipitation,

in-land surface water, geological formation and anthropogenic activities (Ramesh & Elango, 2006; Vasanthavigar et al., 2010). All these factors jointly affect water quality which changes spatially and temporally.

Globally, sub-surface water is being exploited due to the rapid increase in industries, agriculture, irrigation and drinking. The over-exploration of the resource might be a more significant threat to water quality. In addition, excessive pumping, industrial and domestic waste disposal, inappropriate land use, air pollution and wastewater discharge adversely impact sub-surface water quality. Fashae et al., 2014 discussed the impact of anthropogenic effects such as municipal dumpsites and defecation sites on the shallow groundwater in Southwest Nigeria. Similarly, Solanki et al. (2010) studied the untreated domestic waste impact on water quality and contamination in the Andhra Pradesh. According to the study by Babiker et al., (2007), modern agricultural practices, industrial effluents and urban wastewater were increasing the soluble chemicals in groundwater which is a more significant threat to the water environment. Jassas & Merkel (2015) evaluated a study on hydrochemical assessment of groundwater quality for drinking and irrigation in Gomal Basin, Northern Iraq. They observed that the groundwater quality is mainly controlled by rainfall leaching processes (recharge), dissolution of carbonate minerals, alumina-silicate weathering and ionic exchange. Thus, sub-surface water quality is an important issue that needs to be monitored and evaluated for water sustainability and human health.

In India, few studies have been carried out on the sub-surface water quality: for instance, Gujarat (Prakash et al., 2016), West Bengal (Gupta et al., 2008) and other states of India (Shankark et al., 2011). Water Quality Index (WQI) is one of the most efficient methods for detecting and monitoring surface and sub-surface water quality. In addition, the WQI method has been widely used to indicate water quality for drinking and irrigation (Asadi et al., 2007). Jha et al., in 2010, performed GIS and statistical method of Water Quality Assessment. They represented the spatial distribution of sub-surface water quality in Tamil Nadu state through WQI based map.

The present work, assesses the sub-surface water quality in the Surat-Bharuch Industrial region, which has many industries (small and large scale). Therefore, it is assumed that industrial wastewater contains a significant amount of soluble inorganic and organic chemicals and their by-products.

Study Area:

Gulf of Khambat, Western Gujarat, comprises of Surat-Bharuch industrial region. This region covers an area of about 4200 sq. km. and extends between 72°28'E and 73°3'E longitude and 20°59'N and 22°11'N latitude. This region has been a vital hub for economic activities since ancient times. Many industries, such as oil, gas, cotton textile, dyeing, paper, chemical and petrochemicals and new installations are planned in the Hazira and Dahej industrial area (Fig.1).

Rivers Narmada and Tapi intersperse this region and join the Gulf of Khambat. This region is divided into two significant plains: the northern part is Baroda plain and the southern part is Bharuch plain. Geologically, it consists of schists, phyllites and quartzites intruded by basic rocks, granites and pegmatites. The gradient slope is 23.5° north-east which gets reduced to 5° in the south and southwest. The region is endowed with numerous mudflats and marshy vegetation along the coast. The study area falls in the semi-arid and subtropical climatic regions. It receives tremendous annual rainfall from the southwest monsoon between June and September and the intervening month of October. The average annual rainfall ranges between 600 and 850 mm (District Census Handbook, 2011). In this region major aquifers are formed by alluvium with fine clay having silty sand at the top and Deccan trap basalt with moderate to high salinity and shallow water tables (Upadhyaya et al., 2014; CGWB, 2013).

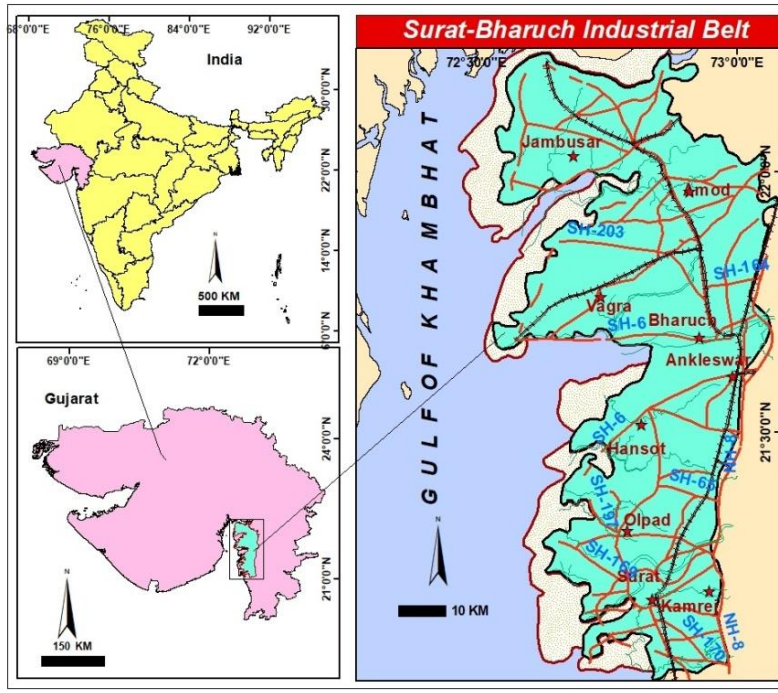

Fig.1: Location Map of the Study Area

The paper is undertaken because it is believed that the sub-surface water quality would be adversely affected by indiscriminate disposal of solid, liquid and gaseous waste from the industries. Disposal of solid waste in open pits and depression, discharge of untreated liquid waste through open drains and emissions of toxic gases into the atmosphere are a few common features generally prevalent in the industrial regions and their vicinity. The problem of contamination is more acute in industrial parts and their fringe areas. In this case, it has been inferred through observation, conducting interviews and applying PRA (Participatory Rural Appraisal) techniques.

Material and Methods:

Data Collection and Sample Analysis

Sub-surface water samples (138) were collected at various depths (<30 m) during pre-monsoon 2017. All samples were stored in plastic bottles and transported to the laboratory for physical and chemical analysis, which followed the standard procedure of APHA (1998). Before use, all glassware apparatus were thoroughly washed and rinsed with distilled water. Chemicals/reagents of analytical grade were used. The entire area of 4,200 sq. km. was gridded into a 5X5 sq. km. area and from each of the grids, at least one sub-surface water sample was collected and analysed (Fig.2). Sampling locations were marked by handheld GPS (Garmin GPSMAP 78S). The sub-surface samples were taken from the bore well and the hand pump, and physical parameters like pH and TDS were determined on-field by a portable instrument (Hanna Make, HI 98129). Esico Flame-Photometer (Model-1385) was used to assess calcium and sodium. Hanna-made Ion Selective Electrodes were used to detect fluoride (HI4110). Elico Double Beam UV- VIS Spectrophotometer (Model S1-210) was used to determine nitrate. All the laboratory work was performed in the laboratory of the Department of Geography, Faculty of Science, The M.S. University of Baroda.

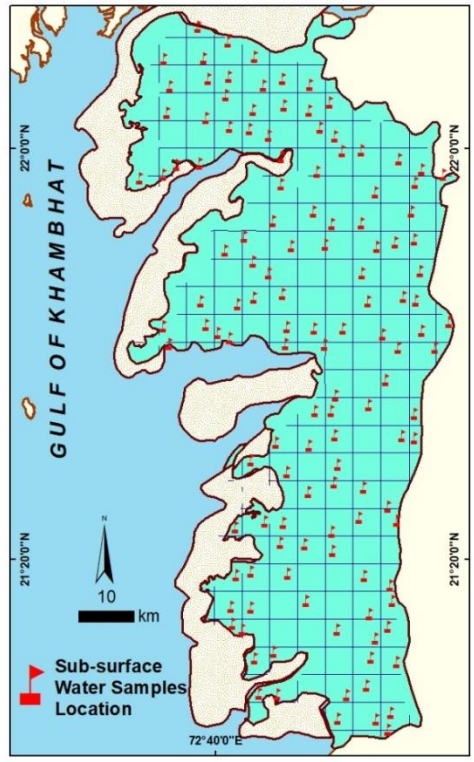

Fig.2: Location of Sub-surface water samples

Spatial Interpolation Method

GIS is a very effective tool for spatial analysis and interpolation methods. The Radial Basis Function (RBF) method produces thematic maps for major cations and anions in sub-surface water. This method followed the deterministic model approach in which the unknown points were computed based on the known points rather than the farthest point (Kawo & Karuppannan, 2018). Each basis function has a different shape and results and it can also predict values from below to maximum measured values (Gunarathna et al., 2016). This method helped categorise the values separately and gave a better visual illustration to understand the present water quality conditions. In the present study, water samples were collected, which were spread over the entire study area (12 talukas). Further, the geostatistical analyst tool generated parameter-wise interpolated surface maps/figures in the ArcGIS environment. For the graphical representation, ArcGIS 10.2 version was used.

Water Quality Index:

The Water Quality Index is an aggregate rating that reflects the composite influence of different water quality parameters (Horton, 1965; Şener et al., 2017). In other words, this method is a mathematical equation primarily used for data reduction of a large number of water parameters into a single number to evaluate the overall water quality at a specific location (Zhang et al., 2019). WQI provides simple and understandable information for decision-makers about water quality for drinking (Reza and Singh, 2010). It generates a score (zero to a hundred) illustrating the water quality status. The lower value of WQI indicates better water quality and the higher value reflects poor water quality. For drinking purposes, the Bureau of Indian Standards (BIS) was considered to interpret WQI.

WQI Calculation

The Water Quality Index was computed using the five measured parameters at each site. The Weighted Arithmetic Index method developed by Horton (1965) and Brown et al. (1970) was applied using the following equation:

$$\text{WQI} = \frac{\sum q_n . W_n}{\sum W_n}$$

Where, q_n = Quality rating of nth water quality parameter, W_n = Unit weight of nth water quality parameter.

Quality Rating ($\boldsymbol{q_n}$)

The quality rating **($\boldsymbol{q_n}$)** is calculated using this equation.

$$q_n = [(V_n - V_{id})/(S_n - V_{id})] \times 100$$

Where,

V_n = Estimated value of nth water quality parameter at a given sample location.

V_{id} = Ideal value for the n[th] parameter in pure water. (V_{id} for pH = 7 and 0 for all other parameters)

S_n = Standard permissible value of n[th] water quality parameter.

Unit weight

The unit weight (W_n) is calculated using the expression given in the following equation.

$$W_n = k / S_n$$

Where,

S_n = Standard permissible value of nth water quality parameter.

k = Constant of proportionality and it is calculated by using the expression given in the equation.

$$k = \left[1/ \left(\sum 1/ S_{n=1,2,..n}\right)\right]$$

Based on the above calculation, the ranges of WQI values were rated as excellent, good, poor, very poor and unfit for human consumption (Table 1).

Table 1 Different types of Sub-surface water and % distribution of samples using WQI (water quality index) range

Water Quality Index Range	Types of Water	% of Sample	% of Area	Probable usage
0-25	Excellent water quality	7.97	3.37	Drinking, irrigation, and industrial purpose
26-50	Good water quality	16.67	13.26	Drinking, irrigation, and industrial purpose
51-75	Poor water quality	14.49	16.98	Irrigation and industrial purpose
76-100	Very Poor water quality	15.94	20.44	For irrigation purpose
Above 100	Unfit for drinking	44.93	45.95	Proper treatment is required for any kind of usage
	Total	100	100	Source: Horton's Method (1965)

Results and Discussion

Descriptive Statistics

Descriptive Statistical analysis of sub-surface water specifications was developed to evaluate the ranges of Physico-chemical parameters and explore their deviation from BIS standards, as produced in Table 2 (Organisation BIS 2012).

Table 2 Descriptive Statistics for Determined Sub-surface Water Parameters

Parameters	Min	Max	Average	STD	Skewness	Kurtosis	S_n (BIS, 2012)	k value	Unit weight
pH	6.05	9.45	7.921	0.463	-0.156	2.31	8.5	0.8619	0.1014
TDS	112.5	7865.4	1171.32	1243.88	3.2	12.77	500	0.8619	0.0017
Sodium (Na^+)	13.4	400	266.996	148.467	-0.406	-1.55	200	0.8619	0.0043
Calcium (Ca^+)	15.5	420	74.306	85.369	3.135	9.44	75	0.8619	0.0115
Fluoride (F^-)	BDL	2.86	1.043	0.723	0.546	-0.52	1	0.8619	0.8619
Nitrate (NO_3^-)	BDL	187.68	21.933	36.396	3.292	11.5	45	0.8619	0.0192

Source– Computed

In the pre-monsoon season, the pH level varied between 6.05 and 9.45, indicating a slightly acidic to alkaline nature (Fig.3a). The mean pH in sub-surface water was 7.92, which depicted the normal condition. The standard deviation value was 0.46, Skewness was negative (-0.16), and kurtosis showed a positive value (+2. 31). The pH value (6.5-8.5) in the entire area was within the range of the drinking water guideline value of BIS (2012). This season, the TDS level ranged between 112.50 to 7865.40 mg/l (Fig.3b). The average value of the data set was 1171.32, with a standard deviation value of 1243.88. The skewness and kurtosis values were +3.20 and +12.77, indicating the data's positive skewness and leptokurtic characteristics. Approximately, 25% of samples in the study area had a TDS value of <500 mg/l, which fell under the freshwater group (Kawo & Karuppannan, 2018).

Calcium concentrations varied from 15.50 mg/l to 420 mg/l (Fig.3c), with an average of 74.31 mg/l. Before the rains, the standard deviation was considerably high (85.37). Both skewness and kurtosis both depicted positive and leptokurtic characteristics (+3.13 and +9.44). 73% of samples of calcium were <75 mg/l, which was within the drinking water guideline set by BIS (2012).

The range of sodium varied between 13.40mg/l and 400 mg/l with a higher mean (267 mg/l) and standard deviation (148.47). Both skewness and kurtosis values were negative (-0.41 and -1.55 respectively). According to Ayenew (2008), the possible sources of sodium in the sub-surface water were weathering of acidic volcanic rocks and rock-water interaction (Fig.3d).

The fluoride concentration ranged from BDL to 2.86 mg/l (Fig.3e). The average fluoride was 1.04 mg/l and the standard deviation was 0.72 in the dataset. Skewness (+0.55) indicated a positively skewed distribution, whereas kurtosis (-0.52) depicted a low degree of peakedness. The primary source of fluoride in sub-surface water is fluoride-bearing minerals such as Fluorspar (Fluorite), Apatite (Fluorapatite) and Phosphorite, which are present in rocks and alluvium of the Deccan Trap aquifer (Prajapati et al., 2017). The nitrate concentration varied from BDL to 187.68 mg/l (Fig.3f). The mean and standard deviations were 21.93 mg/l and 36.40. Skewness (+3.29) and kurtosis (+11.50) showed positive skewness, flatter distribution and leptokurtic dataset. Nitrate contamination in sub-

surface water is caused by agricultural field, waste disposal sites, industrial effluents and organic matter (Zhang et al., 2019).

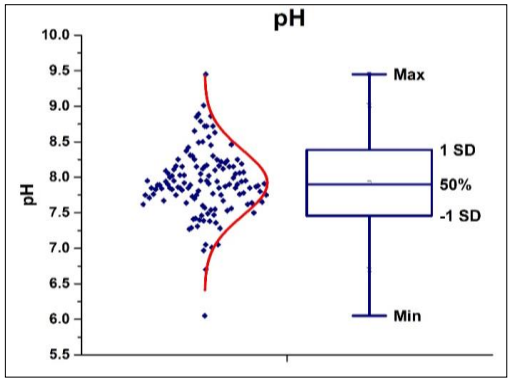

Fig. 3a

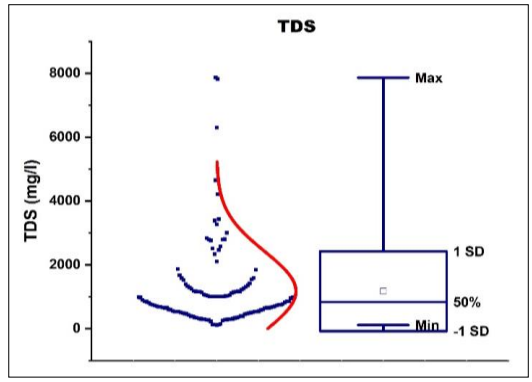

Fig. 3b

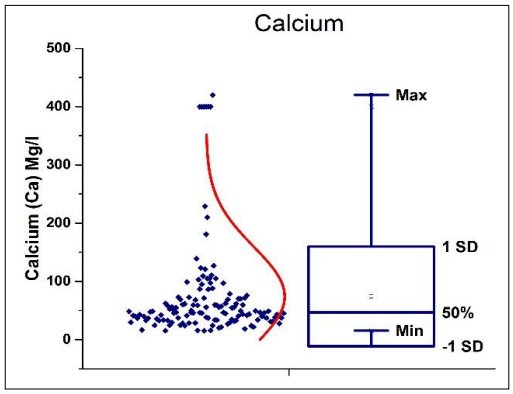

Fig. 3c

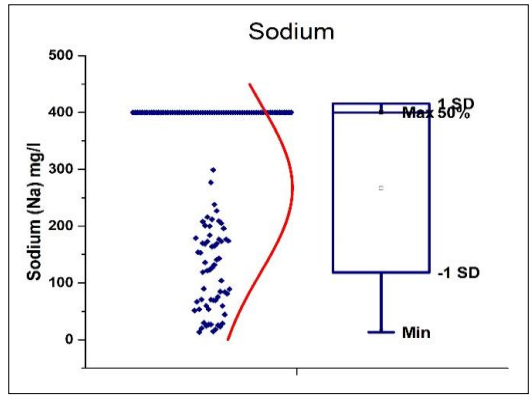

Fig. 3d

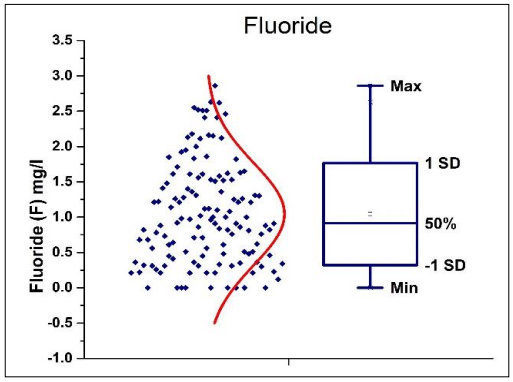

Fig. 3e

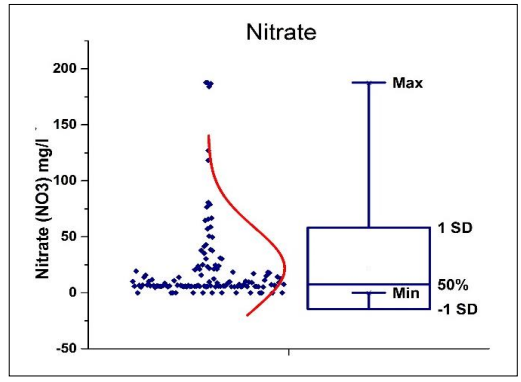

Fig. 3f

Fig. 3(a-f). Spatial distribution of parameters 3a- pH, 3b- TDS, 3c- TDS, 3d- Sodium, 3e- Fluoride, 3f- Nitrite

Spatial Distribution of Sub-surface Water Parameters:

Samples with a pH of >8 were 38.64% and they were spread over an area of 1517.4 sq. km. The western part of the region essentially had >8 of the concentration. Specifically, Vagra taluka in the Bharuch district had the maximum level. pH value (7.51 to 8 range) was observed in 46.21 % of the samples, covering an area of about 48.78 %. These were spread over the entire study area. The concentration range of 7 to 7.5 was noted in 12.88% of the samples, which dispersed across 12.14% of the region. It was seen in small pockets in the southern portion.

Three of the 132 samples had a pH of 7.5, with Amod taluka having the lowest pH value (6.05) (Fig.4a). 2.14% of the region. It was seen in small pockets in the southern portion. Three of the 132 samples had a pH of 7.5, with Amod taluka having the lowest pH value (6.05) (Fig.4a).

TDS value of >2000 mg/l was observed in a small area of the northwestern region. This TDS range encompassed the villages of Tankaria, Nada, Islampur, Devla, Khanpur and Kalak (Jambusar taluka). Only three samples, covering 2.48% of the total area, exhibited concentration ranging between 1500 to 2000 mg/l. The following category of 1000 mg/l to 1500 mg/l included 8.33 % samples, spanning the same region. They were seen in isolated concentrations in the north and south. 500 to 1000mg/l of TDS had 34 samples which covered 27.10% area and were well distributed over the entire study area. 59.85% of samples covering the same percentage of the area had <500mg/l of TDS in sub-surface water. Except for a few pockets, this lower range was observed throughout the entire study region (Fig.4b).

Calcium concentrations above the BIS standard was noted in 78.79% of samples. 56.06% of samples had <50 mg/l calcium, spread over 51.77% of the area. They were distributed over the entire region, particularly in parts where the maximum area is agricultural land. A slightly higher range (50 mg/l to 75 mg/l) was observed in a few segments. It was more pronounced in Amod taluka (Bharuch district) and a long narrow tail was noted along the National Highway. On the other hand, 6.06% of the samples in the Dahej Industrial Region were distributed throughout an area that made up around 4.20 %, with concentrations ranging between 75.1-200 mg/l. 6.06% samples and 12% samples were noted in 100.1 to 125 mg/l and >125 mg/l range. Both ranges were observed in the form of patches in Jambusar, Amod, Vagra and Hansot talukas (Fig.4c).

The sodium concentration in the sub-surface water was <100 mg/l in approximately 19% area and 21.37% of samples. They were observed in the talukas of Vagra, Bharuch and Ankleshwar (Bharuch District) as well as in the city of Surat. It was more prominent in the central to the northern portions of these areas. The sodium content of 100 to 150 mg/l was noted in 9 samples which were spread over 8.76% area. This range was observed over the entire study area in isolated pockets. A higher concentration of sodium (150.1 to 200 mg/l) was found in 15 samples covering 434.05 sq. km of area. 6.11% of samples

covering 7.17% of the area had a concentration of 200.1 to 250 mg/l. Whereas, >54.20% of sub-surface water samples had a sodium content of >250 mg/l that were dispersed over a large area of 55.13%. This belt was observed in two segments: one each in the northern and southern parts and another in the centre, in a small pocket near the Dahej industrial area (Fig.4d).

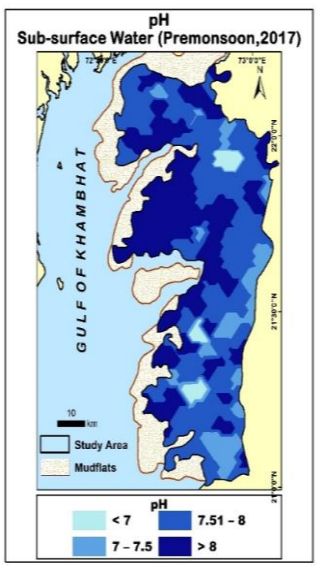

Fig. 4a

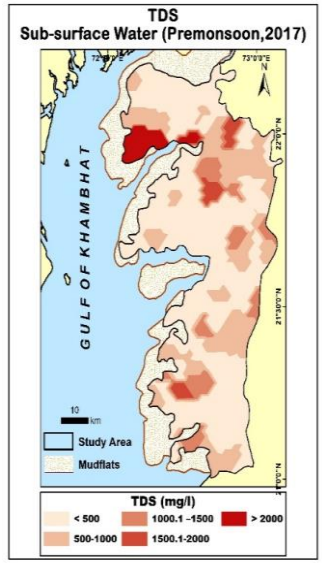

Fig. 4b

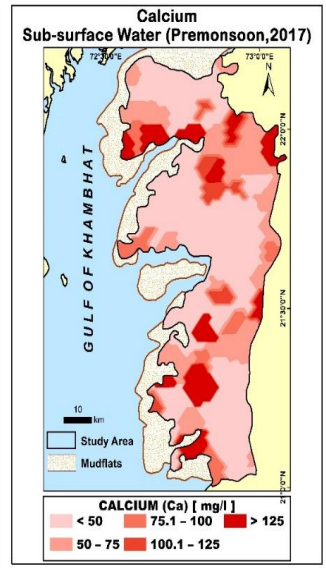

Fig. 4c

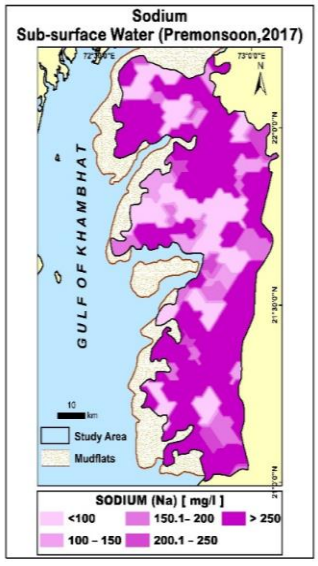

Fig. 4d

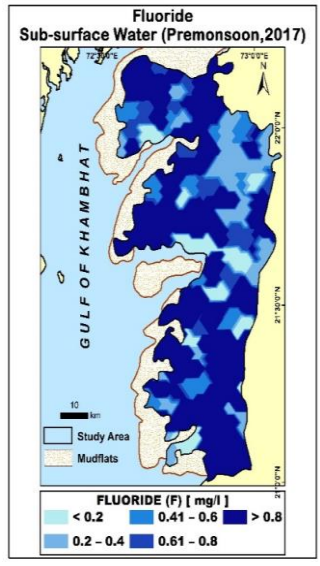

Fig. 4e

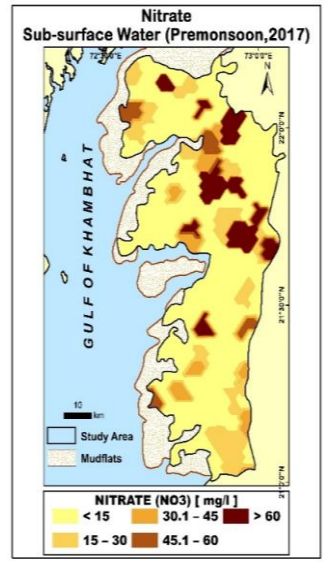

Fig. 4f

Fig. 4(a-f). Spatial distribution of parameters 4a pH, 4b TDS, 4c TDS, 4d Sodium, 4e Fluoride, 4f Nitrite

Fluoride concentrations were less than 0.20 mg/l in 8.40% of the samples. It covered 6.76 % in distinct places scattered over the whole region. Whereas, fluoride values of 0.20 to 0.40 mg/l were observed in 20 samples from the northeastern section, which accounted for 13% of the overall region. 439 sq.km area with 11 samples had fluoride content between 0.41 to 0.60 mg/l. 9.16% of samples spread over a 10.73% area had 0.61 to 0.80 mg/l of the element. They were in isolated scattered pockets near Jambusar, Bharbhut and Mangrol villages (Bharuch District). >0.8 mg/l concentration was identified in 60% of the samples and it was found in almost the same percentage in the industrial zones of Dahej, Vagra, Bharuch, Ankleshwar and Surat (Fig.4e).

The concentration of nitrate in sub-surface water was higher in the northeastern part. In 12 samples, a maximum range of >60 mg/l of the element was observed, accounting for about 10.52% of the total area. In comparison, just 4 samples exhibited nitrate concentration of 45.1 and 60 mg/l, accounting for 5.32% of the area. This range was also found in the form of isolated pockets near Panchppila, Devla and Intola villages (Jambusar taluka). In 9 samples, nitrate concentration ranged from 30.1 to 45 mg/l, accounting for 8.29% of the total area. On the other hand, nitrate values ranging from 15 to 30 mg/l were found in 16.10% of the samples and they were dispersed over 19.35% of the region. Lower nitrate concentrations (15 mg/l) were identified in 62.71% of the samples, which covered around 56.51% of the total study area. (Fig.4f).

WQI Results and Evaluation

In this study, WQI values ranged from 5.51 to 255.22. WQI values ranging from 0 to 25 were found in 7.97% of samples dispersed throughout 3.37 percent of the region. This range was discovered in the villages of Asnera and Nahier in Amod taluka and Manad in Bharuch taluka. Both talukas are located in northeastern and central parts of the study area. 26-50 WQI range was noted in 16.67% of samples, spread over 13.26% of the area.

This range was also recorded in the villages of Wadia, Adwala, Buva, Ranada, Kelod, Ora and Kolavana in the Amod taluka and Kapuria, Bakarpore and Nadiad in the Jambusar taluka. 20 samples and 16.98% of the region under study had WQI values ranging from 51 to 75, indicating "Poor Water Quality." This range was predominantly found in the Bharuch district in the talukas of Jambusar, Amod, Vagra and Bharuch. According to BIS, this water quality may be used for industrial and agricultural purposes. The WQI range of 76-100 labeled as "Very Poor" water quality was observed in 15.94% of samples and spread over 20.44% area. It was seen in the northeastern part of Jambusar taluka, north-western part of Amod taluka, western part of Vagra, north-central part of Ankleshwar taluka in Bharuch district and central part of Olpad taluka in Surat district. 58 samples were in the range of >100, suggesting that they were "Unfit for Drinking" (Table 1). It encompassed 45.95% of the study area (Fig.5). According to the WQI-based spatial variation map, this range was largely seen in the southern talukas of Hansot, Olpad, Surat and Kamrej, as well as in the central portion of Jambusar taluka, the eastern half of Vagra and the southern part of Ankleshwar Taluka (Fig.6). The increased levels of sodium, calcium, nitrate, fluoride and

total dissolved solids in the sub-surface water at these sites were the reason for the increased WQI values. Leaching of ions, water-rock interaction and anthropogenic activities such as excessive pumping, industrial effluents, irrigation and domestic uses can be the probable reasons for the same (Reza & Singh, 2010).

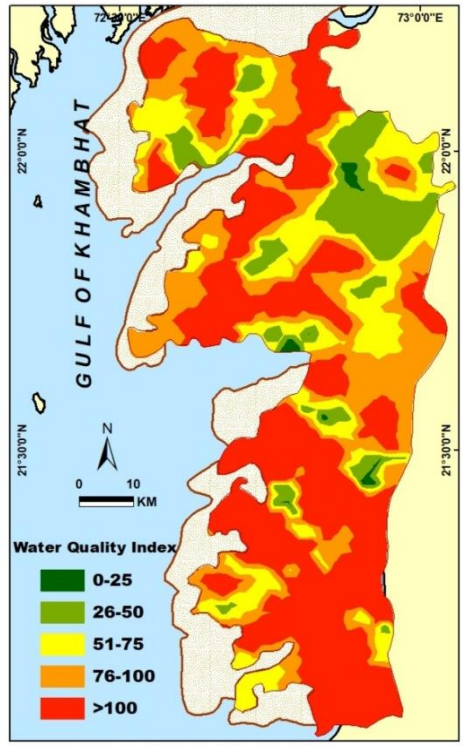

Fig.5: Water Quality Index (WQI) Map of Surat-Bharuch Industrial Region

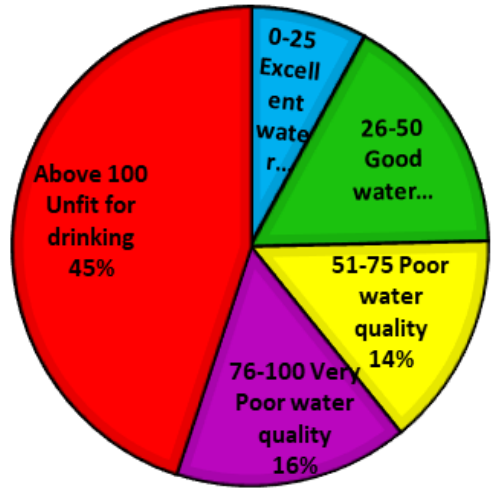

Fig.6: Pie chart showing the WQI category-wise percentage of distribution

Conclusion:

The WQI classification of sub-surface water quality in the Surat-Bharuch Industrial region of Gujarat shows that a significant part of this region has poor water quality - 'Unfit for Drinking'. In this region, natural (sub-surface water influenced by ion leaching process, weathering, percolating and movement) and anthropogenic sources (over pumping, agriculture and domestic use) played a significant role in affecting sub-surface water quality. In general, the highly industrialized and agricultural-based area had an impact on the sub-surface water chemistry of the study area. The investigation suggests that the sub-surface water in these areas requires considerable treatment before use. Some techniques for improving the water quality include- treating industrially contaminated water before discharging it into rivers or ponds, regular monitoring of water quality, revising fertilizer limits for agricultural operations and altering the policy for dumping industrial effluents. The northeastern portion of the research region had acceptable water quality suited for all purposes (drinking, residential, irrigation and industrial) because of the lack of industries in this part.

Acknowledgments

The authors are thankful to the authorities of the Ministry of Earth Sciences (MoES), New Delhi, India, for funding the Major Research Project "Effect of Human Intervention in Fragile Ecosystem along Gulf of Cambay, Mainland Gujarat" (MOES/36/OOIS/Extra/12/2013Dt.-29/05/2015).

References:

1. Asadi, S. S., Vuppala, P., & Reddy, M. A. (2007). Remote Sensing and GIS Techniques for Evaluation of Groundwater Quality in the Municipal Corporation of Hyderabad (zone-V), India. *International Journal of Environmental Research and Public Health*, *4*(1), 45–52. https://doi.org/10.3390/ijerph2007010008
2. Ayenew, T. (2008). The Distribution and Hydrogeological Controls of Fluoride in the Groundwater of Central Ethiopian Rift and Adjacent Highlands. *Environmental Geology*, *54*(6), 1313–1324. https://doi.org/10.1007/s00254-007-0914-4
3. Babiker, I. S., Mohamed, M. A. A., & Hiyama, T. (2007). Assessing Groundwater Quality using GIS. *Water Resources Management*, *21*(4), 699–715. https://doi.org/10.1007/s11269-006-9059-6
4. CGWB. (2013). *CGWB Surat District*. *492001*(0771).
5. Fashae, O. A., Tijani, M. N., Talabi, A. O., & Adedeji, O. I. (2014). Delineation of Groundwater Potential Zones in the Crystalline Basement Terrain of SW-Nigeria: An Integrated GIS and Remote Sensing Approach. *Applied Water Science*, *4*(1), 19–38. https://doi.org/10.1007/s13201-013-0127-9
6. Gunarathna, M. H. J. P., Kumari, M. K. N., & Nirmanee, K. G. S. (2016). Evaluation of Interpolation Methods for Mapping pH of Groundwater. *Ijltemas*, *V*(III), 1–5

7. Gupta, S., Mahato, A., Roy, P., Datta, J. K., & Saha, R. N. (2008). Geochemistry of Groundwater, Burdwan District, West Bengal, India. *Environmental Geology*, *53*(6), 1271–1282. https://doi.org/10.1007/s00254-007-0725-7
8. Isa, N. M., Aris, A. Z., & Sulaiman, W. N. A. W. (2012). Extent and Severity of Groundwater Contamination Based on Hydrochemistry Mechanism of Sandy Tropical Coastal Aquifer. *Science of the Total Environment*, *438*, 414–425. https://doi.org/10.1016/j.scitotenv.2012.08.069
9. Jassas, H., & Merkel, B. (2015). Assessment of Hydrochemical Evolution of Groundwater and its Suitability for Drinking and Irrigation Purposes in Al-Khazir Gomal Basin, Northern Iraq. *Environmental Earth Sciences*, *74*(9), 6647–6663. https://doi.org/10.1007/s12665-015-4664-4
10. Jha, M. K., Shekhar, A., & Jenifer, M. A. (2020). Assessing Groundwater Quality for Drinking Water Supply using Hybrid Fuzzy-GIS-Based Water Quality Index. *Water Research*, *179*, 115867. https://doi.org/10.1016/j.watres.2020.115867
11. Horton RK (1965) An Index Number System for Rating Water Quality. J Water Pollut Control Fed 37(3):300–306.
12. Kawo, N. S., & Karuppannan, S. (2018). Groundwater Quality Assessment using Water Quality Index and GIS technique in Modjo River Basin, Central Ethiopia. *Journal of African Earth Sciences*, *147*(January), 300–311. https://doi.org/10.1016/j.jafrearsci.2018.06.034
13. Prajapati, M., Jariwala, N., & Agnihotri, P. (2017). Spatial Distribution of Groundwater Quality with Special Emphasis on Fluoride of Mandvi Taluka, Surat, Gujarat, India. *Applied Water Science*, *7*(8), 4735–4742. https://doi.org/10.1007/s13201-017-0636-z
14. Prakash, I., Institue, B., & Applicati, S. (2016). *Impact Factor (SJIF): 3 . 632 Assessment of Ground Water Vulnerability to Contamination of Bhavnagar District*. *August*.
15. Ramesh, K., & Elango, L. (2006). Groundwater Quality Assessment in Tondiar Basin. *Indian Journal of Environmental Protection*, *26*(6), 497–504.
16. Reza, R., & Singh, G. (2010). Assessment of Ground Water Quality Status by Using Water Quality Index Method in Orissa, India. *World Applied Sciences Journal*, *9*(12), 1392–1397. http://citeseerx.ist.psu.edu/viewdoc/download?doi=10.1.1.388.1520&rep=rep1&type=pdf
17. Şener, Ş., Şener, E., & Davraz, A. (2017). Evaluation of Water Quality using Water Quality Index (WQI) Method and GIS in Aksu River (SW-Turkey). *Science of the Total Environment*, *584–585*, 131–144. https://doi.org/10.1016/j.scitotenv.2017.01.102
18. Shankar K, Aravindan S, & Rajendran S. (2011). Spatial Distribution of Groundwater Quality in Paravanar River Sub-Basin, Cuddalore District, Tamil Nadu. In *INTERNATIONAL JOURNAL OF GEOMATICS AND GEOSCIENCES* (Vol. 1, Issue 4).
19. Sheikhy Narany, T., Ramli, M. F., Aris, A. Z., Sulaiman, W. N. A., Juahir, H., & Fakharian, K. (2014). Identification of the Hydrogeochemical Processes in Groundwater using Classic Integrated Geochemical Methods and Geostatistical Techniques, in Amol-Babol Plain, Iran. *The Scientific World Journal*, *2014*. https://doi.org/10.1155/2014/419058

20. Solanki, V. R., Hussain, M. M., & Raja, S. S. (2010). Water Quality Assessment of Lake Pandu Bodhan, Andhra Pradesh State, India. *Environmental Monitoring and Assessment*, *163*(1–4), 411–419. https://doi.org/10.1007/s10661-009-0844-6
21. Upadhyaya, D., Survaiya, M. D., Basha, S., Mandal, S. K., Thorat, R. B., Haldar, S., Goel, S., Dave, H., Baxi, K., Trivedi, R. H., & Mody, K. H. (2014). Occurrence and Distribution of Selected Heavy Metals and Boron in Groundwater of the Gulf of Khambhat Region, Gujarat, India. *Environmental Science and Pollution Research*, *21*(5), 3880–3890. https://doi.org/10.1007/s11356-013-2376-4
22. Vasanthavigar, M., Srinivasamoorthy, K., Vijayaragavan, K., Rajiv Ganthi, R., Chidambaram, S., Anandhan, P., Manivannan, R., & Vasudevan, S. (2010). Application of Water Quality Index for groundwater Quality Assessment: Thirumanimuttar sub-basin, Tamilnadu, India. *Environmental Monitoring and Assessment*, *171*(1–4), 595–609. https://doi.org/10.1007/s10661-009-1302-1
23. Villeneuve, J. P., Banton, O., & Lafrance, P. (1990). A Probabilistic Approach for the Groundwater Vulnerability to Contamination by Pesticides: The Vulpest Model. *Ecological Modelling*, *51*(1–2), 47–58. https://doi.org/10.1016/0304-3800(90)90057-N
24. Zhang, Q., Xu, P., & Qian, H. (2019). Assessment of Groundwater Quality and Human Health Risk (HHR) Evaluation of Nitrate in the. *International Journal of Environmental Research and Public Health, 16*(21), 4246.

The Indian Geographical Journal
Volume 96 (2) December - 2021, pp 129-146
ISSN 0019-4824

SIMULATION OF URBAN SPRAWL USING GEO-SPATIAL ARTIFICIAL NEURAL NETWORKS AND CA-MARKOV CHAIN MODELS

Harshali Patil[1], Kanika Pillai[1], Sivakumar V[2*], Shivaji G Patil[3]

[1]COEP, Pune University, Pune, India
[2]Centre for Development of Advanced Computing (C-DAC), Pune, India
[3]Maharashtra Industrial Development Corporation, Pune, India
*Corresponding author: vsivakumar@cdac.in

Abstract

Land use/ land cover (LULC) changes caused by human interferences have extensive consequences at the local and global levels. Rapid urbanization is mainly driven by many factors such as increasing migration to urban areas and rapidly increasing population, especially in developing countries like India. This study, of Pune City, evaluates the changes in the urban area, occurred due to human interferences, in Pune using multispectral satellite imagery. The Machine Learning (ML) method, which is available with Orfeo Toolbox open-source tool, has been used for image classification for the years 1990, 2000, 2010, and 2020. LANDSAT series datasets were used and classified into four classes, viz. urban cover, vegetation, water, and unclassified (vacant, barren land, etc.). The classified outputs were assessed for the accuracy using the open-source Semi-Automatic Classification (SCP) tool. In this study, urban expansion was analysed using certain proximity factors that cause for the growth pattern of Pune city. A hybrid simulation model like Logistic Regression-Markov-Chain and Artificial Neural Network (ANN) were used to predict the future urban sprawl for the years 2030, 2040, and 2050. The validation of output is carried out using actual and simulated outputs. The prediction model results show that 69.63% accuracy with ANN algorithm and 55.25% accuracy with Logistic Regression-Markov-Chain algorithm. The predictions show that the urban area is expected to grow manifolds to 735.52 sq. km in 2050 from 56.943 sq. km in 1990. The result indicates that the integration of remote sensing, GIS, and Artificial Intelligent models help the urban planners for appropriate planning and decision-making processes with most accurate information.

Keywords: GIS, Remote Sensing, Land use / land cover, Logistic Regression-Markov-Chain and Artificial Neural Network, urban growth

Introduction

The term "land cover" refers to the man-made geophysical properties of the earth's surface, including the distribution of plants, water, structures, arid areas, and other physical features [1]. Globally, a significant quantity of agricultural and forested land is being

converted into urban space to accommodate population growth, which immediately affects the composition of the land [2, 3]. This change in land use and land cover in an urban area is a gradual process. With every passing year, the population of a city increases; thus, increasing the demand for infrastructure and services, which initiates the city to expand to satisfy the increasing demand of growing population therein. Different factors like physical, human, and environmental aspects influence the expansion of an urban area. For sustainable development, decision-makers need systems to monitor and observe these change in land cover and accurately predict the future change in land cover [4]. Understanding the change in land cover and urban sprawl of a city would help the decision-makers in making more informed decisions for the future population of the city.

In recent years, Indian metropolises have been witnessing an increasing rate of urbanization. Agricultural or barren land in the peripheral areas of the city is being converted to urban land for the development of infrastructure and facilities. The traditional methods of physically mapping the existing situation are very time-consuming and expensive [5]. The credibility of such data has also been questioned and might affect prediction results [6]. Therefore, the use of remote sensing in the urban planning process along with Geo-Artificial Intelligence or Geospatial-AI (Geo-AI) would help to map such data with credibility and also to generate a more accurate analysis of the existing situation in a cost-effective and time-saving manner. The use of such techniques is slowly being adopted in urban planning procedures.

Artificial Intelligence (AI) is the ability of systems to perform a task that requires human intelligence. Geo-AI is a crucial component of spatial analysis in Geographical Information System (GIS). Geo-AI methods can provide accurate land cover classification reports and also predict the situation in the coming decades by training past and present data sets. With the help of advanced technology, multiple algorithms have evolved in Geo-AI which helps to get precise results and output whole predicting a change in land cover. Artificial Neural Networks (ANN) and Cellular Automata (CA) Markov Chain Models are two widely used models in monitoring and predicting land use change [7]. These methods have been used in order to accurately predict the land cover change in Pune city for the coming decades. The results of this study can be used by the civic bodies and decision makers to facilitate better decisions for the future of the city. In this paper, urban agglomeration in and around Pune City has been studied to predict the future urban cover using ANN and CA Markov Models. To predict the stages of urban growth in Pune over the next few decades, remotely sensed satellite data (LANDSAT series data) from the years 1990, 2000, 2010, and 2020 were employed.

Study Area

Pune is a metropolis in Maharashtra, India. It lies at an altitude of 560m above Mean Sea Level (MSL) on the Deccan plateau. At the centre of the city, the rivers Mula and Mutha converge. It is the eighth-most populated city in India with an estimated population of about 5.05 million as of 2019 (Areas under the jurisdiction of Pune Municipal Corporation (PMC) and Pimpri Chinchwad Municipal Corporation (PCMC) are included). Three

Cantonment Boards, viz. Pune Cantonment Board, Khadki Cantonment Board, and Dehuroad Cantonment Board, are in existence presently in and around Pune city. In the past three decades, the city has become one of the most leading IT centres in India. Due to the presence of many well-known educational institutions, it is also known as the "Oxford of the East". Additionally, the growth of satellite industrial cities like Pimpri-Chinchwad and Chakan has also contributed to an increase in urban cover around Pune City. Similarly, all the incoming highways and bypass roads from other major cities within the state to Pune city are densely populated on both sides due to urbanization process and these exhibit the signs of tremendous rate of development, which results in drastic changes in land cover on both sides of these highways and bypass roads. The population of the city is expected to increase as the city continues to be one of the most liveable cities in the country. This paper primarily examines the study area that sits between 18d 34'31.6147"N to 18d83'13.6237"N latitude and 73d59'17.9289"E to 74d08'81.2515"E longitude, which covers an approximate total area of 2478 sq.km of Pune City (Figure 1).

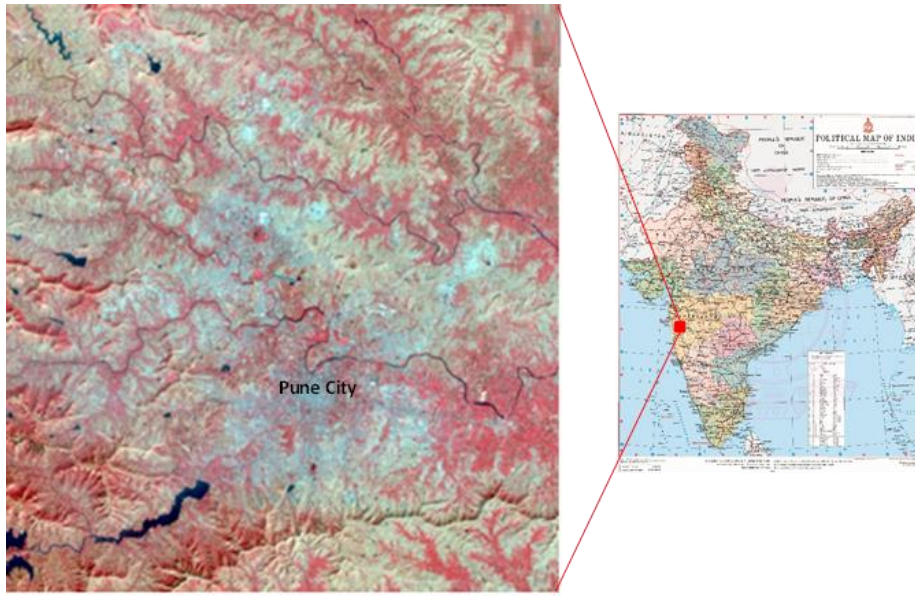

Figure 1. Location map of the study area (India map source: SOI)

Material and Methods

Figure 3 is a flow diagram of methodology of the study. The satellite images were obtained from USGS (earthexplorer.usgs.gov) for the years 1990, 2000, 2010, and 2020 (Figure 2). The details of the satellite data are listed in Table 1. All the satellite images of the recording years were downloaded and stacked. The upper left extent: 73d35'30.4512"E Longitude - 18d20'35.3796"N Latitude and lower right extent: 74d5'17.25"E Longitude - 18d49'52.9032"N Latitude were used for extracting study area and extracted all the images.

The satellite images of the respective four recording years were classified using Orfeo Toolbox, the Machine Learning Algorithm. The obtained classified result is assessed

using the Semi-Automatic Classification Plug-in and predicted and validated using ANN-Molusce and CA- Markov Chain Model. The softwares used to obtain the desired output were QGIS and IDRISI. The classified output is categorized into an urban area with built-up form, Vegetation, Waterbody, and Unclassified (bare land, fallow land, etc.). However, the study gives more emphasise to urban category. The details of the satellite images obtained and used are shown as Figure 2 and a flow diagram of methodology as (Figure 3) in the subsequent sections.

Table 1: Satellite Image specification

Satellite Data	Spatial Resolution (m)	Date of Acquired Data
Landsat 5TM	30	05/05/1990
	30	2903/2000
	30	26/04/2010
Landsat 8 TM	30	07/05/2020

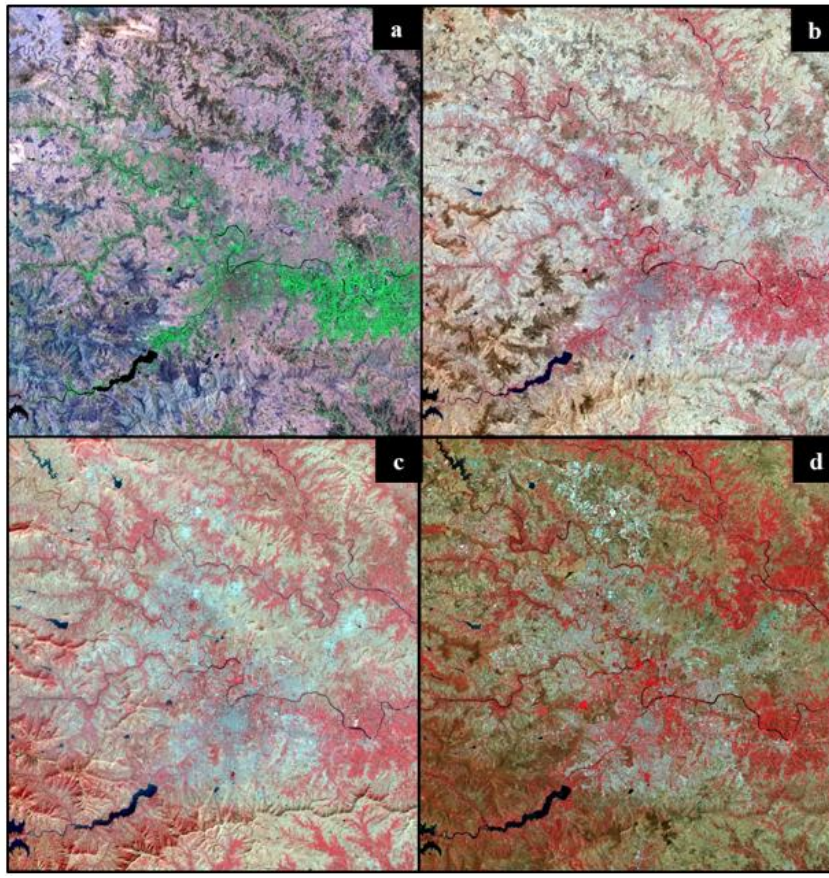

Figure 2. Landsat satellite image of the study area showing different year of acquisition: a) Year 1990 (RGB 345), b) Year 2000 (RGB 432), c) Year 2010 (RGB 432), d) Year 2020 (RGB 543)

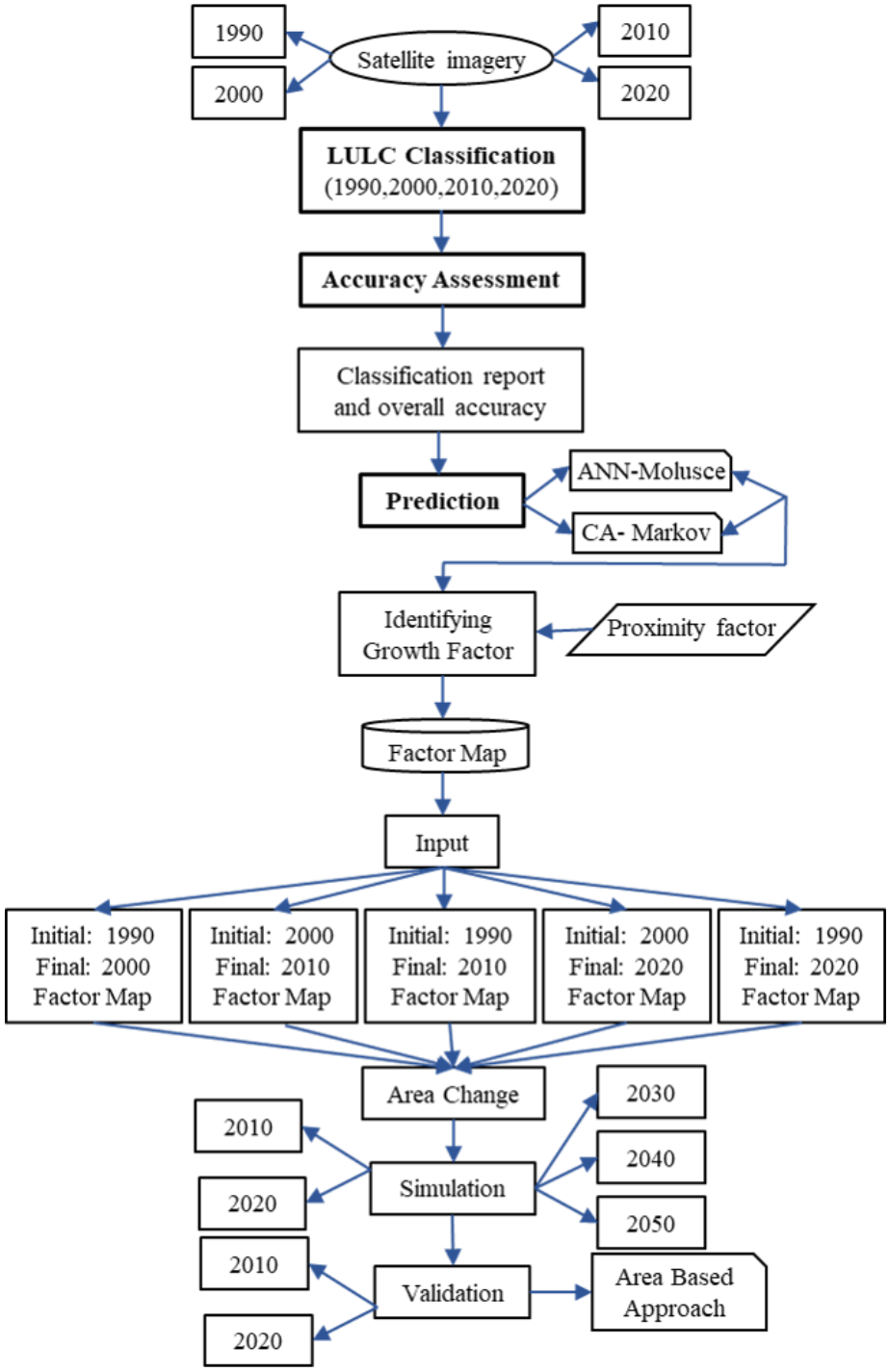

Figure 3. The flow-chart of methodology implemented for LULC classification and future prediction (simulation)

i) Image processing and Classification

Orfeo Tool Box (OTB) is open-source software for image processing. It aids in processing terabyte-scale high resolution optical, multispectral, hyperspectral, and radar pictures. OTB can be used for many different applications such as ortho-rectification or pan-sharpening, supervised or unsupervised classification, feature extraction, and SAR processing. For classification, OTB uses Monteverdi, a lightweight image rendering and processing tool. Monteverdi is a tool for fast visualization of processed results, which can display images in sensor geometry.

Through Image Statistics, Train Image Classifier, and Image classifier, image classification was carried out. It does not replace GIS software, suitable to edit, display, and relate different sources of geographic information both raster and vector. It uses Support Vector Machine (SVM) as a classifier due to its high-quality classification ability for classification and regression. In this method, to train the system, representative samples for each land cover class are selected. Then, "training sites" are applied to the entire image. The first step is to create training samples for each class. Following this, a signature file would generate with all training samples' spectral information. Finally, the signature file is used to run a classification and obtain desired output. Object-based classification was carried out using Support Vector Machine (SVM) algorithm for Supervised Classification. Using OTB, LULC was carried out for 1990, 2000, 2010, and 2020 dataset. In this study, more emphasis is given for urban class extraction and accuracy assessment as it focuses more on urban area growth.

ii) Accuracy Assessment

QGIS based Semi-Automatic Classification Plug-in (SCP) allows access to the accuracy of the image classification result. SCP was used to process raster data, resulting in an automated workflow and simple land cover classification that local practitioners may easily access. It computes classification statistics, band set processing, ROI Creation, and Accuracy assessment. Classified outputs of 1990, 2000, 2010 and, 2020 are assessed using SCP.

In the initial stage, the Classification Report tool in the Semi-Automatic Classification Plug-in is used to generate a report on the area covered by each class. Data is provided in the form of number of pixels, area (in sq. m) and the percentage out of the total area. The Classification reports confirm the observations made from the Image classification results. In this study, multiple data source like open street map, google imagery, town planning maps, NRSC LULC map and published maps from journal / book are used for validating results through online. The Band Set Tool in SCP is used to create a Band set comprising the classification raster that is utilised as an input by other tools for accuracy assessment. Multiple Regions of Interest (ROI) has to be generated which would be used to compare the accuracy of the classified image. The Multiple ROI Creation tool in SCP generates multiple sample pixels which then are assigned a class by comparing to the

initial raster image.This random sample is then used in the accuracy tool to assess the accuracy of the classification. The final step of accuracy assessment is to determine overall accuracy and Cohen's kappa statistics. The key benefit of this method is that it allows one to evaluate accuracy across homogeneous surfaces created automatically from ROIs rather than on single spots only.

iii) Prediction

a) Artificial Neural Network (ANN) -MOLUSCE

MOLUSCE refers to the Model for Land-use Change Evaluation. It analyses, models, and simulates land-use changes. It employs an algorithm that can be developed for LULC analysis, urban analysis, and forest application. It is well suited to analyse land use and forest cover changes, model land-use transition potential, simulate future LULC change and, validate the predicted output with actual LULC [8]. The study uses input as five sets: 1990-2000, 2000-2010, 1990-2010, 2000-2020 and 1990-2020. Hence, the prediction was carried out for 2010, 2020, 2030, 2040 and 2050 respectively and validation was carried out for 2010 and 2020 using both software and an area-based approach as the actual LULC of them is available. Transition Potential Modeling is carried out using ANN, which is the Geo-AI model of neural networks that can predict and provide solutions to complex problems. The ANN method is faster compared to traditional techniques and can solve multiple problems. Due to these advantages, ANN methods have been used in numerous real-time applications [9].

b) Input

Two recording year LULC maps are added to the MOLUSCE Plug-in together with previously processed variables' factors for LULC changes. Roads are one of the contributing factors to urban growth in the study area, therefore, major highways, including the Mumbai-Pune Expressway are used in computing the factors. Distance from the road was calculated to determine the growth factor using proximity Plug-in in QGIS. As the Classified LULC for the recording years 2010 and 2020 are available, the simulated output of 2010 and 2020 is validated with actual classified results.

Growth driver - proximity factor: In order to create a layer with distance-from-nearest-road as a habitat, distance from Road GIS layers employs QGIS for processing spatial information. This layer allows us to generate a probability of occupancy layer and extract distance-from-nearest-road for each location in order to model data. Using Distance from Road in QGIS, spatial variable, raster road tiff file is created. Analysing closeness is done using the spatial analyst tool. The distance toolset includes tools that either assign each cell to the nearest feature or build a raster indicating each cell's distance from a group of features. Tools for measuring distance also determine the quickest route through a corridor between two points to reduce two different sets of expenses. For overlay analyses, distance from any entity is used as inputs. The spatial variable used in this study is the

raster roadway data which is obtained as distance from the road using Proximity Plug-in in QGIS.

c) Land use change

This stage computes transition between the first recording year of LULC and the second recording year of LULC. In this research, five datasets are considered having initial and final recording years. The value of this LULC change in the form of change map is mapped, which would then be used for the fourth stage. The outcomes of the steps are achieved using Transition Probability and Transition Suitability maps. The distribution of each LULC class was projected based on the transition probability p_{ij} between two LULC classes (i and j). p_{ij} was determined over a specific period from time t to time t+1 is presented as Equation (1).

$$p_{ij} = \frac{n_{ij}}{n_i} \qquad (1)$$

$$\sum_{j=1}^{k} p_{ij} = 1$$

Where,

n_i = the total number of pixels of class i transformed over the transition period,

n_{ij} = the number of pixels transformed from class i to j,

k = the number of LULC classes.

The distribution of each LULC class at time t+1(M_{t+1}) was projected forward using the LULC distribution at the beginning time t (M_t) and the transition probability matrix P;

$$P * M_t = M_{(t+1)}$$

d) Transition Potential Modelling

Artificial Neural Network (Multi-Layer Perception), Weights of Evidence, Multi Criteria Evaluation, and Logistic Regression are the four techniques available through MOLUSCE plug-in for predicting LULC change. This study utilised LULC prediction model using an artificial neural network (multi-layer perception) technique. After processing resultant image, the outcome would display the kappa validation value. By using training data and sampling, this method examined the altered pixels between two LULC maps as well as spatial factors. The random sampling mode was specified. Additionally, the model must include the maximum iteration and neighbouring pixels.

ANN is a component of computational intelligence techniques. The utility is justified by the fact that it can be used to address issues wherein a lot of input data is dealt, and where the solution technique is ambiguous or challenging, to employ. It is exceedingly challenging to apply the many analysis parameters linked to terrain or land cover. Because

artificial neural networks implement the principles of fuzzy logic, which is feasible to assess the suitability of a terrain in a continuous range, such as between 0 and 1. The interactions between neurons and the alteration of the weight connections connecting them make up the artificial neural network's essential component. This adjustment is dependent on the supplied information and the anticipated.

e) Simulation

Cellular automata simulation is used to carry out the third year LULC change prediction process because the prior kappa value complies with the assessment standard. The simulation iteration count should be set to 1. Taking into consideration the input dataset, simulation maps for the recording years 2010, 2020, 2030, 2040 and 2050 are predicted.

f) Validation

The validation is processed using the reference map (the third year LULC as it actually occurred), referred to the simulated map (the third year LULC prediction), and computation of the overall Kappa value. Then it is to the cellular automata simulation stage to predict future LULC after the total kappa value satisfies the assessment requirement. The year of prediction is determined by the difference between the final year and the initial year and the following year of prediction can be calculated by adding the difference to the final year.

The Kappa coefficient [12] is calculated using equation (2).

$$\text{Kappa} = \frac{p_o - p_e}{1 - p_e}.. \quad (2)$$

Where,

p_o is the proportion of observed agreements, and p_e is the proportion of agreements expected by chance.

$$p_o = \sum_{c=1}^{i} p_{ij}$$

$$p_e = \sum_{c=1}^{i} p_i T_i T_j$$

Where,

p_{ij}= the i-th and j-th cell of the contingency table,

p_i T= the sum of all cells in i-th row,

pT_j= the sum of all cells in j-th column,

c = the count of the raster category.

iv) Cellular Automata (CA) - Markov Chain Model

The MC model is a stochastic process model that illustrates the concept of changing from one state to another. It has a well-coded algorithm, namely the transition probability matrix [13]. The probabilities of transitioning between these time steps are calculated in the MC model using two LULC of different periods as input. This model has been used to predict urban sprawl and land-use change [13–15], however the MC model is used in this study to confirm the effectiveness. Similarly, with the same input set, prediction and validation is done for recording years using Markov Chain Model. Both the ANN-MOLUSCE and CA- Markov use the same methodology to predict and validate the output. But ANN- MOLUSCE uses the TIFF data file type, whereas CA- Markov Chain Model uses the RST data file type as input and output. The specific formula is presented as equation (3).

Mathematically CA can be expressed as [11],

$$(\{S_{t+1}\} = f(\{S_t\} * \{I_t^h\} * \{V\}) \quad (3)$$

Where,

$\{S_{t+1}\}$=the state of a cell in the CA at time (t +1),

$\{S_t\}$ = the state of a cell in the CA at time (t),

$\{I_t^h\}$ = the neighbourhood,

{V} = the suitability of a cell for urban growth,

f () = the transition rules,

t = the time steps in temporal space,

h = the neighbourhood size.

Results and Discussion

The LULC classification is performed for four recording years as shown in the Figure 4-a, b, c, d using Orfeo Toolbox. Classification report of four recording years is shown in the Figure 5. Accuracy of the output is assessed using Semi-automatic Plug-in and the overall accuracy is shown in the Figure 6. Likewise, using ANN- MOLUSCE and CA- Markov Chain Model, transition matrix is obtained for the all the five input datasets, which are shown in the Table 2.

The transition matrix is obtained for the recording years given in the input dataset through ANN- Molusce and CA-Markov. From 1990 to 2020, urban areas and vegetation have increased by 20% and 17%, respectively. The water body and unclassified landform have been decreased, probably due to urbanisation by 0.5% and 38%, respectively. The transition matrix obtained through ANN- MOLUSCE is more efficient and accurate than CA-Markov due to its high probability outcomes. Growth of IT Parks, industrial areas, educational institutes contribute to the development of the city which needs to accommodate the ever-increasing, pulled and migrated population. The increase in built-up area in the city results in rapid urbanisation.

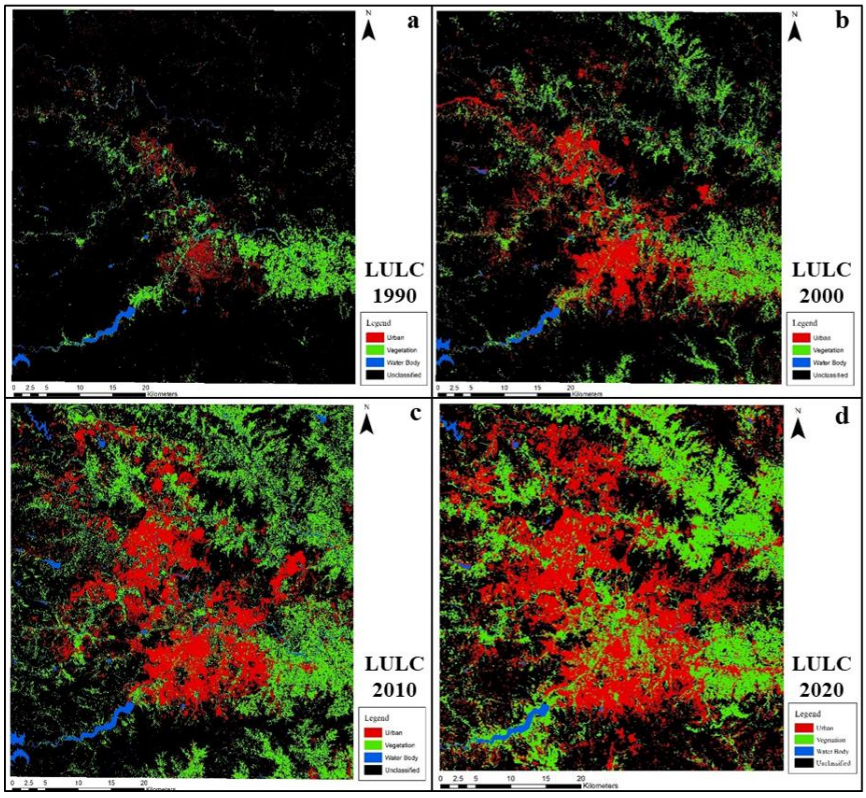

Figure 4. LULC classification map of the study area. Landsat satellite imageries are used to derive the LUCL: a) 1990, b) 2000, c) 2010, d) 2020

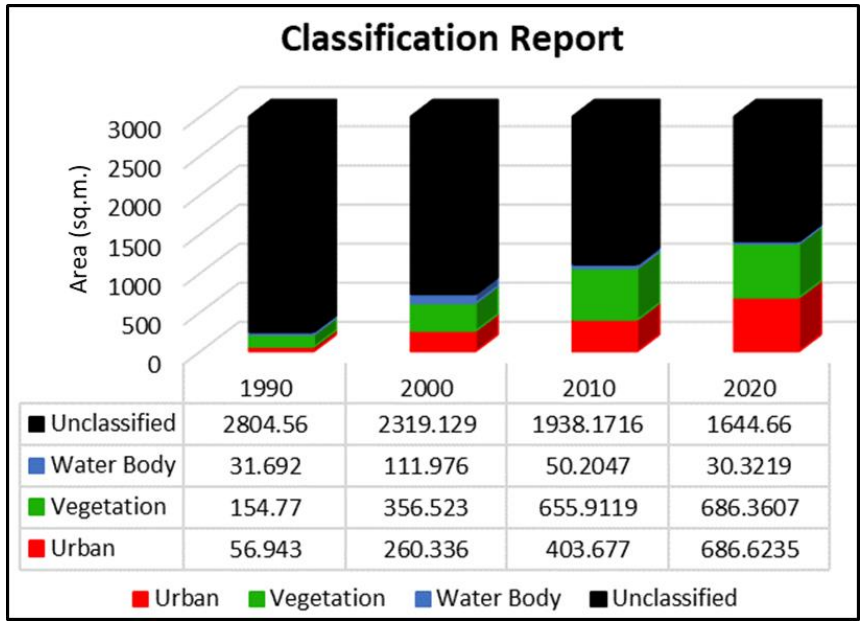

Figure 5. Comparation of LULC classification output with different year

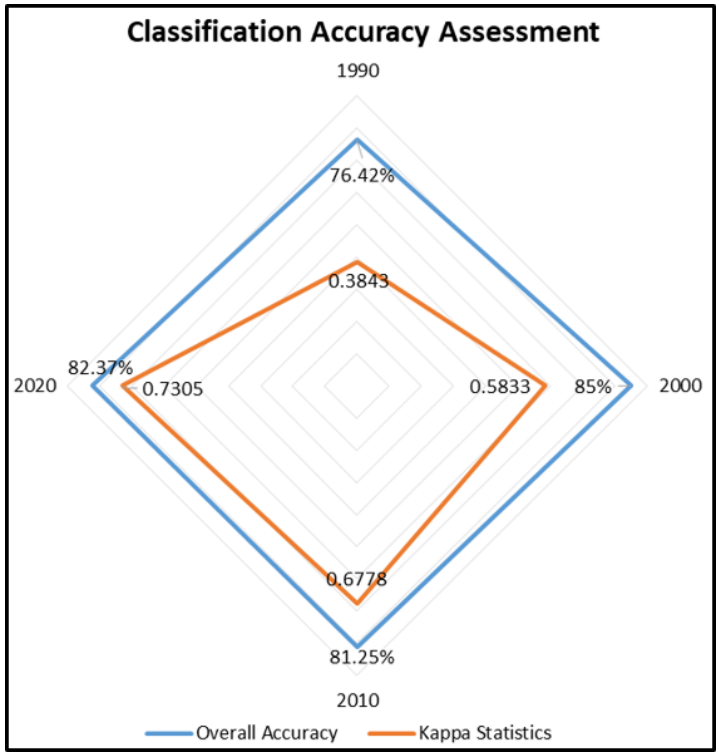

Figure 6. LULC classification accuracy assessment shown in the Radar chart. Blue and orange line show overall accuracy and Kappa statistics, respectively

Simulation is carried for the future recording years 2010-50 and validation for 2010 and 2020 is carried out since the actual LULC is available for same recording years. Figure 7-a, b, c, d, e show the predicted LULC from 2010 to 2050, respectively. The predicted LULC changes (2010, 2020, 2030, 2040, and 2050) provide average Kappa overall accuracy values of 50%. According to the actual LULC, between 1990 and 2020, the built-up area witnessed the highest change, while the barren region observed the biggest change in a drop. During 1990-2020, barren land is transformed into the built-up landform. Also, further validation was carried out for simulated 2010 and 2020, as the actual LULC for both recording years is available. As per the simulated map, the urban class is supposed to expand by 21% in 2030, 23% in 2040, and 26% by 2050 from 1% in 1990. In 2030, the urban expansion is supposed to be blooming along the National Highways, State Highways and around the Chakan industrial belt. In, 2040 and 2050, the same areas are probably strengthened with the core area developing in radially outward. Pune City Mission plans to develop the city in terms of transportation, education, and economy. Hence, the additional pulled and migrated population can be accommodated along with the roadway infrastructure for easy access, decreasing the substance on the core area. The simulated outcomes for future years are predicted and validation was carried out (Table 3, 4).

Table 2: Transition Matrix for the year 1990-2000, 2000-2010, 1990-2010, 2000-2020 and 1990-2020

Class Transition	Method / Algorithm	Transition Year				
		1990-2000	2000-2010	1990-2010	2000-2020	1990-2020
Urban - Urban	ANN	0.605	0.633	0.588	0.656	0.614
	CA - Markov	0.511	0.538	0.545	0.633	0.457
Urban - Vegetation	ANN	0.156	0.147	0.193	0.214	0.283
	CA - Markov	0.135	0.185	0.143	0.199	0.237
Urban - Water Body	ANN	0.011	0.030	0.018	0.011	0.006
	CA - Markov	0.001	0.038	0.016	0.010	0.006
Urban - Unclassified	ANN	0.228	0.190	0.200	0.119	0.097
	CA - Markov	0.200	0.239	0.196	0.099	0.079
Vegetation - Urban	ANN	0.148	0.074	0.155	0.195	0.266
	CA - Markov	0.115	0.093	0.116	0.157	0.228
Vegetation - Vegetation	ANN	0.625	0.632	0.535	0.647	0.612
	CA - Markov	0.430	0.537	0.264	0.623	0.569
Vegetation - Water Body	ANN	0.013	0.013	0.031	0.007	0.015
	CA - Markov	0.007	0.016	0.031	0.007	0.013
Vegetation - Unclassified	ANN	0.214	0.282	0.279	0.151	0.107
	CA - Markov	0.196	0.355	0.247	0.124	0.075
Water Body - Urban	ANN	0.191	0.003	0.123	0.091	0.165
	CA - Markov	0.149	0.003	0.095	0.093	0.097
Water Body - Vegetation	ANN	0.194	0.005	0.176	0.223	0.348
	CA - Markov	0.118	0.005	0.149	0.199	0.299
Water Body - Water Body	ANN	0.483	0.247	0.554	0.660	0.430
	CA - Markov	0.325	0.210	0.539	0.612	0.387
Water Body - Unclassified	ANN	0.132	0.745	0.147	0.026	0.057
	CA - Markov	0.110	0.782	0.129	0.016	0.060
Unclassified - Urban	ANN	0.075	0.091	0.132	0.206	0.236
	CA - Markov	0.046	0.130	0.103	0.147	0.198
Unclassified - Vegetation	ANN	0.088	0.169	0.202	0.186	0.220
	CA - Markov	0.059	0.239	0.165	0.160	0.199
Unclassified - Water Body	ANN	0.004	0.004	0.010	0.003	0.006
	CA - Markov	0.001	0.006	0.009	0.002	0.005
Unclassified - Unclassified	ANN	0.832	0.735	0.656	0.605	0.538
	CA - Markov	0.458	0.625	0.348	0.365	0.457

Table 3: Validation for the year 2010 using an area-based approach

LULC Class	Method / Algorithm	Validation for the year 2010				Validation for the year 2020			
		Actual	Simulated	Validated	% Difference	Actual	Simulated	Validated	% Difference
Urban	ANN	403.68	266.08	-137.6	34.08%	746.8	405.89	-340.9	45.64%
	CA - Markov		220.67	-183	45.33%		382.51	-364.28	48.77%
Vegetation	ANN	655.91	355.05	-300.85	45.86%	746.53	656.6	-90.44	12.11%
	CA - Markov		280.71	-375.19	57.20%		580.94	-165.59	22.18%
Water Body	ANN	50.2	111.84	61.63	55.11%	90.5	50.39	-40.1	44.31%
	CA - Markov		83.81	33.61	66.95%		42.97	-47.52	52.51%
Un-classified	ANN	1938.2	2315	376.82	16.27%	1464.1	1935.58	471.46	32.20%
	CA - Markov		2462.75	5245.84	27.06%		2041.52	577.4	39.43%
% Correctness		ANN= 62.63% CA - Markov= 50.87%				ANN= 71.75% CA - Markov= 59.28%			

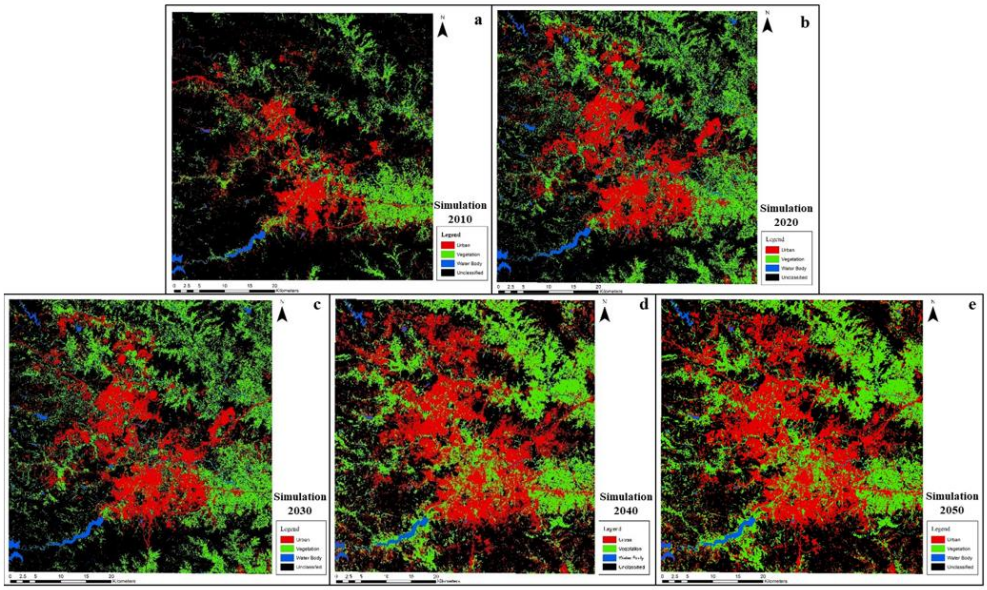

Figure 7. Predicted (simulated) LULC change map, derived through ANN and CA-Markov models using previous year data, a, b, c, d and e represents predicted LULC: a) 2010, b) 2020, c) 2030, d) 2040, e) 2050

Table 4: Validation for the year 2010 and 2020 using software

		2010	2020
% Correctness	ANN	64.18%	69.63%
	CA - Markov	48.86%	55.25%
K value	ANN	0.6122	0.6511
	CA - Markov	0.392	0.4438

The percentage correctness for the years 2010 and 2020 is validated using an area-based approach and software. Table 4 shows the output obtained by both the methods, which is almost the nearby values of one another and indicates that the validation is appropriate. But, as the techniques used, MOLUSCE (ANN based) is more accurate and efficient than Markov model, because percentage correctness using MOLUSCE by both methods is greater than 60% as compared to Markov. In addition, Kvalue is satisfying the value obtained using MOLUSCE than Markov Chain Model.

In the study, the classification is obtained using the Machine Learning Algorithm is not only accurate than traditional superlative method but also the most appropriate tool for predicting land use land cover changes and identifying the trends with different logical conditions. Hence, the predicted and validated outcomes of ANN are more efficient than the Markov Model in terms of probability statistics and percent correctness. The major transition in the future indicates a significant growth of urban land cover due to a rapid increase in population and tremendous growth of industrial areas all around Pune city. Over recent decades, the growth has been more towards the west direction due to: proximity to Mumbai and connectivity with the JNPT Port, near Nhava Shewa; bigger scope for opportunities of employment and businesses; more suitable and better living standards in comparison to other similar tier cities in the country; highly conducive environment for faster and ease of doing business; the large-scale availability of abundant water sources in the study region; and conducive weather conditions.

Conclusion

Geospatial technologies along with artificial intelligence methods demonstrate that urban growth is expected to be occurred along Pune-Bengaluru National Highway, Pune-Ahmednagar State Highway and Pune-Solapur-Hyderabad National Highway, which are proposed to be connected by Ring Road for smoother and efficient traffic and transportation to avoid city traffic congestion. The proposed construction of roads will have bigger impact on the development in the ribbon strips along the roads. Considering the potential of the recent advanced artificial intelligence and geospatial technologies, it is observed that it can detect and predict all the requisite details of the various changes occurring in the land use and land cover. Hence, it is recommended to the administrators, planners and policy/decision makers to make use of Geo-AI technology for urban planning studies, analysis, and decision-making process. The limitation of this study is that the difference between simulated and validated models' results are huge, so "distance to road" factor was only considered. Therefore, other proximity factors like industrial location, rivers, waterbodies and hills should also be included in future research.

Acknowledgement

The authors wish to thank editors and anonymous reviewers for their comments and suggestions that helped to improve the paper. In addition, they thank Prof. Isha Panse, COEP and C-DAC, Pune, for providing facilities and support to complete the work successfully.

References

1 Rawat, J.S. and Kumar, M. (2015). Monitoring land use/cover change using remote sensing and GIS techniques: A case study of Hawalbagh block, district Almora, Uttarakhand, India; The Egyptian Journal of Remote Sensing and Space Science, 18(1):77-84.

2 Li, L.; Lu, D. And Kuang, W. (2016). Examining Urban Impervious Surface Distribution and Its Dynamic Change in Hangzhou Metropolis. Remote Sens-Basel, 8(3).

3 Basommi, L. P.; Guan, Q.; Cheng, D. and Singh, S. K. (2016). Dynamics of land use change in a mining area: a case study of Nadowli District, Ghana; J Mt Sci. 13(4), 633-42.

4 Marwa W.; Halmy, A.; Gessler, P. E.; Hicke, J. A. and Boshra, B. S. (2015). Land use/land cover change detection and prediction in the north-western coastal desert of Egypt using Markov-CA; M.W.A. Applied Geography, 63.

5 Sivakumar, V. (2014). Urban mapping and growth prediction using remote sensing and GIS techniques, Pune, India; The International Archives of the Photogrammetry, Remote Sensing and Spatial Information Sciences; Volume XL-8.

6 Maktav, D.; Erbek, F. S. and Jurgen, S. (2005). Remote sensing of urban areas. International Journal of Remote Sensing, vol. 26, no. 4, 655-659.

7 Liping, C.; Yujun, S.and Saeed, S. (2004). Monitoring and predicting land use and land cover changes using remote sensing and GIS techniques: A case study of a hilly area, Jiangle, China; PLoS ONE 13(7): e0200493.

8 Gismondi, M.; Kamusoko, C.; Furuya, T.; Tomimura, S. and Maya, M. (2014). MOLUSE: An open-source land use Change analyst for QGIS, Documentary on Molusce Plug-in, 20, 612-614.

9 Xia, L. and Yeh, A.G. (2002). Neural-network-based cellular automata for simulating multiple land use changes using GIS, International Journal of Geography Information Science, 16, 323-343.

10 Siddiqui, A.; Siddiqui, A.; Maithani, S.; Jha, A. K.; Kumar, P. and Srivastav, S.K. (2018). Urban growth dynamics of an Indian metropolitan using CA Markov and Logistic Regression, The Egyptian Journal of Remote Sensing and Space Sciences, 21, 229-236.

11 Saputra, M. H. and Lee, H. S. (2019). Prediction of Land Use and Land Cover Changes for North Sumatra, Indonesia, Using an Artificial-Neural-Network-Based Cellular Automaton, Article in Sustainability, 11, 1-16.

12 Arsanjani, J. J.; Helbichb, M.; Kainza, W. and Bolooranic, A. D. (2013). Integration of logistic regression, Markov chain and cellular automata models to simulate urban expansion, International Journal of Applied Earth Observation and Geoinformation, 21, 265-275.

13 opez, E.; Bocco, G.; Mendoza, M. And Duhau, E. (2001). Predicting land cover and landuse change in the urban fringe: a case in Morelia city, Mexico, Landscape and Urban Planning, 55, 271-285.

14 Arsanjani, J. J., Kainz, W. And Mousiv and, A. J. (2011). Tracking dynamic land-use change using spatially explicit Markov Chain based on cellular automata: the case of Tehran, International Journal of Image and Data Fusion, 2(4), 329-345.

The Indian Geographical Journal
Volume 96 (2) December - 2021, pp 147-166
ISSN 0019-4824

MORPHOLOGICAL CHARACTERISTICS OF STREAMS IN EXTREME HUMID AREAS - A CASE STUDY OF THE UM-U-LAH WATERSHED, CHERRAPUNJEE

Andy T. G Lyngdoh * and Bring B. L. Ryntathianng

Department of Geography, Umshyrpi College, Shillong 793004.
*Correspondent author email: andygaland86@gmail.com

Abstract

The morphological characteristics of streams are an essential aspect of all the hydrological and geomorphic processes that occur within the watershed. The present research tries to understand the morphological characteristics of the Um-U-Lah Stream, an initial stream situated in Cherrapunjee well known for receiving the highest rainfall in the world. Various morphological characteristics and morphometric analysis were computed using a GIS environment and manipulated for different calculations. The analysis reveals that the total number and length of the stream is maximum in the first order and decreases as the stream order increases, and the bifurcation ratio between different successive orders is almost constant. Rapid changes in the stream morphology (rapids, potholes, Knick points, pools, riffles, and exposed bedrock) are observed, reflecting the influence of tectonics and structure in this area.

Keywords: Stream, stream morphology, extremely humid areas, climate, rainfall.

Introduction

A river or a stream is a body of flowing water in a channel, and its action is the most ubiquitous landscaping agency. The two basic generalisations about rivers were realised long before geomorphology emerged as an organised science. Streams form the valleys in which they flow and every river functions as a significant trunk segment fed by several mutually adjusted branches that diminish in size away from the main stem. It is generally assumed in fluvial geomorphology that the influence of climate on river morphology is through the magnitude and frequency of flood events, and the same magnitude can have a differing impact depending on the state of the channels. (Huckleberry, 1994; Hooke, 1996).

Morphometric analysis of a watershed provides a quantitative description of the drainage system, an essential aspect of characterising the watershed (Strahler, 1964). The influence of drainage morphometry is very significant in understanding the landform processes, soil physical properties and erosional characteristics. Drainage characteristics of many rivers' basins and sub-basin in different parts of the globe have been studied using conventional methods (Horton, 1945; Strahlar, 1957, 1964; Krishnamurthy et al., 1996).

Morphological characteristics of the river are the intricate components of the river system; such characteristics, in turn, influence the hydrological response and river morphology downstream. The river morphology is determined by the valley topography and the characteristics of the river basin (geology, soil, mechanical properties). The shapes and patterns of the rivers are the results of a long history of climate change, tectonic activities, land use, and human interference. Investigating river morphology and its linkages to the catchment's physical condition provides a holistic understanding of the geomorphology and hydrology of the river system, high and low land and linkages observed in terms of channel morphology, flood, channel stability, and riverine ecology (Van Appledorn et al., 2019).

The research problem here is to understand the morphology of the Um-U-Lah Stream, an initial stream in one of the world's heaviest rainfall regions.

An understanding of the structure and function of morpho-dynamics requires an analysis of not just the channel itself but of the catchment environment as well (Krzemien et al., 1999). The morphological characteristics of a river reach are a dynamic equilibrium between upstream sediment input, discharge regime and grain sizes composing the bed of the reach. A natural or artificial modification of one of these factors can produce changes in channel form at the point of the perturbation and potentially affect several kilometres downstream and even upstream by the consequence of backwater effects. The resulting transformation of the bed is the morphological adaptation toward another dynamic equilibrium corresponding to the new conditions (Benjamin et al., 2010).

Kale (2002), in his paper, emphasised that the rivers of India reveal specific unique characteristics because they undergo large seasonal fluctuations in flow and sediment load. Furthermore, the reproductive success of salmonoids and other riverine communities is influenced by the size of the sediment eroded from and deposited on the channel bed and banks (Montgomery et al., 1996). Channel morphology, a significant component of a river system, is a result of these factors. These factors can be divided into those that are enforced on the watershed (i.e., independent) and those that adjust to the enforced conditions (i.e., dependent) (Hogan and Luzi, 2010).

Stewardson (2005) stated that the variation in the river hydraulic geometry through the stream networks is central to the problem of catchment management. The river hydraulic geometry through the stream networks influences the flow and sediment routing, physical habitat and channel flood plain interaction, and the general definition of hydraulic geometry is a series of functions (normally power function) relating to channel width, water depth and mean velocity at a specific channel cross-section to discharge.

Fannegan et al., (2005) applied the Manning equation and basic mass conservation principles to derive an expression for scaling the steady state, width of a river channel as a function of discharge, channel slopes, roughness, and width to depth ratio. Factors other than the character of sediments can affect the cross-sectional shapes of the channel. (Miller, 1990), for example, the root system of riparian vegetation distinctly decreases bank

erosion and controls channel width. In contrast, large trees that fall across the channel may increase bank erosion.

The main objective is to study the morphological characteristics of the Um-U-Lah Stream as it flows down the channel, which will help to understand the river processes and prescribe countermeasures to address soil conservation and watershed management, flood, bank erosion, and channel avulsion problem.

Methods and Materials:

The study aims to understand the morphological characteristics and the processes that change the river morphology. The basin and morphological variables used in the study were derived from the Topo-sheet No: 78/O/11/SE and satellite imageries available on Google Earth, digital elevation models, and relevant maps. Further, various morphological characteristics and morphometric analyses were computed using map info software and Microsoft Excel to understand the drainage basin's geo-hydrological characteristics of the terrain, features, and flow pattern.

The Um-U-Lah stream is divided into six major sections and 31 minor sub-sections, and a cross-section of each section was surveyed. The different attributes of the stream, namely the channel shape, size, width, depth, and channel pattern, were measured and recorded using numerous instruments such as the laser distometer was used to measure the width of the river channel in the different sub-sections, the Schmidt hammer was used to measure the hardness of the rock surface at various sections and sub-sections of the Um-U-Lah Stream. The measuring tape was used to measure the length of the river from one sub-section to the other of the Um-U-Lah stream to observe the morphological characteristics of streams in extremely humid areas.

The results gathered from the field survey are finally compiled and interpreted along with other relevant reports, research papers and documents.

Regional Settings:

The area chosen for the current work is a micro watershed locally known as Um-U-Lah located in Cherrapunjee, which stands on the southern slope of the Meghalaya plateau, facing Bangladesh. The area extends from 91.715045° east to 91.729592° east longitude and 25.284860° north to 25.268677° north latitude (Singh and Syiemlieh, 2010) and falls under the jurisdiction of the Shell-Bholaganj Community and Rural Development (C&RD) Block. The area experiences an extremely humid climate with a distinct wet season and is famous for receiving the heaviest rainfall globally. According to recent reports, the annual rainfall in Cherrapunjee is about 8101.99 mm in 2021. It has also been recorded that the highest rainfall occurs mainly in July, which is greatly influenced by the southwest monsoon. The area has been deeply eroded by water due to incessant rainfall giving rise to a rugged topography and unique topographical features.

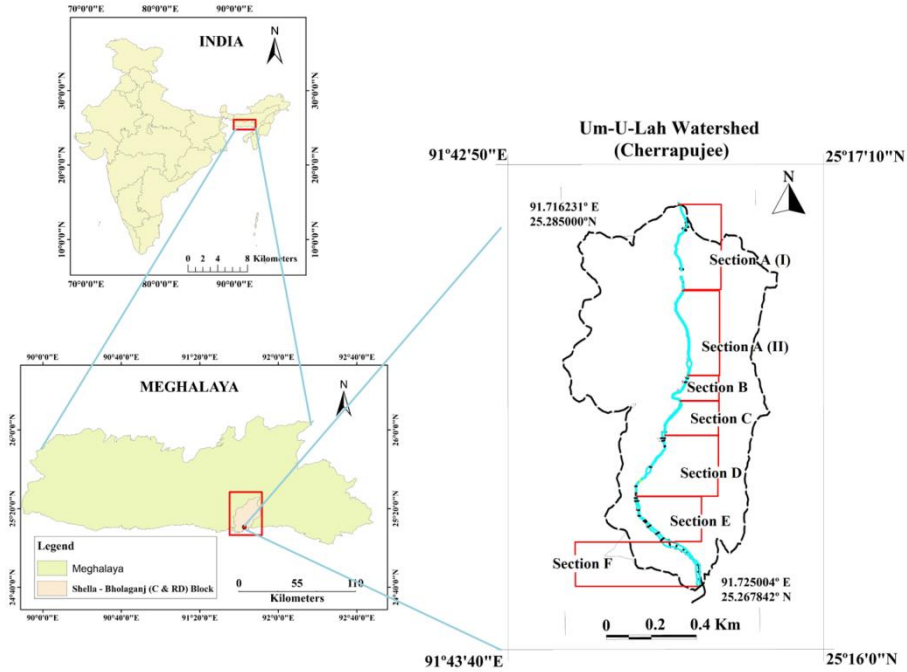

Figure 1: Location Map of the Um-U-Lah Watershed
Source – Compiled by the researcher

Results:

The Um-U-Lah stream follows a dendritic drainage pattern, considered the most common drainage pattern found on the earth's surface. The Um-U-Lah watershed has about 18 steams in the fourth order sprawled over an area of 1.025 km, as shown in figure 2. The first order stream constitutes 7.8 per cent; the second order is 6.82 per cent, the third order is 1.95 per cent, and the fourth order is 1.075 per cent, respectively, showing a decrease in the stream frequency as the stream order increases, which indicates lower the order the higher the number of streams. The highest frequency can be attributed to flat topography and small ridges with numerous tributaries and distributaries. The Drainage Density is the highest in the first order, as shown in table 1 and decreases with increasing stream order, showing an increase in stream population concerning increasing drainage density and vice versa. Further, the highest bifurcation ratio shows the highest overland flow and discharge because of the stream's geology and lithological development.

With the help of the Topo-sheet No: 78/O/11/SE, satellite imagery and map-info software, the longitudinal profile of the Um-U-Lah stream is being generated, which is seen to be slightly concaved (figure 3), still far from the ideal profile of equilibrium. Further, it is seen that the longitudinal profile of the stream is moderately irregular, with two knick points observed along with the profile.

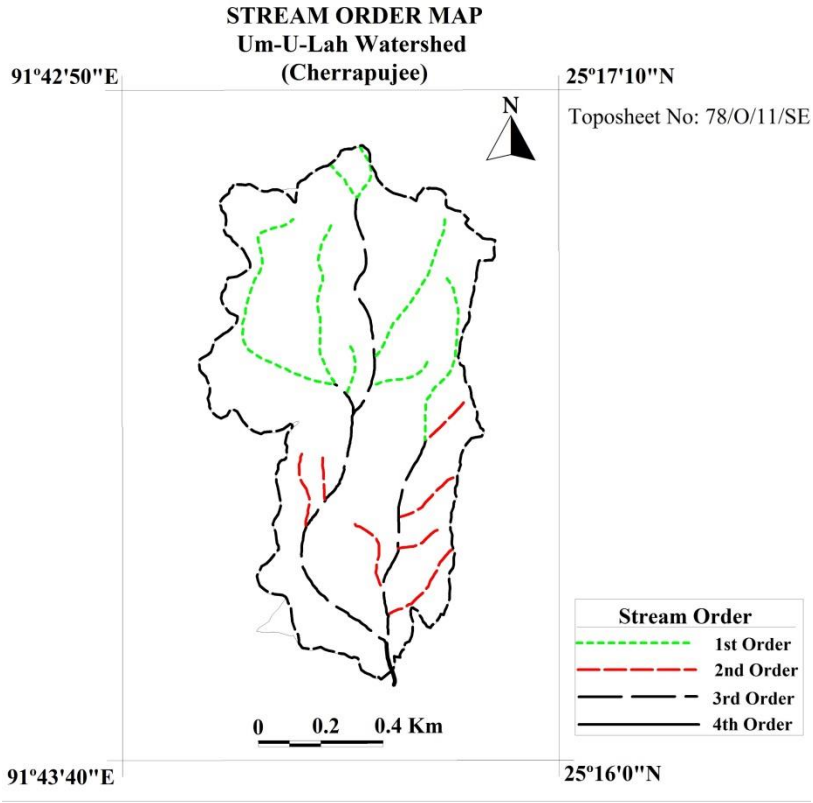

Figure 2: Stream Order Map of the Um-U-Lah Watershed
Source – Prepared by the researcher

Table 1. The Um-U-Lah Watershed Characteristics.

Um-U-Lah Watershed Characteristics					
Stream Order	**1**	**2**	**3**	**4**	**Total**
No of Stream	8	7	2	1	18
Stream Length	3.215	2.135	1.791	0.0529	**7.1939**
Percentage of Stream Length	44.69	30.42	24.89	0.73	**100**
Drainage Density	3.13	2.08	1.74	0.71	**7.66**
Drainage Frequency	7.8	6.82	1.95	1.075	**17.645**
Bifurcation Ratio		1.4	3.5	2	

Source – Prepared by the researcher**.**

The longitudinal profile of the Um-U-Lah stream shows an interrupted profile, especially in the upper part of the stream, with a steep gradient and dense vegetation cover. However, the stream's longitudinal profile becomes more clearly defined in the lower part of the stream, where the stream flows through grasslands and flat lands. The morphological characteristics of the Um-U-Lah stream vary from one section to the other.

The majority of the slope gradient in the area ranges between 10°-18°, with only a few areas falling under the slope gradient between 45°- 90°. Further, each section and sub-sections of the stream is characterised by varying channel width, depth and pattern and accompanied by potholes, ripples, knick points, human interference etc., which affects the water discharge and stream equilibrium resulting in aggradation or degradation. Similarly, the river bed level changes because of the changes in land use, catastrophic floods, and tectonic or neo-tectonic activities.

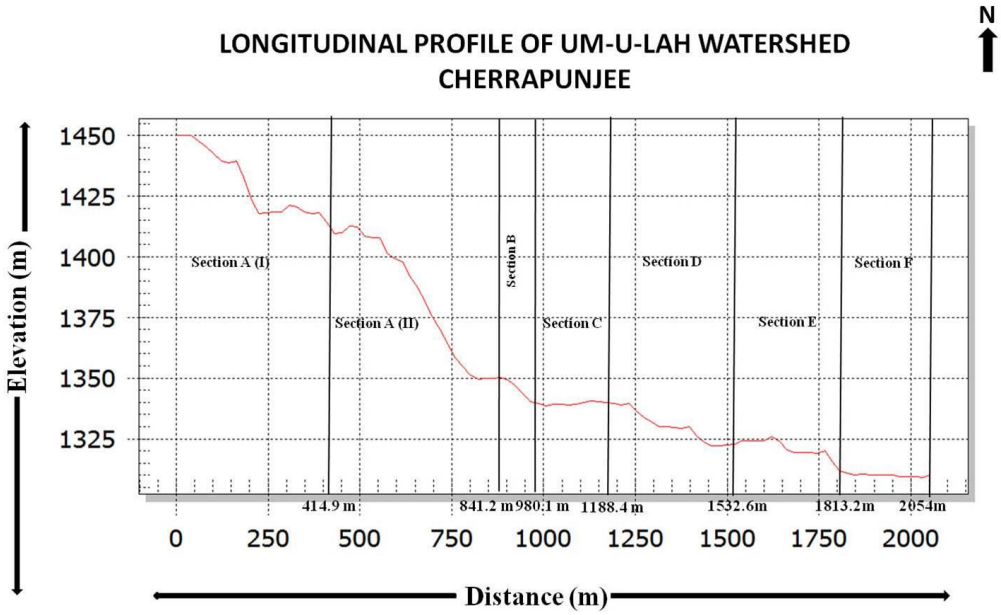

Figure 3: Longitudinal Profile and Cross Section of the Um-U-Lah Watershed
Source – Prepared by the researcher

Discussion:

In the study area, the Um-U-Lah stream shows diverse morphological characteristics. The operation of the exogenetic forces at different rates over a long period has widened the channel pattern and increased the depth, width, and sinuosity, especially in the lower course of the stream. The effect of bank erosion has increased the width of the channel pattern and the sediment discharge. In such an extremely humid region, weathering also plays a significant role in influencing stream morphology. The exogenetic forces combined effect has created a variation in the rock structure and the rock hardness. The rock hardness in this region varies from 34 to 69 R-Value (Rebound Value), indicating that the softer and exposed rocks are easily eroded by weathering agents, leaving the harder rocks behind.

The Um-U-Lah Stream is divided into 6 major sections and 31 sub-sections, and a detailed analysis of the different morphological characteristics such as the channel shape,

size, width, depth, and channel of the stream is done on a section basis. Further, the morphological attributes of the different sections and sub-sections of the Um-U-Lah stream are briefly discussed below:

Section A (I)

This section is the source of the Um-U-Lah stream and is further subdivided into five sections ranging from sections 1 to 5. Numerous small rivulets from high elevated areas joined together to form the youthful stage of the stream. Here, the stream emerges from a drain and spring, which the people have modified for lucrative purposes. The length of the stream in this section is 414.9metres and has a moderate to moderately steep with a gently steep longitudinal profile. The general elevation of this section varies from 1410 meters to 1450 meters.

All the sub-sections slopes vary from moderate to moderately steep, and the degree of slope ranges from 8° to 15°. There is no uniformity in the slope profile to slope angles from the hilltops to the valley's floors in the different sub-sections. The longitudinal profile of the stream in different sub-sections is straight, but it varies significantly as the channel pattern becomes steep and flows downwards. Further, the longitudinal profile of sub-section 1 and 2 is straight and flat. Sub-sections 3 to 5 have a straight, gently sloping longitudinal profile. The length of the stream in sub-sections 1, 2, 3 and 5 varies from 1 meter to 100 meters. However, the length of the stream in sub-section 4 is considered the highest at 201.7 meters.

The channel width of this section ranges from 1.5 meters to 3.6 meters. As the channel moves downwards according to the pattern of the stream, the width tends to increase. The channel width increases mainly due to lateral erosion during the rainy season, and bank erosion is seen to be an essential feature seen along with the channel pattern in this section. In sub-sections 4 to 5, the width has increased to 3.4 meters and 2 meters due to the joining of a small rivulet from a nearby area.

The channel depth of the stream varies considerably from one sub-section to another. On the one hand, sub-sections 1, 2, 4 and 5 have a channel depth of 1 meter; on the other hand, sub-section 3 has a depth of 1.5 meters. The depth of the channel is accompanied by cobbles and a small number of sand deposits brought by the stream during the rainy season.

The channel pattern of the stream in the different sub-sections is straight except for sub-section 3, where it is slightly sinuous towards the right. The river bed in this section remains dry except for sub-sections 1 and 2, where a small quantity of water flows due to human affluence. However, water in sub-section 3, 4, and 5 flows only during the rainy season.

The people residing near the source significantly affect the stream in this section. Modifying the spring that is the stream's source and dumping different kinds of human waste have affected the stream's health and disrupted the ecosystem.

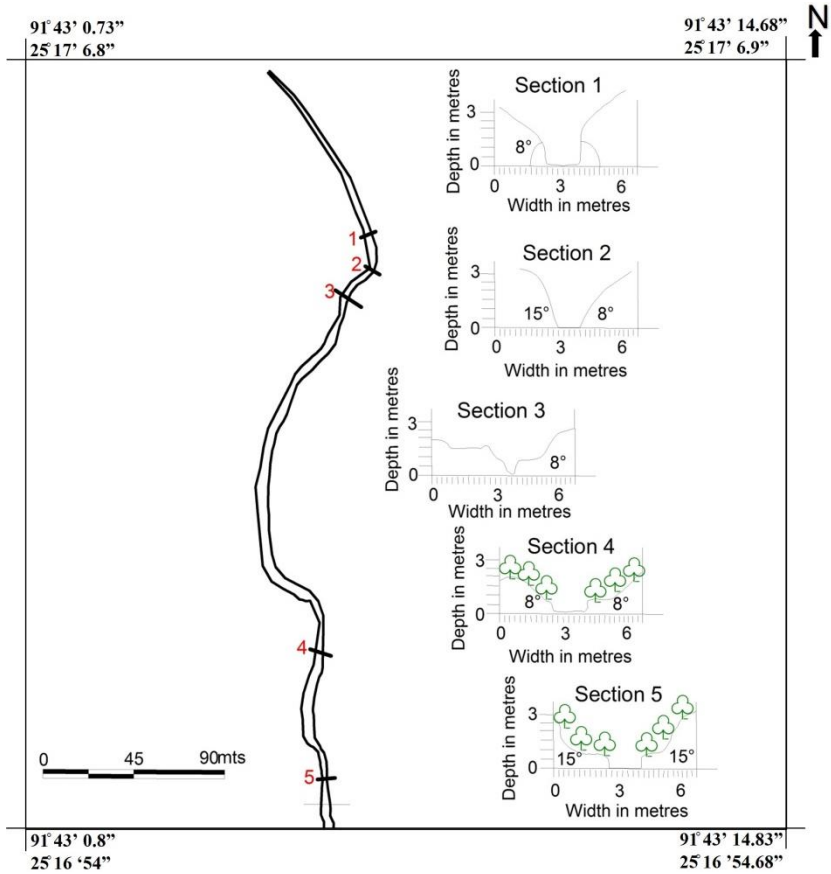

Figure 4: Section A (I) and sub- sections of the Um-U-Lah Stream

Source – Prepared by the researcher

Section A (II)

Section A (II) is divided into two sections, namely, sections 6 and 7. The length of the stream is about 32.9 meters and has a straight and gently sloping longitudinal profile. The lithology of this section is composed of sedimentary rocks, primarily shale and sandstone, having different degrees of hardness. The slope in this section is different from one sub-section to another sub-section. This section has a moderate to moderately steep slope with a 10° slope in sub-section 6 and a 15° slope in sub-section 7.

In both sub-sections 6 and 7, there is hardly any change in the longitudinal profile. The length of the stream in sub-section 6 cannot be attained due to the inaccessibility and very steep slope of the area. However, the length of the stream is measured only in sub-section 7, where it is 32.9 meters.

The channel width of this section varies from 4 meters to 5.5 meters, and it increases downwards according to the pattern of the stream flows. The width of the channel in sub-section 7 is 4.6 meters, and in sub-section 7, it is 5.1 meters, respectively.

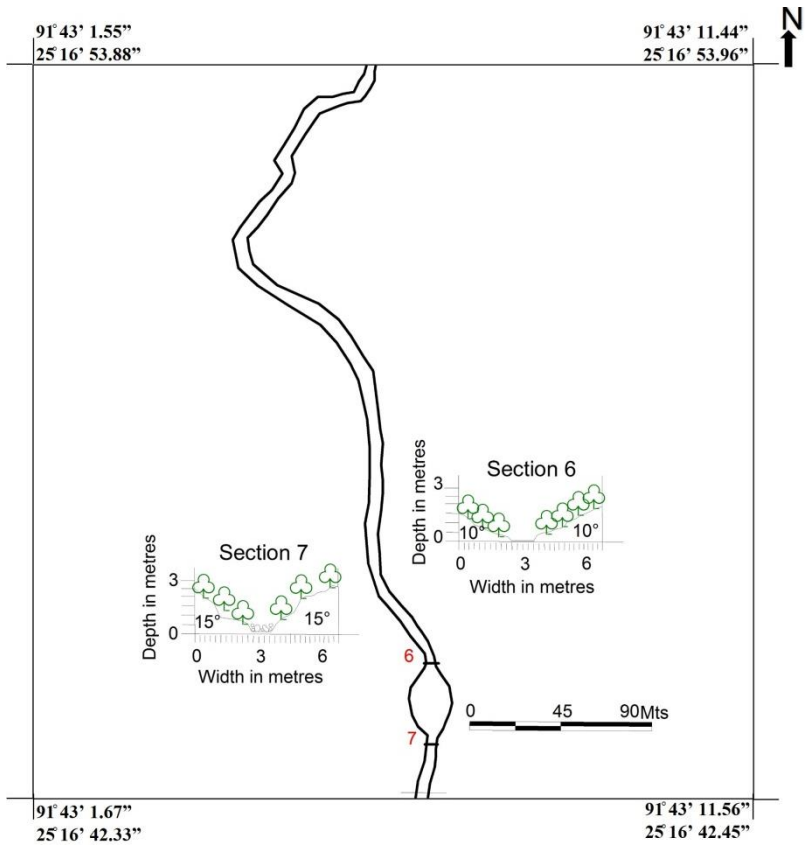

Figure 5: Section A (II) and sub- sections of the Um-U-Lah Stream
Source – Prepared by the researcher

The channel depth of sub-section 6 is 1 meter, and in sub-section 7, it is 2 meters. The channel depth of this section is accompanied by boulders, cobbles, pebbles and a small amount of sand deposit brought by the stream during the rainy season.

The channel pattern in sub-section 6 is straight, while the channel pattern in sub-section 7 is sinuous. The variation in the channel pattern is due to the flow and discharge of the stream. The channel pattern in this section is accompanied by different erosional features of the stream, such as rapids, potholes and an alternate sequence of pools and riffles.

Section B

A moderately steep slope is characterised in section B. The stream length in this section is 138.9 meters, and the longitudinal profile is straight. This section is mainly composed of sandstone and shale; rocks, boulders, cobbles and pebbles of different sizes and shapes are the attributes of this section.

The slope of the different sub-sections in this section varies from moderate to moderately steep. The degree of slope varies from 10° to 18°, and no uniformity is observed in the slope profile. The slope is convex in different sub-sections except in sub-section 10, where the slope is concave.

The stream's length in different sub-sections has been measured and varies significantly from one sub-section to another. The sectional division of the sub-section greatly determines the length of the stream. The stream length in different sub-sections ranges from 50 meters to 60 meters, except for sub-section 10, where the length of the stream is only 30.7 meters. Under the influence of the channel pattern and the stream's direction of flow, the stream's longitudinal profile in sub-section 8 and 9 are straight and slightly steep. However, the longitudinal profile of the stream in sub-section 10 is straight and gently sloping, allowing bed-load transportation downstream.

The channel width in this section ranges from 5 meters to 5.9 meters. It has been observed that the width of the channel increases slowly from one sub-section to another sub-section.

The channel depth varies from 0.7 meters to 1.8 meters, and the channel depth in sub-sections 8 and 9 ranges from 1 to 2 meters, respectively. As the stream flows downwards to sub-section 10, characterised by a plain topography, the channel depth has decreased considerably to 0.7 meters. The channel depth of this section is accompanied by boulders, cobbles, pebbles and sand deposits.

The channel pattern in this section varies significantly from one sub-section to another. As the stream flows downwards, sub-section 8 and 9 are characterised by a straight channel pattern, and sub-section 10 is slightly sinuous. The channel pattern in this section is accompanied by the different erosional features such as riffles, pools, potholes and rapids. Variations in river beds have been observed in sub-sections 8 and 9, while in sub sections 10, a small volume of water flows through the channel.

Further, human interference can also be seen in this section, particularly in sub-section 10 where the people use the stream for different purposes, such as washing clothes and vehicles, which has deteriorated the water and the stream ecosystem.

Section C

Section C is characterised by plain topography, gentle slope, potholes, knick points, rapids, cobbles, pebbles, and fine and coarse sediments. The length of the stream in this section is 203.8 meters and has a straight longitudinal profile. The slope in section C is moderate and ranges from 2° to 10°; however, the degree of slope is not constant, and it changes from one sub-section to another. The slopes in sub-section 11, 13 and 14 are convex, whereas the slope in sub-section 12 is concave.

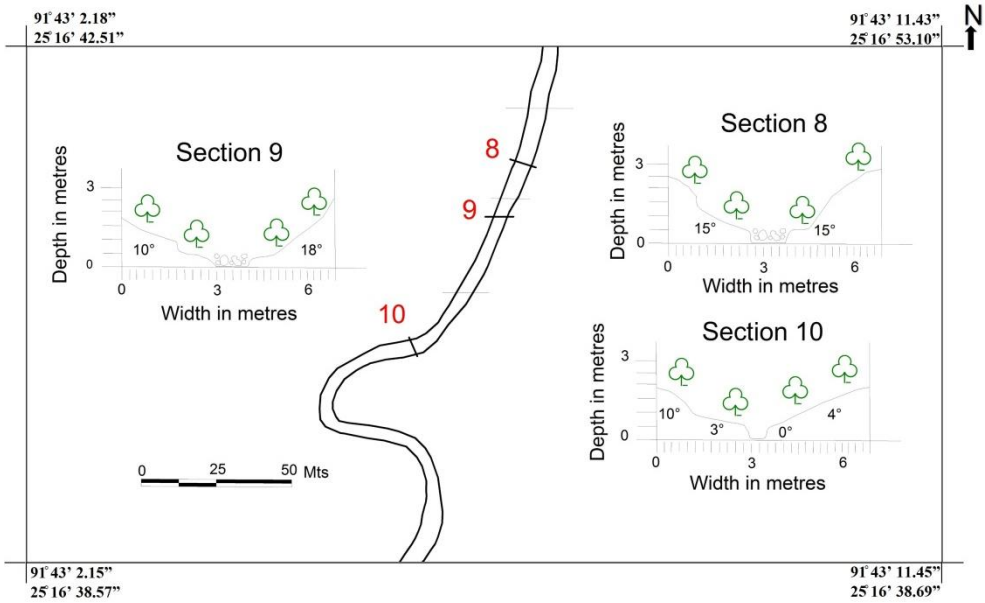

Figure 6: Section B and sub- sections of the Um-U-Lah Stream
Source – Prepared by the researcher

In sub-sections 11 and 12, the length of the stream ranges from 1 meter to 50 meters. Similarly, in sub-sections 13 and 14, the length of the stream ranges from 50 meters to 100 meters. The longitudinal profile of sub-section 11 and 12 is straight, while the longitudinal profile of sub-section 13 and 14 is straight and gently sloping. Such variation in the longitudinal profile is mainly due to the flow direction and the stream's channel pattern.

In this section, the stream's width ranges from 4.2 meters to 7 meters and varies from one sub-section to another. The channel width of the stream is high in sub-section 12, where it is 7 meters and is low in sub-section 11, where it is 4.2 meters.

The channel depth of the different sub-sections that have been measured varies considerably. Sub-sections 11, 13 and 14 are characterised by similar channel depths ranging from 1 to 1.5 meters; however, in sub-section 12, the channel's depth is not deep; it is only 0.25 meters. Under a plain topography, cobbles, pebbles and sand deposits are found at regular intervals in the different sub-sections. Further, the channel pattern of sub-section 11 follows a slightly sinuous pattern, while a straight channel pattern is observed in sub-section 12 to 14.

Section D

Section D is characterised by a plain topography, gentle precipitous slope and knick points. The length of the stream in this section is 344.2 meters, and this section is mainly composed of sandstone and shale. This section has a straight and steep longitudinal profile. The general elevation of the area varies from 1320 meters to 1340 meters.

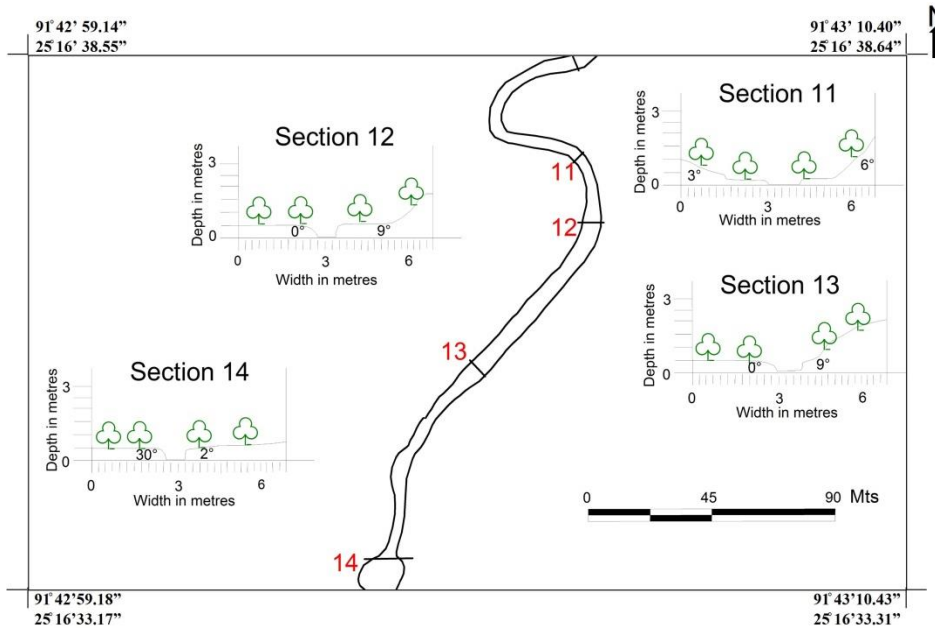

Figure 7: Section C and sub- sections of the Um-U-Lah Stream
Source – Prepared by the researcher

The slope of all the sub-section varies from gentle to steep, and the degree of slope ranges from 2° to 90°. In sub-section 15(a), the degree of slope is enormously high, precipitous, and vertical, and varies from 45° to 90°. Such a high degree of slope in this sub-section is due to the presence of a Knick point (waterfall) where the waterfall height is 8 meters. Sub-section 17 also has a high degree of slope, varies from 12° to 90°, and is moderately steep and wall-like. However, the slope in sub-section 15 (b) to 19 varies from gentle to moderately steep slopes ranging from 2° to 18°.

The longitudinal profile of sub-section 15 (a), 15 (b) and 16 is straight and steeply sloping. However, sub-section 17 to 19 has a straight and gently sloping longitudinal profile. The stream's length in sub-sections 15 (a), 15 (b), 18 and 19 ranges from 1 meter to 100 meters, while the stream length in sub-section 16 ranges from 100 meters to 120 meters. The length of the stream is greater in sub-section 16, where it is 115.6 meters and lesser in sub-section 19, where it is only 9.07 meters.

The channel width of this section ranges from 4.2 meters to 10.4 meters. The variation in the channel width has been observed in the different sub-sections. The channel width is somewhat similar, although specific changes can be seen. Sub-section 15 (b) has a broad channel width of 10.4 meters, and sub-section 18 has a narrow channel width of 4.2 meters, respectively.

The channel depth of the stream varies considerably from one sub-section to another sub-section, and it ranges from 1 meter to 9 meters, respectively. Conversely, sub-

sections 15 (a) and 15 (b) have channel depths of 8 meters and above; conversely, sub-sections 16 to 19 are characterised by channel depths ranging from 1 meter to 3.6 meters. The channel depth of this section is also accompanied by boulders, cobbles, and fine and coarse deposits.

The channel pattern of the stream in the different sub-sections is straight except for sub-section 16, where it is slightly sinuous. This section is also characterised by potholes, lateral erosion, Knick point, rapids, exposed bedrock and an alternate sequence of pools and ripples.

Besides all the above morphological attributes of the stream, the hardness of the rock has also been measured. The hardness of the rock varies significantly, and the variations are mainly caused by weathering the exposed rocks or by the geologic nature of the area. In sub-section 16, the hardness of rocks ranges from 30 to 38 R-value (Rebound value); in sub-section 17, the hardness ranges from 49 to 60 R-value; in sub-sections 18 and 19, the hardness of the rock ranges from 48 to 64 R-value.

The stream in this section has been affected by the people who are dependent on the stream. Modifying the stream by creating a dam in sub-section 17 has caused instability and disrupted the ecosystem. Furthermore, washing clothes by the people in the stream just below the dam degrades the stream's health, affecting the flora and fauna species that thrive on it.

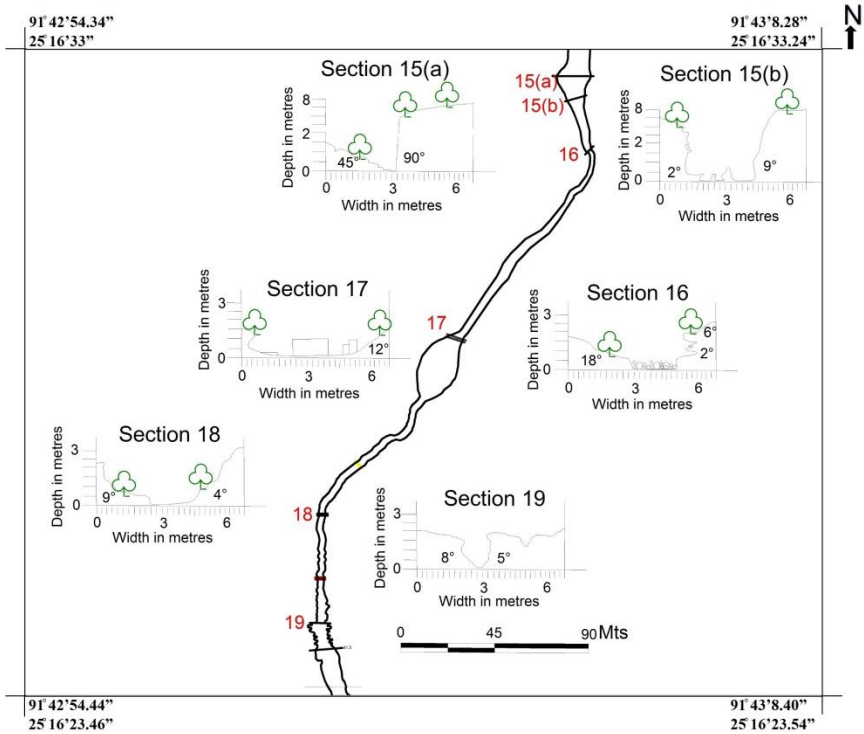

Figure 8: Section D and sub- sections of the Um-U-Lah Stream

Source – Prepared by the researcher

Section E

Section E is characterised by moderate to steep slopes and plain topography. The stream length in this section is 298.6 meters, and the longitudinal profile is straight and gently sloping. The lithology of this section is mainly composed of sandstone and shale; rocks, boulders, cobbles and pebbles of different sizes and shapes are the attributes of this section.

The slope in this section is different from one sub-section to another sub-section. This section has a gentle to moderately slope ranging from 2° to 25°. As topography changes from hills to plains, the degree of the slope also changes from steep to gentle. The slopes in the different sub-sections are convex and concave.

The longitudinal profile of the stream is straight and gently sloping. However, the longitudinal profile varies from one sub-section to another sub-section. The stream's longitudinal profile in sub-sections 21-24 is straight and gently sloping, whereas, in sub-section 25, the longitudinal profile of the stream is straight and steeply sloping. Sub-section 22 has 24.8 meters, which is the shortest compared to other sub-sections, while the length of the stream in sub-section 24 is 102.3 meters, the longest in this section.

The channel width of this section varies from 7.4 meters to 19 meters, and it increases downwards according to the pattern of the stream flows. The width of the channel is broad in sub-section 25, where it is 19 meters and narrow in sub-section 23, where it is only 7.4metres, respectively. Hence, the water and sediment discharge greatly influence the stream's width.

The channel depth in this section varies from 0.25 meters to 1.6 meters. The channel depth of most sub-sections falls below 1 meter, and in sub-section 25, it is 1.6 meters. The channel depth of this section is accompanied by boulders, cobbles, pebbles and a small amount of sand deposit brought by the stream during the rainy season.

The channel pattern in all the sub-sections is straight. The channel pattern in this section is accompanied by different erosional features such as rapids and potholes. Due to low water discharge, the bedrocks are exposed in several sections.

Section F

Section F is characterised by plain topography, grasslands, gentle slope and barren rocks. The length of the stream in this section is 222.8 meters, and it is mainly composed of sandstone and shale. This section has a straight longitudinal profile. This section's attributes are potholes, exposed bedrock, boulders, cobbles, pebbles, and fine and coarse sediments. The general elevation of the area varies from 1310 meters to 1320 meters.

The length of the stream in different sub-sections has been measured and varies significantly from one sub-section to another. The stream length in sub-sections 26 to 31

ranges from 1 to 50 meters. However, the length of the stream in sub-section 27 is above 50 meters. Sub-section 26 has the shortest length of 23.3 meters, while sub-section 27 has the most extended length of 54.6metres.

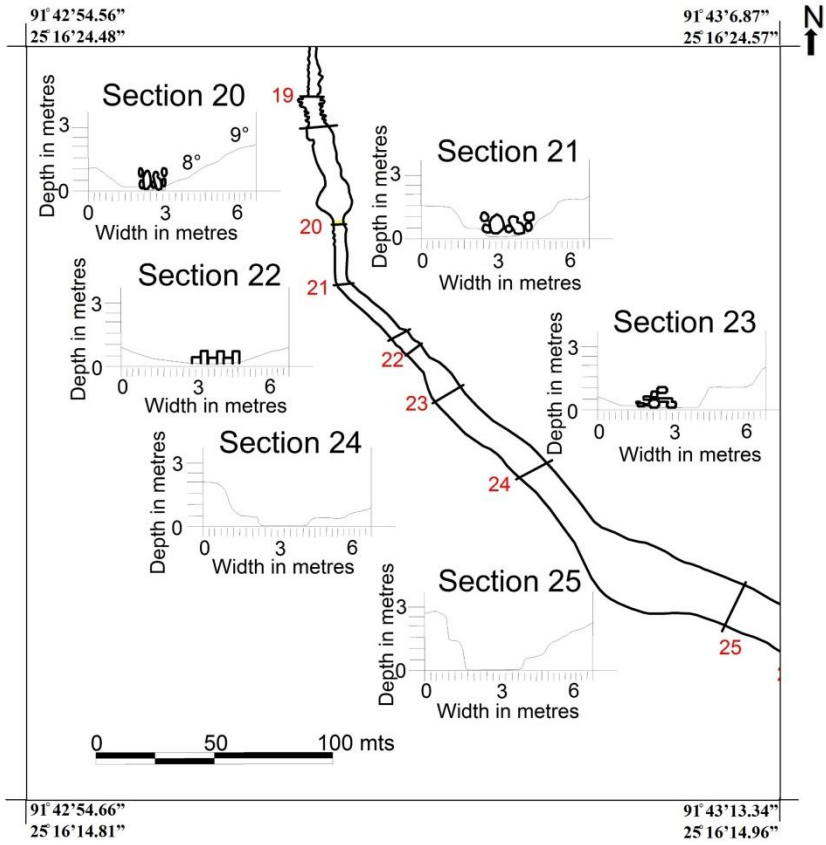

Figure 9: Section E and sub- sections of the Um-U-Lah Stream
Source – Prepared by the researcher

The sub-sections in this section vary from moderate to moderately steep, and the degree of slope ranges from 3° to 15°. In all the sub-sections of this section, the slope and the degree of the slope are similar. However, the nature of the slopes varies considerably from convex to concave.

The longitudinal profile of the stream is similar in all the sub-sections. Being dominated by highly undulating topography, the stream's longitudinal profile in all the sub-sections is straight and gentle sloping.

The channel width of this section ranges from 9.2 meters to 15.9 meters. The variation in the channel width has been observed in the different sub-sections. Sub-section 28 has a broad channel width of 15.9 meters, and sub-section 27 has a narrow channel width of 9.2 meters, respectively.

The channel depth of the stream varies considerably from one sub-section to another and ranges from 0.75 meters to 2.6 meters, respectively. Sub-section 31 has a channel depth of 0.75 meters, which is relatively low, and sub-sections 27 have a channel depth of 2.6 meters, which is relatively high in this section. The channel depth of this section is also accompanied by boulders, cobbles, and fine and coarse deposits.

The channel pattern of the stream in different sub-sections is straight and somewhat similar, and all the sub-sections are characterised by potholes, lateral erosion, exposed bedrock, crumbled boulders in the stream bank, bedrock erosion and undercutting of the rock strata.

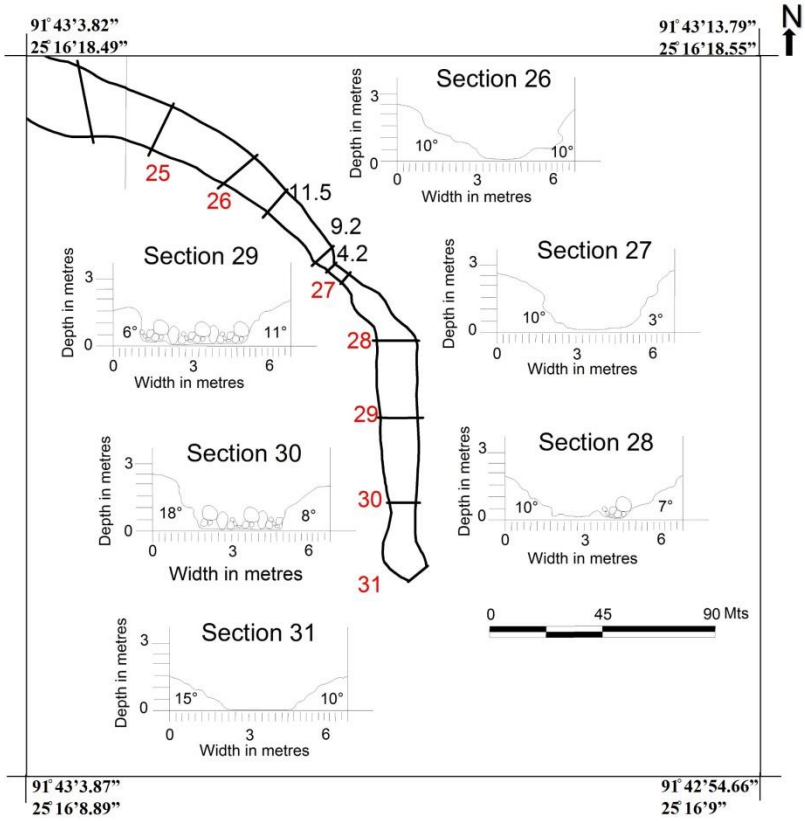

Figure 10: Section F and sub- sections of the Um-U-Lah Stream
Source – Prepared by the researcher

Conclusion:

Located on the southern slopes of the Meghalaya plateau and lying in the path of the South West monsoon, Cherrapunjee is characterised by heavy rainfall, especially during the monsoon season (June – September), and the atmosphere is almost saturated with water vapour, with a relative humidity of 94-95%. The alternating wet-dry annual cycle

with fluctuating rainfall volume between 7,000 mm to 24,000 mm is associated with intense solar radiation in the cool winter months and diurnal temperature changes in different seasons. The weathering processes operating under high fluctuating water levels lead to a considerable variation in the velocities of streams that depend primarily on the volume of rain that plays an essential role in shaping the channels of rivers and streams over old dissected landscapes and resistant rocks from time to time.

The Um-U- Lah catchment is built of limestone complexes of littoral facies. Therefore, the valley floor in those areas is marked by rising limestone mesas of 100-160 m high with a steep slope, ill-defined scarp, and typical karst topographic features like small uvals and different caves systems. The rocks are highly deformed and fractured. The catchment is characterised by rugged and hilly topography consisting of a drainage pattern controlled by the structure and a drainage network of total stream order. With drainage density of 7.6 kilometres reveals the presence of resistant permeable lithology.

The Um-U-Lah stream shows an interrupted profile with a steep gradient, especially in the stream's upper part. However, the longitudinal profile of the stream becomes more clearly defined in the lower part of the stream, where the stream flows through grasslands and flat lands. The stream has a slope of 39 %, indicating that the basin streams are colluvial and a direct receiver of the sediments from slope failure and erosion. Further, the sectional and sub-sectional division of the longitudinal profile shows a significant variation in the morphological characteristics of the stream from one sub-section to the other; this is primarily due to natural processes and human interference from time to time.

Acknowledgement

First, I would express my humble thanks to God who had given me physical and mental strength to complete this paper. I am deeply grateful and would like to express my thankful gratitude to Assistant Professor *Dr. Bring B. L. Ryntathianng,* Department of Geography, Umshyrpi College for his help, professionalism, and valuable guidance throughout this paper without whom this paper will not be fruitful. I would also like to express my gratitude to my father ***Late Amiya Bhuyan*** who had really inspired me in whatever I do.

References:

[1] Agarwal, M. (1989). Geomorphological Studies around Umiam Lake and Adjoining Areas, East Khasi Hills Meghalaya, India. Unpublished M. Phil Thesis, North Eastern Hill University, Shillong. Page: 10 - 120

[2] Agarwal, M. (1994). Geomorphology and Environmental Management of Umiam Basin, East Khasi Hill Meghalaya. Unpublished Ph.D.Thesis, North Eastern Hill University, Shillong. Page: 5 -79.

[3] Bathurst J. C. (1986). Sensitivity Analysis of the Systeme Hydrologique Europeen for Upland Catchment. Journal of Hydrology,vol 87. Page: 103-123.

[4] Beven K. J. (2001). Rainfall-Runoff Modeling - The Primer, John Willey & Son, LTD Chichester. Page: 124- 127.

[5] Beven, K. J., & Kirkby, M. J. (1979). A Physically Based Variable Contributing Area Model of Basin Hydrology. Hydrology Science Bulletin, vol 24. Page: 43-69.

[6] Biswas, S. (1990). Geomorphic study around Cherrapunjee, East Khasi Hills, Meghalaya. Unpublished Ph.D. Dissertation, North Eastern Hill University, Shillong. Page: 1-112

[7] Buffington, J., & Montgomery, D. (2013). Geomorphic classification of rivers. In: Shroder, J.; Wohl, E., (ed.), Treatise on Geomorphology: Fluvial Geomorphology, vol 9. San Diego, CA: Academic Press. Page: 730-767.

[8] Chakraborty, K., Joshi P. K., and Sarma K. K. (2009). Land use/ land cover dynamics in Umnogt Watershed of Meghalaya using Geospatial Tools. Journal of the Indian Society of Remote Sensing, vol 37 (1). Page: 99-106.

[9] Choudhury, B.C. (1985). Morphometric Analysis of the Upper Kaliyani River Basin, Mikir Hills, Assam, North East India. Unpublished Ph.D. Thesis, North Eastern Hill University, Shillong. Page: 1-125.

[10] Devi, H.I. (2000). River Basin Morphology. New Delhi, Rajesh Publication.

[11] Garde, R.J. (2006). River Morphology. New Age International (P) Limited, publisher, New Delhi. Page: 1-125

[12] Germanoski, D., & Schumm, S. (1993). Changes in braided river morphology resulting from aggradation and degradation. The Journal of Geology, vol 101 (4). Page: 451-466.

[13] Ghimire, M. (2014). Basin characteristics, river morphology, and process in the Chure-Terai landscape: A case study of the Bakraha River, East Nepal. The Geographical Journal of Nepal, vol 13. Page: 107-142.

[14] Ghosh, A. K., Mondal, S. K., Singh, S. K., & Sinha, A. (2010). Applicability of surface miner in Nongtrai limestone mine Lafarge Umiam Mining Pvt. Ltd. In Meghalaya, India. Central Institute of Mining & Fuel Research (Council of Scientific and Industrial Research). Department of Science & Technology, Government of India.Barwa Road, Dhanbad 826015, Jharkhand, India. July.

[15] Gogoi, B. (2006). The Noa-Dihing River: The study in Channel Morphology, Hydrology and Fluvial Geomorphology. Hill Geographer, vol 22 (1& 2). Page: 20-31

[16] Goswami, D.C. (1998). Fluvial regime and flood hydrology of the Brahmaputra River, Assam. Kale, V.S. (ed.), Flood studies in India. Geological Society of India, vol 41. Page: 53–76.

[17] Gupta, N., Atkinson, P.M., & Carling, P. A. (2013). Decadal length changes in the fluvial planform of the river Ganga: Bringing a Mega-River to life with Landsat archives. Remote sensing letters, vol 4 (1). Page: 1-9.

[18] Kamykowska, M., Kaszowskik, L., & Krzemień, K. (1999). River Channel Mapping Instruction, Key to the river bed description: River Channel, Pattern, Structure and Dynamics. Cracow, Institute of Geography of the Jagiellonian University.

[19] Matsuda, Iware. (2004). River Morphology and Channel Processes. Eolss Publisher, Oxford, UK. http://www.eolss.net. (Accessed on 13th October 2010).

[20] Morisawa, M. (1985). River Morphology: The Channel. Clayton, K.M (ed.), Rivers: Forms and Processes, London, Longman.

[21] Nongpuir Lyngdoh, Alvareen.R. (2010). Stream Characteristics around Sohra: A Morphological Study. Unpublished Master of Arts dissertation. North Eastern Hill University, Shillong.

[22] Ryntathiang, Bring. B. L. (2012). Morphometric Analysis of the Pynjngithuli River Basin, Cherrapunjee, India. Hill Geographer, vol 28(1). Page: 88-97

[23] Ryntathiang, Bring. B. L. (2014). Channel Morphology on the southern slope of Meghalaya Plateau. Unpublished Ph.D. Thesis, North Eastern Hill University, Shillong. Page: 10 - 120